Synthesis and Evaluation of Multifunctional Nanothiomatrices For an Efficient Antitumor Therapy

A THESIS PRESENTED BY

PRIYA.S.S

TO

SREE CHITRA TIRUNAL INSTITUTE FOR MEDICAL
SCIENCES AND TECHNOLOGY
THIRUVANANTHAPURAM
INDIA

IN PARTIAL FULFILMENT OF THE REQUIREMENTS
FOR THE AWARD OF
DOCTOR OF PHILOSOPHY

2019

CERTIFICATE

I, Priya.S.S, hereby certify that I had personally carried out the work depicted in the thesis entitled, *"Synthesis and evaluation of multifunctional nanothiomatrices for an efficient antitumor therapy"*, except where due acknowledgment has been made in the text. No part of the thesis has been submitted for the award of any other degree or diploma prior to this date.

1/01/2019

Trivandrum

1/1/2019

Priya.S.S

Reg No:2013/PhD/02

Tele : 0471-2340801 Fax : 0471-2341814 / 2340819

श्री चित्रा तिरुनाल आयुर्विज्ञान तथा प्रौद्योगिकी संस्थान
बायो मेडिकल टैक्नोलॉजी विंग
पूजापुरा, तिरुवनन्तपुरम-695 012, इन्डिया

SREE CHITRA TIRUNAL INSTITUTE FOR MEDICAL SCIENCES AND TECHNOLOGY
BIO MEDICAL TECHNOLOGY WING
POOJAPPURA, THIRUVANANTHAPURAM-695 012, INDIA
(An Institute of National Importance under Govt. of India)

CERTIFICATE

Ref: Dr. Rekha.M.R
Scientist F
Division of Biosurface Technology

Date:.....

This is to certify that Ms. Priya.S.S in the division of Biosurface Technology of this Institute has fulfilled the requirements prescribed for the Ph.D degree of the Sree Chitra Tirunal Institute for Medical Sciences and Technology, Trivandrum.

The thesis entitled, "*Synthesis and evaluation of multifunctional nanothiomatrices for an efficient antitumor therapy*", was carried out under my direct supervision. No part of the thesis was submitted for the award of any degree or diploma prior to this date.

Clearance was obtained from the Institutional Animal Ethics for carrying out the study.

1/1/19

Dr. Rekha.M.R
(Research Supervisor)

Trivandrum
1/01/2019

The thesis entitled

SYNTHESIS AND EVALUTION OF MULTIFUNCTIONAL NANOTHIOMATRICES FOR AN EFFICIENT ANTITUMOR THERAPY

Submitted by

Priya.S.S

For the degree of

Doctor of Philosophy

Of

SREE CHITRA TIRUNAL INSTITUE

FOR

MEDICAL SCIENCES AND TECHNOLOGY, TRIVANDRUM

Thiruvananthapuram

Is evaluated and approved by

24.6.19

.....

Dr.Rekha.M.R

(Research Supervisor)

24/06/2019

.....

Examiner

(Prof S.S. Ghosh)

Acknowledgements

It is a pleasure to thank many people for their support during the PhD work which made this thesis possible.

First of all, I wish to express my sincere gratitude to my guide, Dr. Rekha.M.R for introducing me into the exciting field of nanomaterials. I earnestly thank her for her sincere guidance, constant encouragement and inspiration during the entire course of this work. It was only due to her understanding, personal support and great patience that I was able to complete my research work in a respectable manner.

I express my sincere gratitude to the Director, SCTIMST and the Head, BMT Wing for providing with all the facilities needed for the research work. I am very much thankful to the present and previous Deputy Registrars for all the academic assistance in this venture. I am thankful to the Institute for the Institute fellowship during the entire period of my doctoral studies.

I express my sincere gratitude to the Doctoral Advisory Committee members, Dr. Prabha D Nair, and Dr. P.V.Mohanan, for their valuable time, suggestions and encouragements in my work.

I express my sincere gratitude to the Director, RGCB for providing me permission to access the confocal microscopy and flow cytometry facilities in the Institute. I also extend my heartfelt gratitude to Ms.Bindu, Mr.Gopikrishnan and Ms.Joji for giving me adequate assistance in confocal microscopy. I warmly thank Ms.Indu, Ms.Arya for their help in flow cytometry analysis. I wish to thank Dr. Manoj Komath, Dr. Suresh Babu and Mr.Adarsh for their help in FTIR analysis. I thank Dr.Luxmi Varma, Dr. Maya of NIIST for NMR analysis. I am thankful to Dr.Jayasree for her kind permission for using her lab facilities. I thank Ms.Hema and Ms.Resmi of Biophotonics Lab for helping me with the in vivo image analyser. I thank Dr.Maya Nandakumar and Mr.Pradeep of division of microbial technology for providing the facility for microplate analysis. I am grateful to Dr. Harikrishnan, Mr.Manoj, Mr.Pradeep, Ms.Jolly and Mr.Ajimon of DLAS for all the support during my animal work. I thank Dr.Annie and Dr.Harikrishnan for providing me training in animal handling. I also thank Dr.Anil kumar PR and Dr.Naresh for giving me training in confocal microscopy and image analysis. The help and support from Dr.Anil Kumar P.V and all staffs of experimental pathology are gratefully acknowledged. I am also thankful to DR.Anoop of division of molecular medicine for providing facilities for molecular biology work.

I am really thankful to the present and past labmates Ms.Rajalekshmi,Ms.Jasmin, Ms.Annie, Ms.Linsha, Ms.Dhanya, Dr.Susan, Dr.Thasneem, Ms.Mitha and Ms.Caroline for providing a cordial environment to work, their love and support are greatly acknowledged. I also thank Prof. Joachim Kohn, Dr. Ritu Goyal (NJCBM, USA) for selecting me in the International student exchange program. My sincere thank goes to Ms.Neelima, Ms.Nimmy Mohan, Dr.Akhila and Dr.Geetha for their friendship, support and encouragement. I gratefully acknowledge the support and help given by my friends, staff and students of BMT wing of SCTIMST.

I express my sincere gratitude to my Achan and Amma for their genuine love and prayers for me. I also thank my sister, Lekshmi for her motivation and encouragement. I extend my sincere thanks to my beloved husband, Mr.Rajesh for his love, understanding and support, which has helped me for the successful completion of this work.

Above all, I express gratitude and regards from the core of my heart to the Almighty God for His blessings which really helped me to concentrate in my work and successfully completing the thesis work.

Priya.S.S

Table of contents

Declaration by the Student i

Certificate of Guide ii

Approval of Thesis iii

Acknowledgements iv

Table of Contents vi

List of Figures xviii

List of Tables xxi

Abbreviations xxii

Synopsis xxiii

1 Introduction

1.1 Cancer Epidemiology and Social Impact 1

1.2 Cancer Biology: Molecular and genetic basis 2

1.3 The Hallmarks of Cancer 3

1.4 Current Treatment 1of Cancer 4

1.5 Gene Therapy 6

1.5.1 Cancer Gene Therapy 7

1. 6 Polymeric Nanocarriers 10

1.6.1 Barriers for Gene delivery……..…..…10

1.6.2 Gene Packaging 11

1.6.3 Serum stability 11

1.6.4 Intracellular Barriers 12

1.6.5 Endolysosomal Escape 12

1.6.6 Transport through the cytoplasm and nuclear localization ..... .13

1.7 Redox-sensitive polymers ..... .14

1.8 Multidrug resistance in cancer (MDR) ..... .15

1.8.1 ATP dependent transporters (efflux pump) ..... .16

1.8.2 P-gp modulators ..... .17

1.9 Nanotechnological approach against MDR in cancer treatment..... .18

1.10 Role of Thiomers in inhibiting P-gp ..... .20

1.11 Glutathione and chemoresistance.. ..... .21

1.12 p53 and chemoresistance……....22

1.13 Hypothesis……..…23

1.14 Aim…….……..…..24

1.15 Objectives…….……..24

2 Review of Literature

2.1 Redox state and redox environment..... 25

2.2 Reduction-sensitive cationic polymer for intracellular gene delivery……26

2.2.1 Bioreducible polyethylenimine 30

2.3 Thiomers and efflux pump inhibition 33

2.4 Synergistic drug and gene combination for cancer therapy..... 38

2.5 Co-delivery of chemotherapeutics and nucleic acid to promote apoptosis…….……...43

3 Materials and Methods ……...46

3.1 Synthesis and characterization of pullulan-PEI-Cysteine (PPSS)……46

3.1.1 Materials ..... .46

3.1.2 Synthesis of pullulan-PEI..... .47

3.1.3 Thiolation of Pullulan-PEI ..... .47

3.1.4 Oxidation of thiol polymer..... 48

3.1.5 Synthesis of control groups (PEI-CYS(S-S))..... 48

3.1.6 Physiochemical characterization 49

3.1.6.1 Determination of disulfide/ Thiol content 49

3.1.6.2 Determination of primary amine group using $CuSO_4$ assay . 50

3.1.6.3 FTIR analysis 50

3.1.6.4 ^1H NMR 50

3.1.7 Determination of buffering capacity 51

3.1.8 Nanoplex formulation 51

3.1.8.1 Determination of particle size and zeta potential 51

3.1.8.2 Gel retardation assay 52

3.1.8.3 Effect of DTT on the stability of thiolated polyplexes 52

3.1.9 Plasma protein interaction of the polymer (PAGE analysis) 53

3.1.10 Cell culture studies 53

3.1.10.1 In Vitro Cytotoxicity (MTT assay) 54

3.1.10.2 Uptake studies using confocal microscopy 55

3.1.10.3 Uptake studies using flow cytometry 55

3.1.10.4 Pathway studies using endocytosis inhibitors 56

3.1.10.5 Polymer trafficking studies 56

3.1.11 *In vitro* transfection efficiency 57

3.1.11.1 Live and Dead assay 57

3.1.11.2 Propidium iodide (PI) staining 58

3.1.11.3 Annexin V/FITC staining 59

3.1.11.4 p53 immunostaining 59

3.1.12 Efflux pump inhibition studies 60

3.1.12.1 Assessment of P-gp expression in cancer cell lines 60

3.1.12.2 Evaluation of efflux pump inhibition ability of the polymer...61

3.1.12.3 Evaluation of efflux pump inhibition using flow cytometry ... 61

3.1.12.4 DOX retention studies 62

3.2 Synthesis and characterization of pullulan-PEI-mercaptosuccinic acid (PPMSS)

3.2.1 Materials 63

3.2.2 Synthesis of pullulan-PEI 63

3.2.3 Thiolation step 63

3.2.4 Oxidation of thiol polymer..... 63

3.2.5 Synthesis of the control group (PEI-MSA)..... .64

3.2.6 Physicochemical characterization……...64

3.2.6.1 Determination of disulfide/thiol content ..... .64

3.2.6.2 Determination of amino content using $CuSO_4$ assay.……..64

3.2.6.3 Analysis by Fourier Transform Infrared Spectroscopy (FTIR)..64

3.2.6.4 Analysis by ^1H NMR.……..65

3.2.7 Determination of buffering capacity…….....65

3.2.8 Preparation of nanoplexes ..... .65

3.2.8.1 Determination of particle size and zeta potential 65

3.2.8.2 Gel retardation assay 66

3.2.8.3 Effect of DTT on the stability of thiolated polyplexes..... 66

3.2.9 Plasma protein interaction of the polymer (PAGE analysis)..... 66

3.2.10 Cell culture studies..... 67

3.2.10.1 In vitro cytotoxicity (MTT assay)..... 67

3.2.10.2 Uptake studies via confocal microscopy 67

3.2.10.3 Uptake studies using flow cytometry..... 68

3.2.10.4 Pathway studies using endocytosis Inhibitors *68*

3.2.10.5 Polymer trafficking studies *68*

3.2.11 *In vitro* transfection efficiency 68

3.2.11.1 Live and dead assay *69*

3.2.11.2 PI staining *69*

3.2.11.3 Annexin V/FITC staining *69*

3.2.11.4 p53 immunostaining *70*

3.2.12 Efflux pump inhibition studies 70

3.2.12.1 Efflux pump inhibition studies using confocal microscopy *70*

3.2.12.2 Efflux pump inhibition studies using flow cytometry *71*

3.2.12.3 DOX retention studies *71*

3.3 Synthesis and characterization of pullulan-PEI-3,3 dithiodipropionic acid (PPDPA)

3.3.1 Materials 71

3.3.2 Synthesis of Pullulan-PEI 72

3.3.3 Synthesis of pullulan-PEI-3,3 dithiodipropionic acid 72

3.3.4 Synthesis of control group (PEI-3, 3 dithiodipropionic acid) 72

3.3.5 Physicochemical characterization 72

3.3.5.1 Determination of disulfide/thiol content *72*

3.3.5.2 Determination of amino content by $CuSO_4$ assay *73*

3.3.5.3 FTIR analysis *73*

3.3.5.4 ^1H NMR *73*

3.3.6 Determination of buffering capacity 73

3.3.7 Formation of nanoplexes 74

3.3.7.1 Determination of particle size and zeta potential *74*

3.3.7.2 Gel retardation assay *74*

3.3.7.3 Effect of DTT on the stability of thiolated polyplexes *74*

3.3.8 PAGE analysis 75

3.3.9 Cell culture studies 75

3.3.9.1 In vitro cytotoxicity (MTT assay) *75*

3.3.9.2 Uptake studies using confocal microscopy *76*

3.3.9.3 Uptake studies using flow cytometry *76*

3.3.9.4 Pathway studies using endocytosis inhibitors *76*

3.3.9.5 Polymer trafficking studies *76*

3.3.10 *In vitro* transfection efficiency 77

3.3.10.1 Live and Dead assay *77*

3.3.10.2 PI staining *77*

3.3.10.3 Annexin V/FITC staining *78*

3.3.10.4 p53 immunostaining ……..*78*

3.3.11 Efflux pump studies 78

3.3.11.1 Efflux pump inhibition using confocal microscopy……..*78*

3.3.11.2 Efflux pump inhibition studies using flow cytometry…..…*79*

3.3.11.3 DOX retention studies……..*79*

3.4 Synthesis and characterization of pullulan- PEI-3,3dithiodibutyric acid (PPDBA)

3.4.1 Materials…….…….79

3.4.2 Synthesis of pullulan-PEI 80

3.4.3 Synthesis of pullulan-PEI-4,4 dithiodibutyric acid (PPDBA)…….80

3.4.4 Synthesis of the control group (PEI-4,4 dithiodibutyric acid) 80

3.4.5 Physicochemical characterization 81

3.4.5.1 Determination of disulfide/thiol content *81*

3.4.5.2 Determination of amino content by $CuSO_4$ assay *81*

3.4.5.3 FTIR analysis *81*

3.4.5.4 ^1H NMR *82*

3.4.6 Determination of buffering capacity 82

3.4.7 Nanoplex preparation 82

3.4.7.1 Determination of particle size and zeta potential *82*

3.4.7.2 Gel retardation assay *83*

3.4.7.3 Effect of DTT on the stability of thiolated polyplexes *83*

3.4.8 PAGE analysis 83

3.4.9 Cell culture studies 84

3.4.9.1 In vitro cytotoxicity (MTT assay) *84*

3.4.9.2 Uptake studies using confocal microscopy *84*

3.4.9.3 Uptake studies using flow cytometry *85*

3.4.9.4 Pathway studies using endocytosis inhibitors *85*

3.4.9.5 Polymer trafficking studies *85*

3.4.10 *In vitro* transfection efficiency 85

3.4.10.1 Live and Dead assay *86*

3.4.10.2 PI staining *86*

3.4.10.3 Annexin V/FITC staining *86*

3.4.10.4 P53 immunostaining *87*

3.4.11 Efflux pump inhibition studies 87

3.4.11.1 Efflux pump inhibition using confocal microscopy *87*

3.4.11.2. Efflux pump inhibition using flow cytometry *87*

3.4.11.3 DOX retention studies 88

3.4.12 Glutathione activity …….…….88

3.4.12.1 Assessment of glutathione level using monochlorobimane.. 88

3.4.12.2. Role of glutathione in DOX retention 88

3.4.13. Dose-response experiments 89

3.4.14. Drug Release studies..... 90

3.4.15 Immunostaining of membrane P-gp activity in C6 cells ……91

3.4.16 The synergetic effect of p53 in augmenting DOX sensitivity in C6 glioma cells……91

3.5 *In vivo* biodistribution and antitumor efficacy of pullulan-PEI-4,4 dithiodibutyric acid (PPDBA) in mice model

3.5.1. Preparation of PPDBA/ctDNA-DOX nano complex..... .92

3.5.2 *In vivo* organ distribution studies of polymer ..... .92

3.5.3. Antitumor efficacy of PPDBA/p53-DOX nanocomplex in BALB/c mice model……...93

4. Results

4.1. Synthesis of pullulan-PEI…….…….……95

4.1.1 Synthesis and characterization of pullulan-PEI-Cysteine (PPSS)……96

4.1.2 ^{1}HNMR & FTIR…….97

4.1.3. Buffering ability of the polymer……..….101

4. 1.4 Biophysical characterization……...…..102

4.1.4.1 Size and Zeta potential.…….....102

4.1.4.2 Agarose gel electrophoresis.……..…..103

4.1.4.3 Nanoplex stability in presence of DTT.…….....104

4.1.5. Plasma protein interaction with PPSS polymer (PAGE)……..106

4.1.6. Biological analysis……107

4.1.6.1. Cytotoxicity evaluation of the polymer……..107

4.1.6.2. Evaluation of cellular uptake……108

4.1.6.3. Endocytosis inhibition study……..112

4.1.6.4. Polymer trafficking studies……..113

4.1.6.5. Transfection efficiency using Live and Dead assay……114

4.1.6.6. PI staining using flow cytometry……..114

4.1.6.7. Determination of apoptosis by Annexin V staining……115

4.1.6.8. p53 immunofluorescence-confocal microscopy……116

4.1.6.9. Assessment of P-gp activity in cancer cell lines……117

4.1.6.10 Efflux pump inhibition using confocal microscopy……118

4.1.6.11. Efflux pump inhibition studies using flow cytometry……121

4.1.6.12. DOX retention kinetics……122

4.2. Synthesis and characterization of pullulan-PEI-mercaptosuccinic acid (PPMSS)

4.2.1. ^{1}H NMR and FTIR……126

4.2.2. Buffering Capacity……128

4.2.3. Biophysical characterization……..129

4.2.3.1. Size and zeta potential……..129

4.2.3.2. Agarose gel electrophoresis……130

4.2.3.3 Stability of nanoplexes in presence of DTT……131

4.2.4 Plasma protein interaction with the polymer (PAGE)……..133

4.2.5. Biological analysis……..…134

4.2.5.1 Cytotoxicity evaluation of the polymers.……..134

4.2.5.2 Evaluation of cellular uptake ……135

4.2.5.3 Endocytosis inhibitor study ……137

4.2.5.4 Polymer trafficking studies ……138

4.2.5.5 Transfection studies based on live and dead assay.……138

4.2.5.6 PI staining via flow cytometry ……139

4.2.5.7 Annexin V staining ……140

4.2.5.8 p53 immunofluorescence.……141

4.2.5.9 Efflux pump inhibition using confocal microscopy.…. 142

4.2.5.10 Efflux pump inhibition using flow cytometry.……145

4.2.5.11 DOX retention.……146

4.3. Synthesis and characterization of pullulan-PEI-3,3 dithiodipropionic acid (PPDPA)

4.3.1[1]HNM & FTIR…….150

4.3.2 Buffering capacity……153

4.3.3 Biophysical characterization ……154

4.3.3.1Size and zeta potential.……154

4.3.3.2. Agarose gel electrophoresis.……156

4.3.3.3. Stability of nanoplexes in presence of DTT.……157

4.3.4 Plasma protein interaction with the polymers (PAGE)……159

4.3.5 .Biological analysis……160

4.3.5.1.Cytotoxicity evaluation of the polymer.……160

4.3.5.2.Evaluation of cellular uptake.……161

4.3.5.3.Endocytosis inhibitor study.……..164

4.3.5.4.Polymer trafficking studies.……..165

4.3.5.5. Transfection studies based on Live and dead assay.……..167

4.3.5.6 PI staining via Flow cytometry.……..168

4.3.5.7 Determination of apoptosis via annexin V staining.……..169

4.3.5.8 p53 immunofluorescence.……..170

4.3.5.9 Efflux pump inhibition studies using confocal microscopy.……..170

4.3.5.10 Efflux pump inhibition studies using flow cytometry.……..173

4.3.5.11DOX retention kinetics.……..174

4.4. Synthesis and characterization of pullulan-PEI-4,4 dithiodibutyric acid (PPDBA)

4.4.1.[1]HNMR and FTIR……...178

4.4.2 Buffering Capacity ……..……..…….....181

4.4.3 Biophysical characterization ……..…… ……181

4.4.3.1 Size and Zeta potential.……..181

4.4.3.2 Agarose gel electrophoresis.……..183

4.4.3.3 Stability of nanoplexes in presence of DTT.……..184

4.4.4. Plasma protein interaction with the polymer(PAGE)……..…..…186

4.4.5 Biological analysis ……187

4.4.5.1. Cytotoxicity evaluation of the polymer ……..187

4.4.5.2. Evaluation of cellular uptake ……..188

4.3.5.3. Endocytosis inhibitor study.……..191

4.4.5.4. Polymer trafficking studies.…… ……..192

4.4.5.5. Transfection studies based on Live and dead assay ……..194

4.4.5.6. PI staining via Flow cytometry.……194

4.4.5.7. Determination of apoptosis via annexin V staining.……195

4.4.5.8. p53 immunofluorescence.……196

4.4.5.9 Efflux pump inhibition studies using confocal ……197

4.4.5.10 Efflux pump inhibition studies using flow cytometry ……199

4.4.5.11 DOX retention kinetics ……201

4.4.5.12 Role of glutathione.……204

4.4.5.13 DOX mediated cytotoxicity.……207

4.4.5.14 P-gp immunostaining ……210

4.4.5.15. Release study.……211

4.4.5.16. Synergisitic effect of therapeutic gene and drug ……212

4.5.1 *In vivo* organ distribution of PPDBA nanoplexes ……213

4.5.2. Antitumor efficacy of PPDBA/p53-DOX nanocomplex in BALB/c mice model ……..216

5. Discussion

5.1 Pullulan- PEI……..…… ..……..218

5.2. Synthesis and characterization of pullulan-PEI-cysteine (PPSS) and pullulan-PEI-mercaptosuccinic acid (PPMSS) …….……....219

5.3 Synthesis and characterization of pullulan-PEI-3,3 dithiodipropionic acid (PPDPA) and pullulan-PEI-4,4 dithiodibutyric acid (PPDBA)……... 238

6. Summary and Conclusion……..…….……...264

7. References…….....271

8. List of publications ……..….. …283

List of Figures

1. Representation of DNA binding and subsequent intracellular release via disulfide cleavage……...27
2. Cellular factors that contribute drug resistance……..…34
3. Postulated mechanism of efflux pump inhibition by thiomers……...37
4. Antitumor activity of mice containing orthotopic U87 tumor using DOX and TRAIL in a dendrimer based delivery system…….44
5. Co-delivery of anti-angiogenesis drug, candesartan (CD) and wild-type (wt)-p53 plasmids in bPEI grafted with chitosan (CS) system…….….45
6. ^{1}HNMR spectra of Pullulan-PEI, PPSS I, PEICYS(S-S)I 99
7. FTIR spectra of s A) Pullulan-PEI B) PPSSI and C) PEICYS(S-S)I……101
8. Buffering capacity of the polymers PEI (25KDa), PPSS I, PPSS II, PEICYS(S-S)I, PEICYS(S-S)II and saline…….……..102
9. (A) Size measurement and (B) Zeta potential of PPSS1 and PPSSII nanoplexes with different polymer /ctDNA ratio……..103
10. Agarose gel electrophoresis of PPSSI,PPSSII,PEICYS(S-S)I,II nanoplexes with or without plasma……..…104
11. The change in particle size of PPSSI/II polyplexes in presence of DTT (10mM)…….…105
12. Agarose gel electrophoresis of PPSSI/II nanoplexes with DTT and DTT/heparin……..……106
13. PAGE analysis of PPSS I, II,PEICYS(S-S)I,II and PEI……...……107
14. MTT assay of PPSSI and II and PEICYS(S-S)I and II nanoplexes …… 108
15. Cellular uptake of PPSSI and PPSSII using confocal microscopy 110
16. Cellular uptake of PEICYS(S-S) I and II using confocal microscopy 111
17. Cellular uptake of PPSSI /II and PEICYS(S-S)I/II via flow cytometry…....111
18. Endocytosis inhibitor study……...112
19. Polymer trafficking studies of PPSSI nanoplexes…….113
20. Transfection efficacy of PPSSI/II by live and dead assay…….....114
21. Transfection efficiency of PPSSI/II via PI staining …….……..…115
22. Transfection efficiency of PPSSI/II via annexin V staining…….……116
23. p53 immunostaining …….……117
24. Assessment of P-gp activity in cancer cell lines……..…….……118
25. Efflux pump inhibition studies of PPSS nanoplexes in C6 cells…….…...119
26. Efflux pump inhibition studies of PPSS nanoplexes in A549 cells……120
27. Efflux pump inhibition studies of PPSS nanoplexes in HeLa cells……120

28. DOX retention kinetics ……124
29. ^{1}HNMR spectra of PPMSS and PEI-MSA……...……127
30. FTIR of PPMSS &PEI-MSA……..…..128
31. Buffering abilities of PEI, PEI-MSA,PPMSS and Saline…….……129
32. Particle size and zeta potential values of PPMSS and PEI-MSA…….130
33. Agarose gel electrophoresis of PPMSS and PEI-MSA nanoplexes with or without plasma……..…..131
34. The change in particle size of PPMSS and PEI-MSA polyplexes in presence of DTT ……...…132
35. Agarose gel electrophoresis of PPMSS and PEI-MSA nanoplexes with DTT DTT/heparin……..… 132
36. PAGE analysis of PPMSS,PEI-MSA and PEI……...133
37. MTT assay of PPMSS and PEI-MSA nanoplexes ……...…134
38. Cellular uptake of PPMSS and PEI-MSA using confocal microscopy 136
39. Cellular uptake of PPMSS & PEI-MSA via flow cytometry……..…...136
40. Endocytosis inhibitor study……...…137
41. Polymer trafficking studies of PPMSS nanoplexes……....138
42. Transfection efficacy of PPMSS nanoplexes assessed by live and dead assay……139
43. Transfection efficiency of PPMSS assessed via PI staining ……..…140.
44. Transfection efficiency of PPMSS via annexin V staining……..…141
45. p53 immunostaining ……..……..…141
46. Efflux pump inhibition studies of PPMSS nanoplexes in C6 cells……...143
47. Efflux pump inhibition studies of PPMSS nanoplexes in A549 cells…...144
48. Efflux pump inhibition studies of PPMSS nanoplexes in HeLa cells…..144
49. DOX retention kinetics ……....…148
50. ^{1}HNMR spectra of PPDPA & PDPA……..151
51. FTIR of PPDPA & PDPA……153
52. Buffering abilities of PEI, PPDPA I,II,II and PDPA I,II,II……...……..154
53. Particle size and zeta potential values of PPDPA I,II, III & PDPAI,II,III...155
54. Agarose gel electrophoresis of PPDPAI,II,III and PDPA I,II,II nanoplexes with or without plasma…….157
55. The change in particle size of PPDPAI,II,III and PDPAI,II,III polyplexes in presence of DTT 158
56. Agarose gel electrophoresis of PPDPAI,II,III and PDPA I,II,IIInanoplexes with DTT and DTT/heparin…….159
57. PAGE analysis of PPDPAI,II,II and PDPAI,II,III and PEI ……160
58. MTT assay of PPDPA I,II,III and PDPAI,II,II nanoplexes ……...161
59. Cellular uptake of PPDPAI,II,III and PDPAI,II,III using confocal microscopy ……163
60. Cellular uptake of PPDPA I,II,III & PDPA I,II,III via flow cytometry…..164
61. Endocytosis inhibitor study…….165
62. Polymer trafficking studies of PPDPA nanoplexes……..…166

63. Transfection efficacy of PPDPAI,II,III nanoplexes assessed by live and dead assay……167
64. Transfection efficiency of PPDPA nanoplexes assessed via PI staining ..168
65. Transfection efficiency of PPDPA via annexin V staining…….169
66. p53 immunostaining …….....170
67. Efflux pump inhibition studies of PPDPA nanoplexes in C6 cells….....171
68. Efflux pump inhibition studies of PPDPA nanoplexes in A549 cells…….172
69. Efflux pump inhibition studies of PPDPA nanoplexes in HeLa cells….172
70. DOX retention kinetics ……..176
71. ^{1}HNMR spectra of PPDBA & PDBA……....179
72. FTIR of PPDBA & PDBA……..……180
73. Buffering abilities of PEI, PPDBA I,II,II and PDBA I,II,II……181
74. Particle size and zeta potential values of PPDBA I,II, III & PDBAI,II,III.183.
75. Agarose gel electrophoresis of PPDBAI,II,III and PDBA I,II,IInanoplexes with or without plasma……184
76. The change in particle size of PPDBAI,II,III and PDBAI,II,III polyplexes in presence of DTT 185
77. Agarose gel electrophoresis of PPDBAI,II,III and PDPA I,II,IIInanoplexes with DTT and DTT/heparin……..……...186
78. PAGE analysis of PPDBAI,II,II and PDBAI,II,III and PEI ……...187
79. MTT assay of PPDBA I,II,III and PDBAI,II,II nanoplexes ……..188
80. Cellular uptake of PPDBAI,II,III and PDBAI,II,III using confocal ……..190
81. Cellular uptake of PPDBA I,II,III & PDBA I,II,III via flow cytometry…..191
82. Endocytosis inhibitor study…….....192
83. Polymer trafficking studies of PPDBA nanoplexes…….193
84. Transfection efficacy of PPDBAI,II,III nanoplexes assessed by live and dead assay…….194
85. Transfection efficiency of PPDBA nanoplexes assessed via PI staining ...195
86. Transfection efficiency of PPDBA via annexin V staining…….…196
87. p53 immunostaining ……197
88. Efflux pump inhibition studies of PPDBA nanoplexes in C6/A549& HeLa cells……..……199
89. Efflux pump inhibition studies of PPDBA nanoplexes using flow cytometry……..201
90. DOX retention kinetics ……204
91. Glutathione assessment using monochlorobimane (confocal microscopy)……..205
92. DOX retention in presence of glutathione……...206
93. Quantification of DOX in presence of glutathione ……..……...206
94. Dose response curve …….…..208
95. Resistance factor …….…209
96. P-gp immunostaining ……..……211

97. Release studies ……212
98. Synergistic activity of p53 gene and DOX……..……213
99. Organ distribution of PPDBA nanoplexes (*in vivo* image analyzer)…...…215
100.The quantitative measurement of the distribution of PPDBA polyplexes in different organs……..216
101.Antitumor activity Antitumor activity of PPDBA/p53/DOX in the BALB/c mice model…….217

List of Tables

1. Division of tumor bearing BALB/c mice for antitumor evalution ……94
2. Quantification of amino content in PPSSI/II and its controls ……..…97
3. Quantification of thiol/disulfide content in PPSSI/II and its controls…….97
4. Efflux pump inhibition study of PPSS nanoplexes using flow cytometry 121
5. Quantification of thiol/disulfide content in PPMSS and its controls…...…..125
6. Quantification of amino content in PPMSS and its controls …….125
7. Efflux pump inhibition of PPMSS nanoplexes using flow cytometry……...146
8. Quantification of thiol/disulfide content in PPDPAI/II/II and its controls….149
9. Quantification of amino content in PPDPA I/II/III and its controls ……..…149
10. Efflux pump inhibition of PPDPA nanoplexes using flow cytometry ……...174
11. Quantification of thiol/disulfide in PPDBAI/II/II and its controls……..177
12. Quantification of amino content in PPDBA I/II/III and its controls ……..177
13. IC50 values……..……209

Abbreviations

AGE	Agarose gel electrophoresis
ctDNA	Calf thymus DNA
DLS	Dynamic light scattering
DMEM	Dulbecco's modified eagle's medium
DNA	Deoxyribonucleic acid
DTT	Dithiothreitol
EDC	1-Ethyl-3-(3-dimethylaminopropyl) carbodiimide hydrochloride
EDTA	Ethylene diamine tetra acetic acid
FBS	Fetal bovine serum
FTIR	Fourier-transform infrared spectroscopy
GSH	Glutathione
HCl	Hydrochloric acid
kDa	kilo Daltons
MDR	Multidrug resistance
MEM	Minimal Essential Medium
MTT	3-(4, 5-Dimethylthiazol-2-yl)-2, 5-diphenyltetrazolium bromide
mV	milli Volt
Mw	Molecular weight
nm	nanometer
NMR	Nuclear Magnetic Resonance
NTSB	2-nitro 5-thiosulfobenzoate
PAGE	Polyacrylamide gel electrophoresis
PBS	Phosphate buffered saline
PDBA	Polyethyleneimine-4,4 dithiodibutyric acid
pDNA	Plasmid DNA
PDPA	Polyethylenimine -3,3 dithiodipropionic acid
PEI	Polyethylenimine
P-gp	P- glycoprotein
PI	Propidium Iodide
PP	Pullulan-Polyethyleneimine
PPDBA	Pullulan-Polyethyleneimine -4,4 dithiodibutyric acid
PPDPA	Pullulan-Polyethyleneimine -3,3 dithiodipropionic acid
ppm	parts per million
PPMSS	Pullulan-PEI-mercaptosuccinic acid
PPSS	Pullulan-PEI-Cysteine
UV-Vis	Ultra violet-Visible

SYNOPSIS

Cancer is one of the most devastating diseases of the human race in the world today. Undoubtedly, chemotherapy serves the most important strategy to combat cancer in the clinic, but the major obstacle for this curative treatment of malignancies is the emergence of multidrug resistance (MDR). The phenomenon of multidrug resistance (MDR) is that many cancer cells develop resistance to a variety of structurally unrelated chemotherapeutic agents resulting in minimal cell death and expansion of drug-resistant tumors. This defense mechanism contributes to therapeutic failure and tumor relapses for over 90% of cancer patients. Overexpression of efflux transporters, which either inherently expressed by the cancer cells or occurred in response to chemotherapy is an important source of drug resistance. Several efforts have been made for the development of inhibitors/modulators of MDR but their clinical applications remain hindered by lack of specificity, high toxicity, low efficiency, and altered pharmacokinetics when co-administered with anticancer drugs.

To overcome these hurdles, nanotechnology is now recognized as a promising innovative invention to circumvent MDR and combat cancer. Nanomedicine can deliver high concentrations of drugs or inhibitors to the tumor site by evading the membrane P-gp activity. The nanoparticles are too large for diffusion mediated transport which result in endocytosis and accumulation of therapeutics near the perinuclear space, away from P-glycoprotein. This, in turn, enables the nanoparticles to bypass the drug efflux pump. Recently, the combination concepts have been extended to developing carrier materials containing both anticancer drug and antiMDR siRNA. This is advantageous because it can concurrently target different pathways causing MDR.

However, siRNA with certain specific sequences could only inhibit one particular protein and so if several proteins are simultaneously responsible for drug resistance, a mixture of siRNAs should be used to suppress pump resistance which is not feasible. Nanomedicine has been used to incorporate both P-gp inhibitor and anticancer drug together in the same carrier system. These nanotechnological approaches overcomes both the lack of specificity/efficiency of conventional drugs and delivery barriers in solid tumors. It is advantageous if the nanocarriers itself exhibit P-gp inhibitory property apart from the delivering the therapeutic cargo which it carries. Examples for polymeric Pgp inhibitors include α-tocopheryl PEG1000 succinate, non-ionic PEO-PPO-PEO block copolymer, namely Pluronic® P85, Poly(styrene oxide)–poly(ethylene oxide) triblock copolymers, low molecular weight methoxy polyethylene glycol-poly(epsilon-caprolactone) diblock polymer and thiomers. Of which thiomers or thiolated polymers are now established as a potent efflux pump inhibitor. However, there are only limited reports available on the potential benefit of polymer-based systems for the simultaneous effect on P-gp inhibition and therapeutic gene delivery efficacy. Combining these two functions can largely increase the therapeutic potential of the nanomedicine to combat cancer.

In this line, thiolated pullulan based cationic polymers have been synthesized with the purpose of simultaneous P-gp inhibition and therapeutic gene delivery. Pullulan is a non-ionic polysaccharide and is non-toxic, non-immunogenic and non-carcinogenic in nature. The cationicity have been inserted to pullulan by incorporating PEI, a known potent gene transfecting agent. Pullulan contains a flexible hydrophilic group which reduces the heavy surface positive charge in PEI and hence systemic side effects can be minimized. The thiol/disulfide containing moieties have been incorporated into the backbone of pullulan-PEI. The disulfide-containing polymers are also known as bioreducible polymers because of its responsiveness to the

intracellular reduction environment contributed by the high glutathione level (2-10mM). The bioreducible polymers are superior in terms of gene delivery efficacy because it can perform contradictory functions i.e. nanocomplexes will be stable in the oxidizing environment in the systemic circulation but can easily release the therapeutic cargo in the cytoplasm in response to the intracellular reducing environment. These polymers are also successful in overcoming the problems related to cytotoxicity and poor vector unpacking. The transfection efficiency of the disulfide-containing polymers is also reported to be higher than the corresponding cationic counterparts. Thiomers or thiolated polymers are among the most efficient polymeric efflux pump inhibitors currently available. It shows 2.7 fold higher P-gp inhibition effect than PEG and PEG derivatives such as pluronics under physiological conditions. The cationic thiolated pullulan based polymers were synthesized with the dual purpose of gene delivery and efflux pump inhibition in cancer.

The main focus of the study is to develop a nanocarrier which can simultaneously act as a gene delivery vehicle and an efflux pump inhibitor to effectively transfer therapeutic gene and enhance the chemosensitivity of the cancer cells towards anticancer drugs to promote cancer cell death. The thesis consists of six chapters. The first chapter deals with the introduction and background of the study. This part describes the epidemiology of cancer, disease progression, various treatment modalities including the newly advent strategy i.e gene therapy. Cancer is characterized by genetic heterogeneity so treating this disease at the genetic level is an ideal option where the therapeutic gene which is defective in the cancer cells is selectively delivered to the cells without causing any toxicity. In order to carry out the site-specific delivery of a therapeutic gene, an appropriate delivery system is mandatory. The viral vectors have been utilized for the same by considering its inherent property of transfecting a cell but its major disadvantage includes

immunogenicity and insertional mutagenesis. The non-viral vectors have emerged as an alternative strategy to mitigate the problems encountered in the viral counterparts. The different barriers of non-viral vectors and the strategies to overcome the same are also discussed. The chapter also describes the multidrug resistance and various pathways which leads to drug resistance in cancer cells.

The second chapter deals with the bioreducible polymers and its suitability in gene delivery and the significance of thiomers in overcoming P-glycoproteins in the cancer cell membrane. It also describes the combination therapy used for the purpose of targeting different biochemical pathways to overcome multidrug resistance in a heterogeneous tumor. The co-delivery of therapeutic gene and drug can restore the activities of the functional gene which is defective in cancer and can synergistically overcome chemoresistance and thereby retard the progression of cancer.

The third chapter is the materials and methods. It describes the synthesis and characterization of disulfide cross-linked cationic pullulan. Initially, the parent compound pullulan-PEI was synthesized by activating the hydroxyl group of pullulan with carbonyl diimidazole (CDI) and subsequently conjugated with PEI. The thiol moieties were incorporated to the parent compound by two methods i.e. incorporation of the thiol group and followed by oxidation and secondly direct incorporation of in-built disulfide containing moieties to the pullulan-PEI backbone. The first method includes the development of pullulan-PEI-cysteine (PPSS) and pullulan-PEI-mercaptosuccinic acid (PPMSS). The second method involves the synthesis of pullulan-PEI-3,3 dithiodipropionic acid (PPDPA) and pullulan-PEI-4,4 dithiodibutyric acid. The conjugation was confirmed by ^{1}HNMR and FTIR and the quantification of the amino group and thiol group was performed by $CuSO_4$ and Ellman's assay respectively. Nanoplexes of these polymers were then

developed at various ratios. Various characterization techniques were utilized to evaluate the various parameters such as particle size, zeta potential, buffering capacity and the stability of the nanoplexes in presence of plasma as well as in presence of intracellular reducing environment. The plasma protein interactions of the polymers and the cytotoxicity were also assessed. The cellular internalization, endocytosis pathway, and polymer trafficking were determined by using labeled polymers/DNA and imaging by confocal microscopy. Finally, the transfection efficiency of the polymers was analyzed using the therapeutic gene, p53 and its expression was visualized by means of live dead assay using confocal microscopy and the percentage apoptosis was determined by annexin V staining using flow cytometry. The expression of p53 in the transfected cells was analyzed by performing immunostaining with labeled antibody and visualising via confocal microscopy.

A series of cancer cells were screened for efflux pump inhibition studies using the known P-gp blocker i.e verapamil. The DOX retention kinetics was analyzed in different cell lines. The efflux pump inhibition study was carried out in cell lines C6,A549, and HeLa, where the retention of anticancer drug DOX acts as an index of P-gp activity. Based on the performance in transfection and efflux pump inhibition, one of the polymer nanoplexes was chosen for further studies. Nanoplexes developed with the chosen polymer was used to determine the DOX dose-response in A549 and HeLa cells, IC50, resistance factor and release study. The influence of reducing environment on DOX retention was determined by assessing it both in the presence of glutathione monoester and buthionine sulfoximine (BSO) in resistant cell line. P-gp immunostaining was carried out to determine the influence of thiolated polymer on P-gp activity. The *in vivo* organ distribution of the polyplexes was analyzed after tagging the polymer with a fluorophore and the

in vivo antitumor activity was determined by the co-delivery of p53/DOX mediated by the pullulan derivative in the tumor-induced BALB/c mice.

The fourth and fifth chapters are the results and discussion respectively. Here, the gene delivery efficacy and efflux pump inhibition properties of the pullulan based polymers have been evaluated. Both ^{1}HNMR and FTIR showed the conjugation of pullulan-PEI and the thiol group. The size and zeta potential measured via dynamic light scattering showed a particle size of <200nm and a positive zeta potential within +20mV (10-20mV) which is ideal for gene delivery applications. The pullulan derivatives showed high buffering capacity which was comparable to PEI. The gel electrophoresis studies revealed the DNA condensation ability of the polymer. The enlargement in particle size in presence of dithiothreitol indicated its responsiveness to the reductive intracellular environment. The AGE following DTT/heparin treatment of nanoplexes revealed the release of DNA via the combined effect of reducing environment and polyanionic conditions in the cells. The PAGE analysis showed a minimal plasma protein interaction on to the polymer surfaces. The cytotoxicity studies displayed that the pullulan derivatives are non-toxic and safe to use, where it showed >85% viability against <50% viability showed by the controls. The cellular internalization of the nanoplexes was high in the pullulan based polymers compared to the control where cell uptake was poor and notable rupture of the cells was observed. The polymer trafficking studies indicated that following nanoplexes unpacking and successful translocation of DNA to the cytoplasm and nuclei, the polymer was removed from the cell which was indicated by the red fluorescence aligned on to the cell membrane over time. The pullulan based polymers showed high transfection efficiency which was proven by both qualitative and quantitative methods. The efflux pump inhibition study of the pullulan based polymer nanoplexes was analyzed in both P-gp positive or drug resistant cells i.e C6 and A549 and P-gp negative or

drug sensitive cell i.e HeLa. The pullulan based derivatives showed enhanced DOX retention in the P-gp positive cell lines which was confirmed by both confocal microscopy and flow cytometry. The ability of the nanoplexes to retain drug in the resistant cancer cells like A549 and C6 and the extent of P-gp inhibition by the polymer was analyzed by DOX retention kinetics studies. Further, the cytotoxicity of the anticancer drug DOX in the presence of nanoplexes was determined by dose response curve. This revealed that in the resistant cell lines like C6 and A549, the cytotoxicity mediated by the drug was significantly higher than the drug alone treated controls. Based on the dose-response, IC50 and resistance factor was calculated to ensure the effect of nanoplexes in overcoming MDR. The release studies were performed by intercalating DOX with DNA before forming the complex with the polymer and ensured a sustained release of drug over time. Also, it was observed that the nanoplexes were responsive to glutathione level in retaining DOX. The *in vivo* organ distribution studies was conducted to evaluate the behavior of nanoplexes in circulation which revealed that the nanoplexes were removed from the body over time and was not found aggregating in vital organs. The synergistic activity of drug and gene showed an efficient reduction in tumor size and prevention in disease progression in the tumor-induced BALB/c mice.

The sixth chapter deals with summary, conclusion and future work. The redox-sensitive pullulan based polymers form an excellent delivery vehicle for the combined delivery of apoptotic gene and the anticancer drug which caused enhanced cell death even with minimal therapeutic dosage. It is understood that the disulfide cross linked pullulan based nanocarriers forms an efficient platform for cancer therapy.

CHAPTER I INTRODUCTION

1.1 Cancer Epidemiology and social impact

Cancer is a leading cause of death globally, with approximately 9.6 million deaths reported so far in 2018 as per press report released by WHO (World Health Organization). The number of new cases may rise to 22 million within the next two decades. Approximately 70% of cancer death occurs in low and middle- income countries such as Africa, Asia, Central, and South America. Around one- third of cancer death are related to five leading behavioral and dietary risks, i.e., high body mass index, low fruit and vegeTable intake, lack of physical activity, tobacco use and alcohol use (Torre et al., 2016) The overall cancer incidence rate is almost 25% higher in men than in women, where the male incidence rate varies nearly five-fold across the different regions of the world. Based on 2008-2012 reports, the cancer incidence rate is highest among the African American men (261.5 per 100000) and lowest in Asian Pacific Islander women (91.2 per 100000) (Torre et al., 2016). In India, almost 1.4 million people are living with cancer and 0.7 million new cases registered every year. Almost 71% of all cancer-related deaths are occurring in the age group between 30-69 (Noone et al., 2016) However, there is a clear progression in the survival rate of cancer patients across the world due to the emergence of new technologies for cancer diagnosis and treatment (Sullivan et al., 2015).

1.2 Cancer Biology: Molecular and genetic basis

During the past decades, tremendous growth occurred in the understanding of the genetic basis of cancer. Cancer is uncontrolled growth and proliferation of cells, where the cells fail to respond to the normal growth control mechanisms, acquiring the ability to divide uncontrollably. The occurrence of cancer is a multistep process, involving the accumulation of genetic alterations over time. These genetic changes involve activation of a proto-oncogene to oncogenes, deregulation or mutation of tumor suppressor genes and DNA repair genes (Ballestar & Estellar, 2008). Thus, cancer development is due to the accumulation of somatic mutations over time. Typically, the mutation rate in humans gets enhanced due to the effect of the following groups of environmental carcinogens i.e. chemical mutagens, radiation, and tumor viruses. The three major processes of carcinogenesis involve (i) malignant transformation, (ii) invasion of neighboring tissues and (iii) metastasis. The normal cells have to undergo these three phases in order to completely transform to a cancer cell (Krakhmal et al., 2015) Each of these stages contains a series of genetic alterations of cells which are relevant to support the individual changes. One of the best-characterized examples of this multistage carcinogenesis is colorectal cancer. Here the sequence of genetic alteration starts with the activation of K-ras oncogenes from its cellular proto-oncogenes followed by the loss of tumor suppressor genes such as APC (adenomatous polyposis coli) and p53. These genetic events result in the formation of carcinoma. During metastasis, the cancer cells initially break off from the primary tumor and migrate to the distant organ site via systemic/lymphatic circulation and subsequently settle there. In order to sustain tumor development, the growth of new blood vessels (angiogenesis) is necessary, which is contributed by different proteins and small molecules such as vascular endothelial growth factors (VEGF) and basic fibroblast growth factors (bFGF) (Luebeck & Moolgavkar, 2002)

Apart from this, crosstalk between the stromal cells within the ECM and tumor cells are vital for malignant transformation. This includes cleavage of matrix component and release of angiogenic as well as proteolytic factors to promote the growth of blood vessels and cancer cell motility respectively (Guan, 2015). Additionally, the stromal cells within the ECM may also directly transmit the release of oncogenic signals to tumor cells. Furthermore, the genetic analysis of solid tumor revealed the occurrence of a high degree of genetic abnormalities such as aneuploidy, chromosome translocations, etc, which also may contribute to the process of carcinogenesis (Grade et al., 2015).

1.3 The hallmarks of cancer

According to Hanahan and Weinberg, cancer develop certain characteristics which they use for proliferation, survival and metastasis which include i) self- sufficiency in growth signals i.e. tumors usually develop the capacity to proliferate without the presence of external stimuli ii) insensitivity to growth –inhibitory signals, i.e., the tumor cells become non-responsive towards inhibitory molecules iii) evasion of apoptosis i.e., the inactivation of p53 and or overexpression of anti-apoptotic proteins make the tumor cells resistant to programmed cell death iv) defects in DNA repair i.e tumor cells may fail to repair the damage caused by carcinogens or unregulated cellular proliferation v) sustained angiogenesis i.e., the growth of tumour cells is due to the formation of new vascular growth vi) ability to invade and metastasis, i.e., the vast majority of cancer death is due to tissue invasion and metastasis which depends on processes that are intrinsic to the cell or are initiated by signals from microenvironment (Hanahan & Weinberg, 2011).

1.4. Current treatment of cancer

The appropriate diagnosis of cancer is very essential for an effective treatment because every cancer type demands a specific treatment regimen which includes one or more modalities such as surgery, radiotherapy, and chemotherapy. Also, other treatment options include hormone therapy, immunotherapy, angiogenesis inhibition, hyperthermia and gene therapy (Pérez-Herrero Fernández-Medarde, 2015). Surgery is one of the major options to treat cancer which removes the cancerous tumor that is localized to the specific area of the body. However, alongside other types of treatments such as radiation or chemotherapy may be used before or after the surgery. Chemotherapy is one of the potential treatment options for cancer, which uses anti-cancer drugs to kill cancerous cells and works by interfering with the ability of these cells to grow and divide. Anti-cancer drugs either cause damage to the DNA by various mechanisms during different phases of cell cycle or inhibit mitosis by interfering with microtubules (Mukhtar et al., 2014). Chemotherapy may be used alone in combating some types of cancer or in combination with other treatments such as radiation and surgery. Though chemotherapy can be quite effective in combating cancers, it is highly nonspecific, usually toxic to normal cells and hence there may be many side effects during treatment. Another approach is radiation therapy, which uses particles or beam of energy to kill the cells and is used in several ways depending on the type and location of cancer. It ionizes chemicals within cells and the resultant DNA breakage may be repaired or fixed which lead to apoptotic and mitotic cell death. Hence, radiation therapy is efficient in controlling the progression of cancer and helps relieve its symptoms. This approach provide a cure for cancer, control the disease and help to relieve its symptoms. Recent research reported that almost 50% of patients with newly diagnosed cancers benefit from radiotherapy (Siegel et al., 2016). However radiotherapy is also non-specific and damages the neighboring normal tissues. Hormone therapy is also considered as a treatment option for cancer, where it work to add, block

or remove hormones from the body to slow or stop the growth of cancer cells. This therapy is usually advisable for breast cancer and prostate cancer, where the hormones help in the growth of these cancer cells. Tamoxifen is a medication used in hormone therapy to stop the effect of estrogen on the growth of malignant cells in breast cancer. Recently, U.S. Food and Drug Administration (FDA) approved aromatase inhibitors such as Anastrozole and Letrozole to prevent estrogen production and recurrence of breast cancer in post-menopausal women (Schneider et al., 2011). Immunotherapy is a type of cancer treatment where it boosts the body's natural defenses to fight against cancer. For example, the use of monoclonal antibodies can be used as a targeted therapy to block an abnormal protein in the cancer cell. Apart from this, several nonspecific immune therapies also help the immune system to destroy the cancer cells, which are usually given after or at the same time as another cancer treatment such as chemotherapy or radiation therapy.

Formation of new blood vessels (angiogenesis) help the cancer cells to grow, provide cells with oxygen and nutrients and thus allowing cancer cells to multiply, invade nearby tissue and metastasize. An anti-angiogenic therapy may prevent such growth of cancer by blocking the formation of new blood vessels. The FDA has approved the first anti-angiogenesis drug i.e. Bevacizumab to be used along with chemotherapy in patients with metastatic colorectal cancer (Meadows & Hurwitz, 2012). Another treatment option is hyperthermia, where the cancer tissues are exposed to high temperatures of up to 113^{o}F, where it can kill cancer cells and damage proteins and structures within cells but without affecting the normal tissues. This can also be used along with other treatment ways such as radiation and chemotherapy (Jha et al., 2016).

Gene therapy is a new treatment approach which introduces therapeutic genes into the cancerous cells to compensate for abnormal genes. This approach is currently available as a potential treatment for cancer only through clinical trials. This is a highly flexible approach

because a wide range of therapeutic genes can be introduced to the cancer cells using suitably modified vectors.

1.5 Gene therapy

Gene therapy is the use of genes to treat diseases. As such, it holds great potential to cure a wide range of diseases such as cystic fibrosis, heart disease, diabetes, cancer and blood diseases (Collins & Thrasher, 2015). Basically, gene therapy correct a defective gene by using either of the four approaches i) the insertion of a normal gene into a nonspecific location within the genome to replace a defective gene (most common approach) ii) swapping an abnormal gene for a normal one via homologous recombination iii) the repairing of an abnormal gene through selective reverse mutation iv) alteration (degree to which a gene is tuned on or off) in the regulation of a particular gene. There are two types of gene therapy, germline and somatic. In the former type, the gene is transferred to the germ cells and hence the changes are heriTable whereas, in the latter, the introduction of the therapeutic gene is into the somatic cells and hence not heriTable. The delivery of a gene is carried out with the help of carriers called vectors and is of two kinds i.e. viral and non-viral vectors. In the case of viral vectors, the capabilities of viruses to encapsulate and deliver genes to human cells in a pathogenic manner have been exploited where the viral genome are modified and replaced with therapeutic genes. Retrovirus, adenovirus, and adeno associated viruses are suitable and widely used for gene therapeutic approaches. On the other hand, non-viral vectors use cationic polymers and lipids as gene carriers where their efficiency is lower than viral vectors but have the advantage of low immunogenicity and large DNA carrying capacity.

1.5.1 Cancer gene therapy

Current cancer treatments often kill healthy cells and cause toxicity to the patients. Hence the development of treatment modalities which can passively or actively target cancerous cells would always be desirable. The cancer gene therapy offers several potential treatment options because it introduces therapeutic genes into the cancerous cell either to attenuate or override the influence of a malfunctioning gene. Cancer gene therapy basically focuses on three major areas which involves i) to turn off oncogene expression ii) enhance the activity of tumor suppressor genes and iii) to stimulate the immune system against tumor cells (Morris & Chan, 2015). However, a successful translation of this treatment modality into the clinical use often is limited by lack of safe and efficient carrier system.

There have been three different approaches applied to gene therapy and the initial approach, which is the simplest one is the direct injection of free DNA to the tumor site which has shown to produce high levels of gene expression (Hickman et al., 1994). However, this method is restricted to tissues which are easily accessible for direct injection such as skin and muscle and is unsuitable for systemic delivery. This is due to the fact that size, shape, poly-anionic charge of DNA and the serum nuclease activity form a greater barrier which inhibits the systemic administration of the free DNA (Adjei et al., 2014). This has led to the advent of the second approach which is the use of viral vectors as gene transfer vehicles where genetically altered viruses act as gene carriers. The viral vectors are generated by selectively deleting the essential genes in virus genome which allow replication, assembling or infection, and replace it with therapeutic genes. Viral vectors` efficiently carry the modified genome from one host to another, navigate to the cell nucleus and initiate expression of its genome. Viruses such as adenovirus, lentivirus, retrovirus, adeno-associated virus, and herpes simplex viruses can be utilized this way to transfer genetic materials precisely to the host cell by eliminating the possibilities of virus-mediated toxicity (Bouard et al.,

2009). Although viruses used as vectors are transformed into non replicative and nonpathogenic carriers, there are still chances that virus reverts back to the original wild-type virion. Furthermore, they are inherently immunogenic which restricts repeated administrations. Other challenges include lack of target cell specificity and cost of manufacturing viral-based gene therapeutics (Kotterman et al., 2015). These limitations on viral vectors have encouraged researchers to focus on the third approach i.e non-viral vectors. These are mainly cationic polymers and cationic lipids that electrostatically interact with DNA and condense the genetic materials into particles of few tens to hundred nanometers in diameter. Such complexes with cationic lipids and polymers are known as lipoplexes and polyplexes respectively. These nanocarriers have several advantages over viral vectors such as low immunogenic response, capacity to carry large inserts and possibilities of selected modifications. Though transfection efficacy was found to be lower than that of viral counterparts, ease of surface modifications and attachment of ligands to the polymer surface improve the utilization of the non-viral delivery system for systemic application (Yin et al., 2014). Currently, non-viral vectors are considered the most promising gene delivery system and research is now underway in the development of biocompatible vector that can deliver foreign genetic material with transfection efficiency equivalent to viral vectors.

The p53 tumor suppressor gene plays an important role in maintaining genetic heterogeneity in somatic cells. The functional incompetence of p53 destabilizes the genome and quickly leads to cancer. The introduction of wild-type p53 to the cancer cells prevent the progression of cancer by either arresting the cell cycle or leading to apoptosis (Mendoza-Rodríguez & Cerbón, 2001). There are several reports on the use and intracellular delivery use of p53 as a therapeutic gene. Lee *et al*., (2011) reported the delivery of p53 plasmid in a targeted manner using, poly-l-lysine where it was complexed along with two specific peptides. One of which corresponded to the epidermal growth

factor region binding to epidermal growth factor receptor (EGFR) and another to the hemagglutinin glycoprotein region in the membrane. This complex preferentially bound to the hepatic cancer cells and facilitated the release of DNA complexes from the endosome, which ultimately suppressed the growth of human tumors in athymic mice (Lee et al., 2011).

1.6 Polymeric nanocarriers

Many types of polymers have been designed specifically for gene delivery. Mostly, the polymers were designed to address specific hurdles in the intracellular as well as extracellular compartments. The polymeric gene carrier provides protection from the DNases and prolongs the bioavailability of the protected DNA. Most widely reported polymeric non-viral gene delivery vectors include synthetic polymers such as polyethyleneimine (PEI), poly-l-lysine (PLL) and PAMAM. Similarly, the natural polymers investigated for gene therapy include chitosan, collagen, gelatin, alginate, and their modified derivatives (Yin et al.,2014). Among this, chitosan is the most extensively studied natural polymers. However, many factors affect the transfection efficacy of the cationic polymers which include molecular weight, surface charge, charge density, hydrophilicity and the structure of cationic polymers (Hardee et al., 2017).

1.6.1 Barriers for gene delivery

In order to transport genes to the cell nucleus, vectors need to navigate a series of obstacles, both extracellular and intracellular. Unlike viruses, polymeric vectors usually lack one, or several of the necessary functions to address these challenges. For treating a disease like cancer, therapeutics needs to be administered systemically and target specifically to the affected cell. The carrier has to be in the systemic circulation for longer duration without being degraded or removed by the body's defense mechanism. Once in the tumor site, following cellular internalization, there

are further additional obstacles such as endosomal escape, cytoplasm trafficking and nuclear entry that can affect the efficiency of gene delivery system.

1.6.2 Gene packaging

The fundamental design criterion for any gene delivery vector is the ability to neutralize the negatively charged DNA to prevent charge repulsion against anionic cell membrane surface and protect it from the extracellular and intracellular nuclease action. Complexation of DNA mediated by the electrostatic interaction between the positively charged polymer and negatively charged DNA leads to neutralization and compaction of DNA to the small nano-sized structure. This structure further facilitates the easy cellular internalization of nanoplexes into the cell. The process of polyplex formation is entropically driven and each polyplex consists of several DNA molecules along with many polymer chains (Visiliu et al., 2017). An ideal gene delivery vector must balance a sufficient binding strength to initially protect the gene in the extracellular circulation and on the other hand, possess the ability to release plasmid in the cytosol.

1.6.3 Serum stability

Stability of nanoplexes in the circulation is another important criteria for a successful gene carrier vector. The stability is initially governed by the polymer structure and DNA to polymer charge ratio. Neutral polyplexes in the physiological conditions can be ineffective and usually is toxic due to embolization of particles in the lung (Pack et al., 2005). On the other hand, positively charged polyplexes usually invite adsorption of plasma anionic proteins onto the surface which leads to the rapid clearance of polyplexes by the phagocytic cells and reticuloendothelial system. However, the modification of polyplexes with hydrophilic polymers such as polyethylene glycol (PEG) and N-(-2-hydroxypropyl) methacrylate (HPMA), can stabilize polyplexes against interaction with plasma protein and prevent complement activation (Allmeroth et al., 2013).

1.6.4 Intracellular barriers

Once the vector is at the tumor site, the gene delivery vehicles are challenged with new sets of intracellular obstacles and the vector needs to provide specific functionality to overcome each one of it. Usually, polyplexes are internalized by endocytosis, and the endosomes are ultimately trafficked to lysosomes which are acidic vesicles filled with degradative enzymes. The nanoplexes need to escape from these vesicles to reach the cytoplasm for reaching the nucleus. At some point of the transport from cytoplasm to nucleus, the vector must release the DNA, translocate to facilitate transcription in the nucleus (Khalil et al., 2006)

1.6.5 Endolysosomal escape

The predominant way of entry of polyplexes is either via clathrin mediated, caveolae mediated or adsorptive pinocytosis because of the interaction between positively charged polyplexes and negatively charged glycoproteins, proteoglycans, and glycerophosphates in the cell membrane (Rejman et al., 2005). Generally, polyplexes are trafficked into late endosomes where the vesicles are rapidly acidified to Ph (5-6) due to the action of ATPase pump in the membrane, which is subsequently trafficked to the lysosome for degradation. Several strategies have been adopted to overcome this barrier (Akinc et al., 2005). Polymers such as polyethyleneimine (PEI) and polyamidoamine (PAMAM) possess 'proton sponge' effect to escape from the endosome to the cytosol. These polymers contain a large number of secondary and tertiary amines and therefore undergo substantial changes in protonation during endocytic trafficking. It prevents acidification of endocytic vesicles and causes the accumulation of protons which in turn is balanced by the influx of counter ions. The increase in ion concentration ultimately results in the osmotic swelling and rupture of the endosome membrane, this lead to the release of polyplexes into the cytosol. Also, treating the cells with chloroquine at the time of transfection are also known to buffer the

endosomal pH, resulting s in improved gene delivery with some polymers. However, this method is impractical for *in vivo* gene delivery applications (Singh et al., 2015).

1.6.6 Transport through the cytoplasm and nuclear localization

Another hurdle following endosomal escape is the movement of nucleic acid through the cytoplasm and entry into the nucleus. The mobility of large molecules such as DNA is extremely slow in the cytoplasm and also the DNA is susceptible to the cytoplasmic nuclease enzyme. Thus, DNA has to be both protected and also available to enter into the nucleus. Since the DNA is complexed with the polymer, the compaction leads to the increased cytoplasmic mobility and increased stability from the cytoplasmic nucleases. The movement of polyplexes in the cytoplasm is also involves the presence of microtubules where it aid its movement towards the nucleus. It is observed that the plasmid which is directly injected into the cytoplasm is poorly expressed in contrast to those that are directly microinjected into the nucleus (Bremner et al., 2004). These results indicated that the entry to the nucleus is another important barrier for successful gene transfection. The nuclear pore complex (NPC) present in the nuclear membrane allow the passage of molecules up to 9 nm in size (40-60kDa) only and the larger macromolecules require active transport via specific nuclear import proteins (e.g., importins). The polymeric nanocarriers cannot pass through the nuclear membrane as such because it cannot cross the NPC. Hence it relies largely on the nuclear membrane breakdown during cell division for nuclear entry. As such, transfection immediately before cell division is 30-500 times more effective in cells than nondividing cells. Many proteins which are targeting to the nucleus have a small cationic peptide sequence at the N- terminal end called nuclear localization signals (NLS), which can be easily recognized by the protein, importin and facilitates its nuclear entry. It is reported that polyplexes which are also cationic in nature could possibly mimic like NLS to a limited extent (Haberland

& Böttger, 2005). However, this assumptions has turned out to be wrong due to the fact that only a very few polymeric vectors typically reach the nucleus and hence cannot make a generalized statement. Sometimes, the nucleotide sequence in the gene itself could provide nuclear targeting (Young et al., 2003), but the exact mechanism of nuclear entry is yet to be elucidated.

1.7 Redox-sensitive polymers

Recently, reduction sensitive bioreducible polymers have emerged as a promising system for gene delivery applications. The redox-sensitive polymers are designed by incorporating disulfide linkages in the main chain or side chain of the polymer and/or as a crosslinker between two polymers (Gyarmati et al., 2013) The characteristics of redox-sensitive polymers are distinct from other polymeric carriers in terms of the its stability in circulation and extracellular fluid but rapid degradation under reductive environment inside the intracellular compartments. The reductive environment inside the cell is maintained by the high concentration of glutathione (2-10mM), which is almost 1000 times higher than its level in the extracellular medium (Forman et al., 2009). The difference in the reductive environment between both these compartments is utilized in the intracellular delivery of DNA, siRNA, proteins and antisense oligonucleotide (Son et al., 2012. Furthermore, tumor tissue contains at least four-fold higher concentration of glutathione compared with normal tissues, rendering the redox-sensitive polymers suitable for tumor-specific drug and gene delivery. The ease of degradation of bioreducible polymer results in minimizing the toxicity related to the accumulation of high molecular weight polycations and also facilitate enhanced transfection efficacy by the intracellular release of DNA or siRNA inside the cancer cells (Kim & Kim, 2011).

1.8 Multidrug resistance in cancer (MDR)

Chemotherapy is the most potent treatment options for cancer. However, the development of multidrug resistance (MDR) to chemotherapy remains a major challenge (Gillet & Gottesman, 2010). MDR is a phenomenon whereby the tumor cells show resistance to a wide range of structurally and functionally unrelated compounds. It can result from numerous mechanisms. One of the major reasons for MDR is the overexpression of efflux pump (P-gp) in the cancer cells resulting in the active effluxing of anticancer drugs from within the cells (Breier et al., 2013). Alternatively, resistance can also occur due to the reduced drug influx and also enhanced activation of proteins such as cytochrome P450 oxidases which carry out detoxification of anticancer drug and subsequent removal of chemotherapeutics from the cells. Concurrently, the enhanced activation of DNA repair enzyme also contributes to drug resistance. Finally, cancer cells become resistant to drug-induced cell death due to defective apoptotic pathways. This is largely due to non-functional p53 and alteration of ceramide (an apoptotic second messenger) level in tumor cells (Sleiman et al., 2013). Any populations of cancer cells which are exposed to chemotherapy often possess more than one mechanism of multidrug resistance because of the genetically heterogeneous nature of cancer cells.

1.8.1 ATP dependent transporters (efflux pump)

The drug efflux pump proteins are members of ATP binding cassette (ABC) superfamily, which include P-glycoprotein (P-gp/ABCB1), MDR proteins (ABCC) and breast cancer resistant proteins (ABCG2). These proteins play a significant role in decreasing the intracellular concentration of chemotherapeutics and are the most common reason for MDR in cancer. Pgp is the most extensively studied member of ABC transporters. It is reported that Pgp expression, whether acquired or intrinsic, plays a significant role in clinical drug resistance in solid tumors (Binkhathlan & Lavasanifer, 2013). P-gp is a broad spectrum multidrug efflux pump consisting

of 12 transmembrane domains with six extracellular loops and two ATP binding site. Many commonly used anticancer drugs such as doxorubicin, vinblastine, etoposide, and paclitaxel as well as many other pharmaceuticals ranging from antiarrhythmics and antihistamines to statins and HIV protease inhibitors are substrates of P-gp (Ganoth et al., 2015). P-gp pump out these drugs as soon as they enter the plasma membrane or even from within the cells. Following the binding of a drug to the ATP binding site of P-gp, a conformational change in the P-gp protein followed by the hydrolysis of ATP occurs, which ultimately result in the release of drug to the extracellular site (Al-Shawi & Omote ,2005). The P-gp is also expressed in the normal tissues such as in the biliary canaliculi of the liver, epithelial transport regions of the small intestine, colon and proximal tubules of the kidney and the adrenal cortex. The activity of P-gp in normal tissues suggests its crucial role in preventing the transepithelial transport of cytotoxic compounds or xenobiotics into the cells. The endothelial cells of capillaries in the blood-brain barrier contain P-gp localized in the luminal surface preventing the penetration of cytotoxins across the endothelium. Similarly, P-gp is also localized on the apical syncytiotrophoblast surface of the placenta where it protects the fetus from toxic cationic xenobiotics (Staud et al., 2010).

1.8.2 P-gp modulators

Many agents were initially developed to modulate P-gp activity which includes verapamil, tamoxifen, cyclosporin A and several calmodulin antagonists. However, the low binding affinity of these agents necessitated the use of high doses resulting in unaccepTable toxicity (Krishna & Mayer, 2000). In fact, this marked the development of the second generation of P-gp modulators, which include dexverapamil, dexniguldipine, valspodar, and biricodar. These agents were more potent than their predecessors. The best characterized and most studied among these agents is valspodar, which inhibit P-gp with 10 to 20 fold greater activity than cyclosporine A. Though these

modulators have a better pharmacokinetic effect than the first generation, they often show limited clinical usefulness. This is mainly due to that fact that these compounds significantly inhibit the metabolism and excretion of cytotoxic agents. For example, the valspodar inhibit the metabolism of paclitaxel and vinblastine (cytotoxic drugs) via blocking the activity of cytochrome P450. This has resulted in the enhanced serum concentration of these cytotoxic agents (Chico et al., 2001). In addition, many P-gp modulators inhibit the activity of P-gp and related transporters in normal tissues which in turn lead to the greater adverse effect of anticancer drugs. For example in bone marrow, the inhibition of hematopoietic P-gp by the modulators increased the cytotoxicity of chemotherapy drugs on the hematopoietic cells (Alfarouk et al., 2015). These observations led to the development of the third generation of P-gp modulators by using structure-activity relationship and combinatorial chemistry methods to overcome the limitations of the second generation of P-gp modulators (Abdallah et al., 2015). These modulators are highly specific and lacked interaction with the cytochrome P450 system which metabolizes the drug to remove from the cell.

1.9 Nanotechnological approach against MDR in cancer treatment

Recently, nanotechnology has emerged as a promising alternative approach to address MDR in cancer treatments. The nanoparticles have the potential to improve the therapeutic index of drugs along with lowering drug toxicity and maintaining the steady state therapeutic levels over an extended period of time (Tran et al., 2017). The versatile surface chemistry of nanoparticles allows the possible conjugation of targeting ligands to facilitate active drug delivery to the tumor site. Apart from this, nanoparticles improve the solubility and stability of the drug. Generally, the mechanism by which nanocarriers to overcome MDR may vary (Zhang et al., 2017). One reported mechanism is the direct inhibition of P-gp by surfactants such as polyethylene glycol, d- alpha tocopheryl polyethylene glycol 1000 succinate (vitamin E TPGS), tween 80 and pluronics (Yang

et al., 2018). Usually, they act indirectly and non-specifically by interacting with the lipid bilayer and affect the fluidity of the membrane. They can also interact with the polar head regions of the bilayer and establish hydrogen bonding with P-gp. Both these activities impair the membrane surface P-gp activities. Pluronics, on the other hand, inhibit the enzyme ATPase by causing the cellular depletion of ATP. This, in turn, leads to inhibition of the efflux pump because the absence of ATP prevents the sensitization and desensitization of P-gp protein which is essential for the working of the pump. Recent studies have shown that the combination of chemotherapeutics with pluronics have effectively lowered the tumorigenic cell subpopulation and decrease tumorigenicity (Alakhova & Kabanov, 2014). Several nanocarriers such as liposomes, polymeric and or metallic nanoparticles have been engineered in such a way to potentially evade the drug efflux pump and thereby enhancing the retention of drug in cancer cells (Yuan et al., 2016). Nanocarriers possess the ability to co-deliver multiple agents such as chemotherapeutics and MDR inhibitors together. In another study, mesoporous silica nanoparticles were utilized for the simultaneous delivery of doxorubicin and Bcl2- siRNA, resulting in 132 fold increase in the cytotoxicity compared with the free doxorubicin alone treatment in ovarian cancer (Wang et al., 2018). Several reports suggested the suppression of MDR1 by siRNA using nanocarriers, which showed the enhanced sensitivity of drugs in resistant cancer cells (Risnayanti et al., 2018; Yang et al., 2015). However, in contrast to chemotherapeutic drugs, a specific siRNA can inhibit only one particular protein and so if several proteins are involved or responsible for drug resistance as commonly seen in many cancers, a single siRNA cannot satisfy the need. Hence, a combination of siRNAs will be required to suppress drug resistance which is not practically possible. A recent study showed an effective alternative strategy where initially nanocarriers loaded with MDR inhibitors were applied to the tumor site which is then followed by the administration of addition of chemotherapeutics, resulting

in the enhanced drug sensitivity of the cancer cells (Glasgow & Chougule, 2015). Unlike ABC transporter inhibitor which can inhibit only one MDR associated gene, nanomedicine is more powerful in terms of suppressing a variety of mechanism and is thus applicable to multiple cancer types having various mechanisms of MDR (Zahreddine & Borden, 2013). Recently thiomers have gained much attention due to its most potent efflux pump inhibitory properties.

1.10 Role of thiomers in inhibiting P-gp

Thiomers are polymers containing a thiol group. Some of the thiomers include anionic thiolated polymers such as poly-(acrylic acid)-cysteine (PAA-cys), carboxymethylcellulose-cysteine (CMC-cys) and alginatecysteine (alg-cys) and the cationic thiolated chitosan such as chitosan-4-thiobutylamidine (CS-TBA),chitosan-thioglycolic acid (CS-TGA) and chitosan-N-acetyl cysteine (CS-NAC) (Dunnhaupt et al., 2012). The efflux pump inhibition of thiomers was found to be significantly higher (2.7 fold) than PEG and or PEG derivatives like pluronics *in vivo* (Foger et al., 2006). There is two proposed mechanism for the inhibition of efflux pump by the thiomers. The membrane P-gp has 12 transmembrane proteins which contain cysteine residues in domain 2 and 11 at positions 137 and 956 (Laffleur & Bernkop-Schnürch, 2012). Thiomers might enter the channel and may establish disulfide bonding with one or more of the cysteine residue of the channel leading to an allosteric change of the transporter and blocking of the drug efflux pump (Laffleur & Bernkop-Schnürch, 2012). Another explanation is the covalent interaction between free thiol group of the thiomer and membrane surface exposed cysteine residues of P-gp, thus changing the conformation of P-gp and impairing the drug efflux processes. Many studies on thiomers are currently underway evaluating the efficiency towards P-gp inhibition.

1.11 Glutathione and chemoresistance

Glutathione/glutathione disulfide (GSH/GSSG) forms a major redox couple which determines the antioxidative capacity of the cell. The cytosol contains 2 to 3 orders higher level of glutathione (approximately 2-10mM) compared to the extracellular fluid (2-10μM). GSH level was shown to be elevated in different cancers including bone marrow, breast, colon, larynx, and lungs. This elevated GSH level in the tumor cells forms a major contributing factor to drug resistance. The elevated level of GSH may bind or react with drugs, influence the level of ROS, prevents drug induced damage to DNA or proteins or participate in the DNA repair process (Backos et al, 2012). All these limit the effect of cytotoxic drugs on tumor cells. Overexpression of glutathione-s-transferases (GSTs) together with the elevated level of glutathione increases the rate of detoxification of chemotherapeutic agents and thus reduces its effectiveness. Apart from this, GSTs have shown to interact directly with mitogen-activated protein kinases (MAPK) and apoptosis signal-regulating kinases to prevent the downstream signaling of these proteins. Many anticancer drugs induce apoptosis mainly via activation of MAP kinases particularly c-Jun N-terminal kinase 1 and p38. This control of intracellular signaling pathway by the elevated GSTs alters the intracellular balance of kinases in drug treatment which further is an advantage for tumor growth. Another study reported the reversal of resistance of human ovarian cancer cell line to cisplastin by treating with c-Jun antisense oligonucleotide where c-Jun miRNA controlled the detoxifying enzymes via reducing the GSH level (Pan et al., 2002). Studies on buthionine sulfoximine (BSO), an inhibitor of glutathione and oxothiazolidine-4-carboxylate (OTZ), a stimulator of glutathione were used to determine different chemotherapy responses in normal versus tumor cells *in vivo* (Tagde et al., 2014). These results showed that the depletion of GSH could be used to enhance the drug-mediated cytotoxicity without causing any toxicity to the normal cells. Hence, a combination of inhibitors of GSH synthesis together with the utilization of

chemotherapeutics might be a potential treatment strategy to enhance the effectiveness of the current chemotherapeutic approaches.

1.12 p53 and chemoresistance

The tumor suppressor gene, p53 is the most commonly mutated gene in human cancers which plays a pivotal role in the regulation of cell cycle. In response to the stress condition, p53 bind to DNA in a sequence-specific manner and regulate the transcription of genes involved in mediating key cellular processes such as DNA repair, cell cycle arrest, senescence and apoptosis (Qian & Chen, 2010). Studies on different model system indicated that the reactivation or augmentation of p53 activity in cancer cells either alone or in combination with other therapies could significantly improve the efficacy of cancer treatment (Guo & Cui, 2015). A similar finding was noted in a female patient with the inherited mutated p53 gene, who was experiencing progressive pelvis tumor with metastasis to multiple organs. Following several failed attempts with conventional therapies, she was provided with intralesional injection with replicative defective adenoviral vectors containing human p53 cDNA under the control of the cytomegalovirus immediate-early promoter (Advexin). Following seven days of injection, there was an increase in p53 expression together with the transcriptional target of p53 i.e., p21 with the simultaneous increase in caspase 3 and decrease in the apoptosis inhibitor BCL-2 was noted. The tumor size reduced dramatically (Deng et al., 2017). A positive correlation exists between mutant p53 and chemoresistance in cancer cell to a large number of anticancer agents. It was demonstrated in melanoma cell lines that cell having mutant p53 can cause cross-resistance to numerous cytotoxic drugs whereas the MDR1 expression was significantly reduced in the cells containing wild-type p53 (Hientz et al., 2017). It was also reported that the absence of p53 from fibroblast -in p53 nullizygous mice has been associated with resistance to chemotherapeutic agents such as

etoposide, Adriamycin, and 5-fluorouracil. Majority of studies in the promoter region confirmed a downregulation or suppression of ABCB1 promoter by the wild-type p53 and an upregulation or activation by the mutant p53. However, a more defined analysis of *in vivo* systems particularly direct assessment of p53 mutation in the tumor which shows elevated transporter expression is required to give a more clear indication of the correlation between p53 and drug transporter.

1.13 Hypothesis

Nanocarriers based on cationic thiomers that can act as P glycoprotein inhibitor and also simultaneously deliver the therapeutic gene and the chemotherapeutic drug may be more effective in promoting cancer cell death.

1.14 Aim

The purpose of the study is to synthesize and evaluate the disulphide cross linked pullulan based cationic polymers, to assess its efficiency in gene delivery and efflux pump inhibition.

1.15 Objectives

- Development of cationic pullulan based thiolated nanoparticles using organic compound with different carbon chain length
- Physiochemical characterization of Nanothiolmatrices
- The *In vitro* studies to evaluate its suitability as gene/drug delivery vehicle
- Evaluation of the efficiency of nanothiomatrices in efflux pump inhibition and in *vitro* drug release studies
- The *in vivo* evaluation of the optimized nanothiomatrices

CHAPTER 2 REVIEW OF LITERATURE

2.1 Redox state and redox environment

Energy is required to maintain an ordered state of a living system. Here, the movement of electrons from an oxidizable organic molecule to molecular oxygen through electron transport chain releases energy. This creates an overall reducing environment in the cell. The term redox state is used to represent the energy state of an oxidized and reduced form of a specific redox couple involved in the process of electron transport in the cells (Filomeni et al., 2002). The redox couples found inside the cell include glutathione (reduced)/glutathione (oxidized) (GSH/GSSG), nicotinamide adenine dinucleotide phosphate (NADPH/NADP), thiol/disulfide redox couples i.e thioredoxin-1, TRXred/TRXox and cysteine/cystine (Cys/CySS). Among this, the GSSG/2GSH couple forms a very large pool of reducing equivalents, approximately 500 to 1000 fold higher in concentration compared to TRX and NADPH (Jensen et al., 2009). Glutathione is an important antioxidant and has several roles in regulating protein structure and function, detoxification of xenobiotics, cell proliferation, signaling and apoptosis. The concentration of GSH in intracellular and extracellular compartments varies greatly; with almost 2-10mM in the intracellular region against approximately 2.8μM in the extracellular region (Schafer & Buettner., 2001). These differences in the reducing potential between the extracellular and intracellular milieu can be exploited for triggering the intracellular delivery of a variety of bioactive molecules such as siRNA, DNA, an antisense

oligonucleotide, proteins, and low molecular weight drugs (Saito et al., 2003). Furthermore, the concentration of GSH in the tumor site is approximately 4- fold higher than in normal tissues, rendering the reducible bioconjugate valuable for tumor-specific drug and gene delivery (Wu et al., 2004).

2.2. Reduction-sensitive cationic polymer for intracellular gene delivery

Among the various multifunctional polymers synthesized for gene delivery applications, redox-sensitive polymers have gained much attention as it responds efficiently to the redox potential gradient that exists between the intracellular and extracellular environment (Son et al., 2012). Two distinct features of bioreducible polymers make it attractive for gene delivery applications which include its reversibility and its stability in plasma. For example, bioreducible polymers form stable complexes with nucleic acid and remain intact in the extracellular milieu whereas it rapidly undergoes oxidation at the disulfide linkages and releases the therapeutic cargoes in the cytosol (Klein & Wagner, 2014). The intracellular degradation of polymer enhances the transfection efficiency. Apart from this, the degradation of the polymeric gene carrier results in the formation of low molecular weight polymers which in turn causes minimal cellular toxicity. Overall, redox-sensitive polymers have all the characteristics of an ideal gene delivery vector and it ensures stability in the extracellular environment and rapid release of therapeutics in the cytosol of the target cells (Klein et al., 2015). The polyplex formation and its subsequent release of DNA into the cytosol is been depicted in Figure 1.

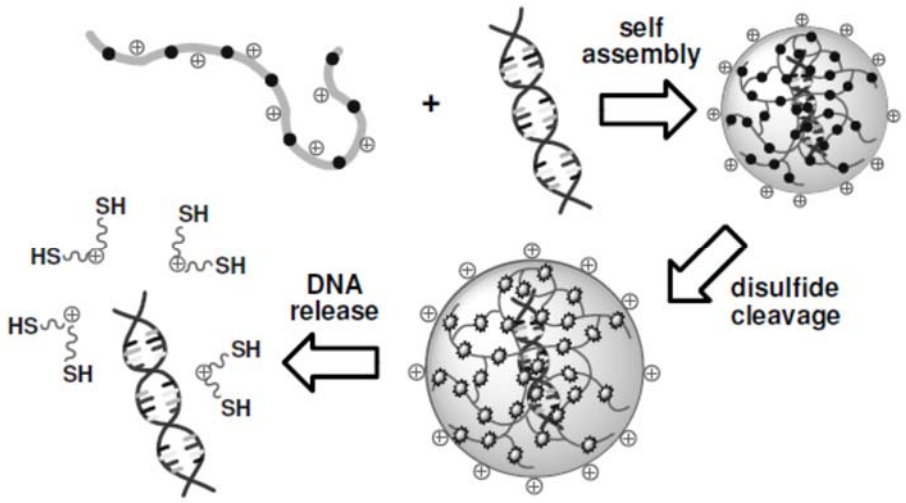

Figure 1: Representation of DNA binding and subsequent intracellular release via disulfide cleavage (Lin & Lou, 2012).

The reduction sensitive cationic polymers can be designed and synthesized, so as to have disulfide bonds either in the polymer back bone or side chain (Ou et al., 2008). The major synthetic routes for developing disulfide cross-linked polymer include

(i) Modification of the polymer chain with thiol containing molecule followed by oxidation of thiol group to form intermolecular linkages.

(ii) Incorporation of disulfide linkages directly into the polymeric backbone

The concept was put forward by McKenzie and colleagues in which a new class of peptide gene delivery agent was synthesized by inserting multiple cysteine residues into short synthetic peptides. The cysteine residue in the peptide chain (substitution of one to four cysteine residue for lysine residue in Cys-Trp-Lys_{18}) spontaneously undergoes oxidation after binding to plasmid DNA to form interpeptide disulfide bonds. The stability of the cross-linked peptide DNA complexes was proportional to the number of cysteines incorporated into the peptides (McKenzie et al., 2000). In another study, Miyata et al synthesized bioreducible polymer by thiolating poly(ethylene glycol)-poly(L-lysine) (PEG-PLL) block polymer with either of two thiolating agents i.e succinimidyl 3-

(2-pyridyldithio)propionate (SPDP) and 2-iminothiolane (Traut's reagent). Both methods were efficient in introducing disulfide linkages to the polymer and the polyplexes have remained stable in the oxidative extracellular environment. It showed higher stability in the circulation and achieved superior gene transfection efficiencies (Miyata et al., 2004). Zugates et al synthesized poly (β amino esters) using the primary amine monomer, 2-(pyridyldithio)-ethylamine (PDA). The pyridyldithio groups in the side chain display selective reactivity with thiol ligands. This property of the PDA based PAE led to the conjugation of cell targeting peptides or ligands for site specific delivery. The thiol reactivity has been demonstrated by binding the PDA PAEs with mercaptoethylamine (MEA) and or the thiol peptide RGDC, the ligand specific for integrin receptor in the cell. Both MEA and RGD based polymer derivatives formed smaller size (approximately 100nm) and exhibited strong DNA binding ability. At the same time, it displayed rapid degradation and release of DNA in response to intracellular glutathione. The polymer also exhibited low cytotoxicity and higher transfection efficiency as compared to PEI in human hepatocellular carcinoma cells (Zugates et al., 2006).

In another study, bioreducible cationic polymers are synthesized by the poly oxidation of dithiol-based monomers containing amino groups. You et al described the preparation of dithiol based poly (2-dimethylaminoethyl methacrylate) (PDMAEMA) oligomers via reversible addition-fragmentation chain transfer (RAFT) polymerization. Here, initially, oligomers of 2-dimethylaminoethyl methacrylate (DMAEMA) containing terminal thiol groups were synthesized by RAFT polymerization and then proceeded with the formation of reducible PDMAEMA by oxidation of the terminal thiol groups, resulting in a polymer with disulfide bonds in the backbone. The polymer showed reduced cytotoxicity and improved transfection activity compared to the non-reducible counterpart (You et al., 2007). Similarly, in another study, reductively cleavable

polycations was synthesized by the oxidation of terminal cysteinyl thiol groups of Cys (Lys) 10Cys. This was then surface cross-linked by using multivalent reactive copolymers of N-(2-hydroxypropyl) methacrylamide (PHPMA) to promote extended circulation in the blood stream. The oxidation was carried out by adding DMSO (Oupicky et al., 2002). This method ensured stability in the extracellular milieu and also exhibited enhanced transgene expression. However, the preparations of these dithiol based oligoamines are time-consuming, and these compounds cannot be stored for a long time due to oxidation of thiol groups by air. A simple alternative approach is the direct addition of disulfide-containing reagent to the polymer backbone. Gosselin et al developed low molecular weight PEI via cross-linking with dithiobis (succinimidyl propionate) (DSP) and dimethyl 3,3 dithiobispropionimidate 2HCl (DTBP) reagents. Both react with the primary amine groups of PEI to form the reducible PEI. The transfection efficiency of these two PEI derivatives was determined in CHO cells. The level of transfection was dependent on various aspects like cross-linking agent, the extent of conjugation and N/P ratio. Though the transfection efficiency was not comparable to PEI, the cytotoxicity was reduced remarkably (Gosselin et al., 2002). Similarly, disulfide containing poly (amido amines) (SS-PAA) was synthesized by the Michael type addition reaction of cystamine bisacrylamide (CBA) to primary, secondary or tertiary amines and bisacrylate monomers. Most of the SS-PAAs exhibited high buffering capabilities at the pH range of 5-7 compared to that of PEI (25kDa). The SS-PAAs form stable complexes on binding with plasmid DNA and rapidly undergo destabilization in presence of 25mM DTT. The structural effect of these PAAs in terms of gene delivery properties was systematically evaluated. It was observed that SS-PAAs containing histidine (HIS), 4-amino-1-butanol (ABOL), 4-amino-1-pentanol (APOL) and 3-methoxypropylamine (MOPA) exhibited high transfection efficiency in COS-7 cells compared to branched-chain PEI (Lin et al., 2007).

The transfection efficiency was based on hydrophobic nature which is in the order of pAPOL>pABOL>pMOPA. Likewise, a number of reducible cationic polymers have been designed that are capable of overcoming gene delivery barriers and leading to detectable gene transfection efficiency (Hoon et al., 2007; Brumbach et al., 2010; Ping et al., 2013). However, both steric hindrance due to the presence of disulfide linkages in the polymer and microenvironment of the disulfide-containing molecules affect the responsiveness of the disulfides to biological stimuli. Hence it is essential to investigate further to ensure the extent of disulfide exchange that occurs within the biological system in both *in vitro* and *in vivo* conditions.

2.2.1 Bioreducible polyethyleneimine

Polyethyleneimine is known as the gold standard for gene delivery applications, and in recent time, the incorporation of disulfide linkage in PEI has drawn enormous attention. Lee et al. reported that cross-linking of PEI with disulfide-containing linkers such as DSP, DTBP, leads to a significant increase in the transfection efficiency. The intracellular reduction of polyplexes by GSH facilitates dissociation of PEI from DNA to enhance the gene expressions (Lee et al., 2007). Similarly, Han et al.cross linked 1800 Da PEI using DTBP. Though the cross-linked PEI/DNA complexes of N/P ratio 10 revealed reduced cytotoxicity and easy unpacking at 3mM GSH compared to PEI 25kDa, it showed poor transfection efficiency (Han et al., 2009). Peng and colleagues prepared disulfide cross-linked PEIs via two approaches such as by thiolation of 800 Da bPEI with methylthiirane at different ratios followed by oxidation and via Michael addition polymerization between cystamine bisacrylamide CBA and 800 Da bPEI (Peng et al., 2009). *In vitro* experiments showed that disulfide cross-linked PEI possess a lower cytotoxicity and comparable or higher transfection efficiency than the 25kDa PEI. It was also observed that fetal bovine serum did not decrease the transfection efficiency. In another study Choi et al reported that

the endosomolytic protein listeriolysin O (LLO) from the intracellular pathogen Listeria monocytogenes conjugated with bPEI via a reversible disulfide linkage to form LLO-SS-PEI could enhance transfection efficiency of the polyplexes (Choi et al., 2009). Breunig and coworkers demonstrated the cross-linking of LMW linear PEI with dithiodipropionic acid or cysteine linkages which resulted in a branched structure. The *in vitro* transfection experiments conducted in seven different cell lines showed superior transfection efficacies and lower cytotoxicities compared to commonly used nonviral commercial transfection agents such as SuperFect, Lipofectamine, and JetPEI (Breunig et al., 2012). In another study, Park et al. designed a reducible linear PEI i.e poly (ethylene imine sulfide) (I-PEIS) with the molecular weight ranging from 10,000 to 20,000 Da by oxidative polycondensation of bismercapto ethylene imine oligomers. The transfection efficiency of I-PEIS was similar to that of 25kDa PEI. In comparison with ExGen 500, a commercial *in vitro* transfecting reagent, I-PEI exhibited low cytotoxicity and was completely degraded inside the cell within 3h. In another study by Carlisle et al, PEI/DNA complexes were coated with poly [N-(2-hydroxypropyl) methacrylamide] (PHPMA) through reducible disulfide linkage between PEI and hydrophilic PHPMA. The resulting complexes were stable and complete release of DNA was attained by the addition of 20mM DTT. The disulfide-linked complexes showed 40-100 fold higher transfection than the corresponding thioether linked counterparts. Hence the hydrophilic polymer coating using reducible disulfide bond represents an efficient strategy to simultaneously fulfill the contradictory requirements for extracellular stability and intracellular release of DNA (Carlisle et al., 2004). Bonner et al prepared 25 kDa bPEI/DNA polyplexes cross-linked with low molecular weight cross-linking agent dithiobis (succinimidyl propionate) (DSP) containing disulfide bond. As compared to the non-cross linked counterpart, it demonstrated increased colloidal stability and reduced interaction with blood components such as albumin and RBCs. The

in vitro experiments demonstrated that the polyplexes were efficiently taken up by the cells and released DNA in response to the intracellular reduction potential and by the addition of 15mM DTT to the transfection medium. The *in vivo* studies in mice also revealed elevated levels of the DSP cross-linked polyplexes in blood, confirming its improved stability in circulation. Furthermore, these polyplexes also exhibited enhanced liver targeting (Bonner et al., 2013). Kim et al. developed polymeric gene carrier with multifunctional properties by prethiolation of LMW PEI with propylene sulfide mixed with R-maleimide-ω-N-hydroxysuccinimide ester PEG (MAL-PEGNHS, Mw: 5 kDa) and cyclic NGR (cNGR) peptide. Further, GSH mediated reductive cleavage of disulfide linkage resulted in an efficient release of pDNA leading to enhanced transfection efficiency in HT1080 cells (Son et al., 2013). In another experiment, PEI-SS polymer in combination with RVG peptide and mannitol successfully delivered neurogenic miRNA into the brain which displayed high efficacy due to the *in vivo* neuron-specific targeting (Hwang et al., 2011). To further enhance the stability of PEI polyplexes in circulation, a combined strategy of PEGylation and reversible surface cross-linking was adopted. PEI has been modified with one or two high molecular weight PEGs (20 or 30kDa) to obtain PEG-PEI diblock or PEG-PEI-PEG triblock type copolymer with DSP. The combined vector showed the synergistic effect by prolonging the blood circulation of the polyplexes *in vivo* (Zhong et al., 2005).

2.3 Thiomers and efflux pump inhibition

Multidrug drug resistance (MDR) is a major obstacle to the successful treatment of local and metastatic cancer. Cancer cells become resistant to the anticancer drug by several mechanisms. Typically, most of the drug molecules diffuse through the cell membrane to enter the cytoplasm where the presence of P-gp in the cancer cell membrane actively transports these drugs out of the cell. This, in turn, leads to low cytosolic as well as nuclear drug concentration. Apart from P-gp

overexpression, several other factors also contribute to the drug resistance in cancer cells which involves i) enhanced activation of DNA repair mechanism ii) activation of detoxifying enzyme (e.g P450 cytochrome oxidase) to change drug metabolism iii) decreased drug influx iv) gene amplification and mutation of target proteins and v) alteration in the apoptotic signaling pathway (Gottesman et al., 2002) (Figure 2).

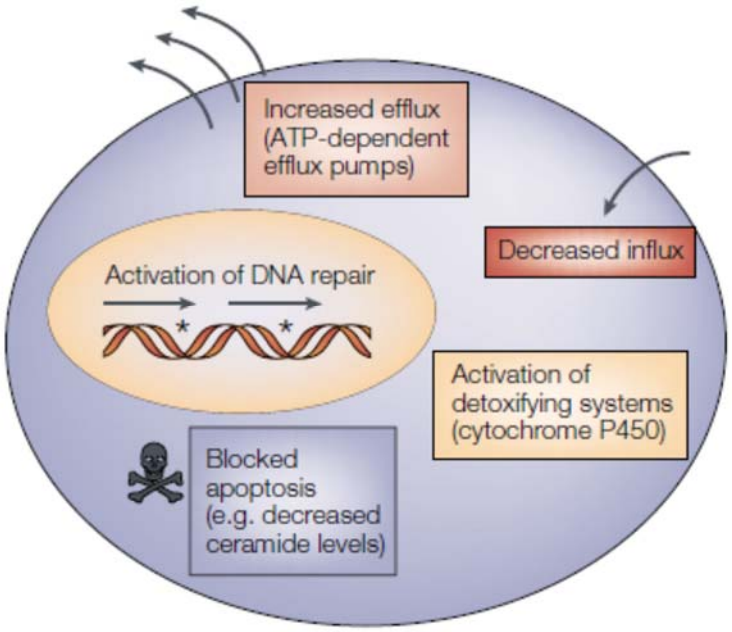

Figure 2: Cellular factors that contribute drug resistance (Gottesman et al., 2002)

Many anticancer drugs such as bisantrene, daunorubicin, docetaxel, doxorubicin, epirubicin, etoposide, idarubicin, methotrexate, mitoxantrone, paclitaxel, teniposide, vinblastine, and vincristine are substrates for various efflux pump transporters. The current pharmacological approaches include co-administration of anticancer drug and efflux pump inhibitor. However, the nonspecific nature of these inhibitors, inherent toxicity and pharmacokinetic interaction with the anticancer drug made it unsuccessful in clinics (Baguley, 2010). At this point, nanocarriers have several advantages because it prolongs the circulation time of drugs and causes selective accumulation of anticancer drugs at the tumor site. Most of the anticancer drugs are small and

hence it can easily passes across the cell membrane where it is largely available for membrane effluxing by P-gp. On the other hand, nanoparticles are too large for diffusion processes across the membrane, hence these particles are carried via the process of endocytosis and accumulate deep into the cell near the nucleus and hence it is unavailable for membrane P-gp activity. (Xiaowei et al., 2010). This enables the nanocarriers to bypass the drug efflux pump and hence leading to enhanced retention of anticancer drugs. A study by Cuvier et al showed that DOX-loaded nanospheres could able to circumvent MDR via bypassing P-glycoprotein and could deliver a high concentration of drug to the cytosol and nucleus (Cuvier et al., 1992). It is well established that active targeting could enhance intracellular drug delivery. In this line, Elbayoumi and co-workers modified the DOX-loaded PEGlyated liposomes (Doxil) with mAb 2C5 (nucleosome specific monoclonal antibody 2C5) and observed an enhanced nuclear drug accumulation and drug-related toxicity compared to the control in DOX-resistant colon cancer cell line (Elbayoumi & Torchilin, 2007). Recently, several studies have shown inhibition of P-glycoprotein in cancer cells by selectively inhibiting the expression of P-glycoprotein using siRNA and or antisense oligonucleotide (AON) (Abbasi et al., 2013; Yin et al., 2012; Yang et al., 2016). These approaches have demonstrated an increase in the accumulation of chemotherapeutic drugs in the cytosol and have improved anti-tumor efficacy *in vivo*. Though the inhibition of P-gp via siRNA and AON are found effective, it is always important to confine its delivery in tumor tissues in order to prevent its action in the normal healthy cells where P-gp play important physiological functions. However, it is always desirable if the polymer itself has the potential to directly inhibit efflux pump and influence its activity. A few examples which can directly modulate P-gp include α-tocopheryl PEG1000 succinate, non-ionic PEO-PPO-PEO block copolymer, namely Pluronic® P85, Poly(styrene oxide)–poly(ethylene oxide) triblock copolymers, low molecular weight methoxy

polyethylene glycol-bpoly(epsilon-caprolactone) diblock polymer and thiomers. Batrakova et al reported that amphiphilic triblock copolymers of poly (ethylene oxide) (PEO) and poly (propylene oxide) (PPO), PEO-b-PPO-b-PEO (Pluronic) is very effective in sensitizing cancer cells to the antineoplastic agent (Batrakova et al., 2010). Pluronics indirectly influence the activity of MDR mainly by two processes such as intracellular depletion of ATP and inhibition of ATPase activity of drug efflux proteins.

Thiomers (thiolated polymer) are considered to be the most potent polymeric efflux pump inhibitors. It is reported to have a 2.7 fold higher effect *in vivo* than PEG and or PEG derivatives such as pluronics P85 (Foger et al., 2006). Unlike other efflux pump inhibitors such as pluronic P85, 6-mercaptopurine, Myrj52, the inhibitory effect of thiomers are completely reversible. Rehmat et al. synthesized hydroxyethyl cellulose (HEC) containing cysteamine as thiol-bearing compound and observed a significant efflux pump inhibition by using rhodamine 123 as the substrate for P-gp when compared with HEC unthiolated form (Rehmat et al., 2012). Schmitz et al. conducted a comparative study of different polymeric and low molecular P-gp inhibitors using rhodamine 123 (Rho-123) as a P-gp substrate and observed a three fold increase in Rho-123 uptake for chitosan -4 thiobutylamidine in combination with glutathione compared to Myrj 52, which showed only 1.8 fold improvement (Schmitz et al., 2007). In another experiment, the potential of thiomers as efflux pump inhibitor was demonstrated *in vivo*, where a significant reduction of tumor growth was observed in rats after oral administration of paclitaxel in combination with thiomers (Foger et al., 2008). Recently, P-gp inhibitory effects were demonstrated using various thiomers both *in vitro* and *in vivo* conditions (Palmberger et al., 2015; Bonengel S & Bernkop-Schnürch A, 2014). The mechanism of action is based on the interaction of thiomers with channel forming the transmembrane domain of P-gp. Two of the transmembrane domain i.e. 2 and 11 have cysteine

residues at position 137 & 956 respectively. Thiomers may enter the channel and subsequently binds with one of the two cysteine residues in the channel. Due to this covalent interaction, a conformational change occurs in the P-gp transporter and which in turn block the active effluxing of anticancer drugs (Figure 3).

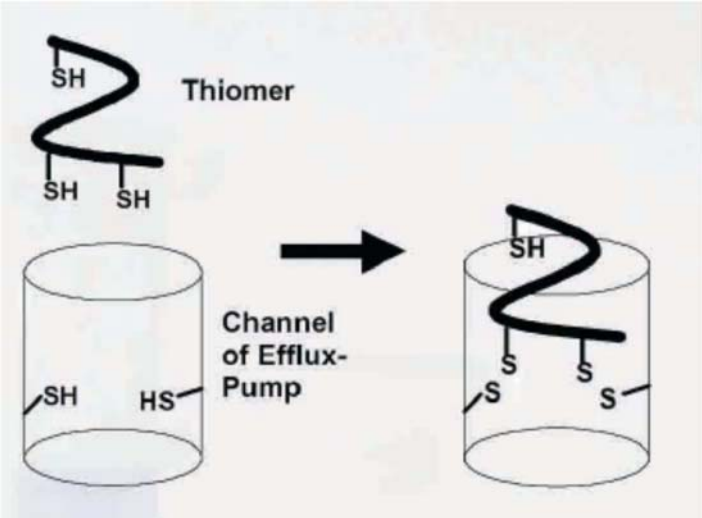

Figure 3: Postulated mechanism of efflux pump inhibition by thiomers (Bernkop et al., 2006).

Apart from this, the thiomers can also form both inter and intra disulfide linkages within thiomers and or with the mucus glycoprotein which result in the enhanced mucoadhesive properties, prolonged disintegration time and control release of drug (Laffleur F & Bernkop-Schnürch A, 2012).

Furthermore, thiomers also have permeation enhancing effect via GSH mediated mechanism and enhances the uptake of hydrophilic macromolecules from the GI tract. Iqbal et al. demonstrated an oral delivery system based on the combination of chitosan-TGA and GSH, which showed enhanced plasma level and increased bioavailability of leuprolide up to 10 fold, indicating the efficacy of thiomer mediated oral delivery system (Iqbal et al., 2012). Similarly, Thierry et al developed thiomers based gene delivery system i.e chitosan-thiobutylamidine. It was demonstrated that chitosan-thiobutylamidine-DNA complex was very stable in the extracellular medium

whereas the nanocomplexes dissociated completely in the cytosol and released approximately 50% of pDNA within 3h. This nanocomplex also showed the high transfection efficiency in Caco-2 cells. It was observed that thiomers undergo thiol-disulfide exchange reaction in presence of glutathione in the cytoplasmic reducing environment resulting in the release of pDNA (Schmitz et al., 2007).

2.4 Synergistic drug and gene combination for cancer therapy

Chemotherapy is a standard treatment regimen for metastatic cancer. However, the clinical benefits are limited owing to various reasons discussed in earlier sections. Besides, cancer therapy using a single anticancer agent may not be sufficient due to genetic heterogeneity or complex nature of cancer cells. Recently combination therapy for treating cancer has gained lot of attention and is in practice. The basic concept of the nanobased combination therapy focus to overcome MDR in cancer cells by targeting different biochemical pathways that influences resistance to anticancer therapy (Longley et al., 2005). In combination therapy, co-delivery of different therapeutics targeting diverse molecular mechanism enhances and ensures tumor destruction in a synergistic way while minimizing the chances of drug resistance and reduces overlapping toxicity. The synergistic effect caused by the action of different chemotherapeutics lead to increased tumor inhibition efficacy, increased sensitivity to therapeutics, reduced therapeutic dosage, decreased adverse effect and prolonged survival.

However, the main issue with combination therapy is the high incidence of toxicity due to drug-drug interactions which is estimated to cause approximately 4% of death in cancer patients (Palleria et al., 2013). This is due to the occurrence of harmful dosage of the prescribed drugs in a given patient. For example, the P-gp inhibitors such as valspodar and tariquidar are highly potent and when co-administered with a cytotoxic drug, is very effective in inhibiting P-gp. But none of

these inhibitors are approved by FDA due to undesirable pharmacokinetic interactions between the inhibitors and cytotoxic drugs which further lead to toxicity to normal cells (Jaramillo et al., 2018).

In this scenario, nanocarriers have emerged as an alternative approach to counteract this problem caused by free drug combinations. Nanocarriers provide prolonged blood circulation of drugs, enhanced tumor accumulation of therapeutics via EPR effect, improved intracellular delivery and reduced side effects (Sunoqrot et al., 2014). Furthermore, 'smart' nanocarriers have been designed that are responsive to specific microenvironment in tumor cells such as pH, temperature, enzyme activity and intracellular reducing conditions for improved drug delivery. Detailed understanding of tumor biology, tumor microenvironment and tumor-host interactions has led to the development of new combination therapy i.e chemotherapy along with nucleic acids (DNA & RNA based therapeutics) (Quail & Joyce, 2013). However, the criterion for combined gene/drug delivery is that the nanocarriers are to be inert in nature, non-immunogenic, non-toxic and at the same time effective in condensing nucleic acid and small molecules. In this line, the biggest challenge is the designing of a suitable carrier due to differences in the chemical characteristics of gene and drug i.e most of the drug components are small hydrophobic molecules whereas nucleic acids are high in molecular weight having negative charge. Saad et al have developed a multifunctional nanocarrier consisting of cationic liposome for the co-delivery of siRNA targeted to MRP1 and BCL-2 mRNA (suppressors of the pump or non-pump cellular resistance respectively) and doxorubicin. This provides an efficient method of co-delivery of DOX and siRNA resulting in cell death induction and suppression of cellular resistance in MDR lung cancer cells. This method has demonstrated an enhanced efficiency of chemotherapy to a level that cannot be achieved by applying individual treatment regimen (Saad et al., 2008).

The use of a single carrier for the co-delivery of drug/gene offers several advantages. The main reason is that unlike a separate carrier system for co-delivery of therapeutics, it is easy to synchronize the pharmacokinetics of both agents and ensure the synergistic effect of both in the same cell. Furthermore, it is possible for the tuning of drug and gene concentration in the *in vitro* condition for an optimal *in vivo* dose administration (Sun et al., 2011).

Liposomes are widely used nonviral gene delivery vector for drug and gene transport. Several of the formulations were successful in clinical trials and have got FDA approval. For example, liposomal doxorubicin (Doxil®, JanssenBiotech, Inc.), and PEGylated liposomal vincristine (Marqibo®, Talon Therapeutics, Inc.). The most important characteristic is that liposomes can carry both water soluble and hydrophobic material within a single carrier, where it can entrap hydrophilic component in the aqueous lumen and at the same time carry hydrophobic drugs in the lipid bilayer. The surface charge, membrane fluidity, and permeability can be adjusted by altering the liposome membrane composition. The insertion of cationic lipids such as N-[1-(2,3-dioleyloxy)propyl]-N,N,N-trimethylammoniumchloride (DOTMA) or N-[1-(2,3-dioleoyloxy)propyl]-N,N,N-trimethyl- ammonium chloride (DOTAP) in the liposome formulation make it suitable for nucleic acid binding and hence used widely for the co-delivery of multiple therapeutic agents (Immordino et al., 2006). Despite many efforts to enhance the efficacy of drug and gene co-delivery, the major challenge of liposomal delivery system is its low gene transfection efficacies and so has not reached a level of observable clinical benefit. However, the combination of various factors including the addition of targeting ligands and insertion of the stimuli-sensitive functional group may help to improve the therapeutic outcome of the liposome-based system (Zhu et al., 2013; Han et al., 2013; Ma et al., 2014). Wang et al, demonstrated the co-delivery of anticancer drug and therapeutic gene in a single polymeric micelle carrier, which was named as P

(MDS- co-CES), consisted of a cationic poly (N-methyldietheneamine sebacate) (PMDS) grafted with N-(2-bromoethyl) carbarmoylcholesterol side chains, where paclitaxel was loaded into the hydrophobic core and the gene which is the interleukin 12 encoding pDNA was electrostatically complexed with the cationic polymer. This combination showed greater tumor reduction compared with gene or drug alone in a 4T1 mouse breast cancer model (Wang et al., 2006). Several polymeric systems have been used for the co-delivery of drug and gene, most importantly cationic moieties such as chitosan, PAMAM, arginine/lysine and bPEI (Tang et al., 2014; Zhan et al., 2012; Fan et al., 2012; Seo et al., 2015 ; Li et al., 2015). However, the major hurdle is that the same cationic polymers are required to bind a hydrophobic small molecule drug having different physicochemical characteristics as compared to pDNA. This is because the process of drug loading may require harsh conditions which in turn will destroy pDNA structure (Ma et al, 2013). Therefore the sequence of addition of DNA and drug to cationic polymers are required to be monitored closely to ensure that the process of pDNA condensation occurs under mild conditions. To address this problem, many polymers for co-delivery have been designed as amphiphilic block copolymers, where it can self-assemble in an aqueous medium to form a micellar structure with a hydrophobic core region and a hydrophilic shell (Kakizawa et al., 2002; Zhang et al., 2012; Jhaveri et al., 2014; Tsouris et al., 2014). The drug can be loaded in the core portion and pDNA binds with the hydrophilic shell. The incorporation of targeting ligands on the micelles may increase the delivery into the tumor cell. However, the major disadvantage is that the micellar system are highly unstable which sometimes leads to premature drug release. In order to achieve an optimum hydrophilic/hydrophobic balance in the co-delivery system, additional components of gene binding and neutralization of cationic moieties are required, which is still more complicated.

Although gene and drug delivery using micelles have shown high efficiency, maintaining stable particle properties for *in vivo* applications remains a major challenge.

Another approach is the drug intercalation with the pDNA. Han et al. combined DOX with pTRAIL in a single carrier, where initially the drug and pDNA formed a gene/drug complex, which was then condensed into nanoparticles using cationic polymers. In this study, the cationic polymer was positively charged PEG-modified polyamidoamine dendrimer conjugated to a tumor-targeting peptide. The free drug was released from the polymer-DOX/pTRAIL ternary nanocomplex into the nucleus after unwinding of pDNA. Delivery of DOX and pTRAIL markedly reduced the tumor burden in mice bearing subcutaneous Bel-7402 liver cancer (Han et al., 2011). There is a growing trend in developing stimuli-sensitive polymers for drug and gene co-delivery mainly because it utilizes the small environmental changes to modify the drug release kinetics and biodistributions. For example, Ko et al reported a redox sensitive polymer which consist of polylactide (PLA) block linked to cationic PDMA by a disulfide linkage (PLA-ss-cPDMA) and incorporated DOX and gene in the micelle and the cleavage of disulfide linkage resulted in >80% release of DOX over a period of 10h (Ko et al., 2015).

2.5 Co-delivery of chemotherapeutics and nucleic acid to promote apoptosis

One of the major hallmarks of cancer is its ability to escape programmed cell death or apoptosis. A balanced network of pro-apoptotic and anti-apoptotic gene regulates apoptosis and prevents the progression of precancerous cells to a cancerous cell. However, an imbalance or dysfunction of these genes leads to tumor progression via multiple gene mutations. Thus, co-delivery of apoptotic gene and apoptosis-inducing anticancer drug to the cancer cells is a good strategy to avoid tumor recurrence and relapse (Wendel et al., 2004). Many cancer cells show a deficiency in p53 activity which in turn fails to activate apoptosis and cell cycle arrest leading to

tumor progression. Also, loss of function of p53 results in the reduction of the therapeutic effect of many chemotherapeutic drugs (Heintz et al., 2017). Ganjavi et al. reported that treatment with wild-type p53 using adenovirus vector significantly increases the sensitivity of osteosarcoma cell line to chemotherapeutics like cisplatin and DOX (Ganjavi et al., 2015). Xu et al. demonstrated that simultaneous delivery of the p53 encoding plasmid along with DOX in a double-walled microsphere improved the activity of the drug (Xu et al., 2012). Liu et al. demonstrated that the delivery of DOX with TRAIL gene in a dendrimer carrier system showed a significantly improved therapeutic effect with delayed tumor progression and prolonged survival time in a tumor-bearing mice model compared to monotherapy using DOX or TRAIL alone (Figure 4.)

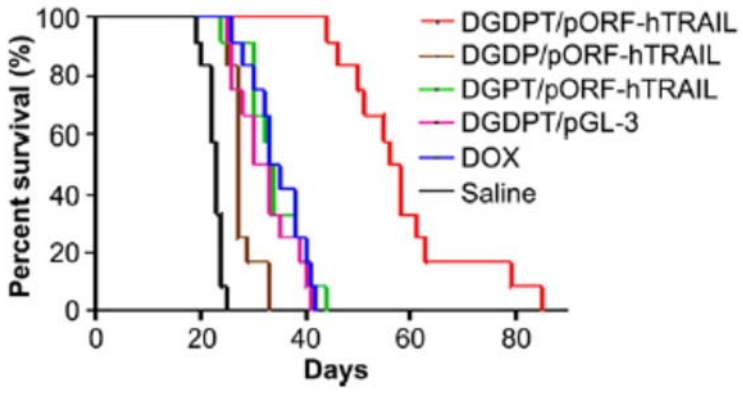

Figure 4: Antitumor activity of mice containing orthotopic U87 tumor using DOX and TRAIL in a dendrimer based delivery system. Survival curves are shown for mice treated with DOX conjugated dendrimer (DGDPT) complexed with TRAIL plasmid DGDPT/pORF-hTRAIL, DGDPT/pGL-3 co-delivery system containing a control Luc gene (pink line), DGDP/pORF-hTRAIL without targeting ligand peptide (brown line), and TRAIL gene monotherapy DGPT/pORF-hTRAIL using DOX-free vector (green line) (Liu et al., 2012).

Similarly, Bao et al. recently developed a multifunctional copolymer conjugate chitosan-graft-polyethyleneimine-candesartan (CPC), which included anti-angiogenesis drug, candesartan (CD) bound with an amide bond to bPEI grafted to chitosan (CS). The drug, CD functions also as a targeting ligand to angiotensin II receptor expressed on various cancerous cells like pancreatic,

breast and ovarian carcinoma. The drug also possesses the endosomal buffering activity. The amide bond linking CD with bPEI were further cleaved by amidase enzyme present in the malignant cells to release free drug inside the cells. The cationic polymer, CPC could also bind with the wild-type p53 plasmid to form CPC/wt-p53. In addition, the co-delivering of both CD and wtp53 gene by the polymer achieved the synergistic angiogenesis suppression by effectively down regulating the expression of vascular endothelial growth factor (VEGF) mRNA and protein via different pathways *in vitro* Furthermore, the combined delivery showed a significant reduction in tumor size in mice compared with CS-grafted bPEI/wt-p53 complexes (CP/wt-p53) and CP/wt-p53 and free drug.

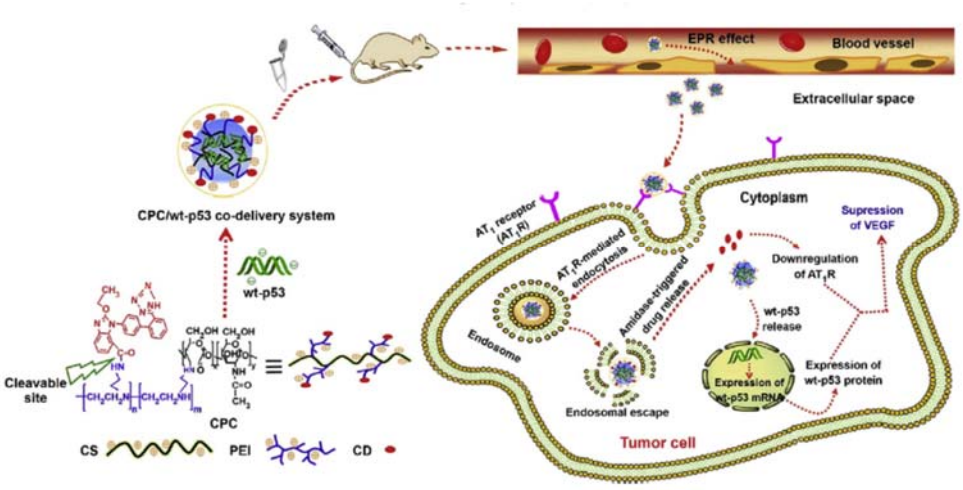

Figure 5: The co-delivery of anti-angiogenesis drug, candesartan (CD) and wild-type (wt)-p53 plasmids in bPEI grafted with chitosan (CS) system for delivery to PANC-1 subcutaneous tumors formed in BALB/c nude mice (Bao et al., 2014).

This synergistic antitumor activity was attributed to increased pDNA uptake and transfection efficiency of CPC/wt-p53 complexes due to both targeting and the endosomal buffering ability of the drug. This work highlights that the combined delivery of drug and gene in a single carrier may create additive/synergistic therapeutic effects. Thus, the combined delivery of gene and drug in a

single carrier exploit the different mechanism of action of the individual therapeutic agent to ultimately give a synergistic effect.

CHAPTER 3 MATERIALS AND METHODS

Thiolated cationic pullulan was synthesized to evaluate its potential towards gene delivery and as an efflux pump inhibitor. The parent compound was synthesized by conjugating the flexible hydrophilic chain of pullulan with the cationic polymer, PEI using CDI as a crosslinker. The resultant compound was then thiolated with different thiol-containing molecules such as cysteine, mercaptosuccinic acid, 3,3 dithiodipropionic acid, and 4,4 dithiodibutyric acid to form pullulan-PEI-cysteine (PPSS), pullulan-PEI-mercaptosuccinic acid (PPMSS), pullulan-PEI-3,3 dithiodipropionic acid (PPDPA) and pullulan-PEI-4,4 dithiodibutyric acid (PPDBA) respectively. Thiolation of pullulan-PEI was carried out by EDC coupling reaction. The control groups were synthesized by conjugating PEI with thiol compounds alone without pullulan.

3.1 Synthesis and characterization of pullulan-PEI-Cysteine (PPSS)

3.1.1 Materials

Pullulan (MW150,000 Da), polyethyleneimine (PEI; MW 25 kDa), cysteine hydrochloride, carbonyl diimidazole (CDI), 1-ethyl-3-[3-dimethyl aminopropyl carbodiimide hydrochloride (EDC),3-(4,5-dimethylthiazol-2-yl)-2,5-diphenyltetrazolium bromide(MTT), DMEM, trypsin, 5,5-dithiobis(2-nitrobenzoic acid) (DTNB; Ellman's reagent), doxorubicin hydrochloride, sodium borohydride ($NaBH_4$), DNase I, glutathione monoesters and monochlorobimane, buthionine sulfoximine, were all purchased from Sigma–Aldrich Chemicals Co, USA. YOYO iodide, Hoechst 33342 from Invitrogen, calf thymus DNA (ctDNA), was purchased from Worthington Biochemical Corp. p53 Dominant-Negative Vector was from Clontech, USA, and FBS was purchased from GIBCO, USA, All other reagents were of analytical grade from Merck, India.

3.1.2 Synthesis of pullulan-PEI

The synthesis of pullulan-PEI was carried out by N, N carbonyl diimidazole (CDI) reaction. Initially, pullulan (250mg) was dissolved in DMSO and the hydroxyl group of pullulan was activated by adding CDI (20mg). CDI is unstable in the aqueous medium and hence the activation step was done in the solvent that is free of water. Following the addition of CDI, the reaction mixture was stirred in magnetic a stirrer at 37°C for 2hr. The activated pullulan was then treated with varying amounts of PEI (200 mg and 100 mg). PEI was dissolved in 20mM borax to carry out the reaction in alkaline medium and the reaction was kept under stirring for 16 hours. After the reaction, acetone was added to the resultant solution to precipitate out the final product. Acetone wash was done twice and the precipitate was collected by filtration. The resultant precipitate was redissolved in water and dialyzed (MWCO 100 kDa) against deionized water.

3.1.3 Thiolation of Pullulan-PEI

In this step, a known quantity of pullulan-PEI (100mg) and different amounts of cysteine (40mg and 80mg) was conjugated by using the crosslinker, EDC (0.1M). The reaction was carried out at pH 6 and kept for magnetic stirring overnight at room temperature. Later, dialysis was carried out using 0.1 M sodium phosphate, 0.15 M NaCl (pH 7.4) and 1mM EDTA in deionized water. Following coupling reaction and dialysis, the thiol content of the resultant conjugant was analyzed by Ellman's reaction.

3.1.4 Oxidation of thiol polymer

A known amount of the pullulan-PEI-cysteine conjugate (100mg) was taken, and the thiol group was selectively oxidized by means of H_2O_2. Initially, the conjugate was mixed with 100mM PBS buffer of pH 3.5 and slowly added 100µL (1%) H_2O_2 and kept for stirring at RT for 2hrs. The reaction was stopped by the addition of PBS, pH 4.5 and stirred again for 6hrs. Later, dialysis was

carried out in deionized water. Thus, the disulfide cross-linked pullulan-PEI-cysteine viz., PPSS I and II were synthesized which varies in the initial amount of PEI and cysteine used.

3.1.5 Synthesis of control groups (PEI-CYS(S-S))

The control groups i.e. PEICYS(S-S) was synthesized with PEI and cysteine alone without using pullulan. Here, initially, a known amount of PEI (200mg and 100mg) and cysteine (40mg and 80mg) were taken and the conjugation was carried out using EDC cross linker at pH 6. The reaction mixture was stirred overnight at room temperature. Later, dialysis was carried out in PBS buffer (pH 7.4). For introducing the disulfide bond, a known amount of the resultant polymer (100mg) was taken, mixed with 100 mM of PBS of pH 3.5 and added 100µl of H_2O_2 to enable the oxidation of –SH group. The oxidation reaction was carried out for 2 hours at room temperature under stirring. The reaction was stopped by adding 0.1M PBS, pH 4.5 and stirred again for 6 hr. The dialysis was performed in deionized water to remove unreacted molecules, leaving behind the disulfide cross-linked PEI derivatives i.e. PEICYS (S-S) I and II.

3.1.6 Physicochemical characterization

3.1.6.1 Determination of disulfide/ Thiol content

The disulfide content of the thiolated polymer was evaluated by using 2- nitro 5-thiosulfobenzoate (NTSB) which was prepared by air oxidation of a solution of 100mg of DTNB (Ellman's reagent) in 10mL of 0.1M Na_2SO_3 at 37°C that yields a yellowish stock solution of NTSB. The working solution was prepared by diluting the stock solution at 1:100 with 50mM glycine, 100mM Na_2SO_3, and 3mM EDTA buffer at pH 9.5. A total of 190 µL working reagent (NTSB) was added to 10 µL (1mg/mL) of the sample per well and incubated at room temperature in the dark for 30 min. Absorbance was read at 405 nm in a microplate reader (Synergy H1, USA).

The disulfide content was measured using cystamine as standard. Simultaneously, the thiol content was measured by using 5,5′- dithiobis-(2-nitrobenzoic acid) (DNTB, Ellman's reagent) assay after reduction of disulfide linkage in the PPSS polymers with sodium borohydride (4%), following a protocol detailed in the literature (Winther & Thorpe 2014). Following reduction, 500µL of the sample (1mg/mL) was used for the assay. Both test sample and standards were prepared in 0.1M sodium phosphate (pH 8.0) reaction buffer. To this 50µL of Ellman's reagent, prepared in 0.1M sodium phosphate buffer at pH 8.0 was added and kept for incubation at room temperature for 15min. The absorbance was measured at 412nm using UV-Vis spectrophotometer (UV Varian Cary, USA). The amount of thiol groups was calculated using the cysteine standard curve. Both reactions were carried out in triplicates, and statistical evaluation was done.

3.1.6.2 Determination of primary amine group using $CuSO_4$ assay

The primary amine group in PEI which is left unreacted following conjugation with pullulan and cysteine was measured using CuSO4 assay. All polymers, that is PPSS I, PPSS II, PEICYS (S-S) I and PEICYS (S-S) II and the parent compound, pullulan PEI of PPSSI i.e PPI and PPSSII i.e PPII were taken at 1mg/mL concentration. To 500µL of the sample, 5mL of CuSO4 solution (0.145mg/mL) was added and mixed thoroughly. The absorbance was measured at 285nm using UV-Vis spectroscopy (UV Varian Cary, USA). PEI (25 kDa) of varying concentration from 0.2 to 2mg/mL was taken as a standard. All experiments were conducted in triplicates and statistical analysis was carried out.

3.1.6.3 FTIR analysis

The FTIR spectra of the representative polymer PPSS I and its corresponding control group PEICYS(S-S) I was recorded in the range 500–4000 cm^{-1} using Nicolet Impact 410.

3.1.6.4 ^{1}H NMR

^{1}H NMR spectra of the thiolated pullulan derivative PPSS I and its corresponding control group was analyzed in D_2O using 500MHz spectrometer (Bruker Avance DPX 300). The analysis was done at 22°C, and the number of transients during the measurement was set as 16. The relaxation time of the instrument during the time of measurement was set as 16.

3.1.7 Determination of buffering capacity

The endo-lysosomal escape of the polymer is one of the cardinal feature required for gene delivery applications. The buffering capacity of PPSS I and II, PEICYS(S-S) I/II, normal saline and PEI was assessed using acid-base titration method over a pH range of 10–4. Initially, the samples were dissolved in normal saline (2.5 mg in 25mL) and adjusted the pH of the solution to 10 using 0.01 N NaOH, which was then titrated against 0.01 N HCl. The change in pH was noted after each addition of a volume of 50 µL of acid. A graph was plotted with pH against the volume of HCl used and assessed the buffering capacity.

3.1.8 Nanoplex formulation

The nanoplexes are formed by the electrostatic interaction between the positively charged polymer and negatively charged DNA. This interaction resulted in small-sized particles with a positive surface charge. The nanoplexes of different weight ratios ranging from 1:1 to 5:1 were prepared by mixing increasing concentration of polymer with the fixed concentration of DNA (10µg) and the final volume was made up to 1mL with distilled water. The mixture was subsequently vortexed for 30sec and kept for 20 min at room temperature.

3.1.8.1 Determination of particle size and zeta potential

The size and zeta potential values of the nanoplexes are crucial factors which affect the passage of nanoparticles through the cell membrane. The size and zeta potential of the nanoplexes of PPSS I/II and its control groups PEICYS(S-S)I/II was measured using Zetasizer Nano ZS (Malvern Instruments Ltd, UK) at a temperature of 25°C. The nanoplexes in the range 1:1 to 5:1 were prepared for each polymer as detailed in the section 3.1.8. The particle size is expressed as mean diameter (z average).

3.1.8.2 Gel retardation assay

The ability of the polymer to condense ctDNA and the stability of the formed nanoplexes were analyzed by means of gel retardation assay. Nanoplexes of varying ratios (1:1-5:1) of the pullulan derivatives (PPSS I/II) and its control (PEICYS (S-S) I/II were loaded in 1% agarose gel prepared in Tris-Acetate-EDTA buffer. Similarly, the influence of plasma proteins on the nanoplexes stability was also analyzed in 1% agarose gel. Here, the nanoplexes were initially incubated with 20µL of plasma for 30 min and electrophoresis was carried out. The electrophoresis was performed in a Bio-Rad electrophoresis system (Bio-Rad Laboratories, USA) at 100V for 60min. Both the gels were digitalized using image analyzer (Fuji LAS 4000) after staining with 2µL of 10mg/mL ethidium bromide.

3.1.8.3 Effect of DTT on the stability of thiolated polyplexes

The stability of the nanoplexes in presence of the reducing agent, DTT was analyzed by means of DLS measurement and agarose gel electrophoresis. Herein, the desired nanoplexes ratios of PPSS I and II such as 2:1, 4:1 and 3:1, 4:1 respectively were chosen and added with 10mM DTT in 150 mM NaCl. The complex was incubated at different time intervals such as 0, 30 min, 1 hr, 2 hr, 3 hr, and 4 hr. The change in size was measured using Zetasizer Nano ZS (Malvern Instruments Ltd, UK) at a temperature of 25°C. Similarly, the influence of DTT in the release of DNA from

the nanoplexes was determined via electrophoresis. Initially, the nanoplexes were incubated with DTT alone (10mM) and/or with heparin (30µg/mL)/DTT (10mM) combination for 1hr and electrophoresis was carried out in 1% agarose gel. The gel was visualized after staining with ethidium bromide, 2µL (10mg/mL) in an image analyzer (Fuji LAS 4000).

3.1.9 Plasma protein interaction of the polymer (PAGE analysis)

Native PAGE analysis was performed to assess the interaction of PPSS I and PPSS II polymers with plasma proteins. The polymer with concentration of 1mg/mL was prepared, of which 100µL of the polymers was taken. PEI incubated with plasma and plasma treated with saline (0.9% NaCl) were considered as positive and negative controls respectively. To the polymer samples, 20 µL plasma (diluted with saline) was added and kept for incubation for 30min. This was followed by centrifugation at 5000rpm for 10 min and subjected to native gel electrophoresis using 7% resolving gel and 4% stacking gel in a Mini-PROTEAN II electrophoresis cell (Bio-RAD, CA, USA). The gel was stained with 0.2% Coomassie brilliant blue R 250 for overnight and destained using 50% v/v methanol in water with 10% acetic acid for almost 4 hrs. The gel was then visualized and the image was digitalized using an image analyzer (LAS 4000, Fuji).

3.1.10 Cell culture studies

Cell culture studies were performed in different cancer cell lines such as C6 glioma cells, A549, HeLa cells, and the normal fibroblast cells, L929. The culturing of these cells was carried out in a different medium such as DMEM/Ham's F12: MEM (1:1) (C6 cells), DMEM (A549 cells), and MEM (HeLa and L929). All contained 10% FBS and 1% antibiotic-antimycotic. Cells were all kept at 37°C in a 5% CO_2 incubator. The cellular uptake and, transfection studies were performed only in C6 cells whereas cytotoxicity and efflux pump inhibition studies were conducted in A549, C6, and HeLa cells.

3.1.10.1 In vitro cytotoxicity (MTT assay)

Cell viability assay of the pullulan based polymer i.e. PPSS I, PPSSII and its control i.e. PEI-CYS(S-S) I, II were carried out in different cell lines. The cancer cell lines such as C6 cells, A549, HeLa and normal fibroblast cell, L929 were each seeded in 96 well plates at a density of $1x10^4$ cells/well. Following overnight incubation, the cells were exposed to selected nanoplex ratios such as PPSS I (2:1 & 4:1), PPSS II (3:1 & 4:1) and PEICYS(S-S) I (3:1 &4:1), PEICYS(S-S) II (3:1& 4:1) in the corresponding growth media for 24hrs and incubated at 37°C in 5% CO_2 incubator. The cells treated with Triton X-100 were taken as positive control. After 24 hour incubation the medium containing polymers were removed and 100µL of MTT was added (0.5mg/mL) and again incubated for 4hrs at 37°C. The formazan crystals formed by the live cells were dissolved in 200µL of DMSO, the absorbance was measured at 570nm using a microplate reader (Synergy H1, USA). The results are presented as percentage value related to the value of untreated control cells. All experiments were performed in triplicate. Cell viability was calculated using the equation given below,

$$\text{Cell viability} = \frac{As}{Ac} \times 100,$$

Where As is absorbance of sample and Ac is absorbance of control

3.1.10.2 Uptake studies using confocal microscopy

The cellular uptake studies were carried out in C6 cells. The cells were seeded in four-well plates with a density of $1x10^4$ cells/well and incubated overnight. Initially, the ctDNA was tagged with YOYO-iodide (2.5µL of 10µM YOYO for 1µg DNA/well) and kept for 1hr. The desired nanoplexes of polymer PPSS I i.e. 2:1 & 4:1, PPSS II i.e 3:1 & 4:1 and the control groups PEICYS (S-S) I 4:1 and PEICYS(S-S) II 4:1 were prepared by complexing the corresponding polymer with

YOYO tagged in Ham's F12 serum-free medium. The complex was kept for incubation for 20 min. The resultant complex was added to the cells and incubated for 3hr at 37°C. The nuclear staining was performed by adding Hoechst 33342 (12µL of 1mM solution) to the cells and incubated for a further half an hour. Cells were then washed in PBS, fixed in 1% formaldehyde and visualized using confocal microscopy (NIKON AIR).

3.1.10.3 Uptake studies using flow cytometry

The cellular uptake of PPSS I/II nanoplexes in C6 cells was quantified by flow cytometry. Initially, the ctDNA was tagged with YOYO-I and kept for 1hr in the dark. The polyplexes of PPSSI and II were formed by complexing the polymer with YOYO-tagged DNA (2.5µL of 10µM YOYO labeled for 1µg DNA/well) at the desired ratios i.e 2:1 and 4:1 for PPSS I and 3:1 and 4:1 for PPSS II in Ham's F12 serum-free medium. The cell were incubated with nanoplexes for 3h. The cells were taken from the incubator and the polyplexes were added after removing the medium. Following this, the cells were washed with PBS and trypsinized. The cells were harvested by centrifuging at 8000rpm for 5 min following PBS wash and were resuspended in sheath fluid in a FACS tube. The quantification of cellular uptake of the nanoplexes was carried out using flow cytometry (BD FACS Aria).

3.1.10.4 Pathway studies using endocytosis inhibitors

The uptake pathways of nanoplexes into the cells were determined by using different inhibitors such as chlorpromazine, filipin, and amiloride, which specifically inhibit clathrin, caveolae, and micropinocytosis mediated internalization respectively. The C6 cells were seeded in 4 well plates ($1x10^4$ cells/well) and incubated at 37°C at 5% CO_2 incubation. The following day, cells were washed and treated with medium containing inhibitors such as chlorpromazine (2µg/mL), filipin (2µg/mL) and amiloride (2.25µg/mL). The cells were subjected to 30min

incubation with inhibitors. After incubation, the medium containing inhibitors were removed and rinsed with fresh media. Following this, the PPSSI nanoplex prepared with YOYO tagged DNA at a ratio of 4:1 (as in section 3.1.10.3) were added to the cells and incubated for 3hrs at 37°C. Nuclear staining was carried out by adding Hoechst 33342 (12µL of 1mM solution) to these cells followed by 30 min incubation. The cells were washed with PBS and fixed in 1% formaldehyde and imaged using confocal microscopy (NIKON AIR).

3.1.10.5 Polymer trafficking studies

The polymer trafficking of nanoplexes inside the cells was analyzed by tagging both polymer and DNA with rhodamine and YOYO-I respectively. This study was conducted in C6 cells using the polymer PPSS I with the nanoplexes ratio 4:1. Initially, a known concentration of the polymer (1mg/mL) prepared in phosphate buffer pH 7.2 was incubated with rhodamine-NHS ester (0.5mg/mL) for an hour. The tagged polymer was then dialyzed at 4°C for 24hrs against PBS 7.2. The YOYO tagged DNA was prepared as mentioned in the previous section (3.1.10.2). Fluorescent nanoplexes of PPSSI at 4:1 ratio was prepared by mixing the labeled polymer with YOYO tagged ctDNA (2.5µL of 10µM YOYO labeled for 1µg DNA/well) and incubated for 20 min at room temperature. The C6 cells were treated with labeled nanoplexes and incubated for different time points of 1hr, 2hr, 4hr, and 7h. The nuclear staining of these cells was carried out using Hoechst 33342 (12µL of 1mM solution) for half an hour. The cells were then washed with PBS (pH 7.4), fixed (1% formaldehyde) and imaged by confocal microscopy (NIKON AIR).

3.1.11 *In vitro* transfection efficiency

The transfection efficiency of the polymer PPSS I and II was analyzed after complexing with the p53 plasmid. The p53 plasmid is meant to cause cellular apoptosis in cancer cells. The experiment was performed in C6 glioma cells. The nanoplexes formation was done with 2.5µg of

plasmid DNA p53 with corresponding polymer PPSS I and II at the ratio 2:1, 4:1 and 3:1, 4:1 respectively to obtain the nanoparticle. Both qualitative and quantitative determination of cell death mediated by p53 containing nanoplexes in C6 cells was evaluated via confocal and flow cytometry analysis. Different methods were adopted to assess the cell death i.e. live and dead assay, PI staining, Annexin V/ FITC staining and p53 immunofluorescence.

3.1.11.1 Live and Dead assay

Live and dead assay were performed to analyze the transfection efficiency of the polymer. The p53 plasmid was used for this purpose. C6 cells were seeded into four well plates ($1x10^4$ cells/well) and incubated at 37°C and 5% CO_2 to allow adherence of cells. Both PPSS I (2:1 and 4:1) and PPSS II (3:1 and 4:1) nanoplexes were prepared with the p53 plasmid in Ham's F12 serum-free medium. Following incubation, the nanoplexes were added to the cells and incubated for 5hrs at 37°C and 5% CO_2. Following this, the medium was replaced with fresh full media (DMEM/Ham's F12: MEM (1:1)) and incubated for another 19hrs. Live and dead assay were performed by using a kit as per the manufacturer protocol. Briefly, 2 µM calcein AM and 4 µM ethidium homodimer 1(EthD-1) in PBS was prepared and added to each well and incubated for 30min. The cells were then washed, fixed with 1% formaldehyde and digitalized by using a fluorescent microscope (Leica DM IRB, Germany).

3.1.11.2 Propidium iodide (PI) staining

The cell death mediated by the transfection of p53 was quantified in C6 cells using propidium iodide (PI) staining. The desired polyplexes of PPSS I (2:1 and 4:1) and PPSS II (3:1 and 4:1) were prepared by mixing the polymer with the p53 plasmid. The experiment was performed as similar to live and dead assay (3.1.11.1) except that following 24hrs of incubation, the cells were washed and trypsinized. The cells were harvested and an aliquot having $1x\ 10^6$

cells/100µL were transferred into FACS tube after resuspending in sheath fluid. The cells were then added with 5µL PI (10µg/mL), mixed gently and kept for 1min incubation in the dark. The percentage of cell death was analyzed using flow cytometry (BD FACS Aria).

3.1.11.3 Annexin V/FITC staining

The p53 mediated apoptosis following transfection in C6 cells using PPSS I and II polymers were analyzed by means of annexin V/FITC staining. The transfection studies were carried out using the desired polyplexes ratios of PPSS I (2:1 and 4:1) and PPSS II (3:1 & 4:1) with the p53 plasmid. The protocol was as similar to live and dead assay (3.1.11.1) except that following 24hrs of incubation, the cells were washed with PBS (7.4) and harvested. The cells ($1x10^6$ cells/mL) were then suspended in 1x annexin binding buffer. The cell suspensions (100µL) were transferred to FACS tube and the apoptotic cells were determined by staining using FITC-annexin V apoptosis detection kit as per manufacturer protocol. The cells were added with 5 µL FITC-annexin V and 1 µL (100µg/mL) propidium iodide (as provided in the manufacturer kit) and incubated in the dark for 15 min. Following this, 1x annexin binding buffer (400µL) was added to each tube and the samples were analyzed by flow cytometry (BD FACS Aria).

3.1.11.4 p53 immunostaining

The immunostaining of p53 was carried out in C6 cells following transfection of p53 using PPSS I/II polymers. Initially, the cells were seeded in a four-well plate at a density of 1x104 cells per well and incubated at 37°C in 5% CO_2 incubator. The cells were treated with the selected nanoplex ratios of PPSS I (2:1 & 4:1) and PPSS II (3:1 & 4:1) for 5hrs. Following this, the medium was replaced with fresh media and incubated for 24hrs as mentioned in the previous section

3.1.11.1. Following this, the cells were washed with PBS three times and fixed using 1% formaldehyde in PBS. The cells were permeabilized using 0.2% Triton X-100 in blocking solution made of 1% BSA in PBS for 20 min. This was again washed with PBS and incubated for another 30 min using 250µL of 1% BSA in PBS. The blocking solution was removed and incubated with 250µL of p53 primary antibody (0.1µg/mL) at 4°C overnight. The antibody was removed and treated with BSA as before. Following the removal of blocking solution, the FITC labeled secondary antibody was added and kept for 1hr in the dark. The cells were then washed with PBS and imaged using confocal microscopy (NIKON AIR).

3.1.12 Efflux pump inhibition studies

The ability of the thiolated polymer in the inhibition of efflux pump in cancer cells were analyzed by evaluating DOX retention in the cells following treatment with polyplex and DOX. Here, DOX is a substrate for efflux pump and hence enhanced retention of DOX in cancer cells mark the inhibition of efflux pump. The experiment was performed in three cell lines such as C6, HeLa, and A549 after screening these cells for P-gp activity.

3.1.12.1 Assessment of P-gp expression in cancer cell lines

The cell lines used were C6, A549, and HeLa, where the cells were seeded in a 24 well plate at a density of $1x10^4$ cells/well and kept for incubation at 37°C for 24hr. Following incubation, the medium was removed and the cells were all treated with a known P-gp inhibitor, verapamil (40µM) for 30 min. Following this, the anticancer drug, DOX (3µM) was added and kept for 24hrs in the incubator. The control group was formed by treating all cells with DOX alone without pretreatment with verapamil. The cells were then washed with PBS and added with 1% Triton X-100 prepared in PBS (0.01M, pH 7.4) and kept for 30 min, followed by twice repeated freeze-thaw cycle. The cell lysate was then centrifuged, and DOX concentration was analyzed after normalizing with the

total protein content of the cells. The protein content in the cell was determined using BCA (bicinchoninic acid). The DOX concentration was measured in a microplate reader (Synergy H1, USA) at an excitation wavelength of 480nm and emission at 580nm.

3.1.12.2 Evaluation of efflux pump inhibition ability of the polymer - confocal microscopy

The efflux pump inhibition properties of the polymer were evaluated in P-gp expressing cell lines C6 and A549 and P-gp negative cell line HeLa. The cells were seeded ($1x10^4$ cells/well) in a four well plates and incubated overnight. The P-gp inhibition was determined by assessing the intracellular retention of DOX in various cell lines. Polyplexes of the polymer PPSS I at desired ratios (2:1 & 4:1) were prepared via complexing with ctDNA. The polyplexes were added to the cells and incubated for 2hrs, following this, the anticancer drug, DOX (3μM) was added and kept for 24hr in the incubator. After incubation, the cells were washed with PBS and fixed in 1% formaldehyde. The cells were imaged using confocal microscopy (NIKON AIR).

3.1.12.3 Evaluation of efflux pump inhibition using flow cytometry

The efflux pump inhibition studies were carried out in C6, A549, and HeLa cells as detailed above in section 3.1.12.2. Following 24hrs of incubation, the cells were washed and trypsinized. The cells were harvested by centrifuging at 8000rpm for 5 min following PBS wash and were resuspended in sheath fluid in a FACS tube. The percentage of cells containing DOX was analyzed by using flow cytometry (BD FACS Aria).

3.1.12.4 DOX retention studies

The DOX retention kinetics was analyzed in different cell lines following exposure with the polyplexes and DOX where both P-gp positive cell lines A549, C6 and Pgp negative cell line HeLa were used. The cells were seeded ($1x10^4$ cells/well) in a 48 well plates and incubated overnight. Initially the polyplexes of PPSS I i.e. 2:1 and 4:1 was prepared by complexing the

polymer with ctDNA. The cells were treated with the polyplexes and incubated at 37°C in 5% CO_2 incubator for different time points such as 1-8 hrs. Following incubation, the cells were washed with PBS and added with 1% Triton X-100 prepared in PBS (0.01M, pH 7.4) and kept for 30 min, followed by twice repeated freeze-thaw cycle. The cell lysate was then centrifuged, and DOX concentration was analyzed after normalizing with the total protein content of the cells. The protein content in the cell was determined using BCA (bicinchoninic acid). The DOX concentration was measured in a microplate reader (Synergy H1, USA) at an excitation wavelength of 480nm and emission at 580nm.

3.2 Synthesis and characterization of pullulan-PEI-mercaptosuccinic acid (PPMSS)

3.2.1 Materials

Pullulan (Fluka), mercaptosuccinic acid, polyethyleneimine (PEI; MW 25,000 Da), 1-ethyl-3-[3-dimethyl aminopropyl) carbodiimide hydrochloride (EDC), carbonyl diimidazole (CDI). All other chemicals used are as listed in section 3.1.1.

3.2.2 Synthesis of pullulan-PEI

The synthesis of pullulan-PEI was as similar as detailed in the previous section (3.1.2). Here, the initial amount of pullulan-PEI used was in the ratio 1:0.8.

3.2.3 Thiolation step

The Thiolation step was carried out in the pullulan-PEI conjugate using mercaptosuccinic acid to improve colloidal stability, targetability and easy release of DNA. Initially, a known amount of pullulan-PEI (100 mg) was taken and conjugated with different amounts of MSA (30mg, 40mg, and 50mg) using crosslinker EDC (0.1M). The reaction conditions and subsequent steps were as similar as detailed in section 3.1.3.

3.2.4 Oxidation of thiol polymer

A known amount of the resultant compound, pullulan-PEI-MSA (100mg) was taken and mixed with 0.1M of PBS of pH 3.5 and added 100µl of H_2O_2 (1%) in order to carry out the oxidation of –SH group in the polymer. The reactions conditions are as similar as detailed in the previous section 3.1.4.

3.2.5 Synthesis of the control group (PEI-MSA)

The control group i.e. disulfide cross-linked PEI-mercaptosuccinic acid (PEI-MSA) was prepared by conjugating PEI with mercaptosuccinic acid (MSA). Here, initially, a known amount of PEI (200mg) was added with different amounts of MSA (30, 40 & 50mg) and the reaction was carried out under the mediation of EDC crosslinker. The subsequent steps were as similar as detailed in section 3.1.5.

3.2.6 Physicochemical characterization

3.2.6.1 Determination of disulfide/thiol content

The disulfide and thiol content of PPMSS and PEI-MSA were measured using 2- nitro 5-thiosulfobenzoate (NTSB) and Ellman's assay respectively. Briefly, the test samples (both PPMSS and PEI-MSA) were prepared at a concentration of 1mg/mL, and the disulfide /thiol content of the polymers was assessed using the protocol as detailed in section 3.1.6.1.

3.2.6.2 Determination of amino content of thiolated polymer using $CuSO_4$ assay

The free amino content of the polymer, PPMSS, and PEI-MSA was evaluated using $CuSO_4$ assay. Both the samples PPMSS and the control, PEI-MSA was prepared at a concentration of 1mg/mL and the experiment was performed as detailed in section 3.1.6.2.

3.2.6.3 Analysis by Fourier Transform Infrared Spectroscopy (FTIR)

The FTIR spectra of PPMSS and PEI-MSA was recorded over an ATR scan range of 500–4000 cm^{-1} using Nicolet Impact 410.

3.2.6.4 Analysis by Proton Nuclear Magnetic Resonance Spectroscopy (^{1}H NMR)

^{1}H NMR spectra of PPMSS and PEI-MSA was analyzed in D2O using 500 MHz spectrometers of Bruker Avance.

3.2.7 Determination of buffering capacity

The buffering ability of the polymers was evaluated by acid-base titration over a pH range of 10 to 4. Initially, both polymers PPMSS and PEI-MSA were dissolved in normal saline (2.5mg in 25 mL) and the pH of the solution was made upto 10 using 0.01 N NaOH, which was then titrated against 0.01 N HCl. The protocol is as similar as detailed in section 3.1.7.

3.2.8 Preparation of nanoplexes

The nanoplexes of different weight ratios ranging from 1:1 to 5:1 were prepared by mixing increasing concentration of PPMSS/PEI-MSA polymer with the fixed concentration of ctDNA (10 µg), and the final volume was made up to 1mL with distilled water. This was subsequently vortexed for 30sec and incubated at room temperature for 20 min.

3.2.8.1 Determination of particle size and zeta potential

The hydrodynamic size and zeta potential of the nanoplexes of PPMSS and PEI-MSA (1:1 to 5:1) were analyzed using Zetasizer Nano ZS (Malvern Instruments Ltd., UK) at a temperature of 25°C. The preparation of nanoplexes is given in section 3.2.8.

3.2.8.2 Gel retardation assay

The gel retardation assay was performed in both PPMSS and PEI-MSA nanoplexes to evaluated the DNA condensation ability of the polymer. The Nanoplexes of varying weight ratios i.e. 1:1 to 5:1 was loaded in 1% agarose gel prepared in Tris-Acetate-EDTA buffer. Similarly, the stability of nanoplexes in presence of plasma proteins was analyzed by agarose gel electrophoresis. The experiment was performed as similar as detailed in section 3.1.8.2.

3.2.8.3 Effect of DTT on the stability of thiolated polyplexes

The stability of the PPMSS nanoplexes in presence of the reducing agent DTT was analyzed by means of DLS measurement and agarose gel electrophoresis. Briefly, both the nanoplexes of PPMSS (3:1 & 4:1) and PEI-MSA (3:1 & 4:1) were incubated with 10mM DTT prepared in 150mM NaCl. The particle size was measured following incubation at different time intervals of 30min, 1,2,3 and 4hrs using Zetasizer Nano ZS (Malvern Instruments Ltd., UK) at a temperature of 25°C. Similarly, the release of DNA following the incubation of nanoplexes with DTT and /or DTT/heparin was analyzed by agarose gel electrophoresis and the experiment was performed as similar as detailed in section 3.1.8.3.

3.2.9 Plasma protein interaction of the polymer (PAGE analysis)

The plasma protein interaction of PPMSS polymer and its control group, PEI-MSA was determined by PAGE analysis. The polymer with concentration 1mg/mL was prepared, of which 100µl of the polymers was taken and 20 µl each of the plasma (diluted with saline) was added. The subsequent step was as similar as detailed in section 3.1.9.

3.2.10 Cell culture studies

Cell culture studies were performed in the cancer cell lines C6, A549, HeLa and the normal fibroblast cell, L929. The appropriate cell culture medium and other maintenance conditions are detailed in section 3.1.10.

3.2.10.1 In vitro cytotoxicity (MTT assay)

The cellular viability of the selected nanoplexes ratios of PPMSS (3:1 & 4:1) and PEI-MSA (3:1 & 41) was evaluated in C6, A549, HeLa and L929 cells using MTT assay. The cells were each seeded in 96 well plates at a density of $1x10^4$ cells/well. After 24hrs, the cells were exposed to the selected nanoplexes ratios of PPMSS (3:1 & 4:1) and PEI-MSA (3:1 & 4:1). The experiment protocol is as similar as detailed in section 3.1.10.1.

3.2.10.2 Uptake studies via confocal microscopy

The cellular uptake of PPMSS nanoplexes and its control groups were analyzed in C6 cells. The cells were each seeded in a 4 well plate at a density of $1x\ 10^4$ cells/well and incubated for 24 hr at 37°C in a 5% CO_2 incubator. Different nanoplexes ratios of PPMSS (3:1 and 4:1) and PEI-MSA (3:1 and 4:1) were prepared with YOYO tagged DNA in Ham's F12 medium and kept for 20min. The experiment protocol is as similar as detailed in section 3.1.10.2.

3.2.10.3 Uptake studies using flow cytometry

The cellular uptake of polyplexes was quantified by means of flow cytometry where the procedure of cellular uptake is as same as detailed in the previous section (3.2.10.2) except that following 3hrs incubation, the cells were washed and trypsinized. The cells were centrifuged for 5 min at 8000 rpm. The harvested cells were then suspended in sheath fluid and the cellular uptake of YOYO tagged DNA was quantified by using flow cytometry (BD FACS Aria).

3.2.10.4 Pathway studies using endocytosis inhibitors

The cellular uptake pathways of the nanoplexes were determined using different inhibitors chlorpromazine, filipin, and amiloride, which specifically inhibit clathrin, caveolae, and micropinocytosis mediated endocytosis respectively. The representative polymer chosen for this study was PPMSS 4:1 ratio. The uptake procedure was carried out with or without inhibitors as detailed in section 3.1.10.4.

3.2.10.5 Polymer trafficking studies

The polymer trafficking inside of the cell was analyzed by tagging, PPMSS with rhodamine and DNA with YOYO-I and nuclei stained with Hoechst. The labeling of the polymer and addition of polyplexes to the cells was as similar to that detailed in the section 3.1.10.5.

3.2.11 *In vitro* transfection efficiency

The transfection efficiency of the polymer PPMSS was performed after complexing with the p53 plasmid in C6 cells. The nanoparticle was prepared by complexing 2.5µg of plasmid DNA p53 with the corresponding polymer amount of PPMSS at ratios 3:1 and 4:1. Both qualitative and quantitative determination of cell death was evaluated in C6 cells using confocal and flow cytometry analysis. Different methods were adopted to assess the cell death i.e. live and dead assay, PI staining, Annexin V/ FITC staining and p53 immunofluorescence.

3.2.11.1 Live and dead assay

C6 cells were seeded into 4 well plates ($1x10^4$ cells/well) and kept at 37°C in 5% CO_2 incubation to allow adherence of cells. PPMSS nanoplexes of different ratios 3:1 and 4:1 were prepared using p53 plasmid in Ham's F12 medium. The nanoplexes treatment to the cells and further proceedings were as similar as mentioned in section 3.1.11.1.

3.2.11.2 PI staining

The C6 cells were seeded in 48 well plates ($1x10^4$cells/well) and incubated at 37°C and 5% CO_2 incubator. The nanoplexes of PPMSS at ratios 3:1 and 4:1 were prepared after complexing the polymer with the p53 plasmid. The treatment of nanoplexes to the cells 11and further processing for flow cytometry analysis is as similar as detailed in 3.1.11.2.

3.2.11.3 Annexin V/FITC staining

The p53 mediated apoptosis following transfection in C6 cells using PPMSS nanoplexes (3:1 & 4:1) were analyzed by annexin V/FITC staining. The experiment was performed as per the protocol detailed in section 3.1.11.3.

3.2.11.4 p53 immunostaining

The Immunostaining of p53 was carried out in C6 cells followed by transfection of PPMSS/p53 3:1 and PPMSS/p53 4:1 nanoplexes. Initially, the cells were seeded in a four-well plate at a density of $1x10^4$ cells per well and incubated at 37°C in 5% CO_2 incubator. The experiment was performed as similar as detailed in the section 3.1.11.4.

3.2.12 Efflux pump inhibition studies

The ability of the polymer to inhibit the efflux pump in cancer cells was evaluated by adding the polyplexes and anticancer drug, DOX in the cells. The enhanced retention of DOX in the cancer cells marked the inhibition of the efflux pump. Herein both P-gp expressed cells i.e. C6 and A549 and P-gp negative cells i.e. HeLa was used. The nanoplexes were prepared by complexing the polymer PPMSS, with ctDNA (2µg) in the ratio 3:1 and 4:1.

3.2.12.1 Efflux pump inhibition studies using confocal microscopy

The P-glycoprotein inhibition properties of the polymer were indirectly assessed by intracellular retention of DOX in C6, A549, and HeLa cells. The cells were seeded in a four-well plate at a density of $1x10^4$ cells/ well and kept overnight at 5% CO_2 incubation. The desired polyplexes ratio of PPMSS i.e. 3:1 and 4:1 was prepared following complexation with ctDNA. The addition of polyplexes to the cells and further processing are as similar as detailed in section 3.1.12.2.

3.2.12.2 Efflux pump inhibition studies using flow cytometry

The efflux pump inhibition of the polymer, PPMSS was determined and quantified by means of flow cytometry analysis. Here, the percentage of cells retaining DOX was determined and both P-gp overexpressed cells C6 and A549 and P-gp negative cells HeLa was used for the study. The cells were seeded in a 48-well plate at a density of $1x10^4$cells/ well and incubated overnight in 5% CO_2 incubator. The method is as same as detailed in the previous section (3.1.12.3).

3.2.12.3 DOX retention studies

The DOX retention kinetics was determined in C6, A549, and HeLa cells. Briefly, the cells were seeded ($1x10^4$ cells/well) in a 48 well plate and incubated overnight. The polyplexes ratio used for this study was PPMSS 3:1 and 4:1 prepared in Ham's F12 medium. The experiment was performed as similar as detailed in the previous section 3.1.12.4.

3.3 Synthesis and characterization of pullulan-PEI-3,3 dithiodipropionic acid (PPDPA)

3.3.1 Materials

Pullulan (Fluka), polyethylenimine (PEI; MW 25,000 Da), 3, 3 dithidipropionic acid, carbonyl diimidazole (CDI), 1-ethyl-3-[3-dimethyl aminopropyl) carbodiimide hydrochloride (EDC), were all purchased from Sigma–Aldrich Chemicals Co, USA. The remaining chemicals were all similar as detailed in section 3.1.1.

3.3.2 Synthesis of Pullulan-PEI

The synthesis of pullulan-PEI, the ratio of pullulan to PEI used and the subsequent steps of the reaction and dialysis were as similar as detailed in section 3.1.2.

3.3.3 Synthesis of pullulan-PEI-3, 3 dithiodipropionic acid

The thiolation of pullulan-PEI was carried out by conjugating with 3,3 dithiodipropionic acid (DPA). Different amounts (30mg,40mg,50mg) of 3,3 dithiodipropionic acid were conjugated with a known amount of pullulan-PEI (100mg) using the crosslinker EDC (0.1M) in pH6.0 and subjected to overnight stirring at room temperature. The experiment protocol was as similar as detailed in section 3.1.3. The pullulan derivatives thus formed were PPDPA I, II and III based on the initial amount of DPA used for conjugating pullulan-PEI.

3.3.4 Synthesis of the control group (PEI-3, 3 dithiodipropionic acid)

The control groups were synthesized by using PEI and 3, 3 dithiodipropionic acid (DPA) alone, where the amount of PEI and DPA took was as similar to that detailed in section 3.3.3. The experiment protocol was as similar as detailed in section 3.1.4.

3.3.5 Physicochemical characterization

3.3.5.1 Determination of disulfide/thiol content

The disulfide/ thiol content of the pullulan based polymers (PPDPA I, II, III) and its corresponding controls (PDPA I, II, III) was determined using a standard protocol as detailed in

the previous section (3.1.6.1). Briefly, the polymers both PPDPAs and PDPAs were prepared at a concentration of 1mg/mL and the disulfide content was analyzed by using 2-nitro 5-thiosulfobenzoate (NTSB). The free thiol content of the polymers i.e. PPDPAs and PDPAs was measured after reducing the disulfide linkage by sodium borohydride (section 3.1.6.1.) and recorded in UV spectrophotometer (Varian Cary, USA) at a wavelength of 412nm.

3.3.5.2 Determination of amino content by $CuSO_4$ assay

The free amino content of the pullulan based polymers i.e. PPDPA I, II and III and its control groups i.e. PDPA I, II & III were evaluated using $CuSO_4$ assay. The sample and control polymers were prepared at a concentration of 1mg/mL. The reaction protocol is as similar to that mentioned in section 3.1.6.2.

3.3.5.3 FTIR analysis

The FTIR spectra of pullulan-PEI, PPDPA II and its corresponding control group PDPA II were recorded using a Fourier Transform Infrared spectrometer (Nicolet Impact 410) over an ATR scan range of 500-4000 cm^{-1}.

3.3.5.4 ^1H NMR

^1H NMR spectra of PPDPAII and PDPA II were measured in D_2O using 500 MHz spectrometers (Bruker Avance).

3.3.6 Determination of buffering capacity

The buffering capabilities of PPDPA I, II and III polymers and PDPA I, II and III polymers were determined by acid-base titration over a pH range of 10 to 4. Each polymer of concentration 0.1mg/mL were titrated against 0.01N HCl. The protocol was as similar as mentioned in section 3.1.7.

3.3.7 Formation of nanoplexes

Nanoplex solutions (1mL) of different polymer to DNA weight ratios (1:1 to 5:1) were prepared by mixing and vortexing a varying quantity of PPDPA I, II, III, and PDPA I, II, III polymer with a fixed amount of ctDNA (10 µg) for 30sec. The total volume was made up to 1mL with distilled water and kept for incubation for 20 min in the room temperature.

3.3.7.1 Determination of particle size and zeta potential

The hydrodynamic size and zeta potential of the PPDPAI, II, III, and PDPAI, II, III nanoplexes (detailed in section 3.3.7) were measured using Zetasizer Nano ZS (Malvern Instruments Ltd., UK) at a temperature of 25°C. The size of the nanoplexes expressed in terms of mean diameter (z average).

3.3.7.2 Gel retardation assay

The ability of the polymer to condense calf thymus DNA was analyzed by gel retardation assay. The nanoplexes of different pullulan based polymers i.e. PPDPA I, II III and its corresponding control groups i.e PDPA I, II, III were prepared as mentioned in section 3.3.7 and the experiment was carried out as similar as mentioned in section 3.1.8.2.

3.3.7.3 Effect of DTT on the stability of thiolated polyplexes

The stability of the nanoplexes in presence of the reducing agent, DTT was assessed by DLS measurement and agarose gel electrophoresis. Initially the desired nanoplexes ratios of PPDPA I (10:1 & 25:1), PPDPA II (3:1 & 4:1), PPDPAIII (3:1 & 4:1) and PDPA I, PDPAII and PDPAIII (all with polyplexes ratio 3:1 and 4:1) were formed and incubated with 10mM DTT prepared in 150mM NaCl. The change in particle size and subsequent release of DNA in presence of DTT and/or DTT heparin was analyzed as mentioned in the previous section 3.1.8.3.

3.3.8 PAGE analysis

The serum protein interaction of PPDPA polymers and its control group, PDPA was determined by PAGE. Each polymer with concentration 1mg/mL was prepared, of which 100µl were taken and incubated with 20 µl each of the FBS (diluted with saline) and placed for incubation for 30min. The experiment protocol was as similar as detailed in section 3.1.9.

3.3.9 Cell culture studies

Cell culture studies were performed in C6, A549, HeLa cells, and the normal fibroblast cell, L929. The culture medium used for each cell lines varies and was as similar as detailed in section 3.1.10.

3.3.9.1 In vitro cytotoxicity (MTT assay)

MTT assay was performed to examine the cytotoxicity of the selected nanoplexes ratios of PPDPA I, II, III, and PDPA I, II and III in C6, A549, HeLa and, L929 cells. The nanoplexes ratios were PPDPA I (10:1 & 25:1), II and III (both 3:1 & 4:1) and the control groups such as PDPA I, II and III (all 3:1 & 4:1). The cells were each seeded in 96 well plates at a density of $1x10^4$ cells/well. After 24hrs, the cells were exposed to selected nanoplexes ratios of PPDPAs and PDPAs for another 24hrs. The experiment protocol was similar to that detailed in section 3.1.10.1.

3.3.9.2 Uptake studies using confocal microscopy

The cellular uptake studies were carried out in C6 cells. The cells were seeded in four well plates ($1x10^4$ cells/well) and incubated overnight. Initially, the ctDNA was tagged with YOYO-iodide and kept for 1hr. The nanoplexes of PPDPA I (10:1 & 25:1), PPDPA II (3:1& 4:1), PPDPA III (3:1 & 4:1) and the control groups PDPA I (3:1 & 4:1), PDPA II (3:1 & 4:1), PDPA III (3:1 &4:1) were prepared with YOYO tagged ct DNA (2.5µL of 10µM YOYO for 1µg DNA/well) in

Ham's F12 serum-free medium and the protocol was as similar to that mentioned in section 3.1.10.2.

3.3.9.3 Uptake studies using flow cytometry

The cellular uptake of the above-mentioned nanoplexes was quantified via flow cytometry. The treatment of nanoplexes to C6 cells was as similar as detailed in the previous section (3.3.9.2) and the experiment protocol was as similar to that mentioned in section 3.1.10.3.

3.3.9.4 Pathway studies using endocytosis inhibitors

The uptake pathways of nanoplexes to the cells were determined by using endocytosis inhibitors chlorpromazine, filipin, and amiloride. The representative polyplex of PPDPA II i.e. 4:1 ratio was used for the study. The protocol is as similar as detailed in section 3.1.10.4.

3.3.9.5 Polymer trafficking studies

The PPDPA polymer trafficking into the C6 cells was analyzed by tagging the representative polymer, PPDPAII with rhodamine. The polyplexes were prepared by complexing with the rhodamine-labeled polymer, PPDPA II and YOYO-I tagged DNA at 4:1 ratio. The experiment was performed as detailed in the section 3.1.10.5.

3.3.10 *In vitro* transfection efficiency

The transfection efficiency of the polymer PPDPA I, II and III was analyzed after complexing with the p53 plasmid. The experiment was performed in C6 glioma cells. The nanoplexes of PPDPA I (10:1 & 25:1), PPDPA II (3:1 & 4:1) and PPDPA III (3:1 & 4:1) were used for the study. Different methods were adopted to assess cell death mediated by p53 transection i.e. live and dead assay, PI staining, Annexin V/ FITC staining and p53 immunofluorescence.

3.3.10.1 Live and Dead assay

The transfection efficiency of the polymer was assessed using p53 plasmid. The nanoplexes of PPDPA I (10:1 & 25:1), PPDPA II (3:1 & 4:1) and PPDPA III (3:1 & 4:1) were prepared by complexing with the p53 plasmid in Ham's F12 medium. Live and dead assay were performed as per the manufacturer protocol as detailed in the previous section 3.1.11.1.

3.3.10.2 PI staining

The cell death mediated by p53 transfection was quantified by PI staining. The polymers (PPDPA I, II, III) were complexed with the p53 plasmid in the desired polyplex ratios i.e. PPDPA I (10:1 and 25:1), PPDPA II (3:1 and 4:1), PPDPA III (3:1 and 4:1). The experiment conducted was as similar as detailed above (section 3.1.11.2).

3.3.10.3 Annexin V/FITC staining

The p53 mediated apoptosis following transfection in C6 cells using pullulan derivatives PPDPA I, II and III were analyzed by annexin V/FITC staining. The transfection studies were carried out using the desired polyplexes ratios of PPDPA I (10:1 & 25:1), PPDPA II (3:1& 4:1) and PPDPA III (3:1 and 4:1) using p53 plasmid. The experiment was performed as per the protocol detailed in section 3.1.11.3.

3.3.10.4 p53 immunostaining

The immunostaining technique was used to determine the expression of p53 in C6 cells following PPDPA nanoplexes mediated transfection. The nanoplexes used for the study is PPDPA I (25:1), PPDPA II (4:1) and PPDPA III (4:1) and the experiment was conducted as per the protocol detailed in section 3.1.11.4.

3.3.11 Efflux pump studies

The efflux pump inhibition property of the polymer was analyzed by using confocal and flow cytometry. Herein, both P-gp expressed cells i.e C6 and A549 and P-gp negative cells i.e. HeLa was used. Different nanoplexes of PPDPA I (10:1 & 25:1), PPDPA II (3:1& 4:1) and PPDPA III (3:1 & 4:1) were selected for the study.

3.3.11.1 Efflux pump inhibition studies using confocal microscopy

The efflux pump inhibition properties of the polymer were demonstrated in P-gp expressing cell lines such as C6 and A549 and P-gp negative cell line, HeLa. The selected polyplex ratios of PPDPA I (10:1 and 25:1), PPDPA II (3:1 and 4:1) and PPDPA III (3:1 and 4:1) were used for the study. The experiment conducted was as similar as detailed in section 3.1.12.2.

3.3.11.2 Efflux pump inhibition studies using flow cytometry

The efflux pump inhibition studies were carried out in C6, A549, and HeLa cells where the selected nanoplexes used were PPDPA I (10:1 and 25:1), PPDPA II (3:1 and 4:1) and PPDPA III (3:1 and 4:1). The anticancer drug used was DOX (3µM). The experiment was conducted as per the protocol detailed in section 3.1.12.3.

3.3.11.3 DOX retention studies

The DOX retention kinetics was assessed in different cell lines such as P-gp positive cells, A549 and C6 and Pgp negative cell, HeLa. The cells were seeded at a density of $1x10^4$ cells/well in 48 well plates and incubated overnight. The selected nanoplexes i.e. PPDPA I (10:1 and 25:1), PPDPA II (3:1 and 4:1) and PPDPA III (3:1 and 4:1) were added to these cells and incubated for 2hrs. This was then followed by the addition of DOX (3µM). The experiments were conducted as per the protocol detailed in section 3.1.12.4.

3.4 Synthesis and characterization of pullulan-PEI-3,3 dithiodibutyric acid (PPDBA)

3.4.1 Materials

Pullulan (Fluka), polyethyleneimine (PEI; MW 25,000 Da), 4,4 dithidibutyric acid (DBA), carbonyl diimidazole (CDI),1-ethyl-3-[3-dimethyl aminopropyl) carbodiimide hydrochloride (EDC), were all purchased from Sigma–Aldrich Chemicals Co, USA. The remaining chemicals were all similar as detailed in section 3.1.1.

3.4.2. Synthesis of pullulan-PEI

The synthesis of pullulan-PEI is detailed in the section (3.1.2). Briefly, the hydroxyl group of pullulan was activated by CDI to form active imidazolyl carbamate intermediate which further reacts with the amino group of PEI to form pullulan-PEI.

3.4.3 Synthesis of pullulan-PEI-4, 4 dithiodibutyric acid (PPDBA)

The thiolation of pullulan-PEI was carried out by conjugating with 4, 4 dithiodibutyric acid (DBA). Different amounts (30mg,40mg,50mg) of DBA were conjugated with a known amount of pullulan-PEI (100mg) using the crosslinker EDC (0.1M) and subjected to overnight stirring at room temperature at pH 6. Dialysis was performed in PBS (pH 7.4). The pullulan derivatives thus formed were coded as PPDBA I, II and III based on the initial amount of DBA used for conjugating pullulan-PEI.

3.4.4 Synthesis of the control group (PEI-4, 4 dithiodibutyric acid)

The control groups were synthesized by using PEI and 4,4 dithiodibutyric acid (DBA) alone, where the amount of PEI used was 200mg and DBA was 30mg, 40mg, and 50mg as given in the previous section (3.4.3). The EDC coupling (0.1M) reaction was carried out to conjugate PEI and DBA as mentioned above. Further, dialysis was performed against PBS at pH 7.4. The control groups are named PDBA I, II and III, based on the amount of DBA used for conjugating with PEI.

3.4.5 Physicochemical characterization

3.4.5.1 Determination of disulfide/thiol content

The disulfide/ thiol content of PPDBA I, II, III and its corresponding controls PDBA I, II, III was determined using a standard protocol as detailed in the previous section (3.1.6.1). Briefly, the pullulan based polymers, PPDBA I, II, III and its controls, PDBA I, II, III were prepared at a concentration of 1mg/mL and the disulfide content was analyzed by using 2-nitro 5-thiosulfobenzoate (NTSB) at a wavelength of 405nm in a microplate reader (Synergy H1, USA). The free thiol content of both pullulan derivatives and its controls were analyzed after reducing with sodium borohydride as detailed in section 3.1.6.1. The thiol content was recorded using UV spectrophotometer (Varian Cary, USA) at a wavelength of 412nm.

3.4.5.2 Determination of amino content by $CuSO_4$ assay

The free amino content of the pullulan derivatives such as PPDBA I, II, III and its corresponding controls i.e PDBA I, II, III were evaluated using $CuSO_4$ assay. The sample and control polymers were prepared at a concentration of 1mg/mL. The reaction was carried out as similar as that mentioned in section 3.1.6.2.

3.4.5.3 FTIR analysis

The FTIR spectra of pullulan-PEI, PPDBA I, II and III, PDBA I, II, III were recorded using a Fourier Transform Infrared spectrometer (Nicolet Impact 410) over an ATR scan range of 500-4000 cm^{-1}.

3.4.5.4 ^1H NMR

^{1}H NMR spectra of PPDBA and PDBA were analyzed in D_2O using 500 MHz spectrometers (Bruker Avance).

3.4.6 Determination of buffering capacity

The buffering capacity of the pullulan derivatives PPDBA I, II and III and its corresponding controls PDBA I, II and III were determined by acid-base titration over a pH range of 10 to 4. Each polymer of concentration 0.1mg/mL was titrated against 0.01N HCl, where the solution was initially made up to a pH of 10 using 0.2 N NaOH. The change in pH was noted after each addition of a volume of 50 µL of acid. A graph was plotted with pH against the volume of 0.1N HCl used and assessed the buffering capacity.

3.4.7 Nanoplex preparation

Nanoplexes of different weight ratios ranging from 1:1–5:1 were prepared by mixing an increasing amount of polymers PPDBA I, II, III, and PDBA I, II and III with a constant amount of DNA (10 µg). The total volume was made up to 1mL with distilled water. The complex was mixed by vortexing for 30sec and kept for incubation for 20 min at room temperature.

3.4.7.1 Determination of particle size and zeta potential

The hydrodynamic size and zeta potential of the PPDBAI, II, III, and PDBAI, II, III nanoplexes were measured using Zetasizer Nano ZS (Malvern Instruments Ltd., UK) at a temperature of 25°C. The preparation of nanoplexes is detailed in the above section 3.4.7. The size of the nanoplexes expressed in terms of mean diameter (z average).

3.4.7.2 Gel retardation assay

The ability of the polymer to condense DNA and its stability was assessed by agarose gel electrophoresis. The nanoplexes of PPDBA I, II, III and its control groups PDBA I, II, III were prepared and electrophoresis was carried out as detailed in section 3.1.8.2. The stability of

nanoplexes in presence of serum was also determined via electrophoresis as detailed in section 3.1.8.2.

3.4.7.3 Effect of DTT on the stability of thiolated polyplexes

The nanoplexes stability in the presence of reducing environment was assessed by incubating different nanoplexes of polymer, PPDBA I, II and III and PDBA I, II and III with 10mM DTT prepared in 150mM NaCl. The polyplexes were then incubated for different time periods such as 30 min, 1, 2, 3, and 4 hrs. The change in particle size and subsequent release of DNA in presence of DTT and/or DTT heparin was analyzed as mentioned in the previous section 3.1.8.3.

3.4.8 PAGE analysis

The native PAGE was performed to assess the interaction of serum proteins with the polymers, PPDBA I, II, III, and PDBA I, II, III. PEI incubated with serum and serum alone (both diluted with normal saline) was considered as negative and positive controls respectively. The experimental protocol was as similar as mentioned in section 3.1.9.

3.4.9 Cell culture studies

Cell culture studies were performed in C6, A549, HeLa cells, and L929 cells. The culture medium used for C6 was DMEM/Ham's F12: MEM (1:1). The medium for A549 and HeLa was DMEM and MEM respectively. The culture medium for L929 was MEM. All medium contained 10% FBS and 1% antibiotic-antimycotic. The cells were grown at 37°C using a 5% CO_2 incubation.

3.4.9.1 In vitro cytotoxicity (MTT assay)

The cytotoxicity of the selected nanoplexes ratios of PPDBA I (3:1& 4:1), PPDBA II (3:1 & 4:1), PPDBAIII (3:1 & 4:1), and PDBA I (3:1 & 4:1), PDBA II (3:1 & 4:1),PDBA III (3:1& 4:1)

were analyzed using MTT assay. The cancer cell lines such as C6 cells, A549, HeLa and the fibroblast cell, L929 were used for the study. The effect of the PPDBA/PDBA nanoplexes on the viability of these cells was assessed. The experiment was carried out as detailed in the previous section (3.1.10.1).

3.4.9.2 Uptake studies using confocal microscopy

The cellular uptake of nanoplexes was carried out in C6 cells by initially tagging the ctDNA with YOYO-I (2.5µL of 10µM YOYO for 1µg DNA/well) and kept for 1hr incubation. The cells were seeded in four well plates ($1x10^4$ cells/well) and incubated overnight. The nanoplexes of PPDBA I (3:1 & 4:1), PPDBA II (3:1 & 4:1) and PPDBA III (3:1 & 4:1) and its controls PDBA I, II, III (all 4:1 ratio) was prepared by complexing polymer and YOYO tagged DNA in Ham's F12 medium and the protocol was as similar as that mentioned in section 3.1.10.2.

3.4.9.3 Uptake studies using flow cytometry

The cellular uptake of the PPDBA and PDBA nanoplexes was quantified via flow cytometry. The experiment was carried out in C6 cells and the protocol was as detailed in the previous section (3.4.9.2). The flow cytometry analysis was the same as mentioned in section 3.1.10.3.

3.4.9.4 Pathway studies using endocytosis inhibitors

The cellular uptake pathways of the PPDBA nanoplexes into the C6 cells were analyzed by using inhibitors such as chlorpromazine, filipin, and amiloride. The representative polymer chosen for this study was PPDBA II 4:1 ratio. The experiment was conducted as same as that detailed in the section 3.1.10.4.

3.4.9.5 Polymer trafficking studies

The polymer trafficking into the cells was analyzed by tagging the PPDBA polymer with rhodamine. The polymer after conjugating with rhodamine was complexed with YOYO tagged

DNA to form the nanoplexes. The representative polymer chosen for this study was PPDBA II 4:1 ratio and the experiment was as similar as detailed in the section 3.1.10.5.

3.4.10 *In vitro* transfection efficiency

The transfection efficiency of the polymer PPDBA I,II and III were analyzed after complexing with p53 plasmid. The experiment was performed in C6 glioma cells. The nanoplex of PPDPA I (3:1 & 4:1), PPDPA II (3:1 & 4:1) and PPDPA III (3:1 & 4:1) were used for the study. Different methods were adopted to assess the cell death i.e. live and dead assay, PI staining, Annexin V/ FITC staining and p53 immunofluorescence.

3.4.10.1 Live and Dead assay

The live and dead assay was performed after complexing the PPDBA I,II, III polymers with the p53 plasmid. The nanocomplexes were then transfected to C6 cells. The nanoplexes were prepared by complexing the polymer with the p53 plasmid at ratios 3:1 and 4:1. The experiment was done as per the protocol detailed in section 3.1.11.1.

3.4.10.2 PI staining

The cell death by the polymer mediated p53 transfection was analyzed by means of PI staining. The nanoplexes of PPDBA I, II, III, were prepared using p53 plasmid at ratio 3:1 and 4:1. The protocol is the same as mentioned previously (3.1.11.2). The cell death was determined by PI staining using flow cytometry (BD FACS Aria).

3.4.10.3. Annexin V/FITC staining

The p53 mediated apoptosis following transfection in C6 cells using pullulan derivatives PPDBA I, II and III were analyzed by annexin V/FITC staining. The transfection studies were carried out using the desired polyplexes ratios of PPDBA I, II and III (all with the polymer to DNA

ratios 3:1 and 4:1) using p53 plasmid. The experiment was performed as per the protocol detailed in section 3.1.11.3.

3.4.10.4 p53 immunostaining

The immunostaining technique was used to determine the expression of p53 in C6 cells following PPDBA nanoplexes mediated transfection of p53. The nanoplexes used for p53 immunostaining was PPDBA I (4:1), PPDBA II (4:1) and PPDBA III (4:1) ratio. The experiment was performed as similar as mentioned in section 3.1.11.4.

3.4.11 Efflux pump inhibition studies

The ability of the thiolated polymer to inhibit efflux pump in cancer cells were analyzed by evaluating DOX retention in these cells following treatment with PPDBA polyplexes and DOX. The experiment was performed in three cell lines where both C6 and A549 were taken as P-gp over expressed cells and HeLa as Pgp-negative cell line.

3.4.11.1 Efflux pump inhibition study using confocal microscopy

The P-gp inhibition was determined by assessing the intracellular retention of DOX in various cell lines viz. C6, A549, and HeLa. The nanoplexes of PPDBA I, II, III were formed after complexing the polymer with ctDNA at a polymer to DNA ratios 3:1 and 4:1. The experiment was performed as detailed section 3.1.12.2.

3.4.11.2 Efflux pump inhibition study using flow cytometry

The efflux pump inhibition studies were carried out in cancer cell lines such as C6, A549, and HeLa where the retention of DOX in these cells was quantified by using flow cytometry. The

nanoplexes used for this study involves PPDBA I, II, III (all 3:1 and 4:1 ratio). The experiment details were as same as mentioned in section 3.1.12.3.

3.4.11.3 DOX retention studies

The DOX retention kinetics was assessed in different cell lines as mentioned previously (section 3.4.11.2). The nanoplexes used for the study involves PPDBA I, II and III with the polymer to DNA ratios 3:1 and 4:1. The experiment was performed as similar as detailed in the section 3.1.12.4.

3.4.12 Glutathione activity

3.4.12.1 Assessment of glutathione level using monochlorobimane

The C6 cells were seeded in four well plates with a density of $1x10^4$ cells per well and cultured for 24hrs at 37°C and 5% CO_2 incubation. The nanoplexes used for the study was PPDBA 4:1 ratio. Following incubation, the nanoplexes were added and kept for 2hrs. The cells were washed and replaced with fresh media. Monochlorobimane (mBCl) prepared in ethanol was added to the medium to give a final concentration of 40μM and kept the cell for 30 min in an incubator at 37°C. Following this, the cells were washed and fixed in 1% formaldehyde before carrying out imaging via confocal microscopy (NIKON AIR).

3.4.12.2 Role of glutathione in DOX retention

To further investigate the correlation between glutathione level and accumulation of DOX, intracellular glutathione concentration was further increased by preincubating the C6 cells with glutathione monoester. The C6 cells were seeded in four well plates with a density of $1x10^4$ cells per well and cultured for 24hrs at 37°C in the CO_2 incubation. The nanoplexes used for the study was PPDBA II 4:1 ratio. Initially, the cells were pretreated with glutathione monoester for 2hrs. This was followed by the addition of PPDBA II nanoplexes 4:1 ratio for 2hrs as described above.

The cells were then treated with DOX (3μM) for 24hrs. The DOX retention of this cells was compared with nanoplex and DOX-treated cells without pre-incubation with glutathione monoester. The DOX alone (3μM) treated cells was taken as controls. In this experiment, another control was set up by pretreating the cells with 2mM of buthionine sulfoximine (BSO) and incubated for 2hrs. The retention of DOX was determined by treating nanoplexes and DOX as mentioned above following the initial exposure of BSO. Following incubation, the cells were washed, fixed and digitalized using confocal microscopy (NIKON AIR). The simultaneous quantification of glutathione using mBCl and corresponding DOX concentration in these cells were carried out in the cell lysate. The fluorescence was measured using a microplate reader (Synergy H1, USA) with an excitation wavelength of 380nm and emission at 461nm.

3.4.13 Dose-response experiments

The C6/A549/HeLa cells were seeded in 24 well plates at a concentration of $1x10^4$ cells per well and incubated for 24hrs at 37°C. After overnight incubation, the cells were then washed and pretreated with PPDBA II/ctDNA of selected nanoplex ratios 4:1 for two hours. This was then followed by the addition of DOX at different concentrations viz., 0.001, 0.01, 0.1, 0.5,1,3,5 and 10 μM. The cell viability following the addition of nanoplex and DOX was determined at different time periods such as 24, 48 and 72h using MTT assay. The control group was DOX alone treated cells which are kept for different time points as mentioned above. Both IC50 and growth inhibition was calculated thereof. MTT assay was used to determine the growth inhibition, where the absorbance was measured at a wavelength of 570nm in a microplate reader (Synergy H1, USA). Cell growth inhibition was calculated by the following equation

Growth inhibition (%) = (1- As/Ac) x 100, where As is absorbance of sample and Ac is absorbance of control. All test were performed in triplicate.

The resistance factor was calculated from IC50 value at the 72 hr time point by dividing the IC50 of A549 cells by IC50 of HeLa cells.

3.4.14 Drug Release studies

The release studies were performed by intercalating DOX (5µM) with DNA(10µg) before forming the complex with the PPDBA polymer to form the nanocomplex with the ratio 4:1. The drug release studies were performed by dialysis method. The selected nanoplex ratio of PPDBA II (4:1) along with the drug DOX (5µM) was sealed in a dialysis bag (molecular weight cutoff 3000) containing a final volume of 2mL, which was immersed in 5mL of phosphate buffer (pH 7.4, pH 6.8) in a 50cc falcon tube. At predetermined time intervals, the solution in every flask was drawn periodically (200µL) and refilled with the same volume of fresh medium. Free DOX content was determined by fluorescence measurement using microplate reader (Synergy H1, USA).

Percent DOX released from the nanoplex was calculated using the fluorescence of free DOX as standard.

3.4.15 Immunostaining of membrane P-gp in C6 cells

The immunostaining of P-gp was carried out in 3 different cell lines C6, A549 (Pgp positive) and HeLa (Pgp negative). The cells were seeded in a four-well plate at a density of $1x10^4$ cells per well and incubated at 37°C at 5% CO_2 incubation. The nanoplex ratios of PPDBA II 4:1 was chosen for this study. The nanoplexes were added to the cells and incubated for 2hrs. This has further followed by the treatment of cells with DOX (3µM) for another 24hrs. Two controls were set up i.e cell alone and DOX-treated. Following this, the cells were washed with PBS (pH 7.4) three times and fixed by using 1% formaldehyde in PBS. This was again washed with PBS and incubated using 250µL of 1% BSA in PBS for 30 min at room temperature. The blocking solution was removed and the cells were incubated with 250µL of Pgp primary antibody (0.1µg/mL) at 4°C

overnight. The antibody was removed and treated with BSA as before. Following the removal of blocking solution, the FITC labeled secondary antibody was added and kept for 1hr in the dark. The cells were then washed with PBS (pH 7.4) and digitalized using confocal microscopy (NIKON AIR).

3.4.16 The synergetic effect of p53 in augmenting DOX sensitivity in C6 glioma cells

Initially, C6 cells were seeded in 24 well plates and incubated for 24hrs with the cell density of $1x10^4$ cells per well in a 5% CO_2 incubator at 37°C. After 24h incubation, the cells were washed and the nanoplexes PPDBA II/p53 4:1 were added. The cells were initially transfected with p53 plasmid as detailed in section 3.4.10.1. The cells were then treated with the nanoplex and incubated for 5hrs. Following this, the medium was replaced with fresh media (DMEM/Ham's F12: MEM (1:1)) and treated with different concentrations of DOX such as 0.5μM,1 μM and 1.5 μM and incubated for another 24hrs. The cells were washed, harvested and the percent cell death was analyzed by flow cytometry (FACS Aria). The cell death was measured via PI staining as detailed in section 3.1.11.2.

3.5 In vivo biodistribution and antitumor efficacy of pullulan-PEI-4,4 dithiodibutyric acid (PPDBA) in mice model

3.5.1. Preparation of PPDBA/ctDNA-DOX nano complex

The PPDBA nanoplex containing DOX was prepared by mixing a fixed quantity of ctDNA (10μg) with DOX (5μM) and kept for incubation for 20 min. The polymer was then added to the ctDNA-DOX complex in 4:1 ratio and the complex was vortexed for 30 sec and incubated for 20 min at room temperature. The resultant PPDBA/ctDNA-DOX was analyzed for hydrodynamic size and zeta potential using Zetasizer Nano ZS (Malvern Instruments Ltd., UK) at a temperature of 25°C.

3.5.2 *In vivo* organ distribution studies of polymer

The polymer, PPDBA of concentration 1mg/mL was conjugated with NIR fluorophore (0.083µg/mg polymer). The NIR fluorophore used was DYLight 750 NHS ester, where it was initially dissolved in DMF (1mg/mL), and an appropriate amount of the reagent was added to the polymer in a reaction tube (for 1mL polymer solution (1mg/mL),8.3µL dye was used) mixed well and incubated for 1hr in room temperature. To remove the unreacted polymer, dialysis was carried out in borate buffer of pH 8.5. The reaction mixture was stored at 4°C, away from light. The nanoplexes labeled PPDBA II was formed by complexing with ctDNA in the ratio 4:1. The complex was then injected via the tail vein of BALB/c mice. The nanoparticle biodistribution kinetics in different organs and clearance was imaged at different time points such as 3h, 6h, 24 and 48hr using live animal imaging system (Xenogen IVIS 200). Three animals each were used for different time points. Imaging was carried out after anesthetizing the animal by intraperitoneal injection of 5mg/kg xylazine and 80mg/kg ketamine. The animal was then dissected and harvested the tissues such as brain, heart, lungs, liver, spleen, and kidney and imaged using the live animal imaging system (Xenogen IVIS 200). Similarly, quantification of the tagged polymer PPDBA II (4:1) in different organs was carried out, where the polymer was tagged with rhodamine NHS ester as mentioned in the previous section 3.4.9.5. The nanoplexes were formed by mixing ctDNA with the tagged polymer. The nanoplexes of PPDBA II 4:1 were injected into the mice tail vein. The animals were dissected following euthanization in CO_2 chamber. Different organs of mice such as the brain, heart, lungs, liver, spleen, and kidney were taken. A known amount of tissue portions (5mg) were homogenized in PBS (5ml) using a homogenizer. The fluorescence of the rhodamine tagged polymer was measured using a microplate reader (Synergy H1, USA) at an excitation wavelength of 480 nm and emission of 580nm.

3.5.3 Antitumor efficacy of PPDBA/p53-DOX nano complex in BALB/c mice model

The tumor was developed in BALB/c mice by injecting tumor cell lines (Dalton's lymphoma cells) suspended in Hank's balanced solution (10^7cells/100µL) into the dorsum hind foot of BALB/c mice. The experiment was started after the tumor size reached a measurable volume. The PPDBA nanoplexes containing p53 was prepared at an optimum ratio of 4:1 in normal saline and the concentration of DOX taken was 5µM, where initially the drug intercalates with the DNA as mentioned in the previous section 3.5.1. The tumor-bearing mice were divided into 4 groups (Table 1) and were given different treatment as mentioned in the Table. The total volume for injection was 200µL, given as single in every alternate day for 35 days. The efficacy of these nanoparticles in reducing the tumor volume was analyzed. The tumor volume was determined by measuring the three orthogonal diameters (d) of the tumors using an ellipsoid volume formula: V=L x W x H x π/6. The survival curve was also plotted.

Sl.No.	Groups
I	Saline alone treated control
II	Dox (5µM) alone treated (drug alone)
III	p53 alone treated (PPDBA/p53 4:1) (gene alone)
IV	PPDBA/p53 4:1/DOX(5µM) (gene and drug combination)

Table 1: Tumor bearing mice is divided into different groups and the treatment modalities in different groups have been mentioned, where n=3

.

CHAPTER 4 RESULTS

The study mainly focused on disulfide modified pullulan based cationic polymer to evaluate the gene delivery efficacy as well as efflux pump inhibiting property of the polymer. To

perform the same, pullulan was first conjugated with the cationic polymer PEI and then with various thiol/disulfide containing groups in varied composition. The various groups added to insert disulfide linkages to the pullulan-PEI backbone are a) Cysteine b) Mercaptosuccinic acid (both of which contain free thiol group which on oxidation form disulfide bonds) c) 3,3 Dithiodipropionic acid d) 4,4 Dithiodibutyric acid (both these contain inbuilt disulfide linkages within the molecule). The control chosen for the study is PEI modified with the corresponding thiol/disulfide molecule.

4.1 Synthesis of pullulan-PEI

Pullulan is a non-ionic polysaccharide which is non-toxic, non-immunogenic, non-mutagenic and non-carcinogenic in nature and is widely used for various biomedical applications. Polyethyleneimine (PEI) is one of most successful gene delivery vehicles, however, its toxicity remains a major obstacle for its use in *in vivo* conditions. Here, the conjugation of pullulan to PEI was carried out to minimize the cytotoxicity and improve the transfection efficiency. The conjugation of pullulan-PEI was carried out by means of CDI reaction where it activates the hydroxyl group of pullulan to form an active intermediate i.e. imidazolyl carbamate. The primary amine group of PEI removes the imidazole group from the active intermediate to form a stable carbamate linkage of pullulan-PEI.

4.1.1 Synthesis and characterization of pullulan-PEI-Cysteine (PPSS)

Pullulan based thiolated cationic polymers were synthesized by conjugating pullulan-PEI with L-cysteine. This thiolated pullulan-PEI was then subjected to oxidation resulting in PPSS I and PPSS II. Similarly, the corresponding control groups were synthesized by coupling PEI and cysteine, followed by oxidation of thiol group to form PEICYS(S-S) I and II. The parent compounds, pullulan-PEI of PPSSI and PPSSII are named as PPI and PPII respectively.

The conjugation of both PPSS and its control groups were established by ^{1}H NMR, FTIR, copper sulfate test ($CuSO_4$) and Ellman's assay. As in Table 2, more number of free amino group was visible in PPSS I compared to PPSSII and correspondingly, in the controls, PEICYS(S-S) I showed more amino content compared to PEICYS(S-S) II. Similarly, the thiol and disulfide content of the polymer was analyzed and evaluated (Table 3). Interestingly, the disulfide/thiol content was found to be higher in those polymers which contained a higher amount of PEI i.e. PPSSI and PEICYS(S-S) I compared to polymers having a lesser amount of PEI i.e. PPSS II and PEICYS(S-S) II. The amino content of the parent compound i.e PPI and PPII are higher than the corresponding pullulan based derivatives.

SL.NO	Sample ID	Amount of Amino group (mg/10mg of polymer)
1	PPSS I	3.17±0.89
2	PPSS II	2.95±0.03
3	PEICYS(S-S)I	5.11±0.024
4	PEICYS(S-S)II	4.03±0.13
5	PPI	3.89±0.08
6	PPII	3.11±0.25

Table 2: The amino content of each polymer determined via $CuSO_4$ assay

Sl.No	Sample ID	S-S linkage (mg/g of polymer)	Thiol content mg/g of polymer
1	PPSS I	71 ±0.06	86±0.01
2	PPSSII	44 ± 0.07	70 ±0.001

3	PEICYS(S-S)I	69±0.011	89 ±0.02
4	PEICYS(S-S)II	61 ±0.02	76 ±0.011

Table 3: Thiol and disulfide content of the polymers quantified by using Ellman's reaction

4.1.2 ^{1}H NMR & FTIR

The conjugation of pullulan, PEI and cysteine in PPSS and PEI and cysteine in PEICYS(S-S) was confirmed by ^{1}HNMR. The representative spectra of the same are given in Figure 6. The signals at region δ=2.5-2.6ppm indicate the characteristic group of PEI i.e, –(CH_2-CH_2-NH)n and is seen in the spectra of pullulan-PEI, PPSS I and PEICYS(S-S) I. The signals at δ=3.4-3.9 ppm, represent – (CH_2-CH_2)-of pullulan and δ=5.2-5.3 ppm indicate the anomeric proton of pullulan. Both the signals were seen in PPSSI and the parent component pullulan-PEI. On the other hand, the signals at δ=2.88 -3.01ppm represent the – (CH_2-S) of cysteine and was clearly seen in both PPSS and PEICYS(S-S) polymers.

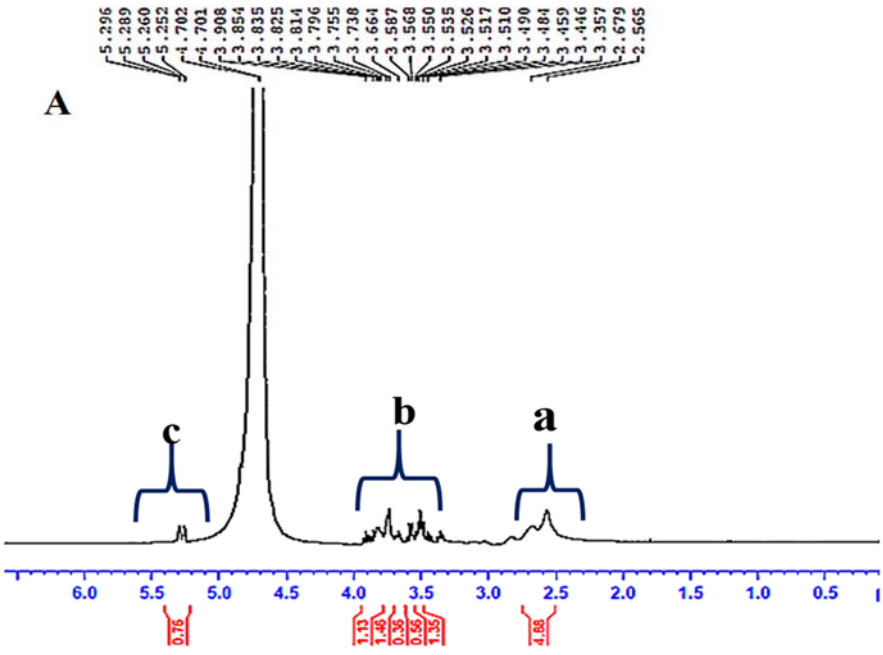

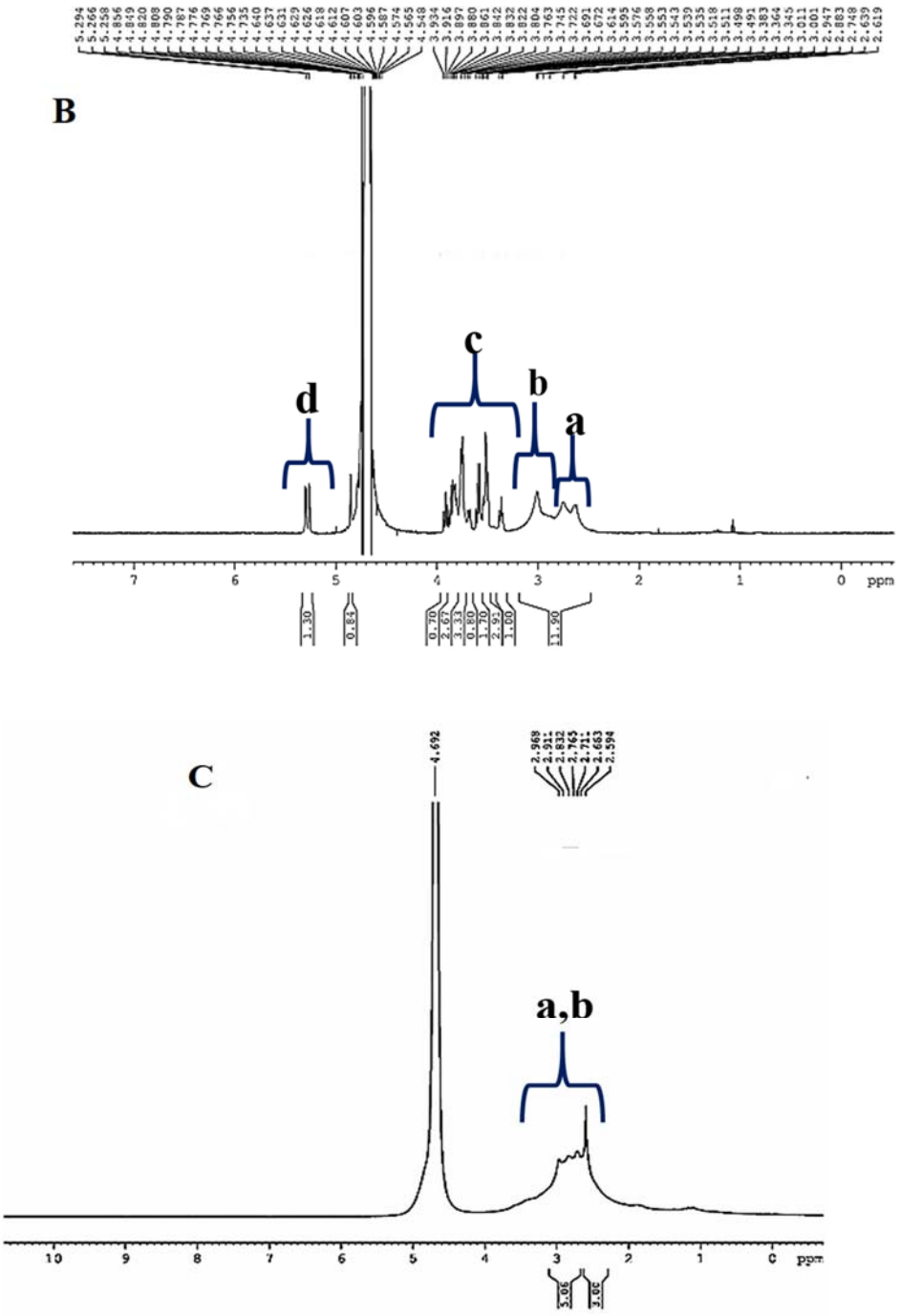

Figure 6. ^{1}HNMR spectra of A) Pullulan-PEI B) PPSS I and C) PEICYS(S-S)I where the notation a denotes the characteristic group of PEI (CH_2-CH_2 -NH)n. b represent the –(CH_2-S) of cysteine. c & d represent –(CH_2-CH_2)- and anomeric proton of pullulan respectively.

The FTIR data also confirmed the conjugation in PPSS and PEICYS(S-S). A broad absorption band visible in PPSS near 3200cm^{-1} is attributed to the –NH and –OH stretching

vibrations of pullulan and PEI. The peaks at 2931cm^{-1} and 2926 cm^{-1} seen in PPSS and PEI-CYS(S-S) respectively are indicative of the –CH stretching vibrations of PEI. Similarly, peaks at 1628cm^{-1} visible in PPSS corresponds to the C=O stretching of amide I band. The additional peaks at 1150cm^{-1} are indicating the C-O-C bond and glycosidic linkage of pullulan. Similarly, the absorption peaks at 858cm^{-1} are showing the glucopyranose unit of pullulan (Figure 7). These peaks are absent in the control groups.

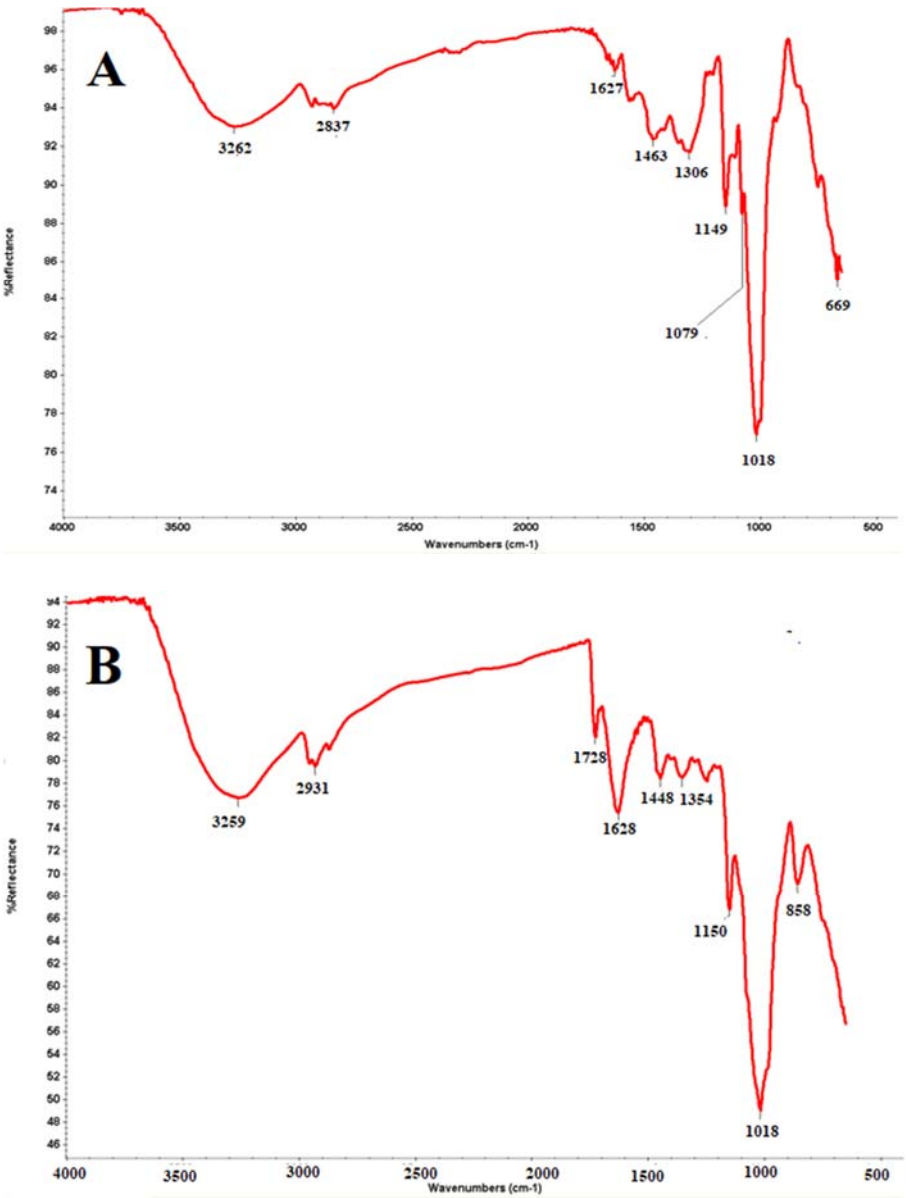

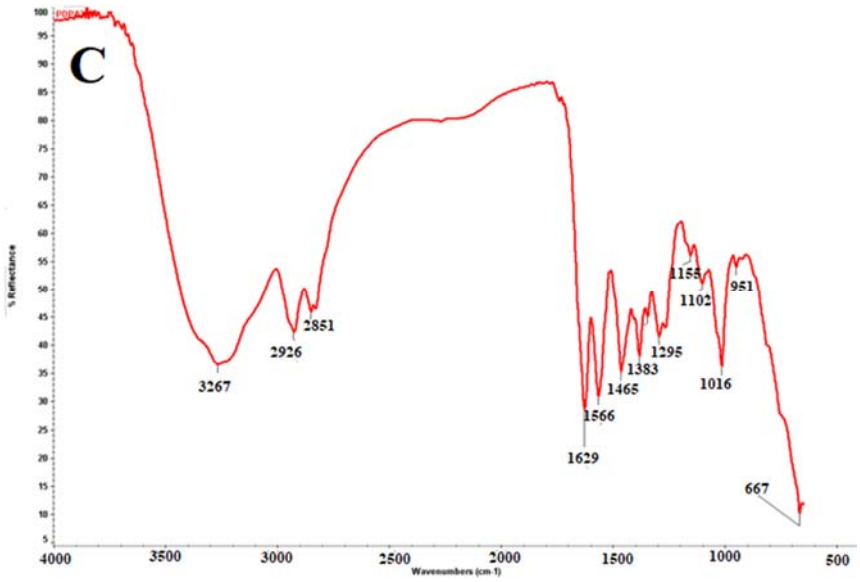

Figure 7: FTIR spectra of s A) Pullulan-PEI B) PPSSI and C) PEICYS(S-S)I

4.1.3 Buffering ability of the polymer

In this study, acid-base titration was carried out to evaluate the proton buffering capacity of the polymer, PPSS and its control PEICYS(S-S) (Figure 8). The results showed that all polymers have good buffering capacity in the pH range of 5-7, whereas normal saline showed nearly a vertical curve indicating its poor buffering ability. The titration of PPSSI and PPSSII showed a similar trend of pH change but there was a slight difference in the buffering capacity between them within the pH range of 7-4. Both the control groups PEICYS(S-S) I & II, exhibited a relatively higher buffering capacity compared to the corresponding pullulan derivatives and displayed lower buffering ability than PEI alone.

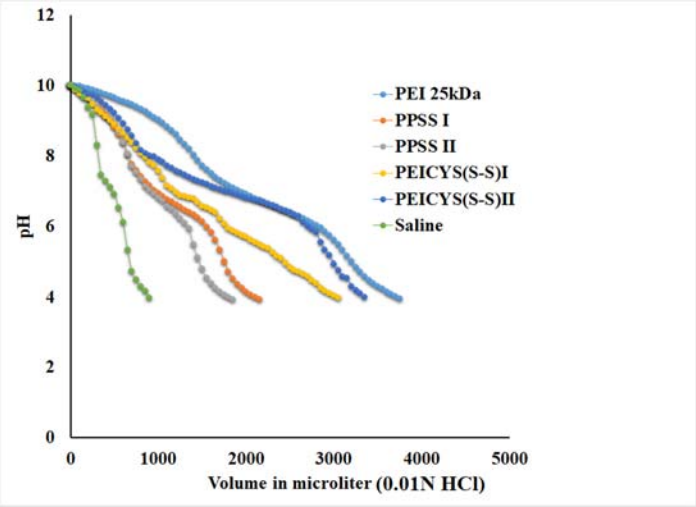

Figure 8: Buffering capacity of the polymers PEI (25KDa), PPSS I, PPSS II, PEICYS(S-S)I, PEICYS(S-S)II and saline.

4. 1.4 Biophysical characterization

4.1.4.1 Size and Zeta potential

The average hydrodynamic diameter of both the polymer nanoplexes, PPSSI, and PPSS II was in the range between 150-200nm with a polydispersity index of <0.2. It was evident from the DLS data that as the ratio of polymer increased from 1:1 to 5:1, the particle size decreased correspondingly. In the case of PPSSI, at initial ratio of 1:1, the average size was 291nm which further decreased to 164nm at 4:1. Similar observation was noted in the case of PPSS II, where at the initial ratio of 1:1, the size was observed to be 276nm, which got reduced to 151nm at the polymer to DNA ratio of 4:1. In the case of control groups, the particle size was in accordance with the previous finding, where also, the reduction was noted to be related to the polymer concentration (Figure 9). The particle size has reached as low as 78nm in the control group, PEICYS(S-S) I at the optimum ratio of 4:1, the zeta potential value was initially negative in both PPSS I and PPSS II polyplexes, which then reached >20mV.

The zeta potential for PPSSI nanoplex reached 23.7mV at 4:1 ratio. The zeta potential value for PPSSII 3:1 and 4:1 were in the range +14 to +19mV, whereas for the control group, it was >25mV.

Considering the small size and positive zeta potential value, two ratios were selected for further studies in both the groups i.e. 2:1 and 4:1 in PPSSI and 3:1 and 4:1 in PPSS II.

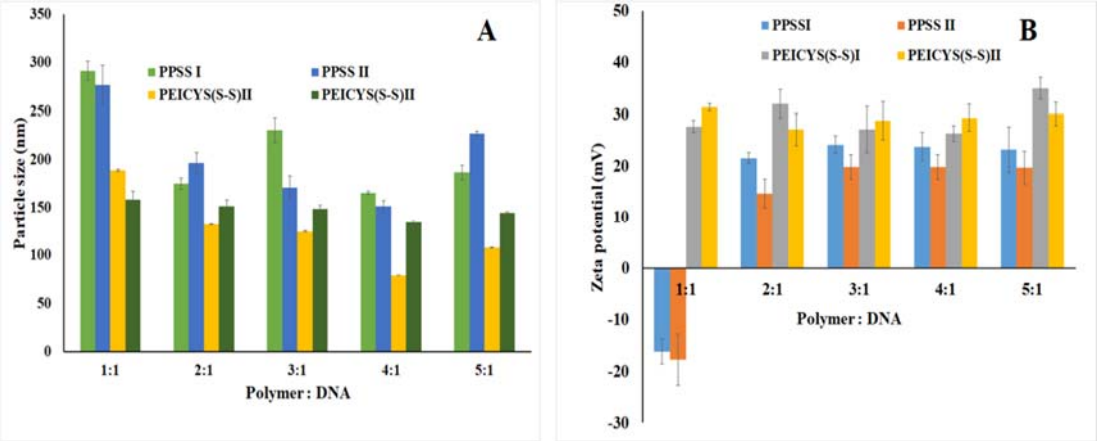

Figure 9: (A) Size measurement and (B) Zeta potential of PPSS1 and PPSSII nanoplexes with different polymer /ctDNA ratio.

4.1.4.2. Agarose gel electrophoresis

The electrophoretic mobility of the polymer/DNA polyplexes was examined to determine the ability of the polymer to stably bind the DNA (Figure 10). Both PPSS I and PPSS II nanoplexes completely inhibited the DNA mobility at all the polymer/ DNA ratios except at the initial polyplex ratio of 1:1. Complete retardation of DNA mobility was observed in all the polyplex ratios of the control group, PEICYS(S-S) I and II also. The interaction of the plasma with the selected nanoplexes ratios of both PPSS I and II also showed a similar trend where the mobility of the DNA was inhibited in all the ratios irrespective of the amount of polymer used (Figure 12).

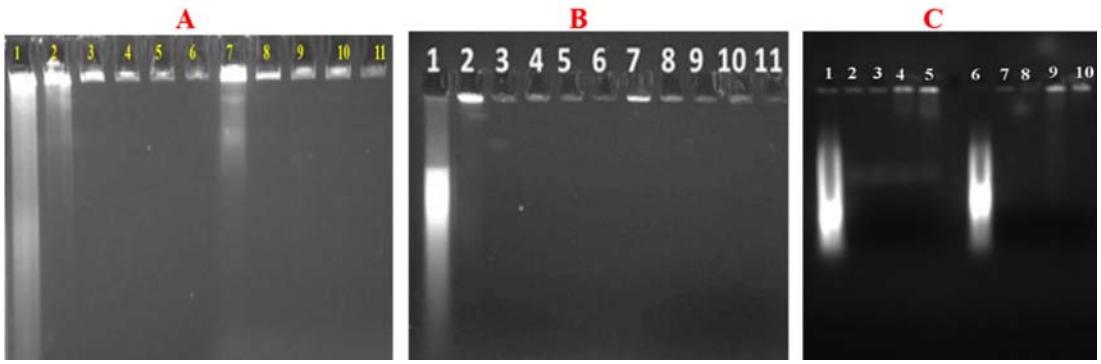

Figure 10: Agarose gel electrophoresis (A) lane 1 indicate the control ctDNA, lane 2 and 7 represent the PPSS I polymer: DNA 1:1 ratio and PPSS II 1:1 ratio respectively. Lane 3-6 indicate PPSSI 2:1-5:1 polyplex ratio and Lane 8-11 show the polyplex ratio of PPSS II 2:1-5:1.Gel (B) , lane 1 is the control ctDNA, 2-6 represent PEICYS(S-S) I polyplex with polymer: DNA 1:1 to 5:1, lane 7-11 indicate the polymer: DNA ratio ranging from 1:1 to 5:1 of PEICYS(S-S) II. The agarose gel (C) , lane 1 and 6 indicate control ctDNA and 2-5 show the PPSS I polymer: DNA ratio 2:1 to 5:1 treated with plasma and 7-11 indicate PPSS II polymer: DNA 2:1 -5:1 treated with plasma.

4.1.4.3 Nanoplex stability in presence of DTT

The reduction sensitive polymer containing polyplexes is expected to remain stable in the extracellular environment and disassemble under intracellular reducing conditions via disulfide cleavage. Therefore, the reducibility of the polymer was investigated by treating the selected polyplexes ratios of PPSS i.e. PPSS I 2:1 and 4:1 and PPSS2 3:1 and 4:1 with reducing agent DTT. The polyplexes were exposed to DTT (10mM) for different time duration and analyzed the changes in particle size. As shown in Figure 13, the particle size changed remarkably over time post exposure with DTT, where PPSSI nanoplexes, i.e. 2:1 and 4:1 showed a particle size of 123nm and 190nm respectively following 1hr exposure with DTT. In the case of PPSS II nanoplexes 3:1 and 4:1, the particle size of 258nm and 230nm were noted at the first-hour incubation with DTT. However at the 4^{th} hour, the particle size of PPSSI 2:1 and 4:1 nanoplexes increased up to 301nm and 440nm and PPSSII nanoplexes 3:1 and 4:1 increased to 425nm and 435 nm respectively. Similarly, it was observed that the size of the control groups also changed in accordance with its exposure to DTT, however, the effect was found to be lower than the pullulan based polymers (Figure 11).

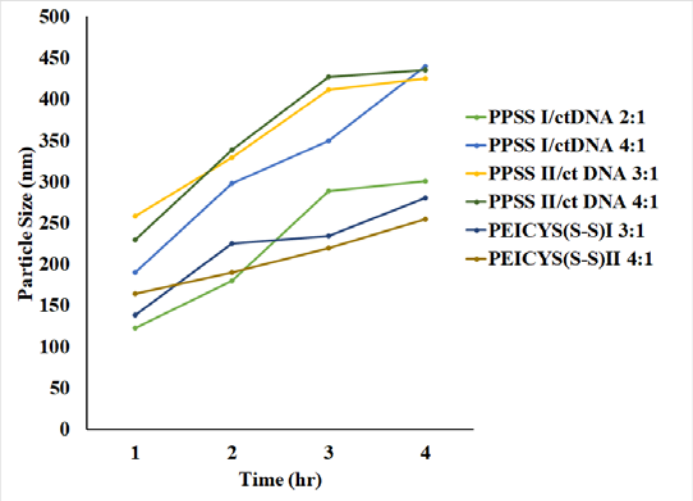

Figure 11: The change in hydrodynamic diameter of the polyplexes in presence of DTT (10mM).

However, it should be noted that the DTT untreated polyplexes of PPSSI and II maintained a particle size of <200nm and no significant change was observed over time. Furthermore, agarose gel electrophoresis was carried out to determine whether the alterations in size in response to DTT are related to the release of DNA from the polyplexes. As shown in Figure 12, following exposure with DTT, the DNA was still found to be retained in the well both in PPSS I/II and its control groups. Hence heparin (which mimick the intracellular polyanionic condition) was added along with DTT and incubated with the polyplexes. The agarose electrophoresis was carried out and observed that the DNA was released from the well (Figure 12).

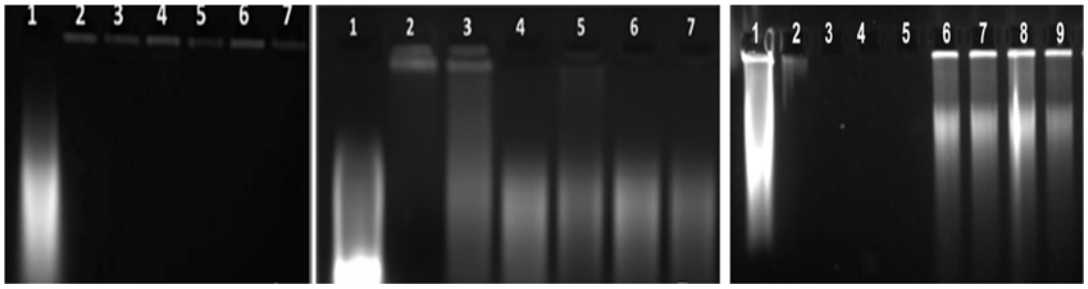

Figure 12: The agarose gel electrophoresis (left), lane 1, ctDNA alone , lane 2-4 indicate, the PPSS I nanoplex ratios 2:1 to 4:1, lane 5-7 indicates nanoplex ratios 2:1 to 4:1, all exposed with DTT(10mM). Next (middle), lane 1 indicates ctDNA, 2-4 indicate PPSS I, 2:1-4:1 polyplex ratios, 5-7 indicates PPSS II 2:1 to 4:1 polyplex ratios, all exposed with DTT/heparin. Again (right) lane

1 shows ctDNA alone, lane 2-3 PEICYS (S-S) I 3:1 & 4:1, lane 4-5, PEICYS(S-S)II 3:1 & 4:1 nanoplex ratios with DTT alone, whereas lane 6-7 and 8-9 indicates the PEICYS(S-S) I/II of 3:1 and 4:1 nanoplexes similar as above but exposed with DTT/heparin.

4.1.5 Plasma protein interaction with PPSS polymer (PAGE)

The interaction of cationic polymers i.e. PPSSI/II and PEI-CYS(S-S) I/II, with the blood proteins were analyzed by incubating the polymers with plasma for 30min. As in Figure 13, it is seen that the proteins corresponding to the globulin fraction of the plasma was totally absent in the PEI polymers and intensity of all other plasma protein bands are faint. But the intensity of the protein bands in the case of PPSSI/II was nearly same as that for the saline-treated plasma. Though the control groups i.e PEICYS(S-S) I/II also showed some reduction in the protein bands, the intensity of protein bands was not as faint as in PEI polymers..

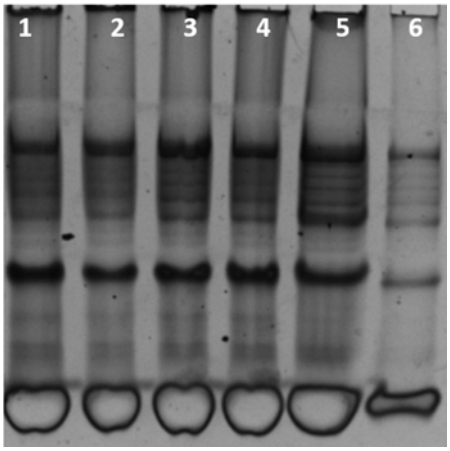

Figure 13: PAGE analysis, Lane 1 & 2: the interaction of PEICYS(S-S) I and II with plasma proteins respectively. Lane 3, 4: the plasma interaction with PPSS I and II respectively. Lane 5 is the, saline treated plasma and Lane 6 is the PEI treated plasma.

4.1.6 Biological analysis

4.1.6.1. Cytotoxicity evaluation of the polymer

The cytotoxicity of the nanoplexes of PPSSI/II and its control groups was analyzed by MTT assay where it was performed in different cell lines such as C6, A549, HeLa and the normal fibroblast cells, L929. As seen in Figure 14, the percentage viability of the cells incubated with the selected nanoplexes ratios of PPSS I and II was found to be >90% in all the cell lines tested i.e. C6, A549, and HeLa. On the other hand, the viability was found to be lower (<50%) in the

cells exposed with the selected nanoplexes ratios of the control groups such as PEICYS(S-S) I and II. Among the pullulan derivatives, the cytotoxicity of PPSS I is lower than that of PPSSII so as the case with control groups PEICYS(S-S) I and II. In L929 cells, the exposure of PPSSI/II nanoplexes exhibited a percentage viability of >85%, whereas the control group showed a viability of around 50%.

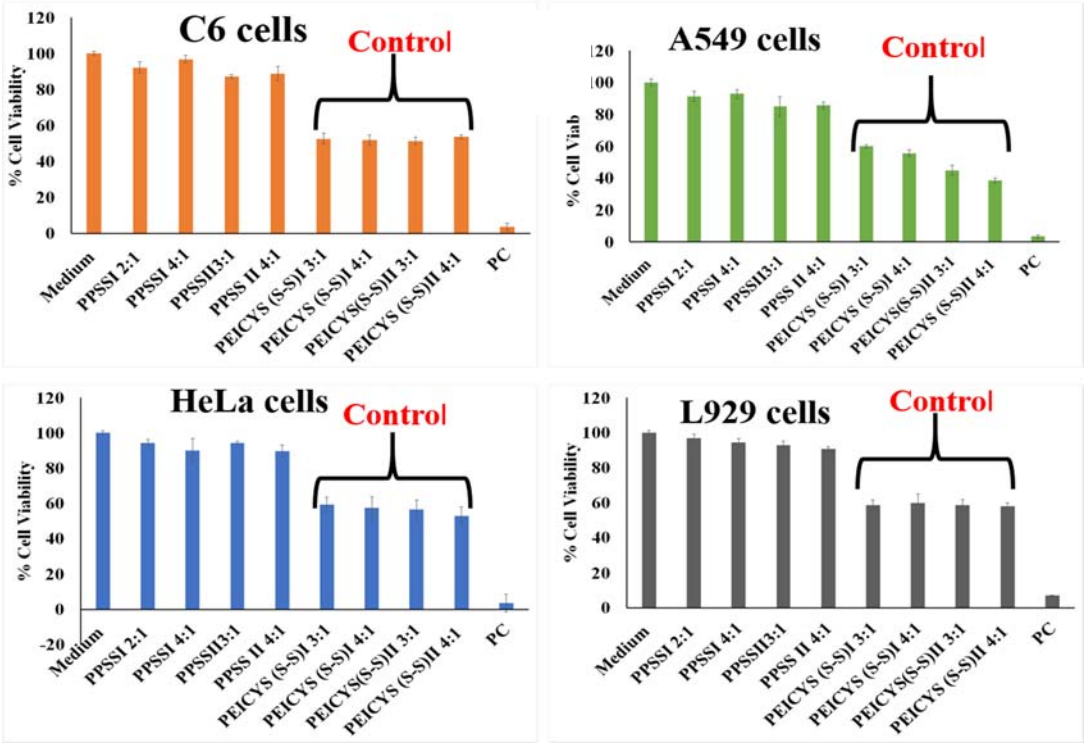

Figure 14: MTT assay of the selected nanoplexes ratios of PPSSI and II with ratios 2:1, 4:1 and 3:1, 4:1 respectively. Likewise, the cell viability was performed with the nanoplexes of PEICYS(S-S) I/II at ratios 3:1, 4:1 in different cells, where n=3 and mean ±SD.

4.1.6.2 Evaluation of cellular uptake

The cellular uptake efficiency of the polymer PPSSI/II and its control groups was evaluated by both qualitative and quantitative methods such as confocal laser scanning microscopy (CLSM) and flow cytometry respectively. The cellular internalization of the nanoplexes was carried out using fluorescently labeled ctDNA (green) and polymer, with the nuclei stained with Hoechst (blue). As seen in Figure 15, a green fluorescence was observed in the cytoplasm as well as the nuclei in both PPSS I/II nanoplexes treated cells following 3h exposure. The fluorescence intensity

was found to be more localized in the nuclear region of the cells exposed with PPSSI nanoplexes. Compared to PPSS I, the polyplexes of PPSS II showed much weaker intensity in the nuclear region whereas more intense green fluorescence was observed in the cytoplasm and perinuclear regions. The high fluorescence signals reveal the greater accumulation of YOYO tagged ctDNA in the corresponding area. Though, the control groups showed cellular uptake of the polyplexes, the cells exhibited noTable necrosis, indicative of the PEI mediated cytotoxicity (Figure 16). On the other hand, pullulan based polyplexes treated cells maintained the normal spindle-shaped morphology. Cellular uptake of polyplexes in C6 cells was quantified by flow cytometry using YOYO tagged ctDNA. The percentage uptake of the nanoplexes is as follows; PPSS I 2:1 (92%), PPSS I 4:1 (92%), PPSS II 3:1 (89%) and PPSS II 4:1 (91%) (Figure 17). Since the control polyplexes caused significant cellular necrosis to C6 cell, it was not taken for flow cytometry analysis.

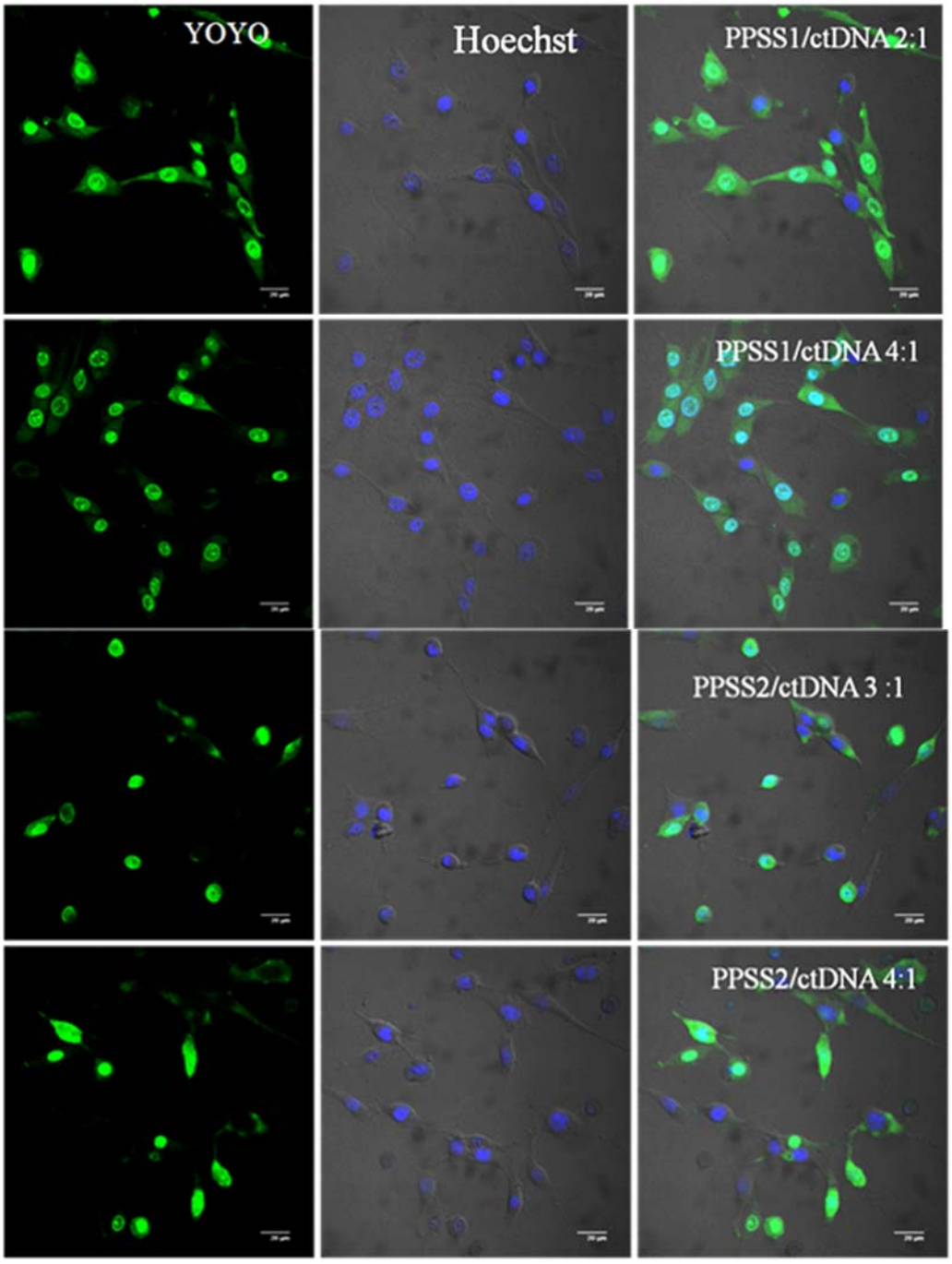

Figure 15: Uptake of YOYO tagged DNA containing PPSS nanoplexes , PPSS I (2:1 & 4:1) and PPSS II (3:1 & 4:1). The green fluorescence indicates the presence of YOYO tagged DNA and the blue color shows Hoechst stained nucleus. The magnification is 60x (confocal microscopy).

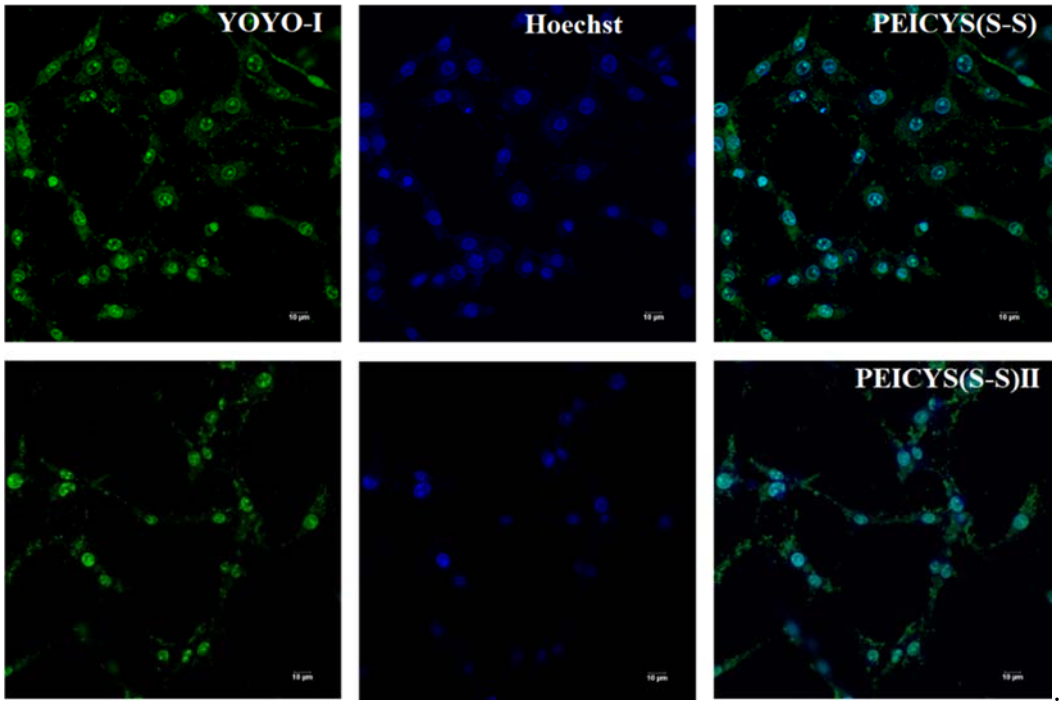

Figure 16: Uptake of YOYO tagged DNA containing PEICYS(S-S) I and II nanoplexes (both 4:1 ratio). The green fluorescence indicates the presence of YOYO tagged DNA and the blue color shows Hoechst stained nucleus. The magnification is 60x (Confocal microscopy).

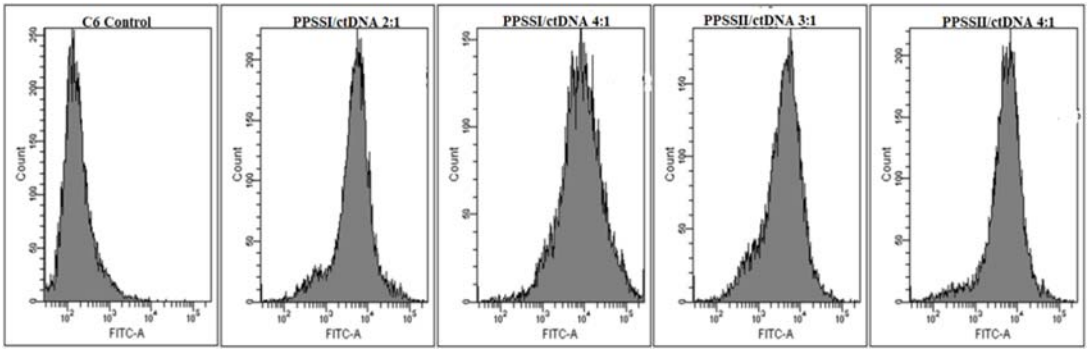

Figure 17: Flow cytometry analysis of cellular uptake of PPSSI/II nanoplexes, percentage uptake of PPSS I/ctDNA 2:1 – 92.38± 3.02% , PPSS I/ctDNA 4:1- 92.77±2.82%, PPSS II/ctDNA 3:1 – 89.12±2.09% and PPSS II/ctDNA – 91.11± 1.89% .

4.1.6.3. Endocytosis inhibition study

The nanoplexes entry into the cell is mediated by a mechanism known as endocytosis, which comprises of different transport mechanisms. Clathrin-dependent, caveolae-mediated and

micropinocytosis form the prominent pathways and these can be inhibited by treating the cells with agents such as chlorpromazine, filipin, and amiloride respectively. The cellular uptake pathways of PPSS nanoplexes was investigated by selectively adding inhibitors to the cells. The cells were initially exposed to these inhibitors and later to nanoplex for 3h. Percentage of nanoplex uptake was measured by using flow cytometry. As seen in Figure 18, the presence of inhibitors has not affected the cellular uptake of nanoplexes and hence all cells displayed almost 100% cellular uptake similar to the uninhibited system (control).

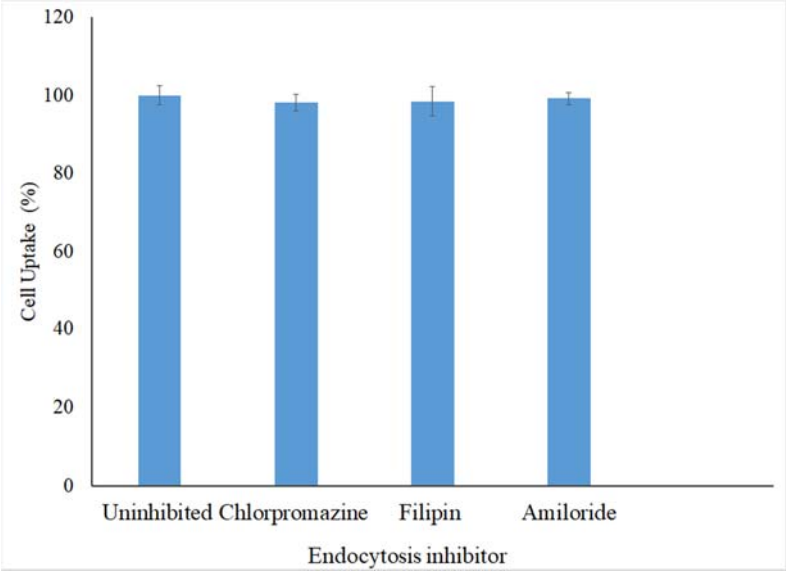

Figure 18: Cellular uptake of the PPSSI/ctDNA nanoplex at 4:1ratio in the presence and absence of inhibitors. The cellular uptake of the uninhibited cells was taken as 100%.

4.1.6.4 Polymer trafficking studies

The polymer trafficking study in the C6 cells was carried out using YOYO labeled ctDNA (green) and rhodamine-labeled polymer (red), the nucleus was stained with Hoechst (blue). Herein, the representative polyplex PPSSI 4:1 was used for the study. The cellular internalization of the nanoplex was monitored at different time points such as 1h, 2h, 4h, and 7h. As seen in Figure 19, the polyplexes were initially seen in the cytosol and mostly confined near the nuclear membrane.

The yellow fluorescence appeared in the cytosol in the 1st hour indicate co-localization of green and red fluorescence in the cytosol. In the 2nd hr, the green fluorescence was found to be merged with the Hoechst stained nucleus, implying the presence of ctDNA in the nucleus, however, the polymer (red) was found to be dispersed in the cytoplasm. In the 4th hour, the red fluorescence representing the polymer was bordered towards the cell membrane. Following this, in the 7th hour, the intensity of red fluorescence in the cell membrane was becoming thicker and was seen to be released from the cell membrane.

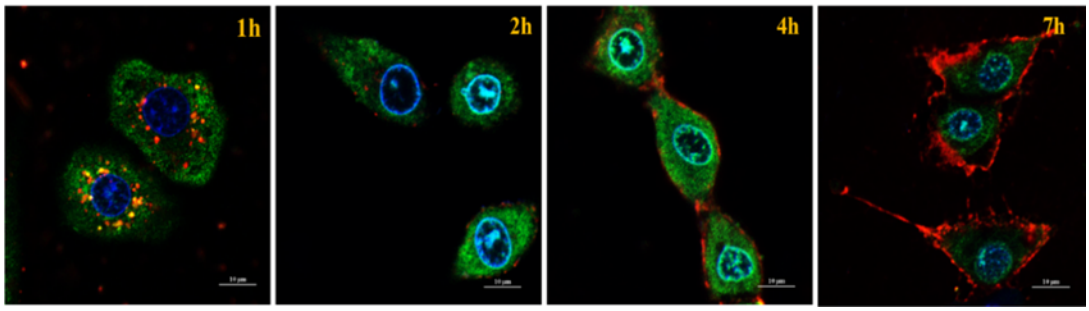

Figure 19: Polymer trafficking studies of the representative polyplex of PPSSI/ctDNA 4:1, where the polymer is tagged with rhodamine (red), ctDNA labelled with YOYO-I (green) and nuclei stained with Hoechst (blue). Magnification is 60x.

4.1.6.5 Evaluation transfection efficiency using Live and Dead assay

The transfection efficacy of the polymer PPSSI and II was analyzed by means of the live and dead assay, where the gene used for transfection was the p53 plasmid. Herein, the transgene expression of p53 is indicated by the presence of dead cells. Following incubation with PPSS I/p53 2:1, PPSSI/p53 4:1 and PPSS II/p53 4:1 polyplexes ratios, the qualitative determination of the red fluorescence or dead cells in C6 cells was carried out by means of fluorescence microscopy. The green fluorescence indicates the presence of live cells. As seen in Figure 20, extensive red fluorescence was seen in both PPSSI 2:1 and 4:1/p53 nanoplexes transfected cells against the very meager presence of red color seen in PPSS II 4:1 treated cells.

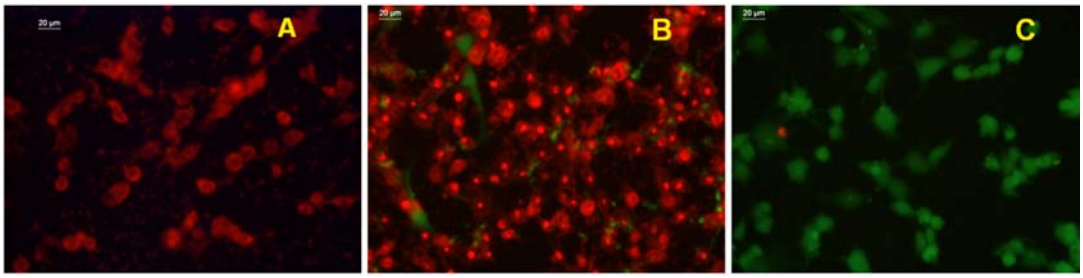

Figure 20: Live and dead assay in C6 cells, A) PPSS I/p53 2:1 polyplexes transfected cells B) PPSSI/p53 4:1 polyplex ratio transfected cells C) PPSS II/p53 4:1 polyplexes transfected cells.Magnification 40x.

4.1.6.6 PI staining using flow cytometry

Transfection efficiency of the PPSS I/II polyplexes was elucidated by means of PI staining in C6 cells by flow cytometry. Following transfection with p53 using PPSSI and II nanoplexes, the quantitative determination of dead cells was carried out by adding propidium iodine (PI) to the cells, where staining of PI indicate the presence of dead cells. As shown in the Figure 21, PPSS I/p53 2:1 and PPSSI/p52 4:1 showed 96.5% and 97.2% cell death respectively, whereas PPSS II/p53 4:1 displayed a cell death of only 15.2%.

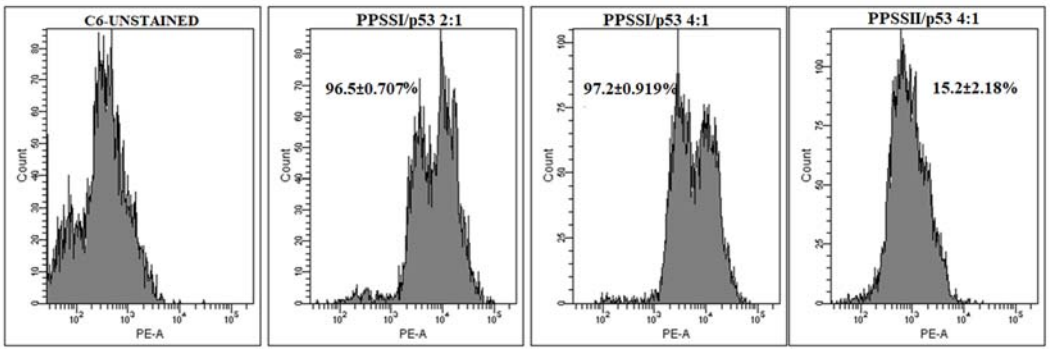

Figure 21: PI staining of PPSSI/p53 2:1, PPSSI/p53 4:1 and PPSSII/p53 4:1 transfected cells measured via flow cytometry which showed 96.5±0.707%, 97.2±0.919% and 15.2±2.18% cell death respectively.

4.1.6.7 Determination of apoptosis by Annexin V staining

The apoptotic activity of PPSS I/II nanoplexes was quantified in C6 cells by flow cytometry using annexin V FITC/propidium iodide (PI) staining. The results revealed that PPSS I/p53 nanoplexes induced higher apoptotic activity than PPSS II nanoplexes, in which PPSS I/p53 2:1, PPSS I/p53 4:1, PPSSII/p53 4:1 caused 88.9±5.02%, 94.1±3.81%, and 13.2±1.11% cell death

respectively (Figure 22). In annexin V staining Q1 represent the necrotic cells, Q2, late apoptotic cells, Q3 is living cells and Q4 is the early apoptotic cells, where percentage apoptosis is indicated by the sum of Q2 and Q4.

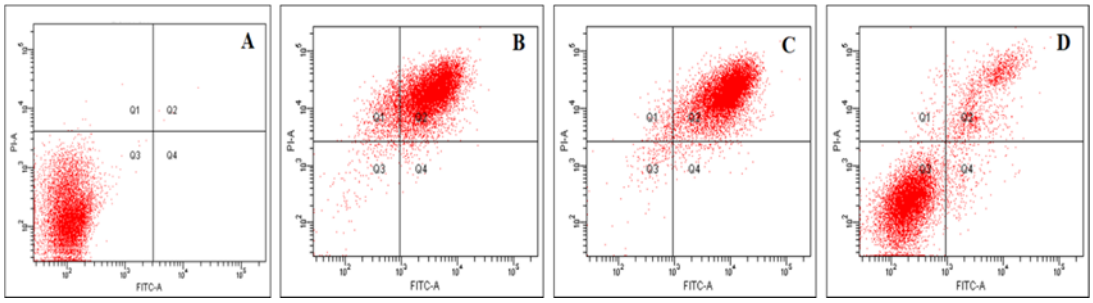

Figure 22: Flow cytometric analysis of cell apoptosis of C6 cells treated with PPSSI/II nanoplexes for 24h, where A) normal control cells stained with Annexin V FITC B) PPSSI/p53 2:1 treated cells where percentage apoptosis is 88.9±5.02% C) PPSSI/p53 4:1 treated cells where percentage apoptosis is 94.1±3.81% and D) PPSSII/p53 4:1 treated cells where percentage apoptosis is 13.2±1.11%.

4.1.6.8 p53 immunofluorescence-confocal microscopy

The expression of p53 in the PPSSI and II nanoplexes treated cells was further confirmed by p53 immunofluorescence study. The green fluorescence represents the presence of p53 protein in the cells. Here the cells were initially incubated with the primary antibody of p53 which was then subsequently treated with FITC tagged secondary antibody. The cells were then monitored via confocal microscopy. As shown in Figure 23, the green fluorescence appeared in the cytoplasm indicate the expression of p53 following its transfection in C6 cells using PPSSI/p53 2:1, PPSSI/p53 4:1 nanoplexes and PPSSII/p53 4:1. The normal cells show very feeble green fluorescence in the cytoplasm, whereas both ratios of PPSSI nanoplexes showed intense green fluorescence (Figure 23). The PPSSII showed negligible green fluorescence.

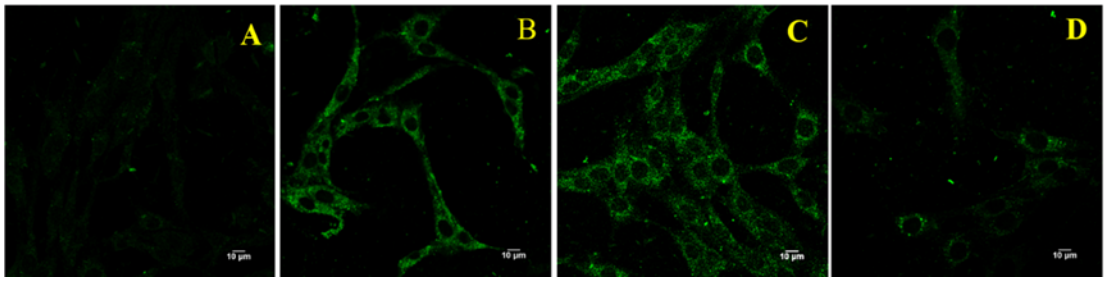

Figure 23: p53 immunofluorescence study in C6 cells where A) Untreated cells B) PPSSI/p53 2:1 nanoplexes transfected cells B) PPSSI/p53 4:1 nanoplexes treated cells D) PPSSII/p53 4:1 nanoplexes treated cells. Magnification is 60x.

4.1.6.9 Assessment of P-gp activity in cancer cell lines

The selection of P-gp negative and positive cell lines has been done with the help of a known P-gp inhibitor, verapamil. The cell lines used were C6, A549 and HeLa. The cells were initially treated with verapamil (40μM) and incubated. This was followed by the addition of DOX and incubated for different time points. The DOX retention at each time point was analyzed in these cell lines. As shown in Figure 24, both C6 and A549 retained drug remarkably in the presence of verapamil where the concentration of DOX reached upto 3μg/mg of protein in A549 where as in C6, it was 2.5μg/mg of protein. It was observed that there is a significant difference in terms of DOX retention in the verapamil pretreated cells compared to the DOX alone treated cells of both C6 and A549 ($P<0.001$). However, in HeLa cells, there was no significant difference in the DOX retention between the control and verapamil pretreated cells.

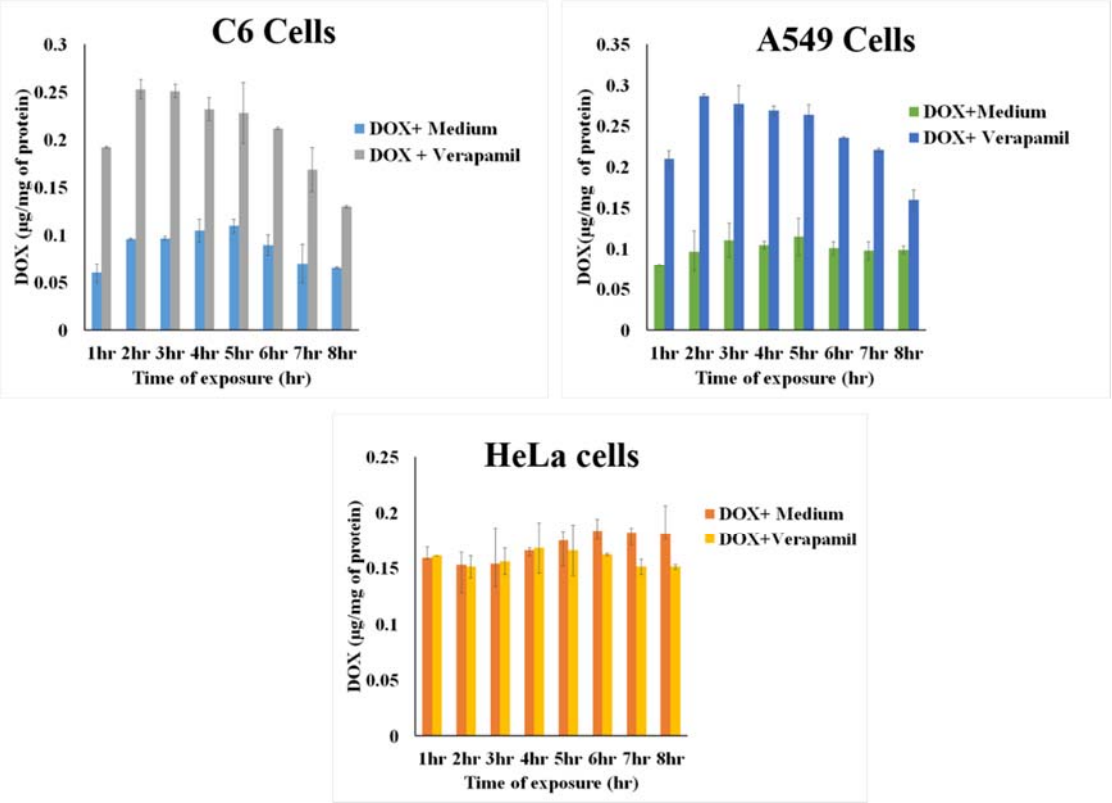

Figure 24: The DOX alone treated cells were compared with verapamil and DOX treated cells. There is significant difference ($P<0.001$) in the DOX retention between untreated and verapamil treated group in C6 and A549. No significant difference was observed in HeLa cells between the groups.

4.1.6.10 Efflux pump inhibition studies using confocal microscopy

Efflux pump inhibition study is meant to evaluate the efficacy of the polymer in inhibiting efflux pump (P-gp). The study was performed in different cell lines such as C6, A549 and HeLa cells, where the anticancer drug, DOX was used as an index for efflux pump inhibition. As seen in Figure 25, the polyplexes (PPSS I 2:1 and 4:1) pretreatment to C6 cells and its subsequent exposure to the anticancer drug, DOX (3µM) led to the enhanced retention of DOX in the cells. This was evidenced by the presence of increased red fluorescence in the cells. Similarly, the intensity of red fluorescence corresponding to the presence of DOX was high in both polyplexes (PPSS I 2:1 and 4:1) pretreated cells of A549 compared to the corresponding control cells where

DOX alone was treated (Figure 26). There was no visible difference in the intensity of red fluorescence observed between the PPSS polyplexes ratios 2:1 and 4:1 pretreated cells of A549 and C6. In contrast, the intensity of red fluorescence was more or less same in HeLa cells in all the groups irrespective of DOX alone and or polyplexes and DOX treatment (Figure 27).

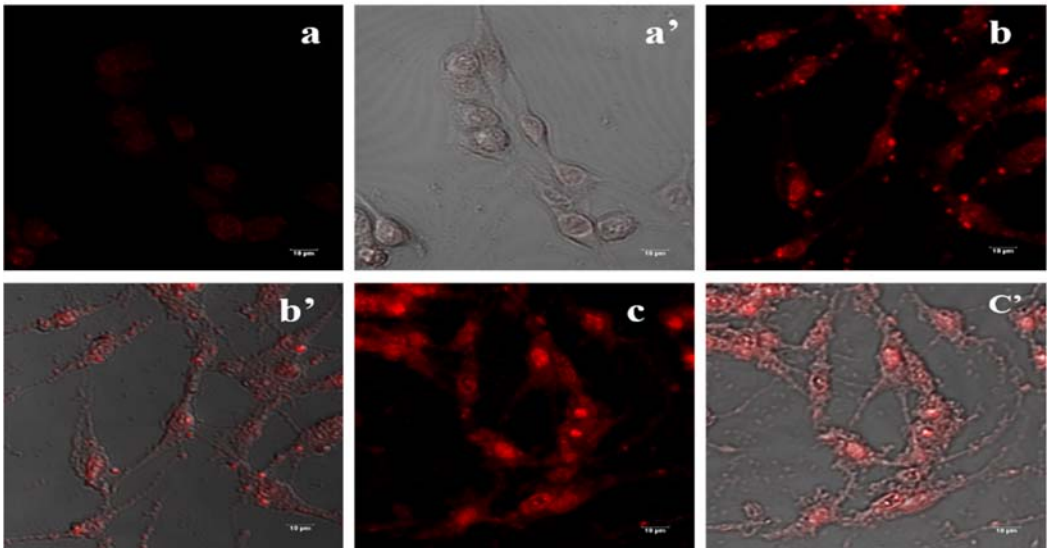

Figure 25: Efflux pump inhibition study in C6 cells where image a and a' is the DOX alone treated control cell and the merged image respectively. Similarly b is PPSS I/ ctDNA 2:1 nanoplexes pretreated cells followed by DOX and b' is the corresponding merged image, c is PPSS I/ctDNA 4:1 nanoplex pretreated cells followed by DOX and c' is the corresponding merged image. The magnification is 60x (confocal microscopy).

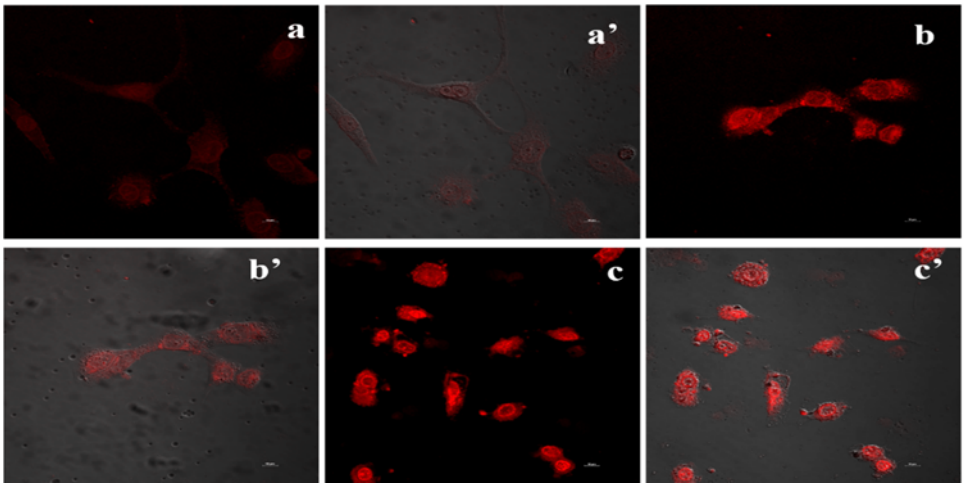

Figure 26: Efflux pump inhibition study in A549 where image a and a' is the DOX alone treated control cells and the merged image respectively. Similarly b is PPSS I/ ctDNA 2:1 nanoplexes

pretreated cells followed by DOX and b' is the corresponding merged image, c is PPSS I/ctDNA 4:1 nanoplex pretreated cells followed by DOX and c'is the merged image. The magnification is 60x.

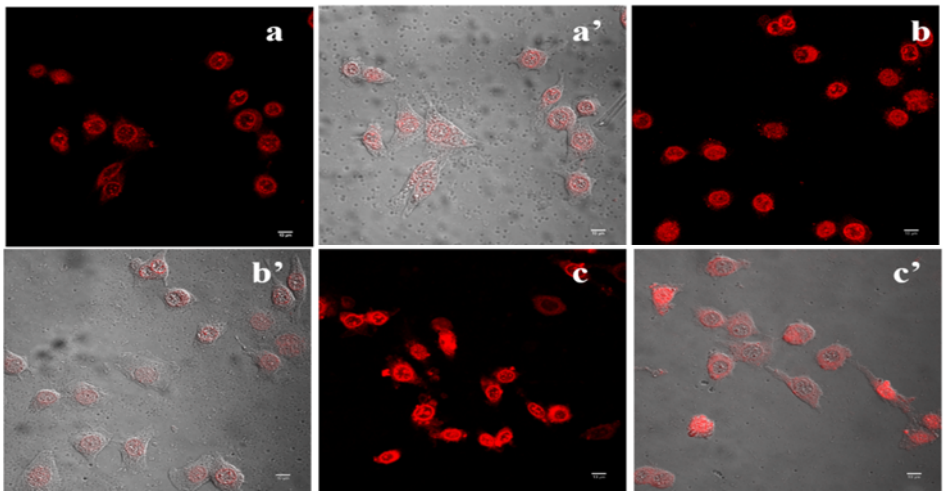

Figure 27: Efflux pump inhibition study in HeLa cells. The image a and a' is the DOX alone treated control cells and its merged image respectively. Similarly b is PPSS I/ ctDNA 2:1 nanoplexes pretreated cells followed by DOX and b' is the corresponding merged image, c is PPSS I/ctDNA 4:1 nanoplex pretreated cells followed by DOX and c'is the corresponding merged image. The magnification is 60x.

4.1.6.11 Efflux pump inhibition studies using flow cytometry

The efflux pump inhibition mediated by PPSSI polymer was determined by flow cytometry by measuring the percentage of cells retaining DOX both in the presence of DOX alone and PPSS and DOX treatment in C6, A549 and HeLa cells . Here, the control group was the cells treated with DOX alone (3μM) whereas nanoplexes treated group was cells pretreated with nanoplexes (PPSS I 2:1 & 4:1) for 2hrs followed by DOX. As shown in Table 4, in both C6 and A549 cells,the percenatge of cells retaining DOX in the control group was 30% and 34% respectively. On the otherhand, the percetage of cells retaining DOX in the PPSSI 2:1 and 4:1 nanoplexes treated

group showed 70% and 78 % respectively in C6 and 69% and 75% respectively in A549 cells. In the case of HeLa cells, the percentage retention of DOX was more or less ame in both control and nanoplexes pretreated group.

Cell lines	% of cells retaining DOX in control group	% of cells retaining DOX in the nanoplexes pretreated group	
		PPSS I/ctDNA 2:1	PPSS I/ctDNA 4:1
C6	30.51±1.18	70.74±2.25	78.52±3.35
A549	34.32±5.43	69.42±1.53	75.21±3.01
HeLa	45.31±1.02	53.11±6.52	47.08±7.91

Table 4: Efflux pump inhibition study using flow cytometry, where the percenatge of cells retaining DOX was measured following DOX alone and/or PPSS nanoplexes pretreatment followed by DOX treatment.

4.1.6.12 DOX retention kinetics

The intracellular DOX retention kinetics was determined in different cell lines such as C6, A549 (P-gp expressed cell lines) and HeLa (P-gp negative cell line), where initially the cells were preexposed with the PPSS I 4:1 nanoplexes followed by DOX (3μM) treatment for different time points. The concentration of the DOX in the cells were analyzed after normalizing with the total protein content of the cell. As shown in Figure 30, there was a significant difference ($P<0.001$) in terms of DOX retention in the nanoplexes pretreated group as compared to the DOX alone control group in both C6 and A549. In the PPSS pretreated group in C6 cells, in the 1st hr, the concentration of DOX reached upto 0.13μg/mg of protein against 0.06 μg of DOX /mg of protein

in the control group. Similarly, the concentration of DOX raised to 0.18 µg/mg of protein in the 2nd hour against 0.08 µg/mg of protein in the controls. From the 3rd hour onwards, the concentration of DOX was found to decrease with time. However, the C6 cells maintained a significant difference ($P<0.001$) in the DOX retention compared to the control upto the 7th hr. In the case of A549, following 1hr exposure to DOX, the concentration reached 0.15 µg/mg of protein in the PPSS nanoplexes pretreated cells whereas it was 0.08 µg/mg of protein in the control cells. As shown in Figure 28, there was a gradual increase in the DOX concentration was observed over time in A549 and it reached to the maximum level at the 4th hour where it was 0.182 µg of DOX/mg of protein. Though there was a decrease in DOX concentration occurred following 4th hr, the A549 cells maintained a significant difference in DOX retention between the control and nanoplexes pretreated group even in the 8th hr. On the other hand, HeLa cells maintained a high DOX retention in the control cells and the nanoplexes treated cells. The initial concentration of DOX was 0.16µg/mg of protein and was keep increasing till 8th hour where it was noted as 0.19 µg/mg of protein. It should be noted that the nanoplexes pretreated cells also maintained a DOX concentration similar to the controls.

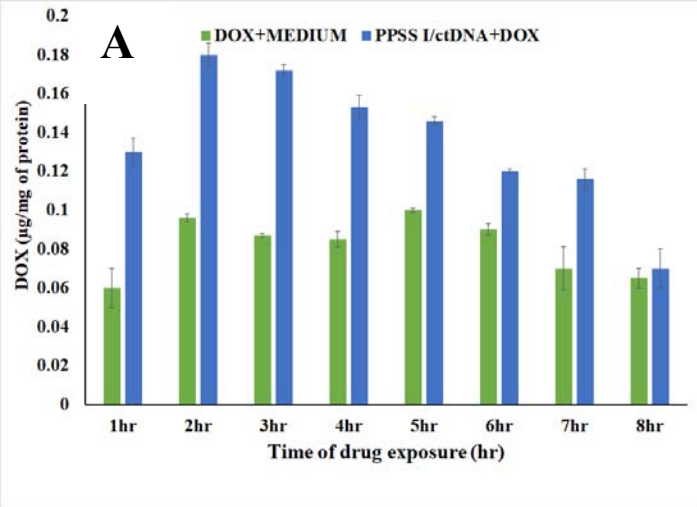
A
DOX+MEDIUM
PPSS I/ctDNA+DOX
DOX (µg/mg of protein)
0.2
0.18
0.16
0.14
0.12
0.1
0.08
0.06
0.04
0.02
0
1hr
2hr
3hr
4hr
5hr
6hr
7hr
8hr
Time of drug exposure (hr)

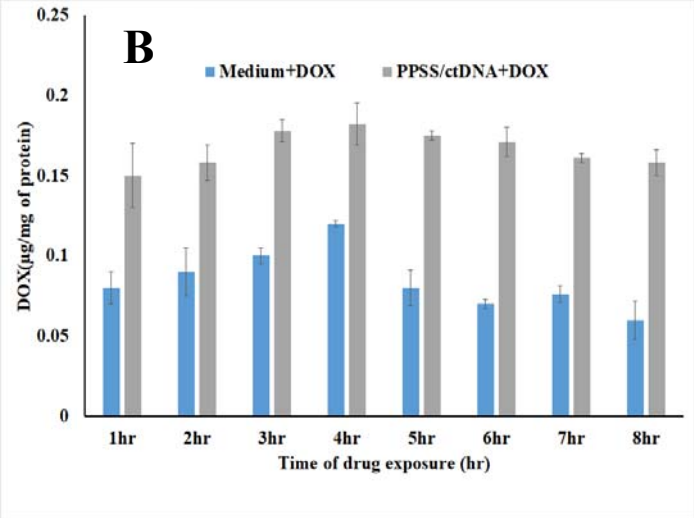
B
Medium+DOX
PPSS/ctDNA+DOX
DOX(µg/mg of protein)
0.25
0.2
0.15
0.1
0.05
0
1hr
2hr
3hr
4hr
5hr
6hr
7hr
8hr
Time of drug exposure (hr)

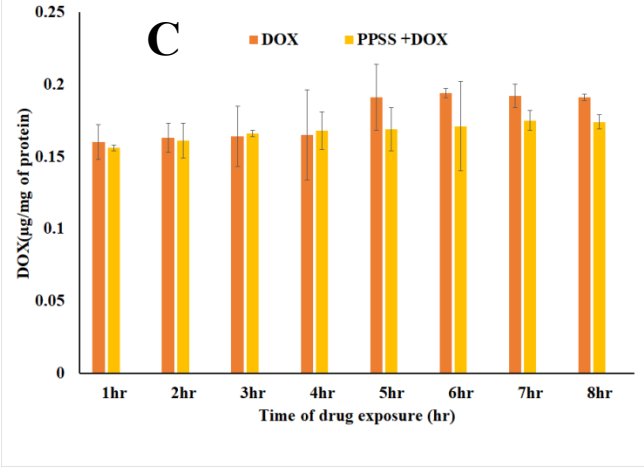
C
DOX
PPSS +DOX
DOX(µg/mg of protein)
0.25
0.2
0.15
0.1
0.05
0
1hr
2hr
3hr
4hr
5hr
6hr
7hr
8hr
Time of drug exposure (hr)

Figure 28: DOX retention in different cell lines A) C6 cells B) A549 and C) HeLa cells. The DOX alone treated group was compared with the PPSS 4:1 nanoplexes pretreated and DOX treated group in C6, A549 and HeLa.

4.2. Synthesis and characterization of pullulan-PEI-mercaptosuccinic acid (PPMSS)

Pullulan-PEI-mercaptosuccinic derivatives were synthesized by conjugating pullulan-PEI (PP) with varying amounts of mercaptosuccinic acid (MSA). The thiol groups thus introduced were oxidized to form disulfide cross-linked pullulan-PEI (PPMSS) via the addition of hydrogen peroxide. The control groups were synthesized by conjugating MSA with PEI and further oxidation with H_2O_2 i.e. PEI-MSA. The quantification of thiol and disulfide content in the polymer, PPMSS and PEI-MSA was analyzed by Ellman's and NTSB assay respectively. As shown in the Table 5, PPMSS III, which showed the highest MSA content in the polymer, exhibited high content of thiol and disulfide linkages. The thiol contents of both PPMSS polymers and its control groups were analyzed by initially reducing the disulfide group with sodium borohydride (Table 6).

SL.NO	Sample ID	S-S linkage mg/g of polymer)	Thiol content mg/g of polymer
1	PPMSS I	44±0.006	55±0.01
2	PPMSS II	50±0.007	61±0.013
3	PPMSS III	61±0.004	68±0.001
4	PEI-MSA I	54±0.012	72±0.012
5	PEI-MSA II	68±0.002	77±0.02
6	PEI-MSA III	70±0.011	75±0.01

Table 5: The thiol and disulfide content of the pullulan derivative, PPMSS polymers and its corresponding controls PEI-MSA.

The quantification of the free amino content in the PPMSS and PEI-MSA polymers were analyzed by CuSO4 assay. The amino group in the PEI was involved in conjugation with pullulan so as the case with MSA. Hence as the degree of substitution of MSA increases in the polymers, the amino content correspondingly decreases (Table 6). However, It should be noted that further evaluation of the zeta potential values of polymers showed a corresponding negative or lower positive surface charge in the polymers having a higher MSA content such as PPMSS II and PPMSS III. Hence for further studies, PPMSS I alone was chosen to carry out both gene delivery and efflux pump inhibition studies.

SL.NO	Sample ID	Amount of amino group (mg/10mg of polymer)
1	PPMSS I	3.09±0.32
2	PPMSS II	2.51±0.03
3	PPMSS III	2.01±0.12
4	PEI-MSA I	4.98±0.08
5	PEI-MSA II	4.55±0.11
6	PEI-MSA III	4.76±0.12

Table 6: Amino content of PPMSS and PEI-MSA polymers determined via $CuSO_4$ assay

4.2.1 ^{1}H NMR and FTIR

The conjugation of pullulan, PEI and mercaptosuccinic acid was verified by ^{1}HNMR. The signals of –SH protons of alkyl thiols in the MSA are visible at δ 1.2 and δ 1.8 ppm in PEI-MSA, whereas the same is not clearly appeared in PPMSS. ^{1}H NMR peaks showed a characteristic PEI peak of – (CH_2-CH_2-NH) at δ 2.5-2.6 ppm in both PEI-MSA and PPMSS. The spectra indicated a chemical shift of protons of pullulan at δ 3.7-3.8ppm. The presence of anomeric protons of maltotriose was seen between δ 4.5 to 5.4 ppm (Figure 29).

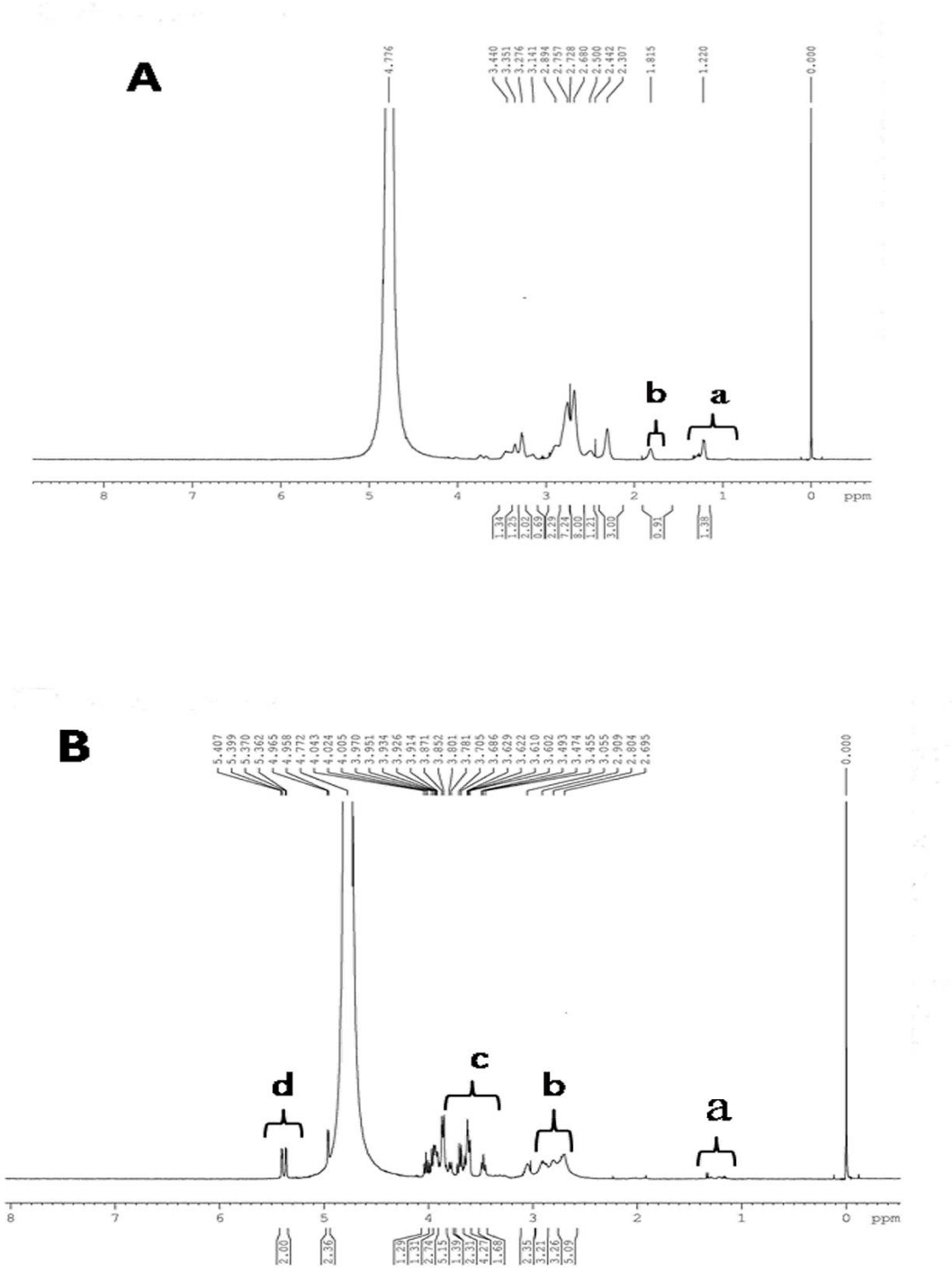

Figure 29: [1]HNMR spectra of A) PEI-MSA and B) PPMSS. The notations a and b demonstrates the presence of -SH protons of alkyl thiols of MSA and (CH_2-CH_2-NH) n of PEI respectively. The c and d denotes -(CH_2-CH_2) and anomeric protons of pullulan respectively.

The FTIR data also supports the conjugation of pullulan-PEI-MSA. A broad absorption peak observed in both Pullulan PEI (PP) and PPMSS at around 3200 cm^{-1} is due to –OH stretching vibration and peak at 932 cm^{-1} is due to C-O-C stretching of α (1-4) glycosidic linkage of pullulan. Similarly, the band at 1149 cm^{-1} and 1151 cm^{-1} in pullulan-PEI and PPMSS is assigned to the valence vibrations of the C-O-C bond and glycosidic linkage of pullulan. However, the same is absent in the control group, PEI-MSA. The strong peaks at 2923cm^{-1} and 2825cm^{-1} observed in PEI-MSA are indicative of the C-H stretching vibration of PEI. Similarly, peaks at 1629cm^{-1} in PEI-MSA and 1655cm^{-1} of PPMSS, are indicative of the C=O stretching of amide I band (Figure 30).

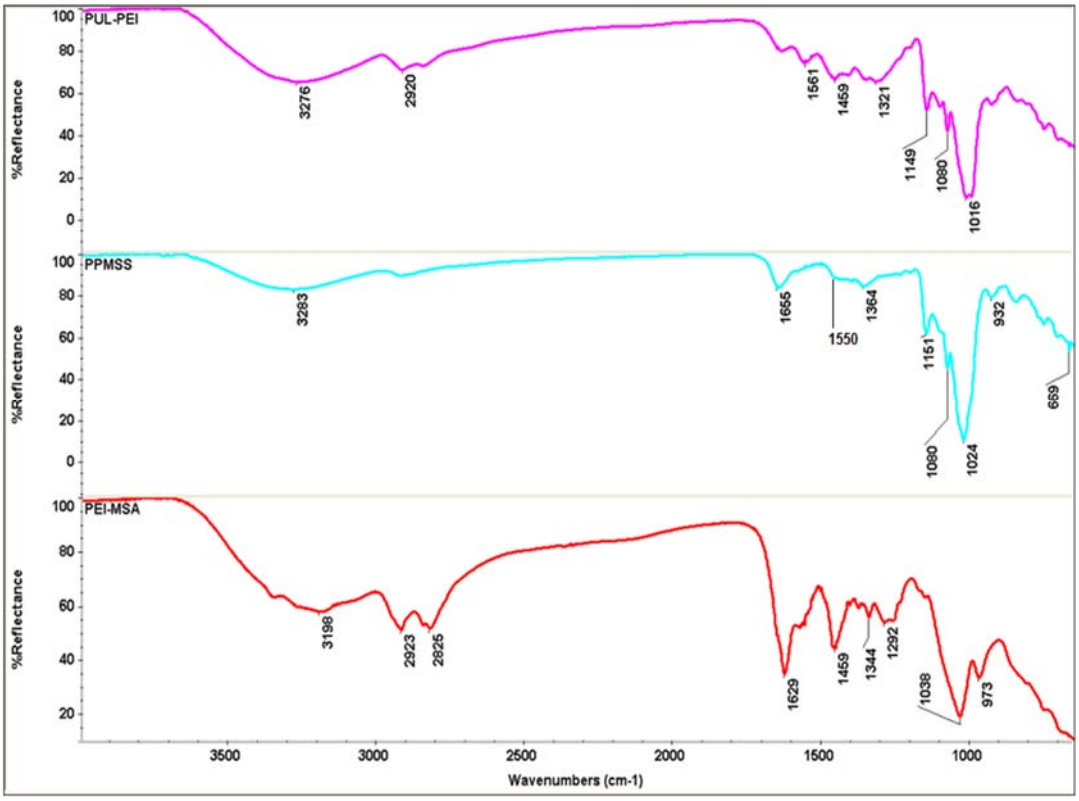

Figure 30: FTIR spectra of Pullulan-PEI, PPMSS and PEI-MSA

4.2.2. Buffering Capacity

The acid-base titration studies were performed to determine the buffering ability of the polymers at the pH range of 10-4, which determines the endosmolytic properties of the same. Generally, cationic polymers containing many amino groups exhibit low pKa values between the physiological and lysosomal pH (pH 7-4) and acts as a good buffer at this range. The quantification of buffering capacity of different polymers i.e PEI, PEI-MSA and PPMSS were carried out by the serial addition of HCl (0.01N) at 50µL aliquots. As indicated in Figure 31, both PPMSS and its control, PEI-MSA possess good buffering ability in the specified pH range where a slightly higher buffering capabilities was showed by PEI-MSA. The buffering abilities of the pullulan based polymer, PPMSS and its control was comparable to the PEI polymer.

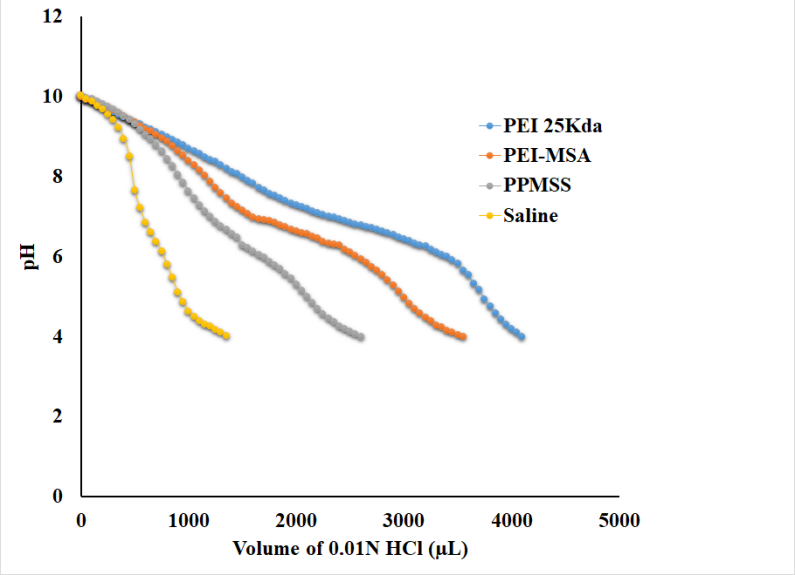

Figure 31: Buffering abilities of PEI, PEI-MSA, PPMSS and Saline

4.2.3. Biophysical characterization

4.2.3.1. Size and zeta potential

The whole process of gene delivery starts with the condensation of negatively charged DNA with positively charged polymer and form small nanosized structures called nanoplexes. The

particle size and zeta potential of PPMSS/PEI-MSA nanoplexes were analyzed via dynamic light scattering (DLS). Both PPMSS and PEI-MSA based polymers showed smaller particles of size less than 200nm (Figure 32). Both the polymer and the control group showed a net positive change at all polymer to DNA ratios ranging from 1:1 to 5:1. The zeta potential values of PPMSS nanoplexes were in the range +10 to +19mV against +25 to +32mV in PEI-MSA.

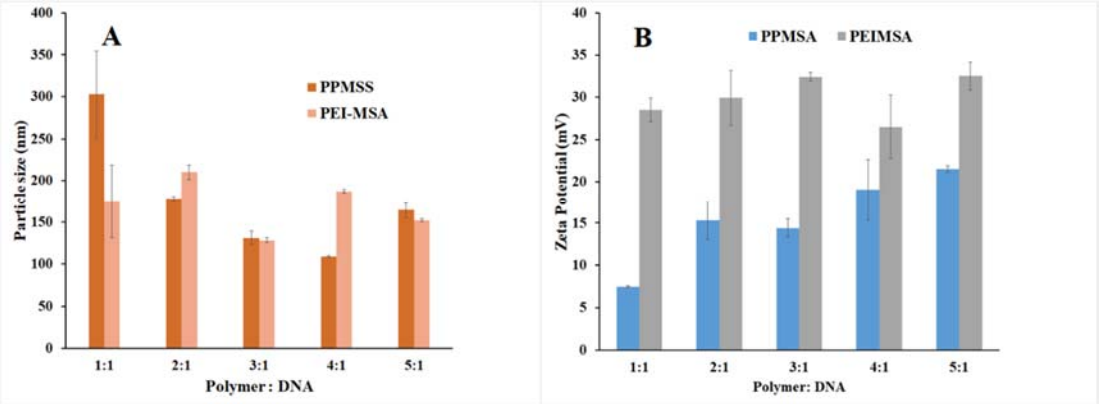

Figure 32: Particle size and zeta potential values of PPMSS and PEI-MSA nanoplexes with the polymer to DNA ratio ranging from 1:1 to 5:1.

4.2.3.2 Agarose gel electrophoresis

The ability of the polymer to condense ctDNA and the stability of the formed nanoplexes were analysed using agarose gel electrophoresis. DNA alone was taken as control. (Figure 33). The bright intensity of bands observed near the well indicated the inhibition of DNA, confirmed the strong interaction between the polymer and DNA. However in the case of DNA alone it can be seen as a smear in the first well. The effect of plasma proteins on stability of nanoplexes was also evaluated by AGE. As shown in Figure 35, the DNA is retained in the well indicating the stability of the PPMSS and PEI-MSA nanoplexes in presence of plasma also.

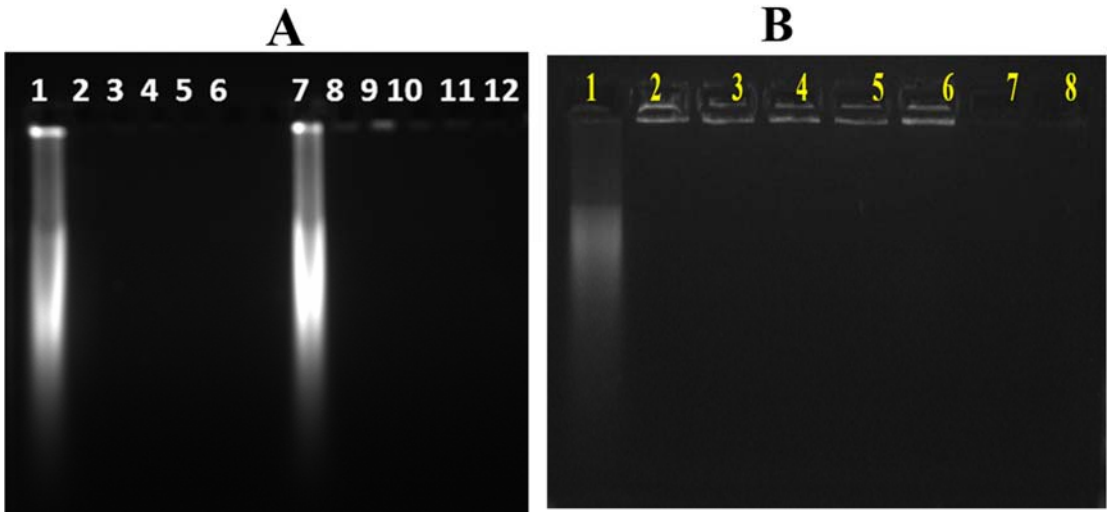

Figure 33: Agarose gel electrophoresis. The gel A lane 1 and 7 indicate the control ctDNA alone, lane 2-6 and 8-12 represent the nanoplexes of PPMSS and PEI-MSA ranging from 1:1 to 5:1 ratios respectively. The gel B indicated the selected nanoplex treated with plasma, where lane 1 is the ctDNA alone, lane 2-5 show the nanoplex of PPMSS ranging from 2:1 to 5:1 and 6-8 indicate the nanoplex of PEI-MSA, 2:1 to 4:1.

4.2.3.3 Stability of nanoplexes in presence of DTT

The stability of PPMSS/ctDNA complexes in response to 10mM DTT was determined by agarose gel electrophoresis and size measurement by DLS. The time-dependent changes in particle size distribution were monitored using dynamic light scattering for up to 4h. As seen in Figure 34, the exposure of the PPMSS/ctDNA and PEI-MSA/ctDNA complexes to DTT, rapidly increased the mean particle size (>400nm), suggesting the formation of large aggregates within hours. Even in the first hour of exposure of PPMSS/ctDNA 3:1 nanoplexes to DTT have remarkably changed the particle size. That is from 131 nm in the absence of DTT to around 340 nm. Similar changes were observed in PPMSS/ctDNA 4:1 nanoplex which increased to 325nm in the initial hour from the original untreated size of 109nm. Both reached around 450nm by 4^{th} hr. However, to determine the consequences of reduction sensitive size alterations of PPMSS/ctDNA polyplexes on genetic payload, agarose gel electrophoresis was performed following incubation of polyplexes with DTT.

As shown in Figure 35, a complete retardation of DNA in the well following DTT incubation with the polyplexes was observed but exhibited the release of DNA from the well in the combined treatment of DTT and heparin.

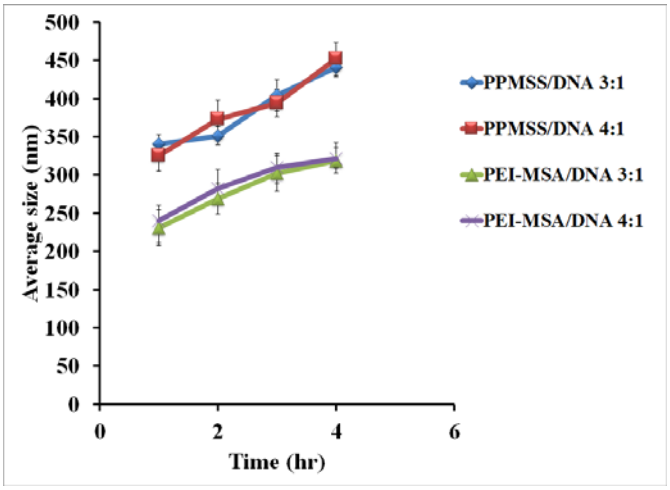

Figure 34: Size change of PPMSS/ctDNA and PEI-MSA/ctDNA nanoplexes on exposure with DTT at different time periods.

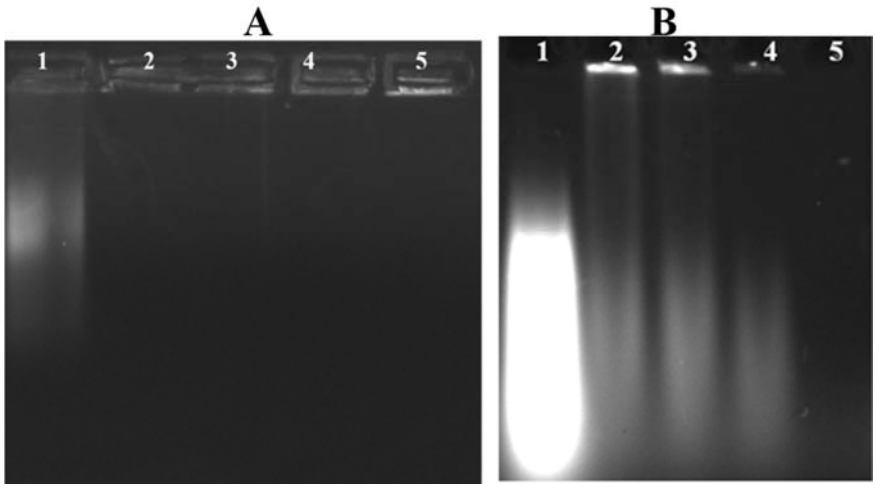

Figure 35: Agarose gel electrophoresis : The gel A, lane 1 –ctDNA control, lane 2-3, PPMSS/ctDNA 3:1 and 4:1, lane 4-5 PEI-MSA/ctDNA 3:1 and 4:1, all treated with DTT except the control. The gel B, lane 1 indicates ctDNA , lane 2-3, PPMSS/ctDNA 3:1 and 4:1, lane 4-5 PEI-MSA/ctDNA 3:1 and 4:1 nanoplexes respectively, all treated with heparin/DTT.

4.2.4 Plasma protein interaction with the polymer (PAGE)

The plasma protein interaction of PPMSS, PEI-MSA and PEI polymer was analyzed after incubating the polymers with plasma, the plasma supernatant collected after incubation with polymers were subjected to PAGE. As seen in Figure 36, the number of protein bands as well as the intensity of the protein bands corresponding to PEI treated plasma is faint. The control group i.e. PEI-MSA also showed a reduction in the protein bands but not as similar as in PEI, mostly due to the reduction in surface charge. On the other hand, the pullulan based derivative i.e. PPMSS showed the presence of protein bands as similar to that of plasma alone, implies that the interaction between the polymer and plasma proteins did not result in significant adherence of proteins.

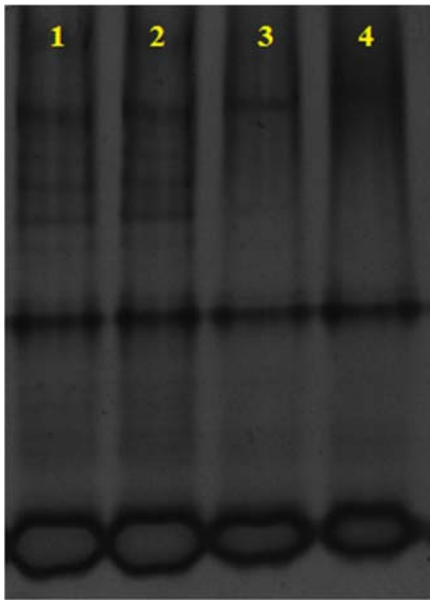

Figure 36: PAGE analysis. Interaction of different plasma proteins with polymers PPMSS, PEI-MSA and PEI in comparison with the protein profile of plasma treated with normal saline. Lane 1) Plasma, Lane 2) PPMSS, Lane 3) PEI-MSA and 4) PEI.

4.2.5. Biological analysis

4.2.5.1. Cytotoxicity evaluation of the polymer

The cytotoxicity of the selected nanoplexes ratios of PPMSS i.e 3:1 and 4:1 and its control group, PEI-MSA 3:1 and 4:1 was evaluated in C6, HeLa, A549 and L929 cells by using MTT assay. Triton X-100 was used as the positive control. As seen in Figure 37, all the cancer cell lines i.e C6, A549 and HeLa incubated with the PPMSS nanoplexes showed >85% cell viability whereas the control group showed the viabilty of <60%. The cytotoxicity of the nanoplexes were performed in the L929 cells also to find out if it causes any toxicity to the normal cells. As shown in the Figure 37, the cells incubated with PPMSS showed >80%viability against 30% showed by cells exposed with the nanoplexes of PEI-MSA in L929.

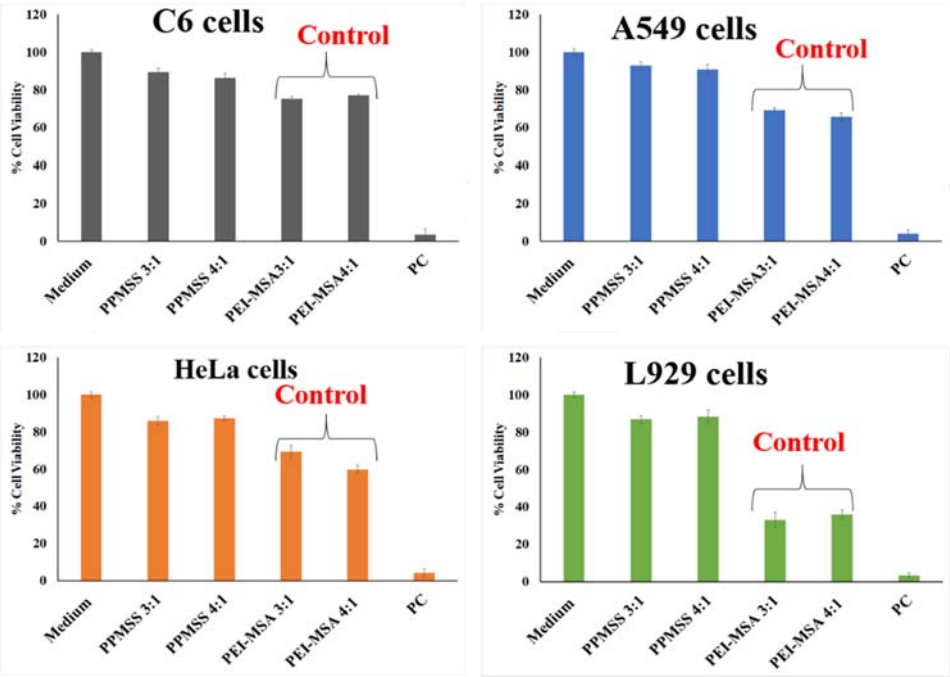

Figure 37: MTT assay of the selected PPMSS and PEI-MSA nanoplexes at polymer to DNA ratios of 3:1, 4:1 in different cancer cell lines such as C6, A549 and HeLa and the normal fibroblast cell, L929. Data is shown as mean ±SD, n=3.

4.2.5.2. Evaluation of cellular uptake

The cellular uptake of PPMSS (3:1 &4:1) nanoplexes were analyzed by using confocal laser scanning microscopy and flow cytometry in C6 cells after tagging the DNA with YOYO-I. The

image shown in Figure 38 reveals good cellular uptake of PPMSS/ctDNA nanoplexes at both ratios i.e. 3:1 and 4:1. It could be seen that YOYO tagged DNA is localized more in the nuclear region than in the cytoplasm following 3h exposure to cells with PPMSS nanoplexes. On the other hand, the control group i.e PEI-MSA 4:1 nanoplexes showed no observable cellular uptake but displayed noTable necrosis of cell with the appearance of fragmented Hoechst stained nucleus. The flow cytometry analysis of cellular uptake also have substantiated the confocal microscopy analysis and showed a cellular uptake of 75% for PPMSS 3:1 nanoplex and 78% for PPMSS 4:1 nanoplex in C6 cells (Figure 39).

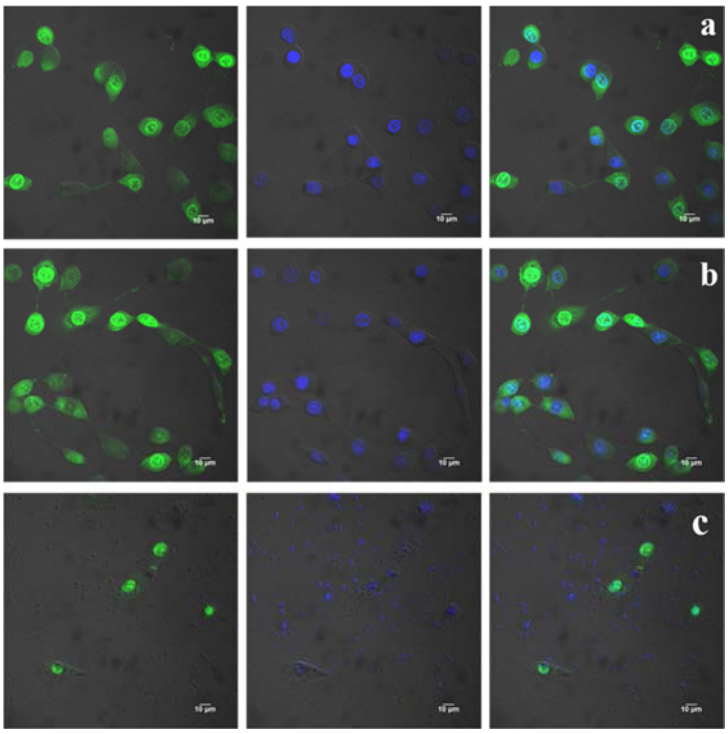

Figure 38: Cellular uptake of a) PPMSS/ctDNA nanoplex at 3:1 ratio b) PPMSS/ctDNA nanoplex at 4:1 ratio and c) PEI-MSA nanoplex at 4:1 ratio. In each row the green flurescence represent the YOYO tagged DNA and the blue image indicates the Hoechst stained nucleus and finally the merged image.(Magnification 60X)

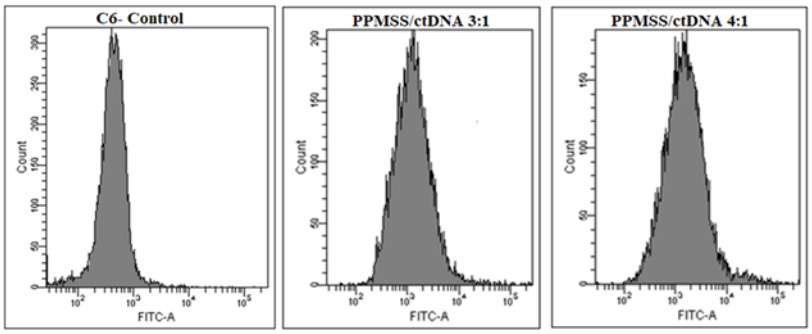

Figure 39: Percentage cellular uptake of nanoplexes PPMSS/ctDNA and PPMSS/ctDNA at 3:1 and 4:1 ratios respectively with YOYO tagged DNA. Where PPMSS/ctDNA 3:1 showed 75.22±5.11% uptake and that of PPMSS/ctDNA 4:1 78.43±3.05%.

4.2.5.3 Endocytosis inhibitor study

The endocytosis pathway of the PPMSS nanoplexes was evaluated by means of endocytosis inhibitor study using flow cytometry. The PPMSS/ctDNA 4:1 polyplex was chosen as the representative polymer for the uptake study. The drugs chlorpromazine, filipin, and amiloride were used to respectively block the endocytosis pathways such as clathrin-mediated, caveolae-dependent and micropinocytosis. Following initial exposure with the drugs, cells were allowed to carry out normal cellular uptake process. From Figure 40, it is revealed that all the three endocytosis inhibitor individually didn't affect the uptake process and PPMSS nanoplex showed almost 100% cellular uptake similar to the uninhibited system (Figure 40). Here, the uninhibited cellular uptake process of the PPMSS nanoplexes was considered as 100% uptake. It should be noted that none of the inhibitors showed any significant influences in the PPMSS cellular internalization process.

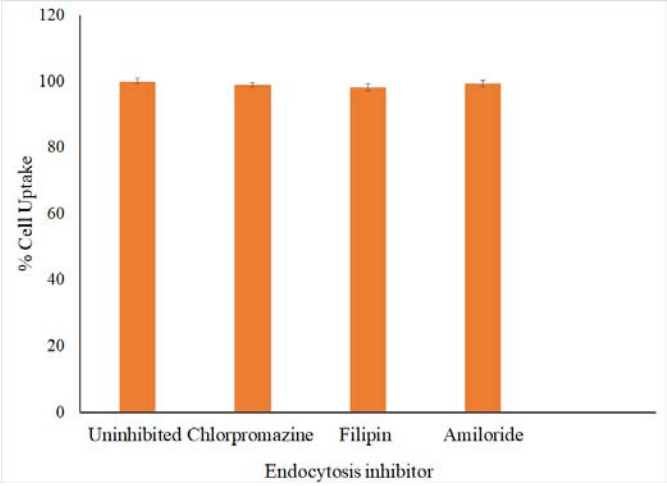

Figure 40: Endocytosis inhibitor effect on the cellular uptake of the, PPMSS/ctDNA nanoplex at 4:1 ratio. The control group is the uptake of polyplex without pretreatment with the inhibitor, where it is taken as 100%.

4.2.5.4 Polymer trafficking study

Polymer trafficking study was performed with PPMSS/ctDNA nanoplex at 4:1 ratio, where polymer and ctDNA was labeled with rhodamine (red) and YOYO iodide (green) respectively. From Figure 41, it is revealed that after 1h incubation, most of the green fluorescence appeared inside the nucleus and some in cytoplasm whereas the red fluorescence was mostly localized in the cytoplasm and or towards the cell membrane. In the 2nd hour, the distinction was more obvious and the red fluorescence was seen spread in the cytoplasm while the green fluorescence seen overlapped with the blue fluorescence in the nucleus. This is indicative of the transport of DNA to the nucleus and the retention of polymer within the cytoplasm. However, in the 4th and 7th hour, the intensity of red fluorescence was found to be minimal in cytoplasm and tend to confine towards the membrane region.

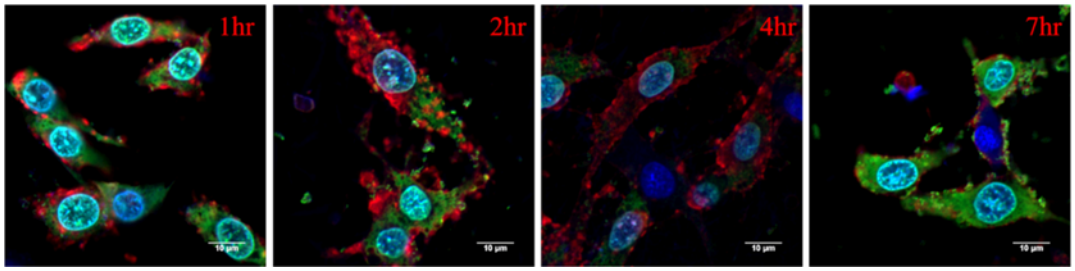

Figure 41: Localization of rhodamine labelled polymer inside the cytoplasm following uptake of nanoplexes of PPMSS/ctDNA 4:1 at different time period, where blue color indicate Hoechst stained nucleus and the red color represents rhodamine conjugated polymer and green fluorescence indicate YOYO tagged DNA.

4.2.5.5 Transfection studies based on Live and dead assay

The transfection of p53 plasmid in C6 cells via PPMSS carrier was evaluated using live and dead assay. Herein, the cellular apoptosis was caused by p53 expression and the dead cells were stained by ethidium homodimer dye which gives a red fluorescence. Since PEI-MSA caused a cellular rupture in the uptake studies due to high toxicity, it was not found suitable for transfection studies. Here, the normal untreated cells appeared green due to the cleavage of calcein CM dye in live cells, which emits green fluorescence. As seen in Figure 42, both PPMSS nanoplexes treated cells appeared mostly in red color and control cells appeared green, where the red color indicates dead cells and green indicate live cells. The results showed successful transfection of p53 gene.

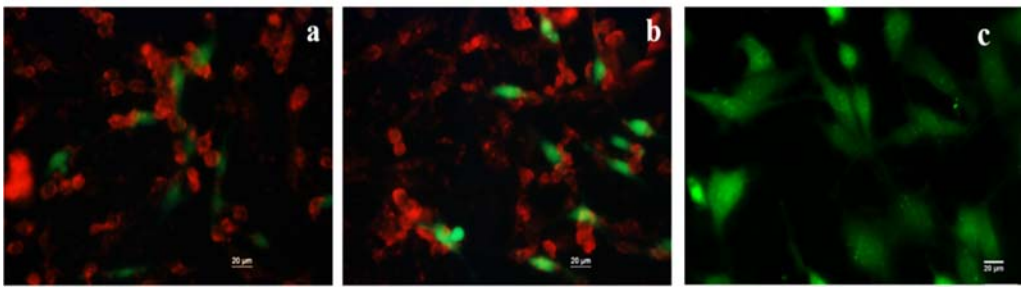

Figure 42: Live and dead assay a) PPMSS/p53 3:1 b) PPMSS/p53 4:1 and c) normal untreated cells, where red color indicate dead cells and green indicate live cells . The magnification is 40X.

4.2.5.6 PI staining via flow cytometry

The quantification of dead cells in PPMSS/p53 transfected cells was carried out using PI staining by flow cytometry. Propidium iodide is permeable to dead cells only, hence in dead cells it can enter and intercalate with the DNA to give red fluorescence. Herein, the dead cells indicate the transgene expression of p53. As seen in Figure 43, more than 70% of cells were dead following the transfection with p53 gene where PPMSS/p53 4:1 nanoplexes showed 78% cell death and PPMSS/p53 3:1 caused 71% death.

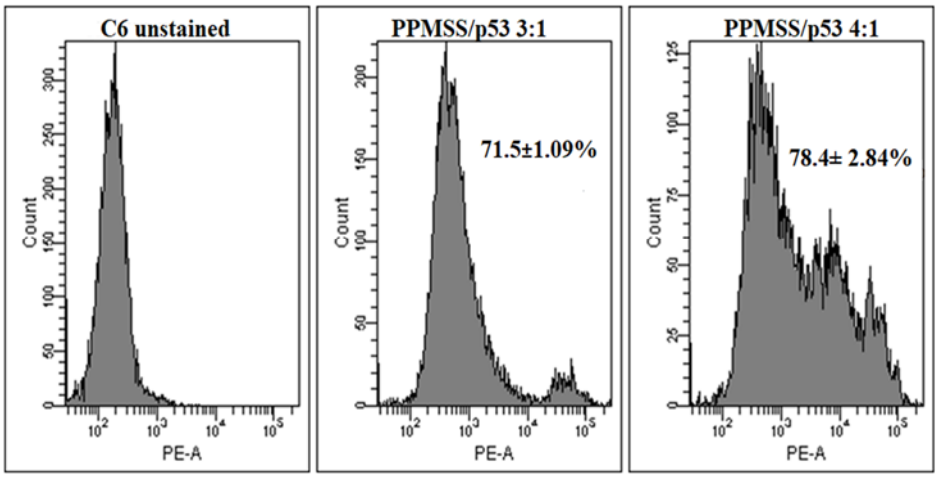

Figure 43: PI staining by flow cytometry, where PPMSS/p53 3:1 and PPMSS/p53 4:1 treated cells showed 71.5 % and 78.4% cell death respectively.

4.2.5.7 Determination of apoptosis by annexin V staining

It is known that p53 induce cellular apoptosis. Here, FITC-AnnexinV/propidium iodide (PI) method was utilized to investigate whether C6 cell death caused by the PPMSS polymer was associated with p53 expression and related apoptosis. C6 cells were transfected with nanoplexes of PPMSS/p53 at ratios 3:1 and 4:1. Twenty four hour post transfection, the cells were subjected to FITC-AnnexinV/PI staining. The cells without treatment with the nanoplexes were used as control. As shown in Figure 44, the percentage apoptosis was calculated by the sum of early and late apoptosis which is 73% and 80% by PPMSS/p53 3:1 and PPMSS/p53 4:1 respectively. This in turn indicates that more than 70% cells were transfected with p53 gene.

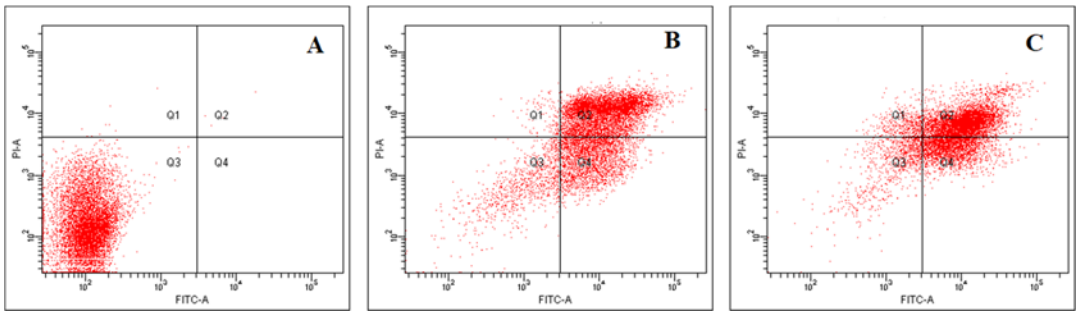

Figure 44: FITC-Annexin V/PI staining, A) untreated normal cells B) PPMSS/p53 3:1- 73.3±2.11% and D) PPMSS/p53 4:1- 80.2±4.02% cell death, where Q1 is necrotic cells, Q2 is late apoptosis Q3 is live cells and Q4 is early apoptosis. Percentage apoptosis is given as Q2+Q4.

4.2.5.8 p53 immunofluorescence – Confocal microcopy

The presence of p53 protein in the cytosol following the transfection of p53 gene mediated by PPMSS polymer was analysed by using labeled antibody and visualized in confocal microscopy. The binding of tagged antibody gives fluorescent signals which is indicative of the presence of apoptotic protein,p53. As seen in Figure 45, PPMSS/p53 nanoplexes treated cells showed intense green fluorescence, indicating the successful transfection of p53 and its corresponding expression in C6 cells. The p53 expression in turn is mediating cellular apoptosis.

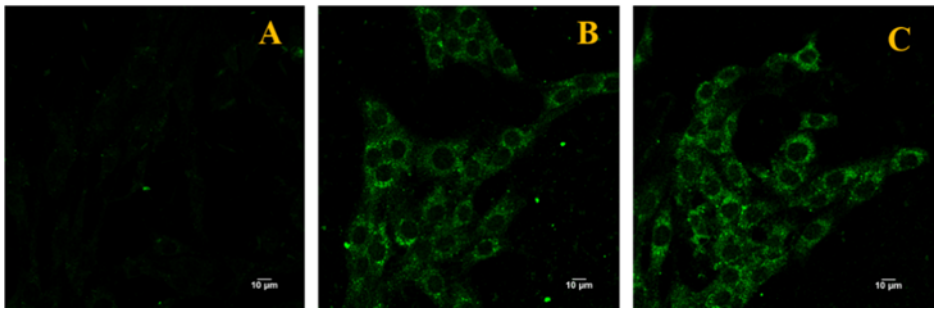

Figure 45: p53 immunofluorescence A) untreated control cells B) PPMSS/p53 3:1 nanoplex transfected cells C) PPMSS/p53 4:1 transfected cells, where green fluorescence indicate p53 expression.

4.2.5.9 Efflux pump inhibition studies using confocal microscopy

The efflux pump inhibition study was meant to evaluate the efficacy of PPMSS polymers in inhibiting efflux pump in different cancer cells. This, in turn, increases the accumulation of chemotherapeutics in the drug-resistant cells. The experiment was performed with the anticancer drug, DOX in different cells lines like C6, A549, and HeLa. The red fluorescence in these cells corresponds to the presence of DOX. The cells were initially preexposed with the PPMSS nanoplexes and were then followed by DOX treatment. As seen in Figure 46, the C6 cells showed increased intensity of red fluorescence in the PPMSS 3:1 and 4:1 nanoplexes pretreated cells compared to the DOX alone treated control cells. Similarly, in the case of A549 cells, the intensity of red fluorescence was remarkably increased in both PPMSS 3:1 and 4:1 nanoplexes pretreated cells compared to the control cells (Figure 47). However, as in Figure 48, the HeLa cells showed no visible difference in terms of DOX retention in both PPMSS (3:1 & 4:1) nanoplexes pretreated cells and DOX alone treated control cells. In fact, the intensity of red fluorescence was same in both the groups.

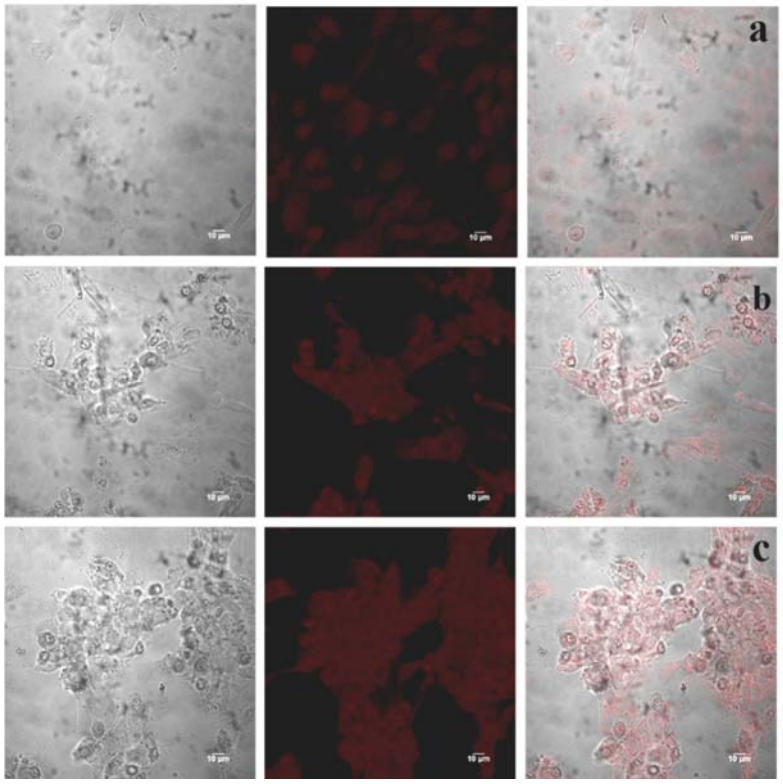

Figure 46: Efflux pump inhibition study in C6 cells using PPMSS polymer. a) merged image of bright field and DOX alone treated control cells, (b) bright field merged image of cells pretreated with PPMSS nanoplex at 3:1 ratio followed with DOX (c) bright field merged image of cells pretreated with PPMSS nanoplex at 4:1 ratio followed with DOX. (Magnification is 60X)

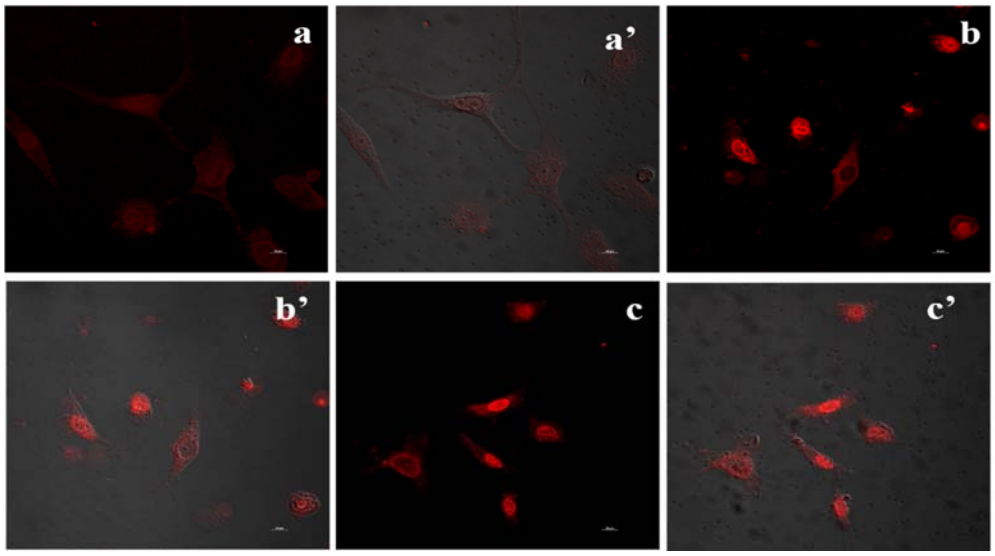

Figure 47: Efflux pump inhibition study in A549 cells, (a) DOX alone treated cell (a') bright field merged image of a (b) cells pretreated with PPMSS nanoplex at 3:1 ratio followed with DOX (b') bright field merged image of b (c) cells pretreated with PPMSS nanoplex at 4:1 ratio followed with DOX (c') bright field merged image of c The magnification is 60x.

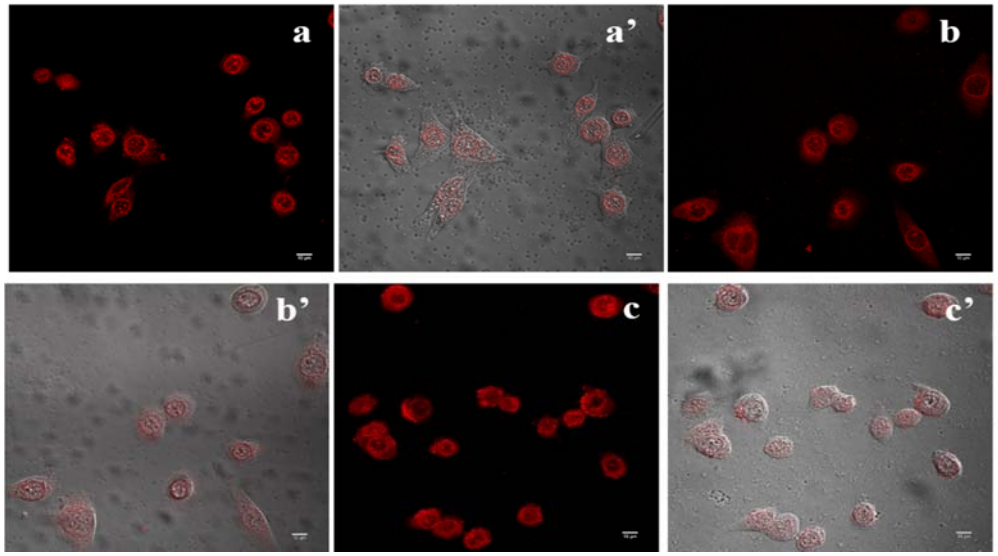

Figure 48: Efflux pump inhibition study in HeLa cells, (a) DOX alone treated cell (a') bright field merged image of a (b) cells pretreated with PPMSS nanoplex at 3:1 ratio followed with DOX (b') bright field merged image of b (c) cells pretreated with PPMSS nanoplex at 4:1 ratio followed with DOX (c') bright field merged image of c The magnification is 60x.

4.2.5.10 Efflux pump inhibition studies using flow cytometry

The efflux pump inhibition properties of the polymer, PPMSS were quantified via flow cytometry. The cell lines used were C6, A549, and HeLa. The DOX alone (3μM) treated cells was taken as the control group. The efflux pump inhibition by the polymer was assessed by initially exposing the cells with PPMSS 3:1 and 4:1 nanoplexes followed by the treatment with DOX (3μM). The percentage of cells retaining DOX in each group was quantified by flow cytometry. Herein, only 30% and 34% of cells retained DOX in the control groups of C6 and A549 respectively (Table 7). In the case of nanoplexes pretreated group of C6 cells, the percentage of cells retaining DOX was high and was 67% and 81% for PPMSS nanoplex ratios 3:1 and 4:1 respectively. The retention was almost similar in A549 cells, where 70% and 79% of cells retained DOX following exposure with PPMSS nanoplexes at 3:1 and 4:1 respectively. On the other hand, the control group of HeLa cells showed that 45% of cells retained DOX whereas nanoplexes pretreated group showed 44% and 50% respectively for PPMSS nanoplex ratio 3:1 and 4:1. This observation was in accordance with the confocal microscopy analysis.

cell lines	% of cells retaining DOX in control group	% of cells retaining DOX in the nanoplexes pretreated group	
		PPMSS/ctDNA 3:1	PPMSS/ctDNA 4:1
C6	30.51±1.18	67.4 ± 5.43	81.31 ± 6.82
A549	34.32±5.43	70.35 ± 8.21	79.62 ± 3.33
HeLa	45.31±1.02	44.69 ± 2.86	50.42 ± 5.05

Table 7: Efflux pump inhibition study using flow cytometry. The DOX alone treated cells is the control group. In the test group the cells were subjected to pretreatment with PPMSS I nanoplexes at ratios 3:1 and 4:1 followed by DOX exposure. Quantification of the percentage of cells retaining DOX was carried out using flow cytometry.

4.2.5.11 DOX retention kinetics

The retention kinetics of DOX in various cell lines was quantitatively determined by analyzing the concentration of DOX in cell lysate following nanoplexes pre-exposure and DOX treatment. The cells were initially treated with PPMSS 4:1 nanoplexes for 2hr followed by DOX treatment (3μM) and incubated for different time periods. As shown in Figure 49, In the case of C6 cells, the PPMSS nanoplexes pretreatment elevated the DOX concentration within the cells. In the first hour the DOX concentration reached upto 0.11μg/mg protein versus 0.06μg/mg of protein in the control group. The concentration of DOX further reached up to 0.14 μg/mg of protein in the 2nd hr and was found to be decreasing with time. Similarly, in A549 cells, the concentration of DOX reached up to 0.16μg/mg of protein in the 3rd hr against 0.09 μg/mg of protein in the control. Though the level of DOX was found to be decreasing over time in control groups, it maintained a high concentration 0.12 μg /mg of protein in the polyplexes pretreated group upto 7th hour. On the contrary, HeLa cells showed a DOX concentration of more or less same in both controls as well as polyplexes pretreated group.

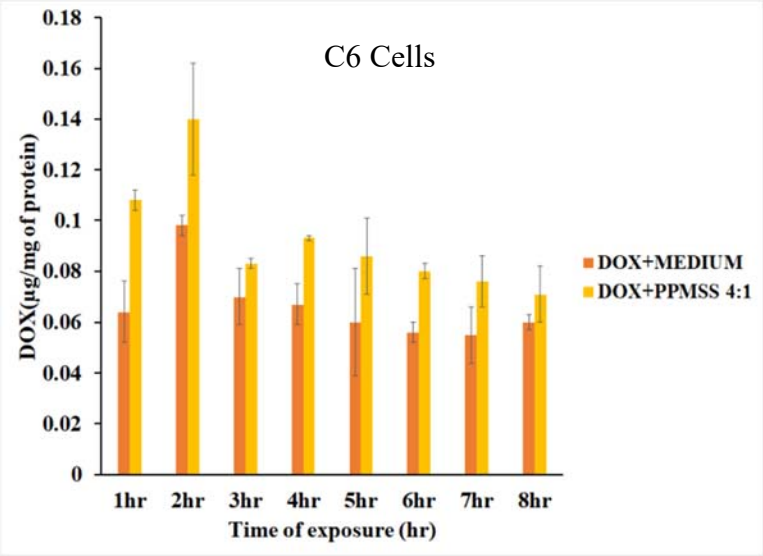
C6 Cells
DOX(µg/mg of protein)
0.18
0.16
0.14
0.12
0.1
0.08
0.06
0.04
0.02
0
1hr
2hr
3hr
4hr
5hr
6hr
7hr
8hr
Time of exposure (hr)
DOX+MEDIUM
DOX+PPMSS 4:1

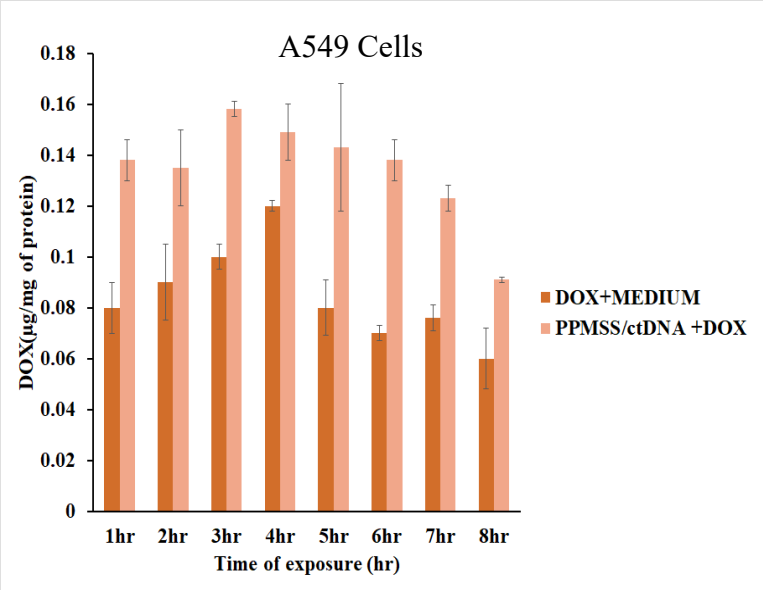
A549 Cells
DOX(µg/mg of protein)
0.18
0.16
0.14
0.12
0.1
0.08
0.06
0.04
0.02
0
1hr
2hr
3hr
4hr
5hr
6hr
7hr
8hr
Time of exposure (hr)
DOX+MEDIUM
PPMSS/ctDNA +DOX

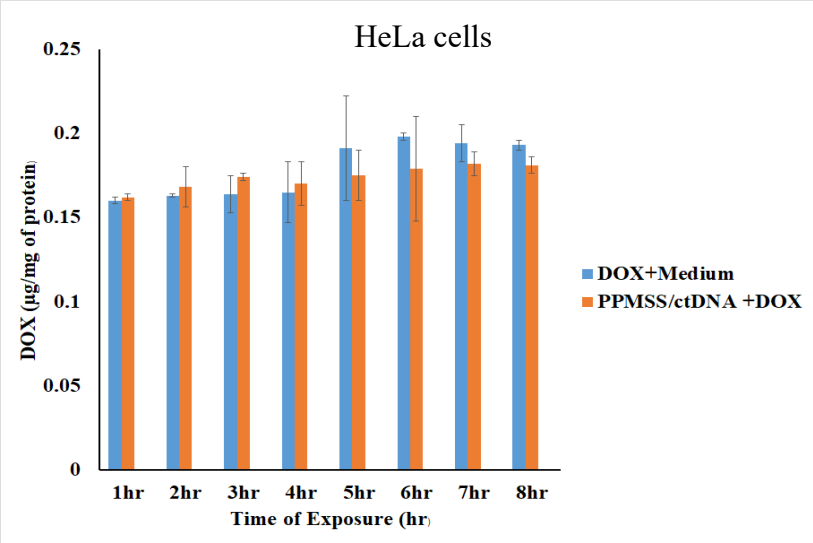

Figure 49: DOX retention kinetics in C6, A549 and HeLa. The cells were treated with PPMSS nanoplexes for 2hrs and followed by DOX treatment for different time points.

4.3. Synthesis and characterization of pullulan-PEI-3,3 dithiodipropionic acid (PPDPA)

The synthesis of pullulan-PEI-3,3 dithiodipropionate (PPDPA) was carried out by conjugating 3,3 dithiodipropionate (DPA) to the pullulan-PEI backbone via EDC coupling reaction. Depending on the amount of DPA added to pullulan-PEI conjugate, three PPDPA derivatives were synthesized i.e PPDPA I, II and III. The corresponding control groups were synthesized by conjugating PEI with DPA and were -coded as PDPA I, II and III. The disulfide as well as thiol content of these polymers were quantified and is given in Table 8. The thiol/ disulfide content of the polymer was in the order PPDPA III>PPDPAII>PPDPA I.

SL.NO	Sample ID	s-s linkage (mg/g of polymer)	Thiol content (mg/g of polymer)

1	PPDPA I	50.12±0.02	67.31±0.001
2	PPDPA II	64.08±0.007	71.04±0.034
3	PPDPA III	72.11±0.01	76.45±0.01
4	PDPA I	61.31±0.008	85.22±0.002
5	PDPA II	72.57±0.02	91.05±0.01
6	PDPA III	78.22±0.002	88.26±0.001

Table 8: The thiol and disulfide content of the pullulan derivative, PPDPA polymers and its corresponding controls PDPA.

The amino content of the polymer was evaluated by $CuSO_4$ assay and is given in Table 9. The amino content of the polymer is in the order PPDPA I > PPDPA II> PPDPA III which infact is reverse in order as compared with the thiol/disulfide content.

SL.NO	Sample ID	Amount of amino group (mg/10mg of polymer)
1	PPDPA I	3.23 ± 0.03
2	PPDPA II	2.93 ±0.11
3	PPDPA III	2.89 ±0.21
4	PDPA I	4.78 ±0.09
5	PDPA II	4.19 ±0.06
6	PDPA III	4.23 ±0.03

Table 9: Amino content of PPDPA I/II/III and the control group PDPAI/II/III polymers determined via $CuSO_4$ assay

4.3.1 ^{1}HNMR and FTIR

The formation of pullulan-PEI-dithiodipropionate (PPDPA) was verified by ^{1}H NMR. The characteristic peak of PEI representing the repeating units – (CH_2-CH_2-NH) - was at δ 2.5- 2.6

ppm which is clearly visible in the pullulan-PEI, PPDPA and PDPA (Figure 50). The signals at the region between δ 3.1 -3.2 ppm was visible in pullulan-PEI, PPDPA and PDPA represents – $CONHCH_2$. The signals corresponding to δ 3.4 -3.9 ppm in PPDPA were mainly associated with the $–CH_2-CH_2-$ group of pullulan. The signals at δ 5.25-5.29 ppm in PPDPA was due to the anomeric protons associated with α-(1-6) glycosidic linkage of maltotriose in pullulan. Most importantly, two ethylene groups neighbouring a disulfide linkage was observed at δ 2.7-2.8ppm in both PPDPA and PDPA. However, the more prominent presence of the corresponding signals was seen in PDPA control groups compared with the PPDPA polymers, mainly due to the influence of other chemical shifts in PPDPA polymers. This confirms the successful incorporation of disulfide groups in the polymer.

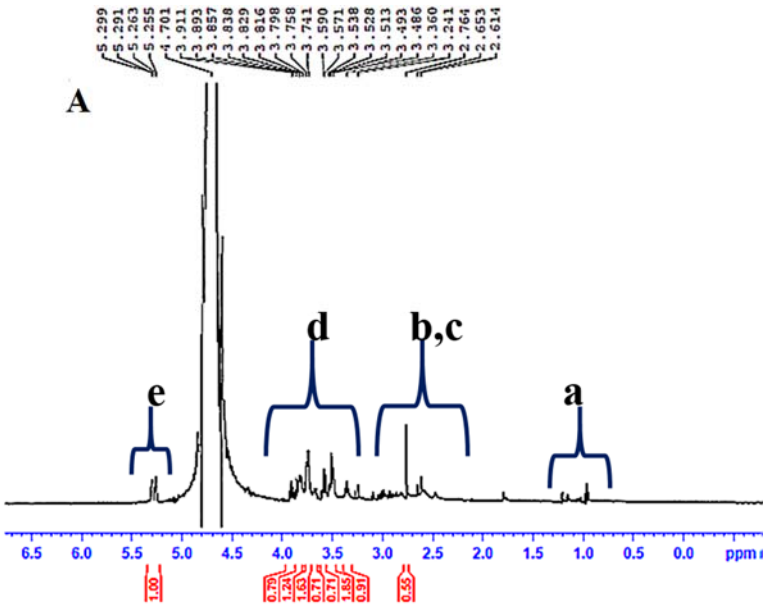

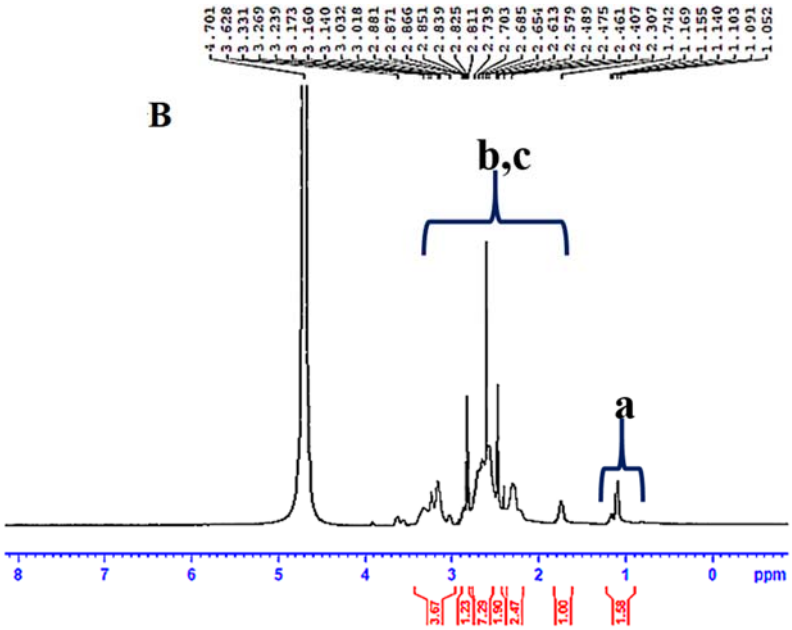

Figure 50: [1]HNMR spectra of A) PPDPA B) PDPA where the notations a represent the alkyl group of 3,3 dithiodipropionic acid. b and c indicate characteristic group of PEI i.e, –(CH_2-CH_2 -NH)n and two ethylene groups neighbouring a disulfide linkage respectively. The notation d and e in PPDBA indicate -CH_2-CH_2 - backbone and anomeric protons in pullulan respectively.

The FTIR spectra also support the successful conjugation of PEI to pullulan and also the conjugation of 3,3 dithiodipropionic acid to pullulan-PEI. In the spectrum, the absorption peaks around 848 cm^{-1} is indicative of D-glucopyranose units in pullulan and peak at 754 cm^{-1} observed in the PPDPA polymer is assigned to α (1,4) glycosidic bonds and that around 932 cm^{-1} proves the presence of α (1,6) glucosidic bonds in pullulan. The peaks at 1149cm^{-1} visible in the PPDPA polymer indicate the C-O-C stretching vibrations. The band in the PPDPA polymers at 2925 cm^{-1} is due to the stretching vibration of CH and CH_2 groups. The prominent broad band near 3283 cm^{-1} in PPDPA polymers are attributed to the overlapping of –OH and –NH stretching vibrations of both pullulan and PEI. On the other hand, the sharp peaks observed at 3268cm^{-1} seen in the control groups such as PDPA are due to the –NH stretching vibrations of PEI. Similarly, peaks near 1629cm^{-1} in PDPA polymers and 1635cm^{-1} in the PPDPA polymers are due to amide I bond owing to C=O stretching (Figure 51).

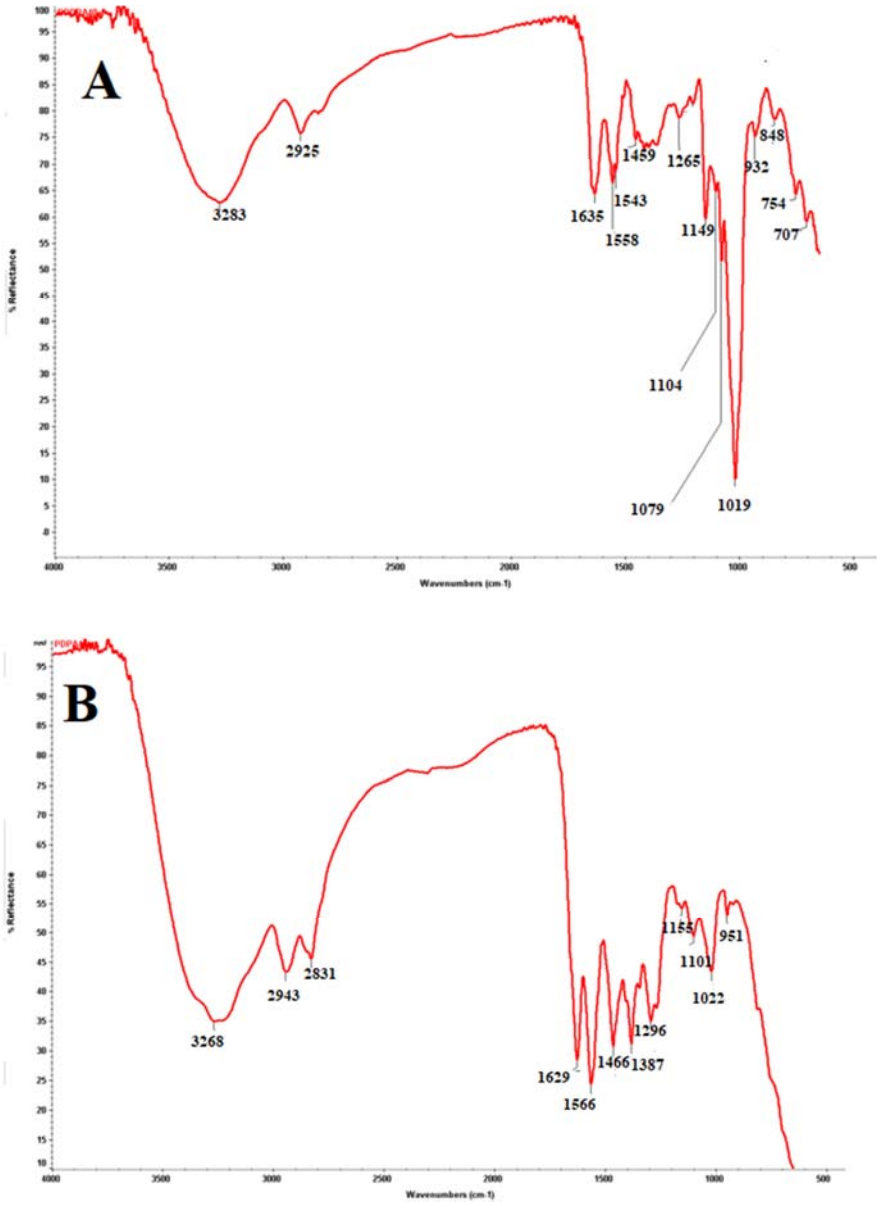

Figure 51: FTIR spectra of A) PPDPA II B) PDPA II

4.3.2 Buffering capacity

Buffering ability of the polymer is very important for the escape of nanoplexes from the endosome and also to promote transfection efficacy. This has been associated with the buffering abilities of non-viral vectors within the pH range of 10-4. Here, acid-base titration was carried out

to assess the buffering abilities of the polymers PEI, PPDPA I/II/III and the corresponding controls PDPAI/II/III. As seen in Figure 52, PEI showed the highest buffering capacity due to the presence of the dense amino group in the polymer. On the other hand, when comparing the buffering capabilities of pullulan based polymers, PPDPA I showed higher buffering ability at the specified pH range compared to the other two i.e. PPDPA II and III. Both PPDPAII and III have almost the same titration curve but was found to be lower compared to PPDPA I. The PEI derivatives such as PDPA I, II and III also showed a reduction in the buffering abilities compared to PEI but higher when compared with pullulan-PEI based derivatives.

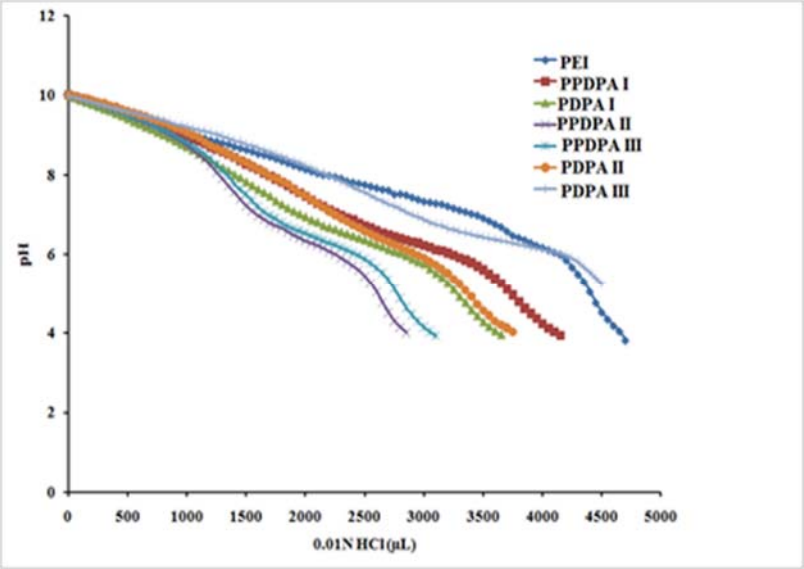

Figure 52: Acid-base titration curve of PEI, PPDPA I/II/III and PDPA I/II/III against 0.01N HCl.

4.3.3. Biophysical characterization

4.3.3.1 Size and Zeta potential

The hydrodynamic size of PPDPA I, II and III polyplexes were analyzed and compared with the corresponding control groups i.e. PDPA I, II and III. The PPDPA I polyplex ratios ranging from 1:1 to 5:1 showed a particle size of < 200nm but have failed to attain an appropriate zeta potential value, hence higher polyplex ratios i.e. 10:1 to 30:1 were evaluated. The optimum size

and zeta potential values were recorded at 10:1 and 25:1, where the size measured was 124.6± 2.01 and 124.3±1.34nm and zeta potential value as 12.8±2.47 & 13.2±2.55mV respectively. In contrast, the control PDPA I polyplexes (1:1 to 5:1) showed smaller size and positive surface charges with > 25mV even at lower polyplex ratios. For the control, the optimum size was obtained at 2: 1 and 4:1. On the other hand, the hydrodynamic size of both PPDPA II and III were less than 200nm both the cases. The particle size of PPDPA II nanoplexes were 192±6.1nm and 142±4.76nm for at 3:1 and 4:1 ratios respectively. Similarly, for PPDPA III, it was137± 1.8nm and 159± 6.3nm respectively. The zeta potential values of these nanoplex at ratios of 3:1 and 4:1 of both PPDPA II and III were in the range between 8-12mV against > 25mV for the control groups PDPA II and III (Figure 53). The size and zeta potential values of the nanoplexes at 3:1 and 4:1 ratios were found suitable for gene delivry applications in the case of PPDPA II and III and 10:1 and 25:1 in case of PPDPA I. Hence these ratios were selected for further studies.

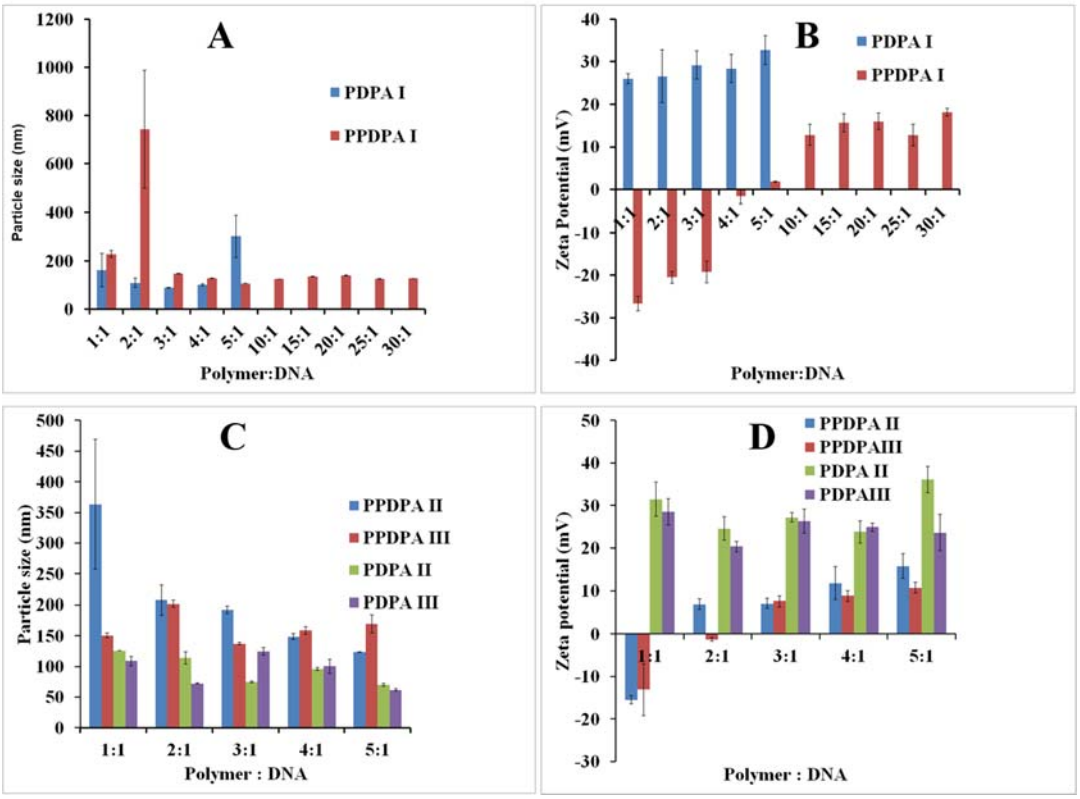

Figure 53 : Size and zeta potential values of A) hydrodynamic size of PDPA I and PPDPA I B) zeta potential of PPDPA I and PDPA I C) size of PPDPA II, PPDPAIII and PDPA II and PDPA III and D) zeta of PPDPA II,PPDPA III, PDPAII and PDPA III.

4.3.3.2 Agarose gel electrophoresis

Agarose gel electrophoresis was carried out to understand the stability of polyplexes or the condensation ability of the polymer. Complete retardation of DNA was observed in the control groups PDPA I, II and III at all polyplex ratios. However, in the case of PPDPA I, II and III, complete inhibition of DNA mobility required higher amounts of the polymer (Figure 54). As in Figure, the DNA bands were visibly trailing in the gel which infers unstable complex formation at PPDPA I polyplex ratios of 1:1-5:1 and initial two polymer:DNA ratios of PPDPA II and III. However, at an optimal polymer to DNA ratios, i.e 10:1, 25:1 for PPDPA I, at 3:1 and 4:1 for PPDPA II & III respectively, the DNA mobility was completely retarded and was observed to be

retained in the wells. The stability of the polyplex was also assessed by incubating with plasma. As shown in Figure 54, the nanoplex was found to be stable and the DNA was seen confined in the well, implying the strong interaction of the polymer with the DNA even in the presence of anionic protein.

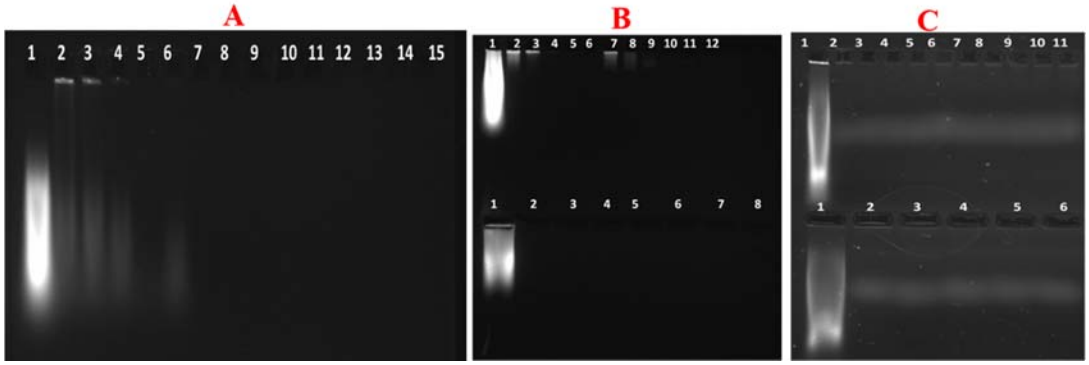

Figure 54: Agarose gel electrophoresis A) Lane 1: ctDNA, Lane 2-6: PPDPA I/ctDNA 1:1 to 5:1 and lane 7-11: PPDPA I/ctDNA 10:1, 15:1, 20:1,25:1 and 30:1 respectively. Lane 12-15: PDPA I /ctDNA ratios 2:1 to 5:1. B) Lane 1 upper and lower indicate ctDNA, lane (upper 2-6) shows PPDPAII/ctDNA 1:1 to 5:1 and 7-11 indicate PPDPA III/ctDNA 1:1 to 5:1 Lower lane 2-4 indicate PDPA II and lane 5-8 represent PDPA III/ctDNA nanoplex ratio 2:1-5:1. C) Lane 1 upper and lower indicate ctDNA and plasma, lane 2-5 indicate PPDPA I/ctDNA 10:1,15:1,20:1 and 25:1, whereas lane 6-8 indicate PPDPA II/ctDNA nanoplex ratio 2:1 -4:1 and lane 9-11 corresponding to PPDPA III/ctDNA 2:1 -4:1. Lower lane represents PDPA I/II and III to DNA ratios 2:1 & 4.1, 3:1 & 4:1 and 4:1 respectively.

4.3.3.3 Stability of nanoplexes in presence of DTT

It is known that the reduction potential in the cytoplasm is much higher than that in the plasma. In order to study the reduction response of the polyplexes formed by the polymer i.e. PPDPA I/II/III and PDPA I/II/III, DTT was applied as a model reducing agent. The effect of DTT on polyplexes

was analysed by means of size measurement and gel retardation assay. As shown in Figure 55, in the presence of DTT, the particle size of the polyplexes of the polymer PPDPAI/II/III was gradually increasing with time, starting from around 150nm and reached around 250nm over time. However, there was no observable size variation seen with respect to time in the selected polyplexes of PPDPA I/II/III without DTT, which remained around 200nm in 4hr. However, though the control groups also showed some changes upon DTT exposure, it was not as significant as the pullulan based counterparts. Figure 56, shows gel retardation results of the selected polyplex ratios of PPDAI/II/III and PDPA I/II/III in the presence of DTT, it can be seen that the addition of DTT has not released DNA from the corresponding polyplexes, while the combined treatment of heparin/DTT resulted in release of DNA from the selected polyplex of PPDPA and PDPA. There was sufficient dissociation of the polyplexes resulting in nearly complete release of DNA owing to the combined treatment.

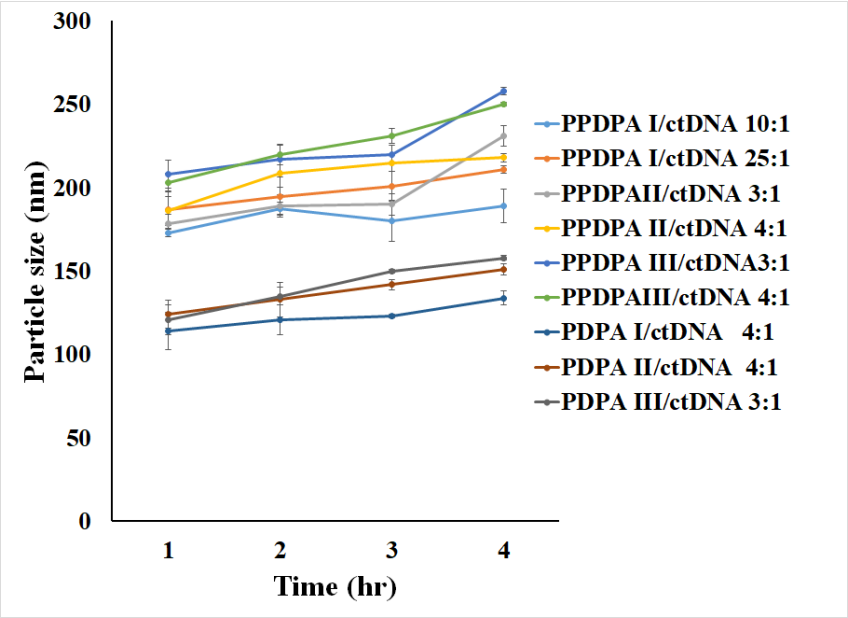

Figure 55: Particle size measurement of selected polyplex ratios of PPDPAI/PPDPAII/PPDPAIII and PEI-CYS(S-S)I/II/III in presence of DTT (10mM)

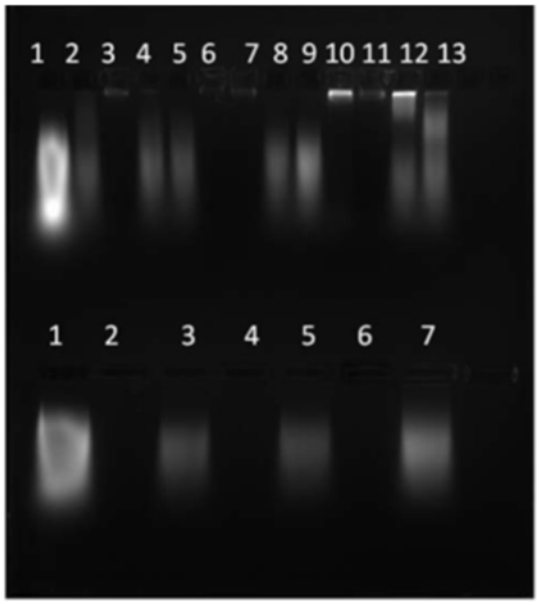

Figure 56: Lane 1 upper and lower indicate free ctDNA, lane 2-3(upper) PPDPA I10:1 & 25:1 with DTT alone treated, lane 4-5 (upper) nanoplex with both DTT/heparin treated. Similarly lane 6-7 and 10-11 corresponding to DTT alone treated one with PPDPA II and III polyplex ratios 3:1 and 4:1 respectively. Lane 8-9 and 12-13 shows the DTT/heparin treated one. Lane 2,5,6 (lower)is PDPA I 4:1, PDPA II 4:1 and PDPA III 3:1 with DTT alone treated and lane 3,5,7 is the corresponding DTT/heparin treated one.

4.3.4 Plasma protein interaction with the polymers (PAGE)

Blood contains various abundant proteins which can interact with nanoparticles during their transport in the systemic circulation leading to alterations in its circulation time or resulting in early clearance. Herein, PPDPA I/II/III , PDPA I/II/III and PEI were incubated with serum for 30min. The resulting supernatant following centrifugation was subjected to PAGE. As seen in Figure 57, the proteins bands are all present in the untreated serum (negative control) whereas there is a marked reduction in protein bands in the case of PEI (positive control), which is mostly due to the adsorption of proteins on to the surface of the polymer. Similar to PEI, the control groups such as PDPA I, II, III also showed a corresponding reduction in the protein bands as compared to the serum alone, indicating active adsorption of the proteins on to the particle surface (Figure 57).

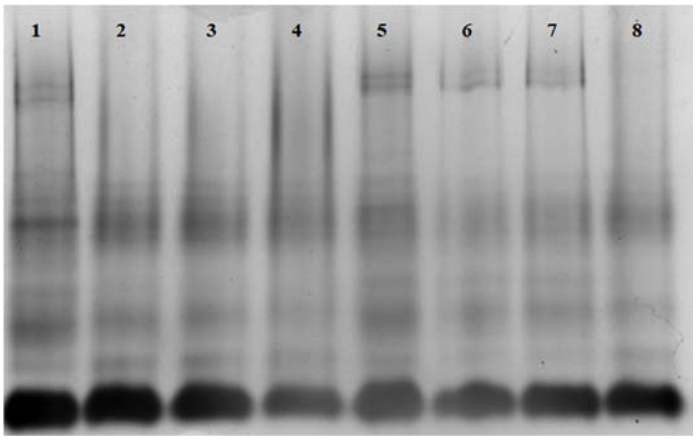

Figure 57: PAGE analysis. Interaction of different plasma proteins with polymers PPDPA I, II, III and its control PDPA I, II, II and PEI in comparison with the protein profile of serum treated with normal saline. Lane 1 is serum (positive control) Lane 2-4 is PDPA I/II/III with serum respectively and lane 5-7 is PPDPA I/II/III with serum respectively with . Lane 8 is PEI with serum (negative control).

4.3.5 Biological analysis

4.3.5.1 Cytotoxicity evaluation of the polymer

The cytotoxicity of the selected nanoplexes ratios of PPDPA I, II, III and PDPA I, II, III were evaluated in different cancer cell lines such as C6, HeLa and A549 along with the normal fibroblast cell i.e L929 by means of MTT assay. As shown in Figure 58, the percentage viability was found to be higher (>85%) in both PPDPA I and II polyplexes as compared to PPDPA I (~81%). In the case of control group PDPA I,II, III treated cells, the viability was <50%. Moreover, in the fibroblast cell, L929, cell viability was maintained above 81% with all the PPDPA polyplexes of PPDPA polymers I/II/III with higher values observed in PPDPA II polyplex i.e 87%. On the contrary, the control groups showed a very low viability of around 30% in the L929 cells which is lower than that of the toxicity observed in cancer cell lines. The percentage viability was found >85% in all the cancer cell lines tested when it is treated with PPDPA II and III nanoplexes whereas the viability was approximately 80% in the PPDPA I nanoplexes exposed cells.

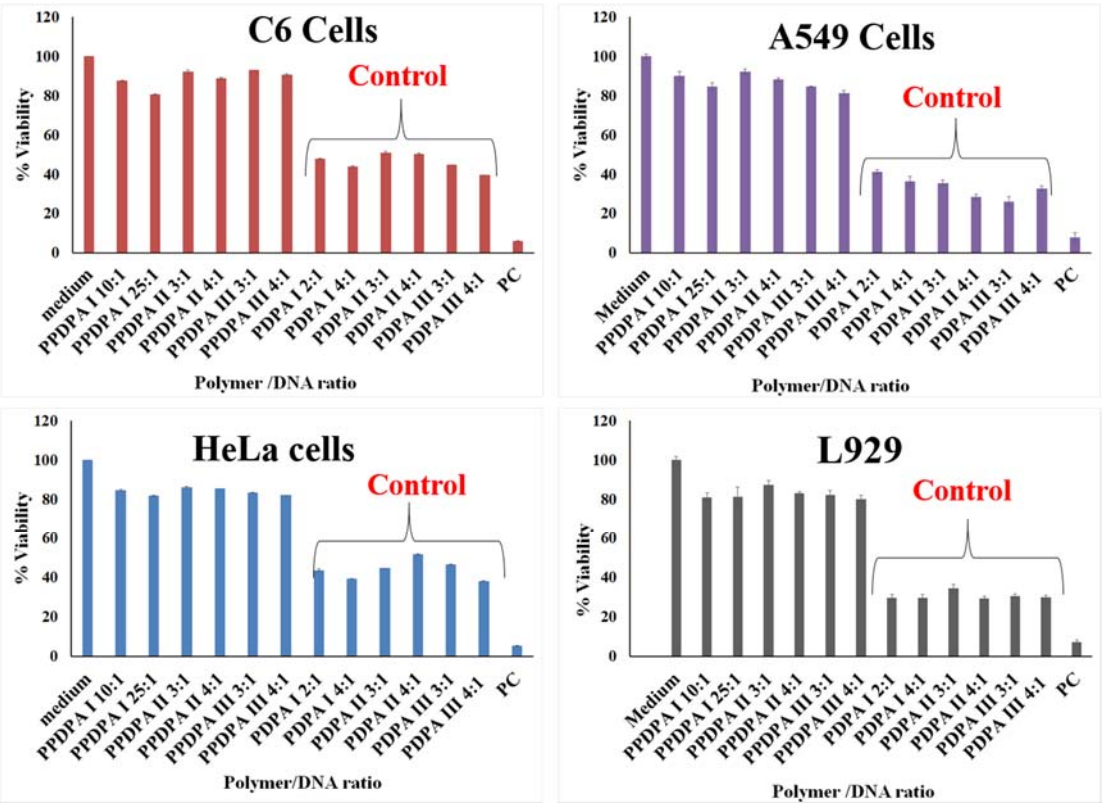

Figure 58 : The percentage cell viability of the selected nanoplexes ratios of PPDPA I (10:1 & 25:1), PPDPA II (3:1 & 4:1) and PPDPA III (3:1& 4:1) in different cell lines measured using MTT, where data represent mean ±SD (n=4).

4.3.5.2 Evaluation of cellular uptake

To visualize the intracellular DNA transport, YOYO-I was tagged to ctDNA to produce green fluorescence, making it traceable under biological conditions. The selected nanoplexes ratios of PPDPA I/II/III and its corresponding control groups i.e PDPA I/II/III were incubated to C6 cells for 3hr. The cell nuclei were stained with Hoechst. Confocal images demonstrated that YOYO tagged ctDNA could be detected in almost all the cells after 3h exposure (Figure 59). More specifically, most of the green fluorescence was mainly localized in the nucleus by coinciding with blue fluorescence in the nucleus, whereas some signals were found localised in cytoplasm of C6 cells. However, the control groups formed by the PDPA I/II/III nanoplexes showed neither cellular

nor nuclear uptake and the cells were visibly damaged. Simultaneously, the cellular uptake process was quantified by means of flow cytometry. The PPDPA I/ctDNA nanoplex at ratio 10:1 showed an uptake of 84.5 % and PPDPA I/ctDNA 25:1 showed a 90.3% uptake. Similarly, PPDPA II/ctDNA 3:1 nanoplex and PPDPA II/ctDNA 4:1 showed a cellular uptake of 91.1 % and 93.4% respectively. On the other hand, PPDPA III/ctDNA 4:1 exhibited an uptake of 76.9 % (Figure 60). These results clearly reveals that PPDPAs polymer based polyplexes could successfully deliver ctDNA into the nucleus.

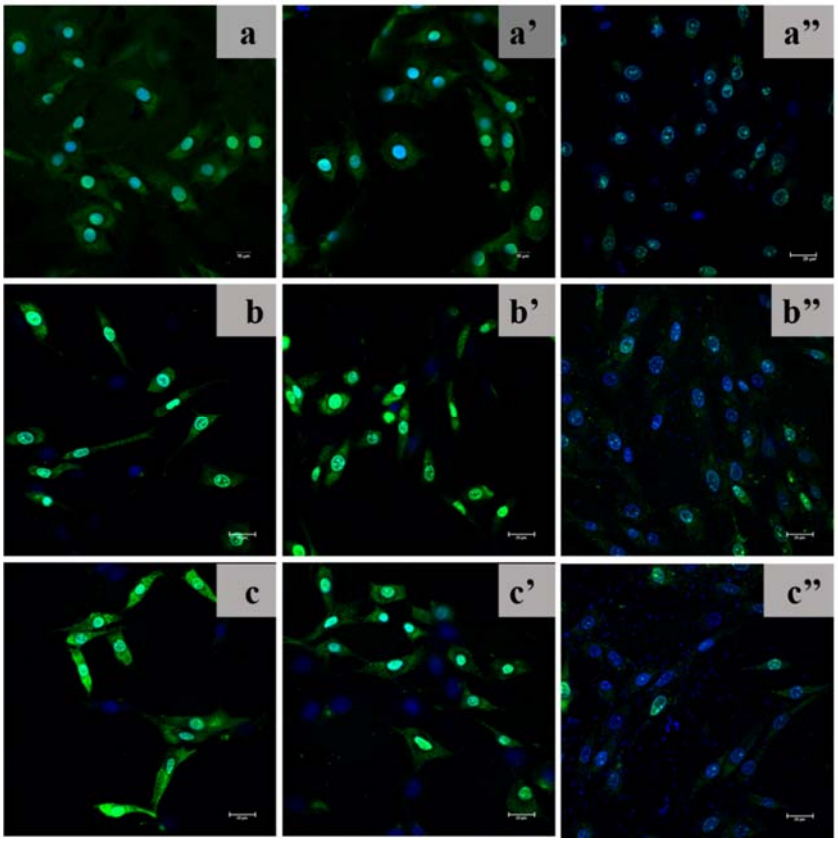

Figure 59: Cellular uptake of PPDPA polymers where nucleus is stained with hoechst and DNA with YOYO-I a) PPDPA I/ctDNA 10:1 nanoplexes a') PPDPAI/ctDNA 25:1 nanoplexes a'')

PDPA I/ctDNA 4:1 nanoplexes b) PPDPA II/ctDNA 3:1 b') PPDPA II/ctDNA 4:1 b'') PDPA II/ctDNA 3:1 c) PPDPA III/ctDNA 3:1 c') PPDPA III/ctDNA 4:1 and c'') PDPA III/ctDNA 3:1 nanoplexes.(Magnification is 60X)

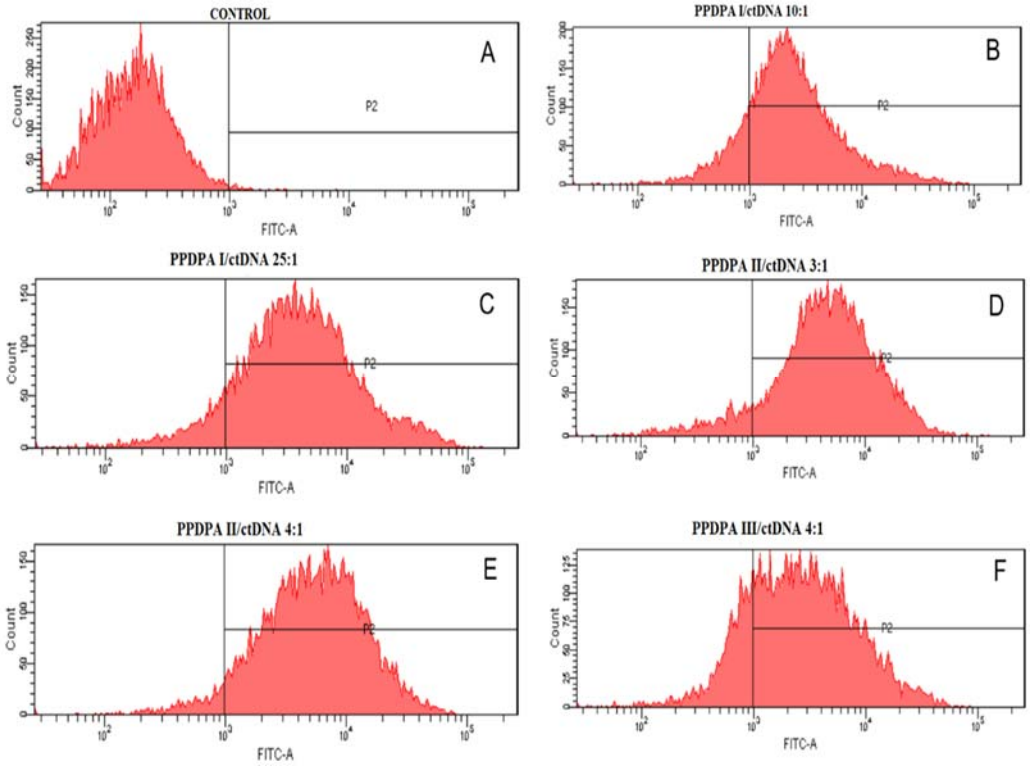

Figure 60: Flow cytometry data of A) control unstained B) PPDPA I/ctDNA nanoplex of ratio 10:1 with percentage uptake of 84.5 ± 3.62 % C) PPDPA I/ctDNA 25:1, percentage uptake is 90.3± 3.81% D) PPDPA II/ctDNA 3:1 nanoplex with uptake of 91.1±4.1% E) PPDPA II/ctDNA 4:1 F) PPDPA III/ctDNA 4:1 with percent uptake of 93.4±2.7 and 76.9 ±4.1 respectively.

4.3.5.3 Endocytosis inhibitor study

The pathway of entry of PPDPA nanoplexes into the cell was illustrated using endocytosis inhibitors targeting different key endocytosis pathways. As shown in Figure 61, chlorpromazine which specifically inhibits the clathrin-mediated endocytosis pathway in the cell did not adversely influence the cellular internalization of the PPDPA polyplexes (99% uptake compared to the untreated control cells). Similarly, filipin and amiloride which shut down the two crucial endocytosis pathways such as caveolae-mediated and micropinocytosis respectively, failed to prevent the entry of nanoplexes into the cells and formed 98% and 97% of cellular entry

respectively. The individual effect of these inhibitors was such that none was capable to adversely influence the endocytosis process of the nanoplexes. The flow cytometry analysis showed a near 100% entry of the nanoplexes comparable to that of the untreated cells, where the percentage uptake of the untreated cells was taken as maximum.

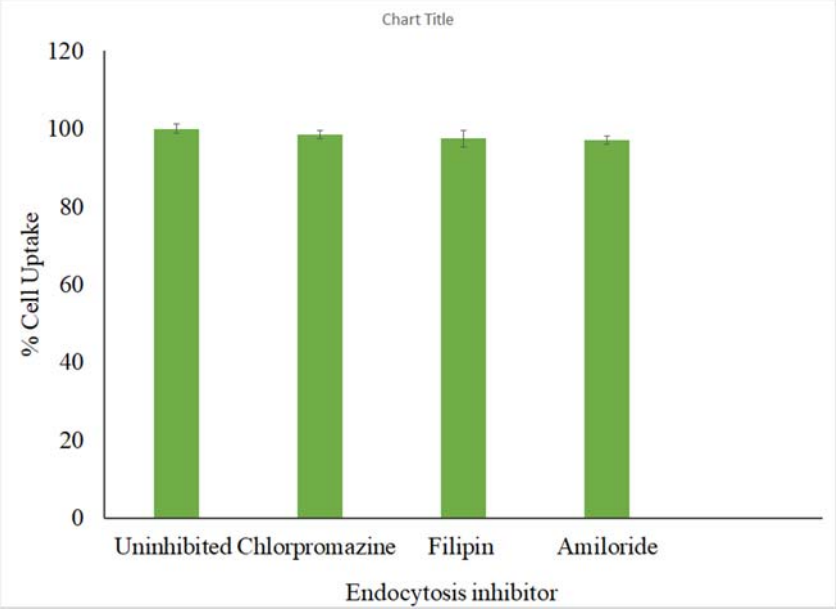

Figure 61: Cellular uptake of PPMSS/ctDNA 4:1 in presence endocytosis inhibitors. The control group is the nanoplex treated cells without endocytosis inhibitors.

4.3.5.4 Polymer trafficking studies

The gene transfection efficacies of the cationic polymer are closely related to the intracellular kinetics and internalization pathways. Therefore the cell uptake and intracellular transport of PPDPA polyplexes were explored at different time points. The distribution of both DNA and the polymer was monitored by using fluorescent dyes such as YOYO-I and rhodamine respectively. As shown in Figure 62, the cellular uptake increased with incubation time. Though the green fluorescence observed in the nucleus coincided with blue fluorescence in the 1st hour, the intensity was visibly lower. However, in the 2nd hour, both green and red fluorescence was found to be

prominent and the intensity of green fluorescence appeared very clear and intense in the nucleus whereas some traces were observed in the cytoplasm. In the 4th hour, the scenario was still the same, with more pronounced appearance of green fluorescence in the nucleus with traces in the cytoplasm and the red fluorescence mainly confined to the membrane region. By 7th hour, red fluorescence was still more intense but aligned towards the cell membrane (Figure 62). It should be noted that red fluorescence always remained outside the nucleus either in the cytoplasm or the cell membrane surface and have not entered into the nucleus per se.

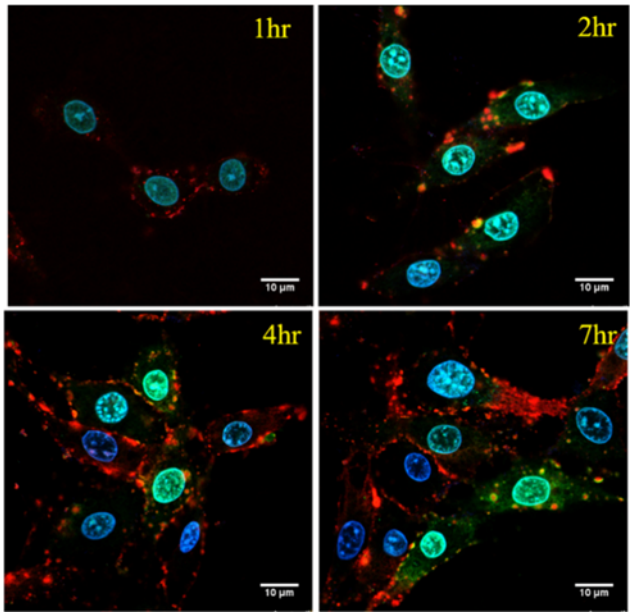

Figure 62: Time dependent observation of cellular uptake of nanoplexes. Naoplexes are prepared with rhodamine tagged PPDPAII and YOYO tagged DNA at 4:1 ratio. The internalisation is monitored at specified time intervals as shown in image.

4.3.5.5 Transfection studies based on Live and dead assay

The *in vitro* transfection efficiency of different PPDPA polymers i.e PPDPA I/II/III was evaluated using live and dead assay, where p53 was used as the gene of interest. The transfection

efficiency was directly visualized, where red fluorescence indicates dead cells and green fluorescence represented live cells. Here, two selected nanoplexes ratios of each PPDPA polymers were used for the study i.e. PPDPAI /p53 10:1, PPDPA I/p53 25:1, PPDPA II/p53 3:1, PPDPA II/p53 4:1 and PPDPA III/p53 3:1 and PPDPA III/p53 4:1 ratio. The C6 cells were transfected with the above mentioned nanoplexes and the gene expression was evaluated using live dead assay. The p53 gene expression lead to cell death and is identified by the red fluorescence owing to the intercalation with ethidium bromide. As shown in Figure 63, it can be seen that both ratios of PPDPA I/II express more red color than PPDPA III.

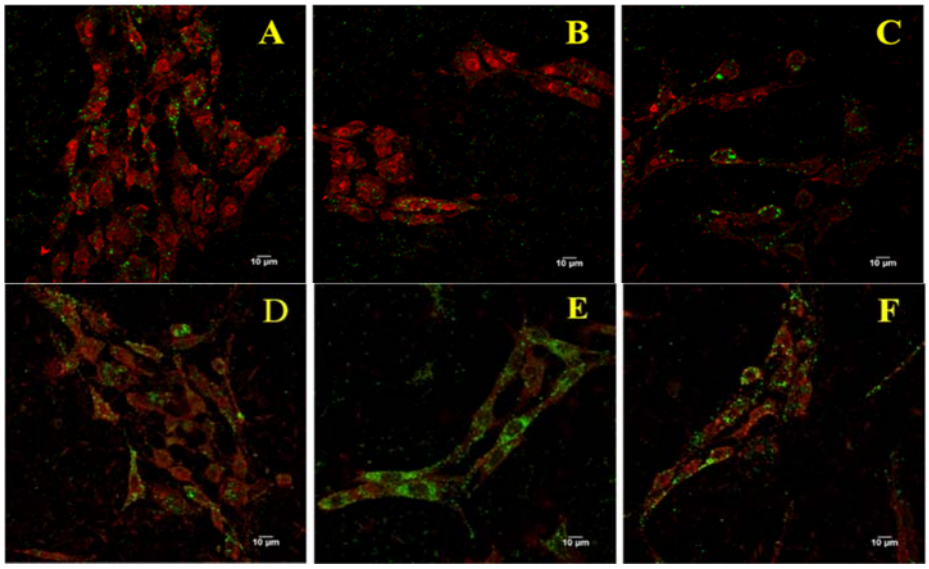

Figure 63: Live and dead assay A)PPDPA I/p53 10:1 transfected cells B) PPDPA I/p53 4:1 C) PPDPA II/p53 3:1 D) PPDPA II/p53 4:1 E) PPDPA III/p53 3:1 F) PPDPA III/p53 4:1 treated cells.

4.3.5.6 PI staining via Flow cytometry

The transfection efficiency of PPDPA polymers was further determined by means of staining. Propidium iodide (PI) cannot cross the membrane of live cells hence it can be used to differentiate dead cells from healthy cells. The percentage cell death identified by using PI staining indicates the extent of cell death caused by the polyplex transfection. As shown in Figure 64, PPDPA I

showed higher cell death of 88% and 92% for PPDPA/p53 10:1 and 25:1 nanoplexes respectively. On the other hand, PPDPA II/p53 3:1 and 4:1 nanoplexes exhibited 76% and 78% of cell death and PPDPA III/p53 3:1 and 4:1 showed 51% and 52% respectively. This results clearly showed that extensive cell death occurred in the PPDPA I nanoplex treated cells compared to PPDPA II and III., PPDPA III nanoplexes treated cells showed a minimal cellular death of around 50% compared to PPDPA I/II.

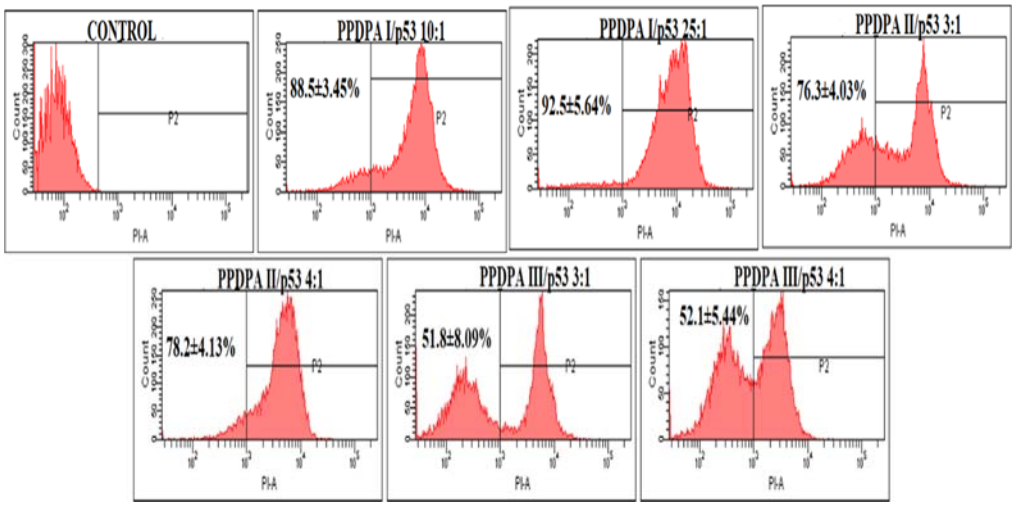

Figure 64: Cell death measured by PI staining: the percentage cells death following the transfection of selected nanoplexes ratios of PPDPA I/II and III in C6 cells.

4.3.5.7 Determination of apoptosis via annexin V staining

The cell death mediated by apoptosis was specifically determined via annexin V staining, where the apoptotic activity of the polymer based nanoplexes of PPDPA I/II and III were determined. As seen in Figure 65, the percentage apoptosis for PPDPA I/p53 10:1 and 25:1 transfected cells is 64% and 65% respectively. Similarly, the PPDPA II/p53 3:1 and 4:1 polyplexes

mediated transfection showed 60% and 64% and PPDPA III/p53 3:1 and 4:1 caused 54% and 44% apoptosis respectively. The untreated cells are taken as a control group.

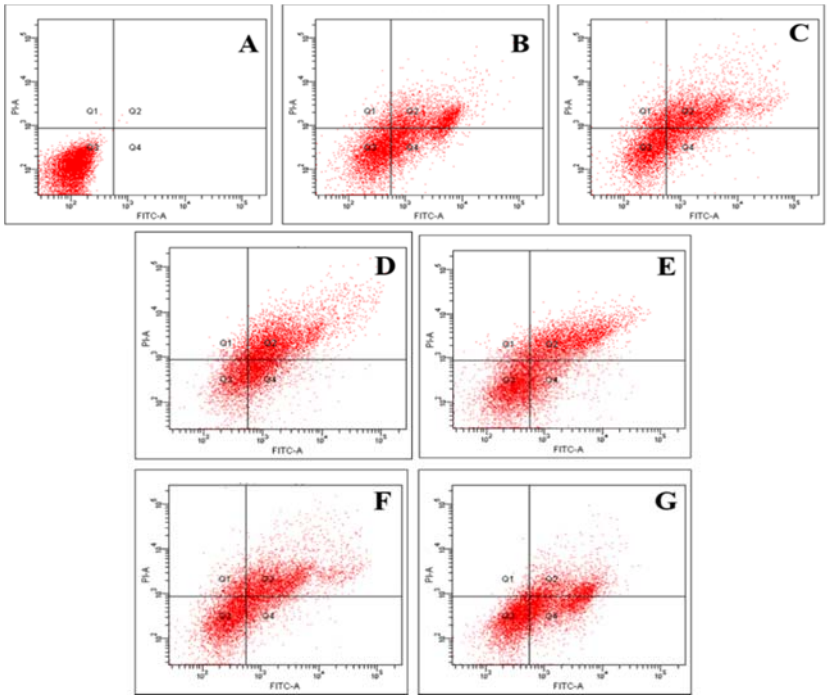

Figure 65: PPDPA/p53 nanoplexes mediated apoptosis, where A) normal control cells B) PPDPA I/p53 10:1 treated cells with percentage apoptosis is 64.3±2.76% C) PPDPAI/p53 25:1, percentage apoptosis= 65.2±3.22%, D) PPDPA II/p53 3:1,percentage apoptosis= 60.8± 5.88% E) PPDPA II/p53 4:1, percentage apoptosis=64.4 ± 3.98% F) PPDPA III/p53 3:1, percentage apoptosis is 54.8±4.09% G) PPDPA III/p53 4:1, % apoptosis= 44.5 ±4.17 %.

4.2.5.8 p53 immunofluorescence

The p53 transfection by the polymer PPDPA was further confirmed by immunofluorescence study. As observed in Figure 66, the three representative nanoplexes of PPDPA i.e PPDPA I/p53 25: 1, PPDPA II/p53 4:1 and PPDPAIII/p53 4:1 showed expression of p53 in the cytosol which is evidenced by the presence of green fluorescence in the cytoplasm. The green fluorescence

indicates the presence of the protein, p53, which shows the successful transfection of PPDPA/p53 based nanoplexes in C6 cells.

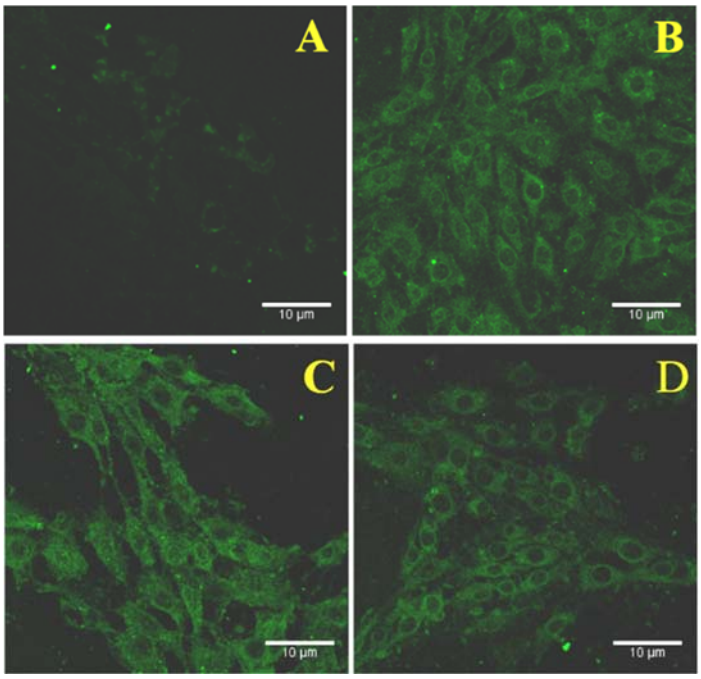

Figure 66: p53 immunofluoresence A) untreated control cells B) PPDPAI/p53 4:1 treated cells C) PPDPA II/p53 4:1 nanoplexes D) PPDPAIII/p53 4:1 nanoplexes treated cells, where green fluorescence indicate the expression of p53.

4.3.5.9 Efflux pump inhibition studies using confocal microscopy

The efficacy of the PPDPA polymers in inhibiting efflux pump or P-gp in cancer cells was analyzed using confocal microscopy. Three different cell lines were used i.e C6, A549 and HeLa, where the anticancer drug, DOX was used as an index of efflux pump inhibition. As shown in Figure 67 and 68, the nanoplexes (PPDPA I/ctDNA 25:1,PPDPA II/ctDNA 4:1 and PPDPA III/ctDNA 4:1) pretreated cells of C6 and A549 showed enhanced intensity of red fluorescence compared with the control group following the treatment with DOX(3µM). The remarkable difference in the fluorescence intensity between the control and the nanoplexes pretreated cells

indicate the enhanced accumulation of DOX in the nanoplexes treated cells. On the other hand, HeLa cells following exposure with PPDPA I/II/III nanoplexes and DOX showed good fluorescence intensity. The red fluorescence observed in the control cells were also same as that showed by the nanoplexes pretreated cells (Figure 69).

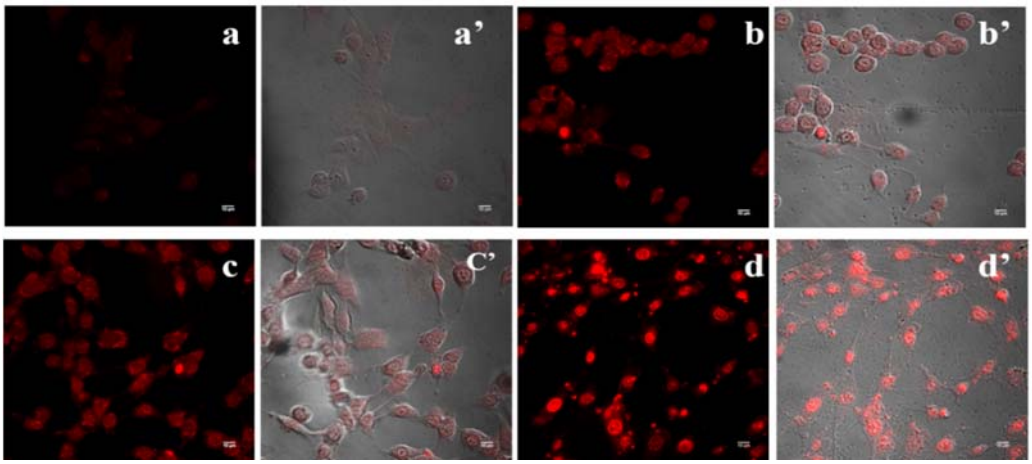

Figure 67: Efflux pump inhibition study in C6 cells, (a) DOX alone treated cell (a') bright field merged image of a (b) cells pretreated with PPDPA I nanoplex at 25:1 ratio followed with DOX (b') bright field merged image of b (c) cells pretreated with PPDPA II nanoplex at 4:1 ratio followed with DOX (c') bright field merged image of c, and (d) PPDPA III nanoplexes 4:1 exposed cells followed with DOX treatment (d') bright filed merged image of d. The magnification is 60x.

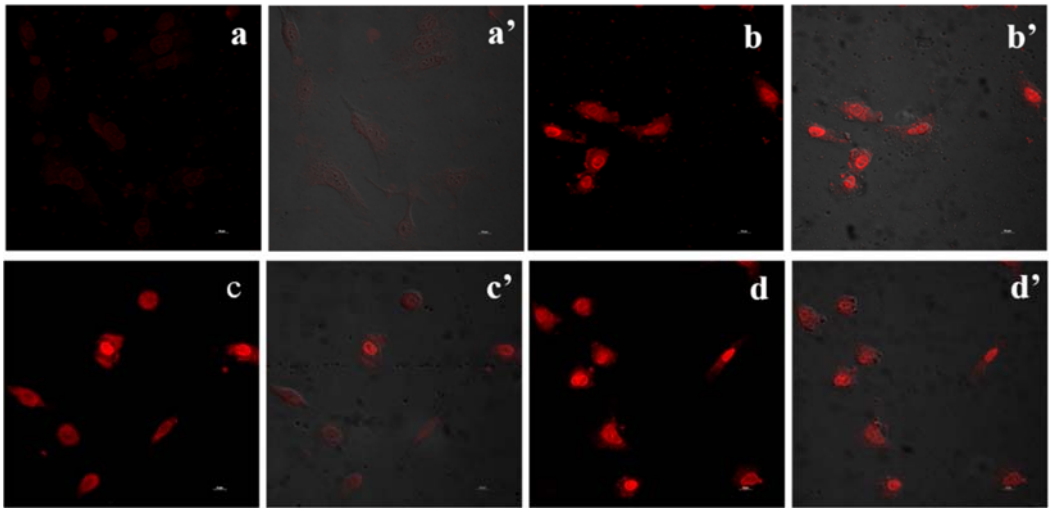

Figure 68: Efflux pump inhibition study in A549 cells, (a) DOX alone treated cell (a') bright field merged image of a (b) cells pretreated with PPDPA I nanoplex 25:1 followed with DOX (b') bright field merged image of b (c) cells pretreated with PPDPA II nanoplex at 4:1 ratio followed

with DOX (c') bright field merged image of c, and (d) PPDPA III nanoplexes 4:1 exposed cells followed with DOX treatment (d') bright filed merged image of d. The magnification is 60x.

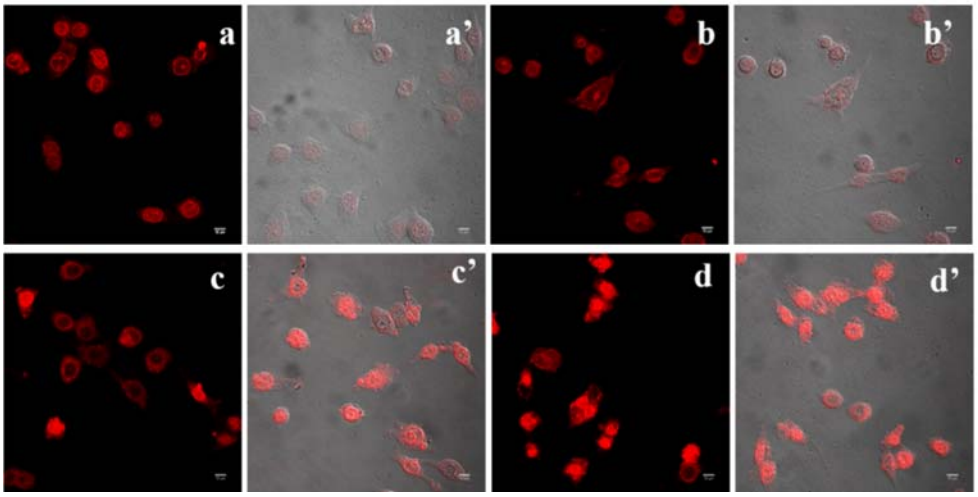

Figure 69: Efflux pump inhibition study in HeLa cells, (a) DOX alone treated cell (a') bright field merged image of a (b) cells pretreated with PPDPA I nanoplex at 25:1 ratio followed with DOX (b') bright field merged image of b (c) cells pretreated with PPDPA II nanoplex at 4:1 ratio followed with DOX (c') bright field merged image of c, and (d) PPDPA III nanoplexes 4:1 exposed cells followed with DOX treatment (d') bright filed merged image of d. The magnification is 60x.

4.3.5.10 Efflux pump inhibition studies using flow cytometry

The efflux pump inhibition study was performed to evaluate the efficacy of thiolated polymer to inhibit efflux pump. As in previous studies, the cell lines used were C6 and A549 (Pgp positive) and, HeLa cells (Pgp negative). Initially, the cells were treated with nanoplexes of PPDPA I (ratios 10:1 & 25:1), II (ratios 3:1& 4:1) and III (ratios 3:1 & 4:1) for 2hours. On completion of 2 hours to the cells. DOX (3μM) was added. Following this, the percentage of cells retaining DOX was determined by flow cytometry. The DOX alone treated group was taken as the control group. The results showed that the percentage of cells retaining DOX was found to be high in the PPDPA I/II/III polyplexes pretreated group compared to the corresponding control group in C6 and A549 (Table 9). In both C6 and A549, the values of polyplexes pretreated group are more or less same. It should be noted that among the nanoplexes pretreated group in C6 and A549, the cells retaining DOX was found to be slightly higher in both PPDPA II and III compared to PPDPA I nanoplexes

pretreated group. On the other hand, both the control and nanoplexes treated group in HeLa cells showed no significant differences (Table 10).

Cell lines	The % of cells retaining DOX in control group	The percentage of cells retaining DOX in the nanoplexes pretreated group					
		PPDPA I 10:1	**PPDPAI 25:1**	**PPDPA II 3:1**	**PPDPA II 4:1**	**PPDPAIII 3:1**	**PPDPA III 3:1**
C6	33.82±2.42	76.52 ±3.65	77.18± 6.77	83.96± 4.11	82.32± 3.99	87.93± 5.38	91.35± 6.32
A549	37.12±4.76	79.31 ±8.12	83.22± 6.87	84.93± 1.49	90.21± 5.06	91.14± 3.21	93.28± 5.55
HeLa	46.3±2.32	52.61 ±1.25	50.33± 3.27	55.32± 3.25	52.82± 3.26	49.74± 6.35	51.36± 2.58

Table 10: Efflux pump inhibition study using flow cytometry, where the percentage of cells retaining DOX was measured following DOX alone and/or PPDPA I,II and III nanoplexes pretreatment followed by DOX treatment.

4.3.5.11 DOX retention studies

The DOX retention kinetics in different cell lines was determined by exposing the cells with the nanoplexes of PPDPA I, II and III at selected ratios followed by the treatment of DOX for different time periods. The concentration of DOX in these cells was determined by normalizing with the total protein content of the cells. As seen in Figure 70, the DOX retention kinetics in HeLa cells was similar in both free drug as well as the nanoplex and drug-treated group. As shown in results, there is a gradual increase in the concentration of DOX in the PPDPA nanoplex pre-

treated cells overtime with more pronounced effect observed in PPDPA III and II compared with PPDPA I. The cellular DOX level in A549 reached up to 0.239 µg/mg of protein in the PPDPA III nanoplex treated cells and 0.230µg/mg of protein in case of PPDPA II and 0.201 µg/mg of protein with PPDPA I in the 4th hr. The DOX level was sustained at same concentration for almost 7hrs. However, the concentration of DOX in the untreated cell was only half that of the nanoplex treated cells. In the case of C6 cells also, a similar observation was seen. Here, the DOX concentration attained the peak level of 0.24 µg by 2nd hr in PPDPA III and 4th hour in PPDPA II which sustained more or less the same way in both the polymers up to 6 hrs. The reduction in the concentration of DOX occurred following 6hrs of drug exposure in C6 cells. In both C6 and A549, there was a gradual increase in DOX concentration followed by a decrease over time. Compared to PPDPA II and III, the DOX retention was found to be less in case of PPDPA I but was higher than the control group.

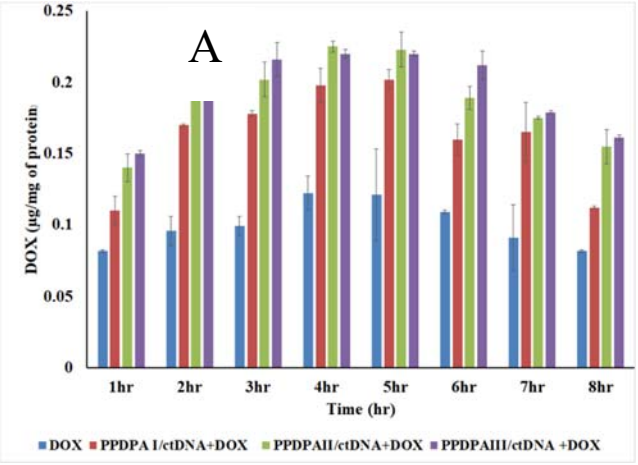

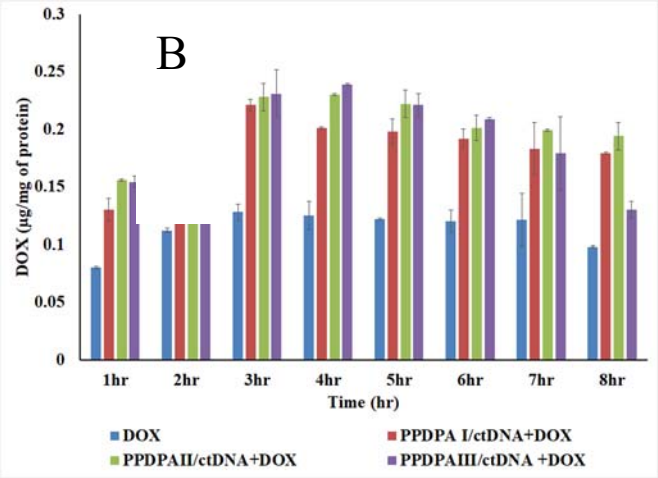

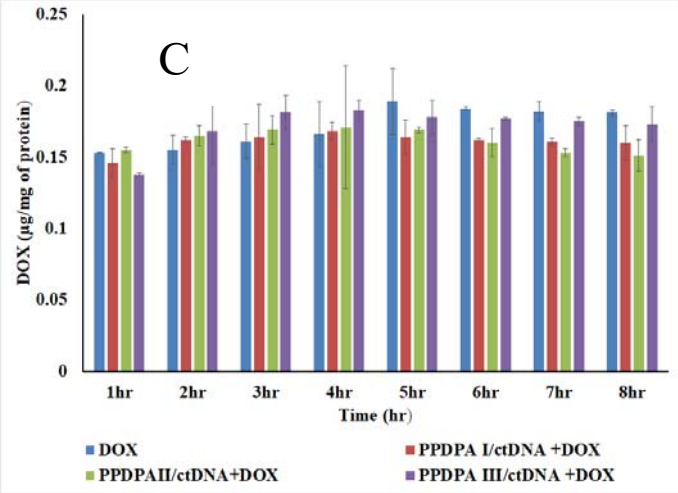

Figure 70: DOX retention in different cell lines A) C6 cells B) A549 and C) HeLa cells. The DOX alone treated group was compared with the PPDPA I/ctDNA (25:1), PPDPA II/ctDNA (4:1) and PPDPA III/ctDNA (4:1) nanoplexes pretreated and DOX treated group in C6, A549 and HeLa.

4.4. Synthesis and characterization of pullulan-PEI-4,4 dithiodibutyric acid (PPDBA)

The synthesis of pullulan-PEI-4,4 dithiodibutyric acid (PPDBA) was carried out by conjugating the thiol containing group i.e 4,4 dithiodibutyric acid (varying amount) on to the backbone of pullulan PEI by means of EDC reaction. Based on the amount of 4,4 dithiodibutyric

acid added, three different groups were formed i.e PPDPA I, II and III. The control group was synthesized by conjugating PEI with 4,4 dithiodibutyrate (DBA) using EDC as crosslinker. The polymers were named as PPDBAI, II and III and the controls as PDBA I, II and III. The thiol/ disulfide content of the respective polymers was in the order of PPDBA III>PPDBAII>PPDBA I (Table 11).

SL.NO	Sample ID	s-s linkage (mg/g of polymer)	Thiol content (mg/g of polymer)
1	PPDBA I	54.12±0.02	72.21±0.011
2	PPDBA II	71.05±0.017	75.14±0.34
3	PPDBA III	78.11±1.55	84.25±2.32
4	PDPBA I	65.31±0.98	87.08±0.42
5	PDBA II	79.27±2.02	95.05±3.01
6	PDBA III	83.22±0.013	98.16±0.31

Table 11: The thiol and disulfide content of the pullulan derivative, PPDBA I, II, III polymers and its corresponding controls PDBAI, II and III.

The amino content of the polymer PPDBA I, II and III and its control was evaluated by means of $CuSO_4$ assay. Among the pullulan derivatives, the amino content was highest for PPDPA I and is in the order PPDPA I> PPDPA II > PPDBA III. More the conjugation with DBA, lesser is the amino content of the polymer (Table 12).

SL.NO	Sample ID	Amount of amino group (mg/10mg of polymer)
1	PPDBA I	3.03 ± 0.13
2	PPDBA II	2.83 ±0.12
3	PPDBA III	2.79 ±0.32
4	PDBA I	4.28 ±0.01

Table 12: The amino content of PPDBA I, II, III and PDBAI, II, III polymers determined via $CuSO_4$ assay.

5	PDBA II	4.09 ±0.03
6	PDBA III	4.12 ±0.21

4.4.1 ^{1}HNMR and FTIR

The conjugations were established by ^{1}HNMR (Figure 71). The peaks corresponding to the repeating units – (CH_2-CH_2-NH) - of PEI were visible at around δ 2.6ppm in both the control and PPDPA. The characteristic peak of PEI was less prominent in both PPDBA and PDBA, due to the influence of pullulan and dithiodibutyric acid. The peaks at δ1.1 to 1.8 ppm represent the alkyl group of 4, 4 dithiodibutyrate, and was clearly seen in PDBA but was observed to be slightly shifted to δ1.9ppm in PPDBA. The peaks at δ 2.7-2.8ppm denote the two ethylene groups neighbouring a disulfide linkage and was seen in both PDBA and PPDBA. Similarly, the peaks observed in PPDBA at the wide region from δ 3.4 -3.9 ppm was associated with the –CH and –CH_2 backbone of pullulan and the peaks at δ 4.7 is indicative of –OH group. The same was absent in PDBA. A slight shift occurred in the anomeric protons associated with maltotriose unit in pullulan and the signals were seen at δ 5.33-5.38 ppm (Figure 71).

In the FTIR spectra, the prominent broad band observed near 3282 cm^{-1} in PPDBA polymers are due to the overlapping –OH and –NH stretching vibration of pullulan and PEI and the sharp peaks at 3272 cm^{-1} corresponds to the –NH stretching vibrations of PEI, which was observed in PDBA. The aliphatic -CH stretching was observed at 2928cm^{-1} and 2824cm^{-1} in PPDBA and 2939cm^{-1} and 2827cm^{-1} in the control group. A sharp peak at 1559cm^{-1} was assigned to the –OH stretching in PPDBA. The peaks at 1627cm^{-1} and 1624cm^{-1} in PPDBA and PDBA, was assigned to the amide

I bond of C=O stretching and peaks at 1459cm^{-1} in both was due to the –NH bending of amide II bonding (Figure 72).

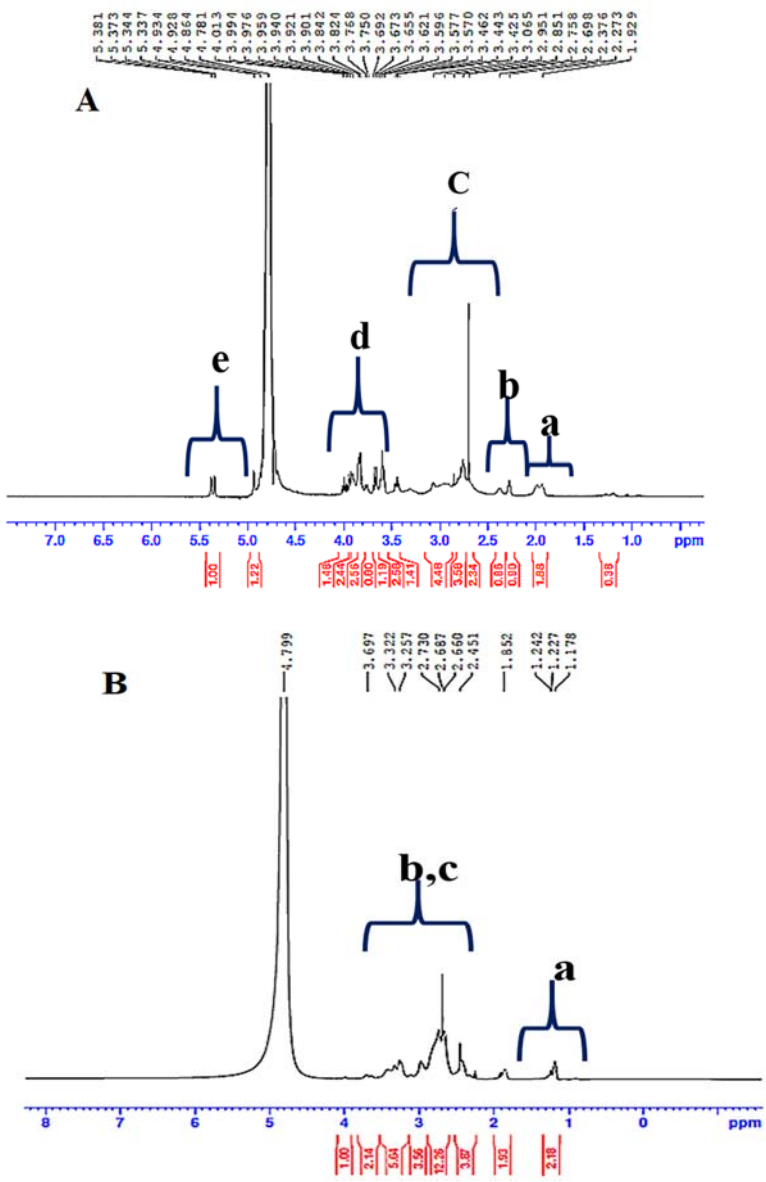

Figure 71: [1]HNMR spectra of the representative polymer A) PPDBAII B) PDBAII where the notations a represent the alkyl group of 4,4 dithiodibutyric acid. b and c indicate characteristic group of PEI i.e, –(CH_2-CH_2 -NH)n and two ethylene groups neighbouring a disulfide linkage respectively. The notation d and e in PPDBA indicate -CH_2-CH_2 - backbone and anomeric protons in pullulan respectively.

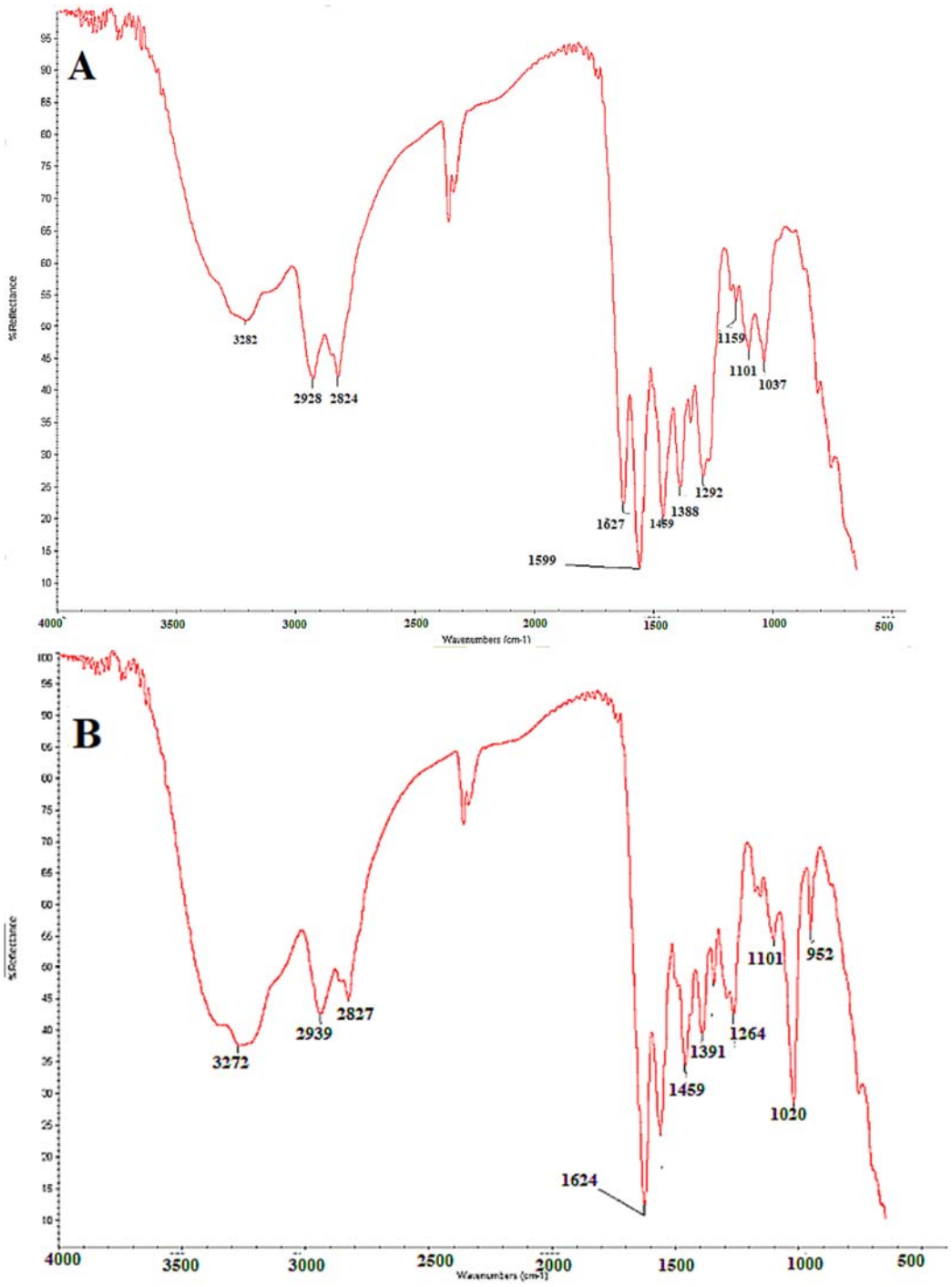

Figure 72 : FTIR spectra of A) PPDBA II and B) PDBAII.

4.4.2 Buffering capacity

The buffering capacity of PPDBA I/II/III, PDBA I/II/III and PEI was determined by acid-base titration in the pH range 10 to 4. As shown in Figure 73, the titration curve confirmed that both pullulan based polymers and PEI derivatives are displaying good buffering capacity. The titration curve of PPDBA I/II and III had a relatively steep slope in the pH region of 5-7, showing that the polymers had a good buffering capability at this range. However, the buffering ability of PPDBA polymers was relatively lower compared to that of PEI and PEI derivatives i.e PDBAI/II and III but the results showed that all were comparable to that of PEI. Among the polymers, the buffering capacity was in the order PPDBA I> PPDBA II > PPDBAIII,

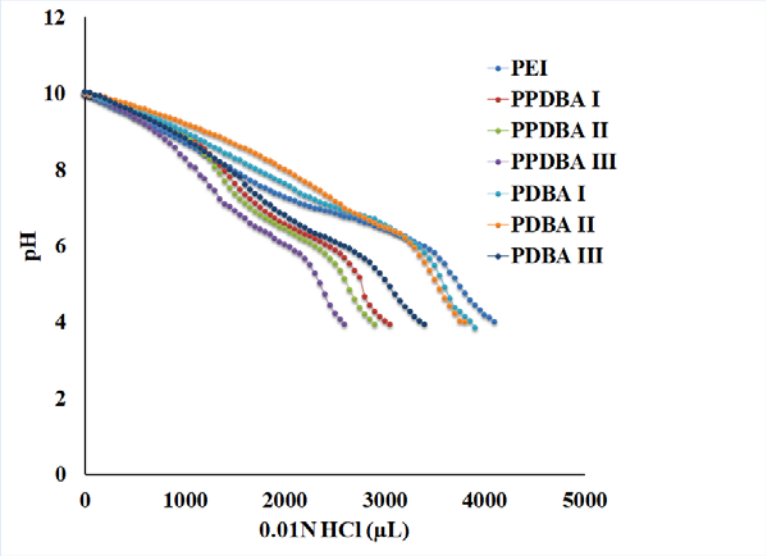

Figure 73: Buffering capacity of PPDBA I/II/III , PDBA I/II/III and PEI.

4.4.3 Biophysical characterization

4.4.3.1 Size and Zeta potential

The size and surface charge of the nanoparticle are important physicochemical parameters in designing drug/gene delivery vehicle. The PPDBA polyplexes had a hydrodynamic size within the desired range of 150-200nm, especially in the polymer to DNA ratio ranging from 2:1 to 5:1 (Figure 74). The initial polyplexes ratio, 1:1 of all PPDBA polymers resulted in larger size compared to the other ratios. All control polymers PDBA I, PDBA II and PDBA III were able to

form relatively uniform sized nanoplexes with mean sizes in the range 60-120nm. The optimum size of polyplexes PPDBA I, PPDBA II and PPDBA III based on the cationic polymer to DNA were at ratio 3:1 and 4:1. The particle size of PPDBA I 3:1 and 4:1 was noted as 114 nm and 140nm, and PPDBA II 3:1 and 4:1 as 155nm and 161nm and PPDBA III 3:1 and 4:1, the particle size was 167nm and 158nm respectively.

As indicated in the Figure 74, all the polyplexes of PPDBA I, II and III showed similar levels of zeta potential values with an increase along with the increase in the polymer to DNA ratio, which was ranging from 4 to14mV. As compared to the corresponding controls, the initial values were all negative for the polymer nanoplexes. The optimum zeta potential value was obtained at 4:1 ratio in all PPDBA polymers i.e PPDBA I, II and III, it was 14mV, 13.2mV and 13.6mV respectively and the value was found sharply declined at the ratio 5:1 in all the polymers. The optimum nanoplex ratio selected for PPDBA I, II and III was 3:1 and 4:1 in each polymer category.

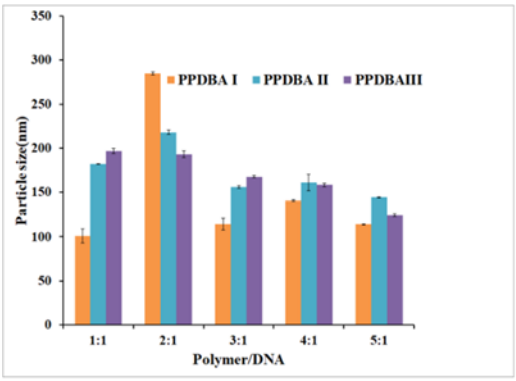

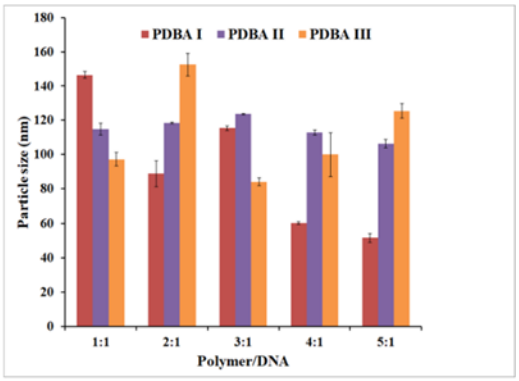

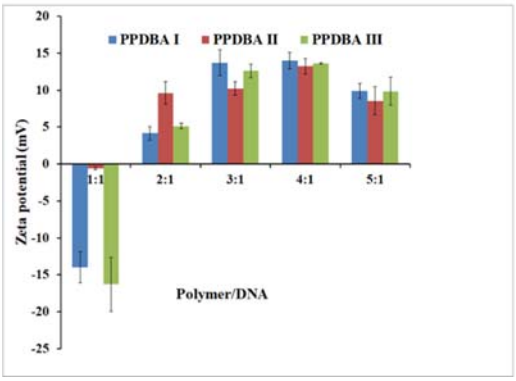

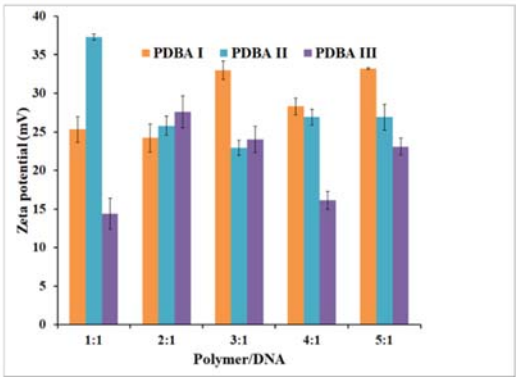

Figure 74: Particle size and zeta potential value of PPDBA I, II and III and the corresponding control group PDBAI, II and III

4.4.3.2 Agarose gel electrophoresis

Agarose gel electrophoresis was carried out with the nanoplexes of polymers i.e PPDBA I, II and III and the control groups i.e PDBA I, II and III indicate the DNA condensation capability of the polymer. The nanoplexes formed from the corresponding polymer showed complete inhibition of DNA mobility at all ratios except the initial ratio of 1:1, where the DNA was seen trailing in the gel. However, higher nanoplex ratios showed a complete retardation of DNA mobility and was seen restricted to the well (Figure 75). The selected ratios of the control groups were also found to be completely retained in the well. Further, studies on the stability of nanoplexes in presence of plasma proteins also showed a similar result, where DNA was found to remain complexed with the polymer. .

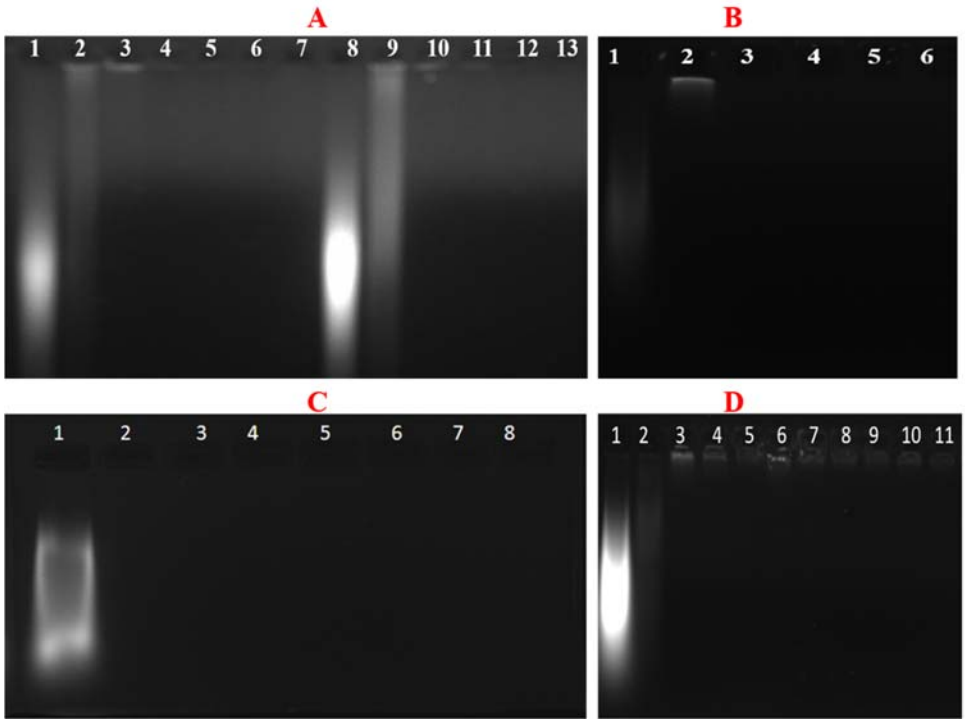

Figure 75: Agarose gel electrophoresis A) Lane 1 and 8: ctDNA, Lane 2-6: PPDBA I/ctDNA 1:1 to 5:1 and lane 8-13: PPDBA II/ctDNA 1:1 to 5:1 respectively. B) Lane 1: ctDNA, lane 2-6 PPDBA III /ctDNA ratios 1:1 to 5:1. C) Lane 1 ctDNA, lane 2-4 shows PDPAI/ctDNA 2:1 to 4:1

and 5-6 indicate PDBA II/ctDNA 3:1 to 4:1,lane 7-8 indicate PDBA III/ctDNA 3:1 and 4:1 respectively D) Lane 1 indicate ctDNA and plasma, lane 2-5 indicate PPDBA I/ctDNA 1:1-4:1 polymer : DNA nanoplex with plasma, whereas lane 6-8 indicate PPDBA II/ctDNA nanoplex ratio 2:1 -4:1 with plasma and lane 9-11 corresponding to PPDBA III/ctDNA 2:1 -4:1 with plasma.

4.4.3.3 Stability of nanoplexes in presence of DTT

The stability of the PPDBA/ctDNA polyplexes in the reductive media was investigated using DTT as the reducing agent. The DTT induced degradation of the disulfide cross-linked polyplexes of PPDBA was investigated using agarose gel retardation assay and size measurements. No considerable size change was seen in the DTT treated nanoplexes in comparison with untreated ones. After incubation with DTT for 4hr at room temperature, the size increased from around 150nm up to 270nm in the case of PPDBA II and III, whereas as seen in Figure 76, less pronounced change has occurred in PPDBA I. In the meantime, there was no considerable size variation occurred in the case of control groups ie PDPA I/II/III (Figure 76). Agarose gel electrophoresis (Figure 77) shows that on incubating with 10mM DTT, the DNA bands at the sample loading site become more brighter with a tail like portion observed outside the well in case of PPDBA II/III polyplexes.. However, no such band of the free DNA was observed both in PPDBA I and control groups PDBA I/II/III when exposed with DTT. On the other hand, the combined treatment of heparin/DTT on the selected polyplex ratios of PPDBA I/II/III and PDBA I/II/III released the DNA bands in the gel.

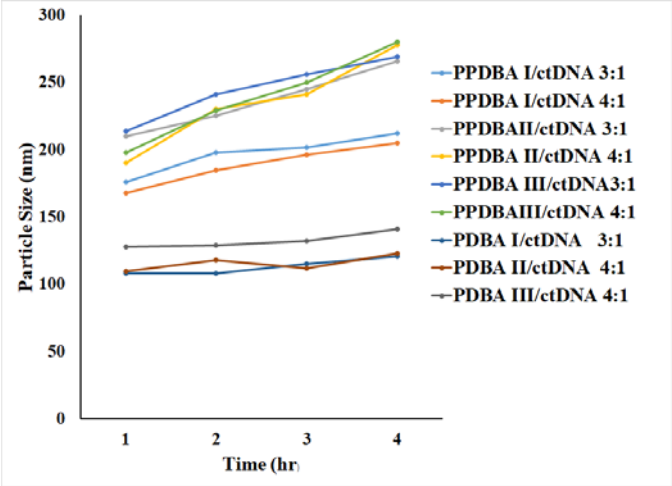

Figure 76: Size variations of PPDBA I/II/III and PDBA I/II/III nanoplexes on exposure with 10mM DTT, measured using DLS.

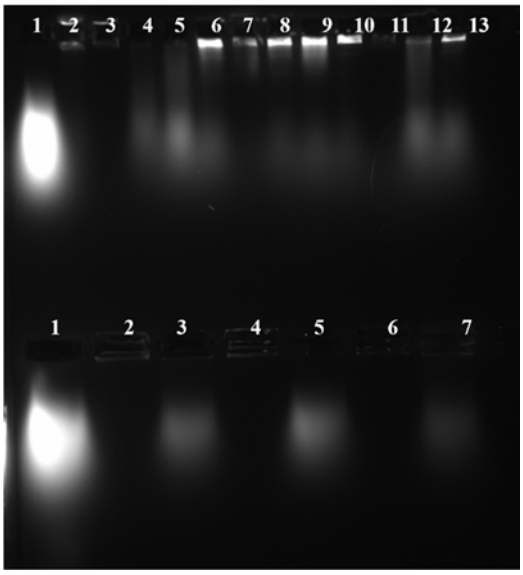

Figure 77: agarose gel electrophoresis (upper) lane 1- ctDNA alone control, 2-3 PPDBA I/ctDNA polyplexes, lane 6-7 PPDBA II/ctDNA polyplexes, lane 10-11 PPDBA III/ctDNA polyplexes, all with polymer to DNA ratios 3:1 & 4:1, treated with DTT alone. Whereas lane 4-5, PPDBA I/ctDNA polyplexes, lane 8-9 PPDBA II/ctDNA polyplexes, lane 12-13 PPDBA III/ctDNA polyplexes, all with polymer to DNA ratios 3:1 & 4:1, treated with heparin/DTT. Lane I (lower) indicates ctDNA, lane 2,4,6 (lower) indicates the control PDBAI/II/III polyplexes respectively where treated with DTT alone, whereas lane 3,5,7 (lower) shows the above polyplex with heparin/DTT treatment.

4.4.4 Plasma protein interaction with the polymer (PAGE)

When nanoparticles are administered systemically, the proteins which tend to adhere on the surfaces may greatly affect the circulation and biodistributions. Adsorption of proteins on the polymer surfaces was assessed by incubating the pullulan based derivatives such as PPDBAI/II/III and its control groups i.e PDPA I, II, III with serum and was compared with cationic PEI and serum alone which forms positive and negative controls respectively. Herein, the PEI adsorbs proteins on to the surfaces resulting in absence of protein bands on PAGE analysis. The control groups such as PDPA I/II/III also showed more similar result as PEI but the intensity of bands were slightly improved than that of PEI alone control group. On the other hand, the pullulan based derivatives exhibited more or less the same protein bands as the negative control indicating that the hydrophilic nature of pullulan prevents the adsorption of proteins (Figure 78).

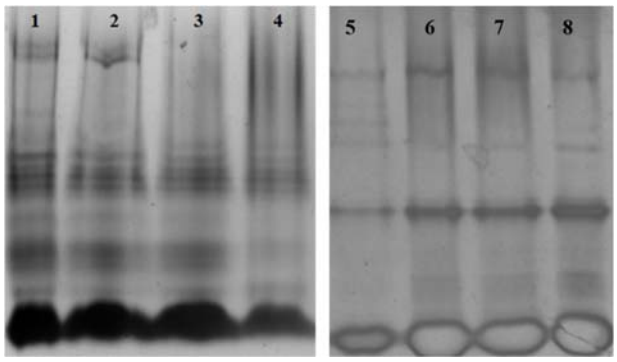

Figure 78: PAGE, lane 1 shows serum alone, lane 2-4 shows the protein bands corresponding to the pullulan based derivatives i.e PPDPA I/II/III , lane 5 indicates PEI and serum, lane 6-8 shows the protein bands on the control group i.e PDBA I/II/III respectively.

4.4.5 Biological analysis

4.4.5.1 Cytotoxicity evaluation of the polymer

The *in vitro* cytotoxicity of the selected nanoplexes ratios of PPDBA I (3:1 & 4:1) , PPDBA II (3:1 & 4:1) and PPDBA III (3:1& 4:1) were evaluated in C6, A549 and HeLa cell lines and fibroblast cell, L929 by MTT assays. The pullulan based nanoplexes showed >85% viability in all the cell lines tested, whereas the selected nanoplexes of the controls i.e PDBA I/II/III polyplexes remained toxic to cells. Both PDBA I/II showed a viability of around 55% against 38% showed

by the PDBA III polyplexes in all the cell lines tested. However, a slight difference in terms of cell viability was observed in the C6 cell for PDBA III, where it remained around 35%. The toxicity level remained low in the normal fibroblast cells (> 82% viability) when exposed with the selected nanoplex ratios of PPDBA I/II/III (Figure 79).

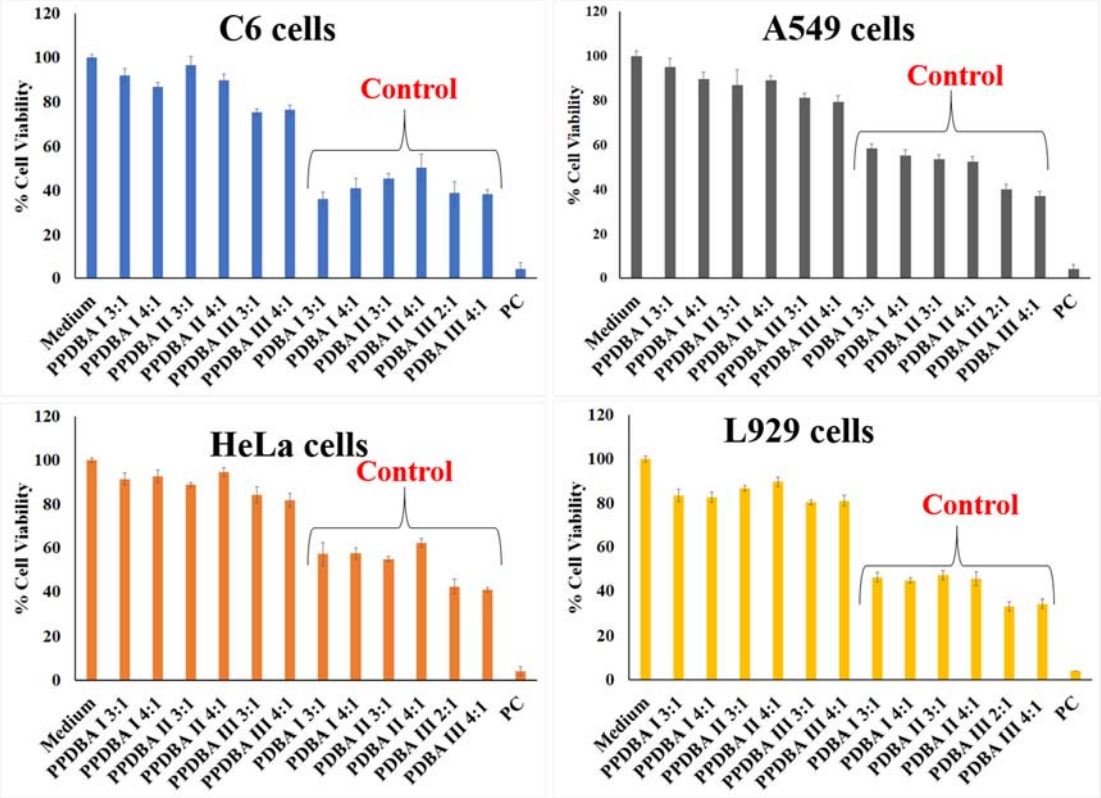

Figure 79: MTT assay of the selected PPDBA and PDBA nanoplexes at polymer to DNA ratios of 3:1 and 4:1 in different cancer cell lines such as C6, A549 and HeLa and the normal fibroblast cell, L929. Data is shown as mean ±SD, n=4

4.4.5.2 Evaluation of cellular uptake

The cellular uptake of PPDBA polyplexes was analyzed by using labeled nanoplexes in which DNA was tagged with YOYO-I. The confocal laser scanning microscopy (CLSM) images revealed that polyplexes were effectively taken up by the C6 cells as evidenced by the extensive cytoplasmic distribution of YOYO-I-DNA post 3h incubation (Figure 80). It should be noted that YOYO-I-DNA was widely confined to nuclei. Most of the green fluorescence was found to be

coincided with the blue fluorescence in the nuclei at all selected ratios of PPDBA polyplexes i.e PPDBA I/ctDNA 3:1 & 4:1, PPDBA II/ctDNA 3:1 & 4:1 and PPDBA III/ctDNA 3:1 & 4:1. On the contrary, the PDBA nanoplex treated cells showed visible signs of toxicity. Though it maintained normal spindle-shaped structure in most of the cells, nuclear membrane rupture was clearly visible. The flow cytometry analysis was simultaneously carried out with all the selected ratios of PPDBA nanoplexes and the percentage uptake was as follows, PPDBAI/ctDNA 3:1 nanoplex is 96.5% and PPDBAI/ctDNA 4:1 is 95.8%. Similarly, the percentage uptake of PPDBA II/ctDNA 3:1 and 4:1 is 96.4% and 91.3% and PPDBA III/ctDNA3:1 and 4:1 is 90.2% and 74.6% respectively (Figure 81).

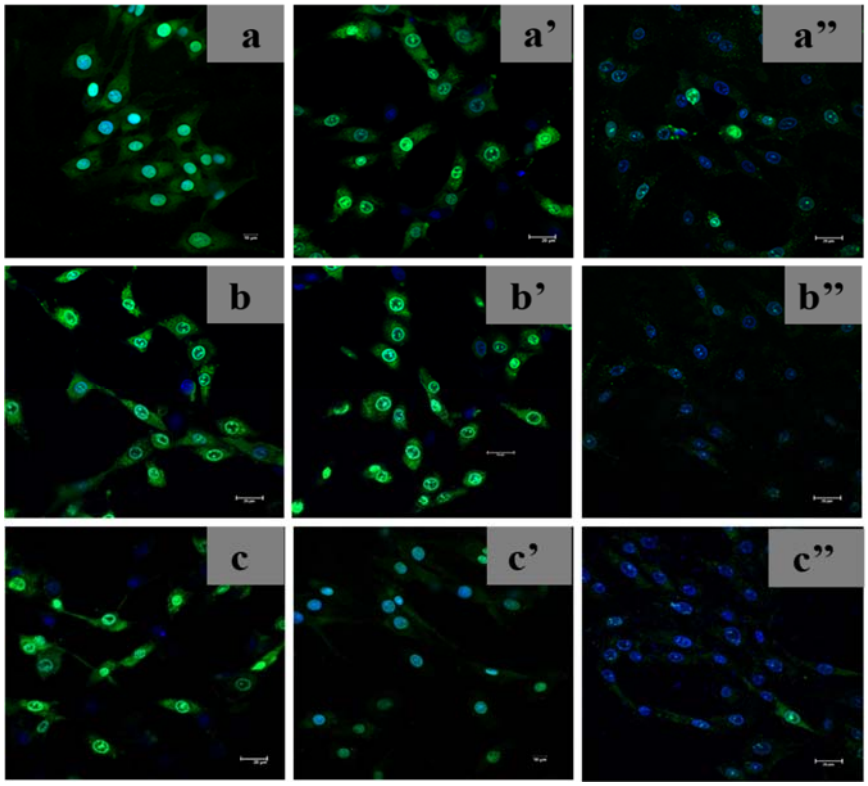

Figure 80: Cellular uptake of PPDBA polymers based nanoplexes where nucleus is stained with hoechst and DNA tagged with YOYO-I a) PPDBA I/ctDNA 3:1 a') PPDBAI/ctDNA 4:1

nanoplex a'') PDBA I/ctDNA 4:1 nanoplex b) PPDBA II/ctDNA 3:1 b') PPDBA II/ctDNA 4:1 b'') PDBA II/ctDNA 3:1 c) PPDBA III/ctDNA 3:1 c') PPDBA III/ctDNA 4:1 c'') PDBA III/ctDNA 3:1 nanoplexes.Magnification is 60x.

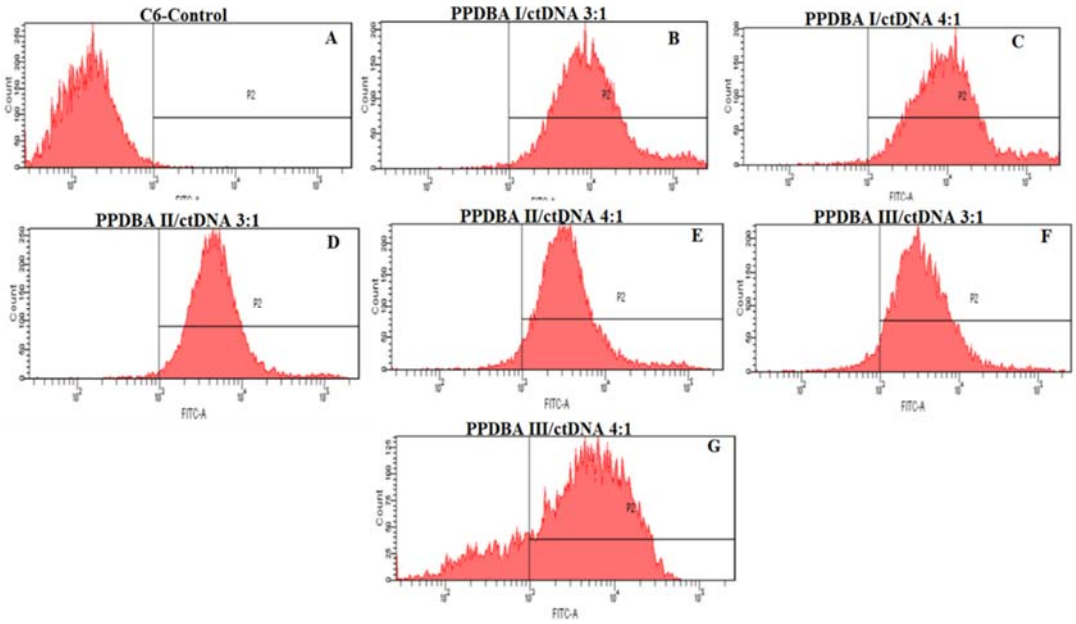

Figure 81: Flow cytometry data of A) control unstained B) PPDBA I/ctDNA nanoplex of ratio 3:1 with percentage uptake of 96.5 ± 8.12 % C) PPDBA I/ctDNA 4:1, percentage uptake is 98.8± 1.81% D) PPDBA II/ctDNA 3:1 nanoplex with uptake of 96.4±2.21% E) PPDBA II/ctDNA 4:1 is 91.3% F) PPDBA III/ctDNA 3:1 & 4:1 with percent uptake of 90.2±3.65 and 74.6 ± 5.4% respectively.

4.3.5.3 Endocytosis inhibitor study

The internalization pathway of the polyplexes was probed by using different endocytosis inhibitors. Chlorpromazine inhibit clathrin-mediated endocytosis and similarly, filipin and amiloride inhibit caveolae-mediated and micropinocytosis respectively. Cellular uptake in presence of inhibitors was investigated using PPDBA II/ctDNA nanoplex at 4:1 as a representative. The cell uptake level was not reduced in any of these cases where each individual inhibitor was evaluated for its inhibitory effect in the endocytosis pathway. It was noted that all

the inhibitors individually maintained more or less 100% cellular uptake as similar to the uninhibited control cell. Here, the cellular uptake of the PPDBA nanoplex without inhibitor was maintained as 100% which was then compared with the uptake of individual inhibitors (Figure 82).

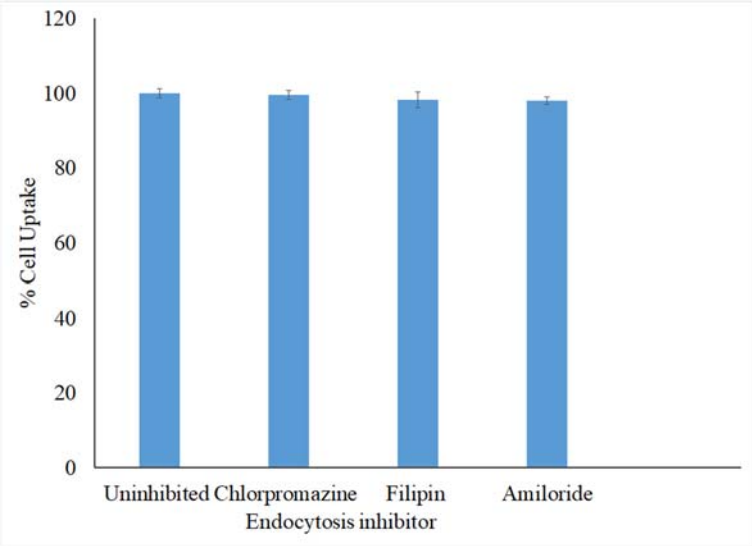

Figure 82: The cellular uptake of the PPDBA/ctDNA nanoplex at ratio of 4:1 in presence of endocytosis inhibitors.

4.4.5.4 Polymer trafficking studies

To illustrate PPDBA nanoplexes fate inside the cell, both polymer and DNA was tagged with rhodamine and YOYO-I respectively. The intracellular trafficking of polyplexes and the corresponding fate of DNA and polymer was monitored at different time points such as 1hr, 2hr, 4hr and 7hr using confocal laser scanning microscopy. Herein, the representative polyplex of PPDBA polymer i.e. PPDBA/ctDNA 4:1 was used for the study. As seen in Figure 83, after incubation of 1hr, the ctDNA was found to be mostly localized in the nucleus, where the green fluorescence was merged with blue fluorescence in the nuclei. The red fluorescence was clearly separated from the green fluorescence and was seen localized in the cytoplasm. As the incubation time increased, in the 2nd hour, the demarcation of green and red fluorescence became clearer and

the green fluorescence was seen in the cytoplasm and nuclei. Yellow fluorescent dots within the cells denotes the co-localization of polymer and DNA. In the 4th hour, most of the green fluorescence was seen coincided with the blue fluorescence and some traces of green was sparingly visible in the cytoplasm. The red fluorescence was visible towards the membrane. In the 7th hour, no traces of yellow fluorescence or co-localization of the nanoplexes visible with all most all the ctDNA or green fluorescence appeared in the nuclei. Red fluorescence became more intense at the cell membrane surface (Figure 83).

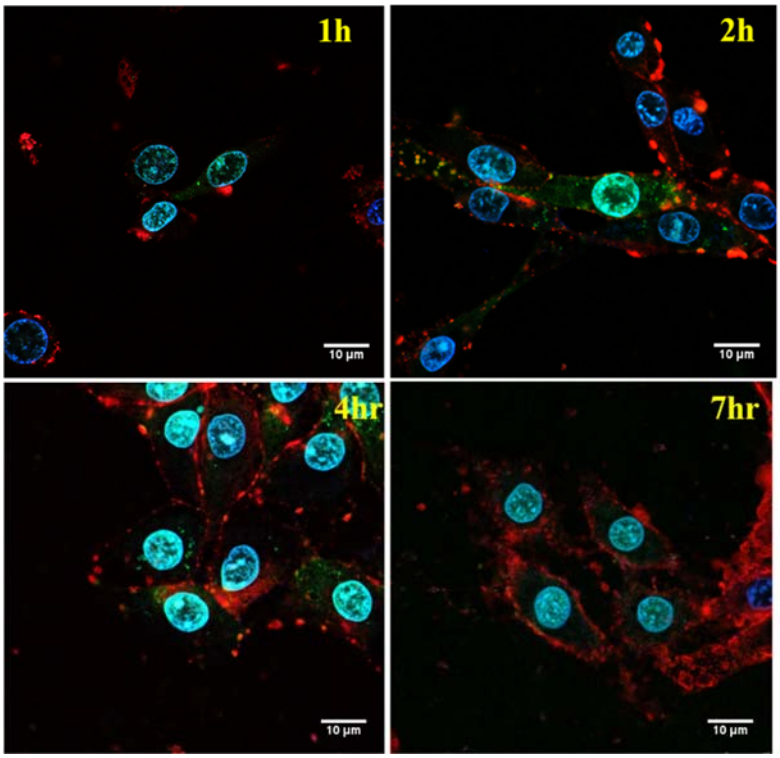

Figure 83: The nanoplex internalization kinetics of PPDBAII/ctDNA 4:1 ratio, monitored at different time points. Nuclei stained with Hoechst (blue), YOYO-I-DNA (green) and rhodamine tagged polymer (red).

4.4.5.5 Transfection studies based on Live and dead assay

The transfection efficiency of PPDBA polymers was studied in C6 cells. The selected nanoplex ratios of PPDBAI/II/III (all with the polymer to DNA ratio 3:1 & 4:1) were chosen to

transfect C6 cells after complexing with the p53 plasmid. Higher transfection efficiency of the polymer is associated with a greater number of dead cells which in turn appears as red fluorescence. As in Figure 84, all nanoplex ratios of PPDBA I i.e PPDBA/p53 3:1 and 4:1 showed superior transfection efficiency compared to PPDBAII and III. The nanoplex ratios of PPDBA II i.e 3:1 and 4:1 also showed good transfection efficiency indicated by the number of dead cells as compared to PPDBA I. However, the number of dead cells was minimal in PPDBA III nanoplexes treated cells, indicating it as a poor transfecting agent.

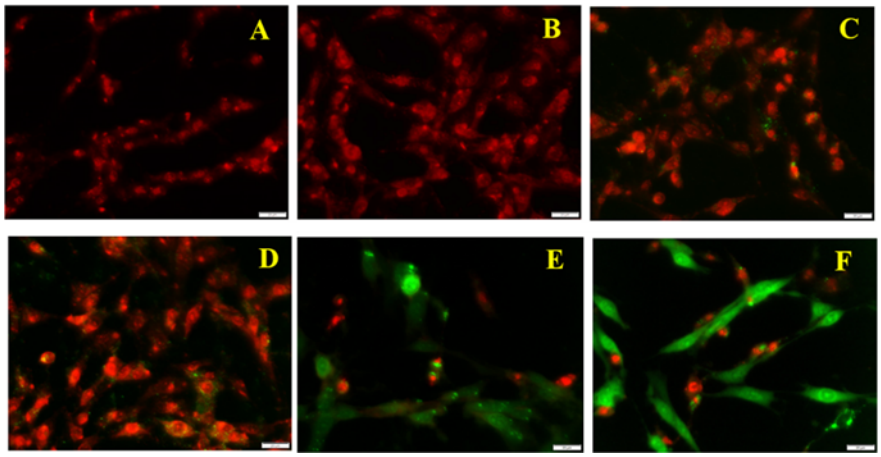

Figure 84: Live and dead assay of A)PPDBA I/p53 3:1 transfected cells B) PPDBA I/p53 4:1 C) PPDBA II/p53 3:1 D) PPDBA II/p53 4:1 E) PPDBA III/p53 3:1 F) PPDBA III/p53 4:1 treated cells. The red colour represents dead cells and green colour indicate the live cells. The magnification is 60x.

4.4.5.6 PI staining via Flow cytometry

The transfection efficacy of the polymer was quantified by means of PI staining via flow cytometry. The gene, p53 is meant to cause apoptosis, resulting in cell death. As seen in Figure 85, the percentage of cell death measured with PI staining was higher in PPDBAI nanoplexes compared to PPDBA II and III. The polyplex, PPDBA I/p53 3:1 and 4:1 showed 88% and 96% cell death whereas PPDBA II/p53 3:1 and 4:1 formed 72% and 59% cell death and PPDBA III/p53

displayed cell death of 52% and 50% respectively. Overall, the cell death detected by PI staining was in the order of PPDBAI > PPDBAII >PPDBAIII.

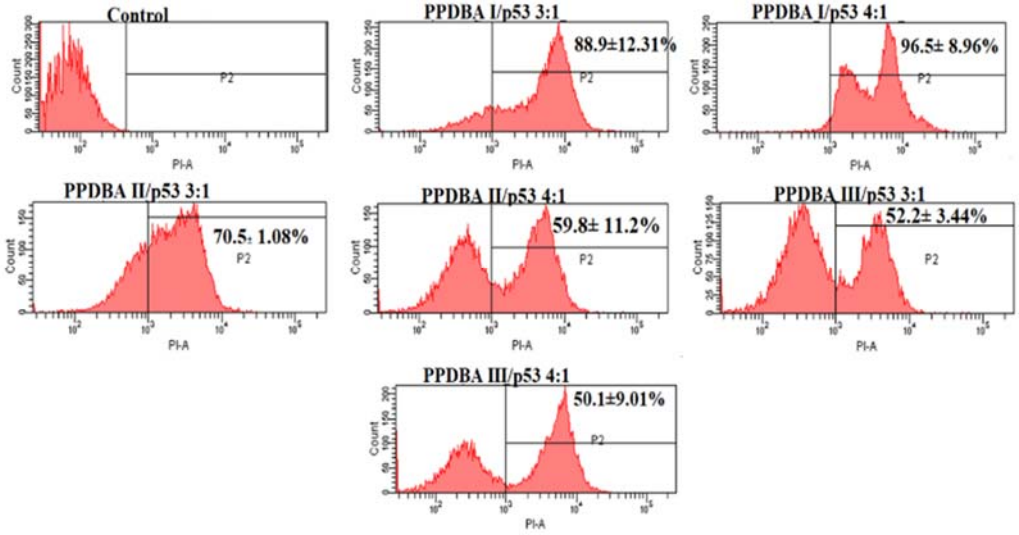

Figure 85: Determination of transfection efficiency by PI stainin. The percentage cell death was measured in C6 cells treated with different nanoplex ratios of PPDBA polymers.

4.4.5.7 Determination of apoptosis via annexin V staining

The p53 gene plays a critical role in the cellular apoptosis. The apoptotic activity mediated by PPDBA/p53 nanoplexes was investigated in C6 cells by flow cytometry using annexin V FITC/propidium iodide (PI) staining. The results revealed that the nanoplexes induced apoptosis, where higher apoptotic activity was shown by the PPDBAI compared to PPDBAII/III. PPDBAI caused 85% and 87% for the polymer to DNA ratio of 3:1 and 4:1 ratio respectively. Similarly, the PPDBAII/p53 displayed apoptosis of 64% and 52% for 3:1 and 4:1 ratio and PPDBAIII showed around 50% for both polyplexes ratios (Figure 86). The percentage apoptosis mediated by PPDBA nanoplexes in C6 cells determined via annexin V staining are in the increasing order of PPDBAIII<PPDBA II<PPDBA I.

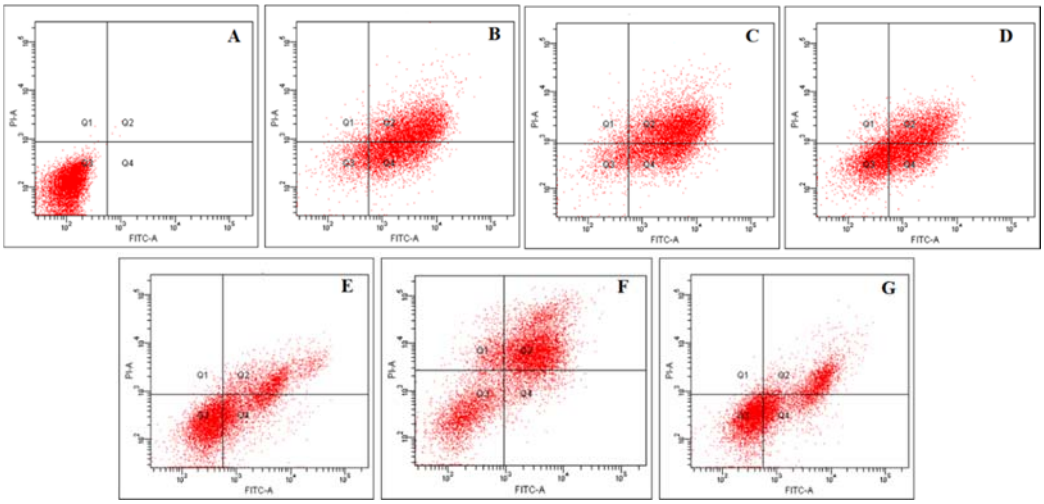

Figure 86: Apoptosis by annexin V staining, where A) normal untreated control B) PPDBAI/p53 3:1 nanoplexes treated cells, percentage apoptosis is 85.5±5.23%, C) PPDBAI/p53 4:1 nanoplexes with percentage apoptosis is 87.8±9.62% D) PPDBAII/p53 3:1 ratio, percent apoptosis is 64.1±8.01% and E) PPDBA II/p53 4:1, percentage apoptosis is 52.9±4.22%, F) PPDBAIII/p53 3:1 and the percent apoptosis is 53.1±5.38% and G) PPDBAIII/p53 4:1, percentage apoptosis is 50.1±11.2%.

4.4.5.8 p53 immunofluorescence

The presence of the apoptotic protein, p53 in the C6 cells was analyzed by immunocytochemistry. As seen in Figure 87, the untreated control group showed no fluorescence signals whereas all the PPDBA/p53 nanoplexes treated cells showed green fluorescence in the cytoplasm, indicating the expression of the p53 gene. The absence of green fluorescence shows lack of p53 protien in the cell, whereas the appearance of green fluorescence showed its presence. This, in turn, shows successful transfection of p53 in the PPDBA nanoplexes treated cells and its corresponding expression of the gene in the cytoplasm.

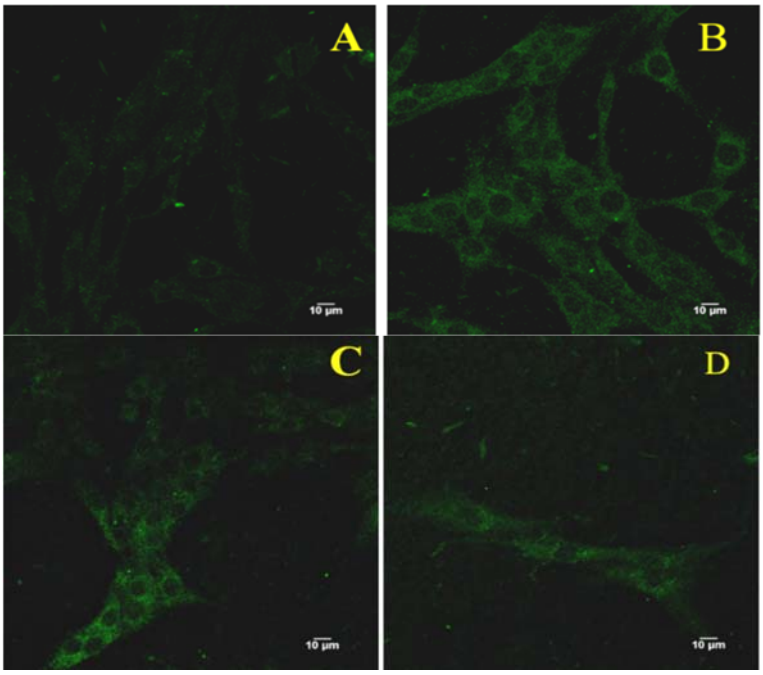

Figure 87: Immunofluorescence analysis to establish p53 expression in C6 cells. (A) Control cell without any treatment (B) cells treated with PPDBA I/p53 nanoplex at 4:1 ratio (C) cells treated with PPDBA II/p53 nanoplex at 4:1 ratio and (D) cells treated with PPDBA III/p53 nanoplex at 4:1 ratio.

4.4.5.9 Efflux pump inhibition studies using confocal microscopy

The efflux pump inhibition studies were carried out in different cell lines such as C6, A549, and HeLa. Herein, the efflux pump inhibition studies were performed to evaluate the efficacy of PPDBA polymers in inhibiting the efflux pump. Here, the anticancer drug DOX was used as an index of efflux pump activity, where the intensity of red fluorescence in the cells is directly proportional to the concentration of DOX. The representative nanoplexes ratio used for the study is PPDBA I,II, III 4:1. Both C6 and A549 showed enhanced red fluorescence in the cells preincubated with PPDBA nanoplexes followed by DOX treatment compared to the DOX alone treated control cells (Figure 88). The efflux pump inhibition studies in HeLa cells showed the appearance of red fluorescence more or less in same intensity in both PPDBA nanoplexes pretreated and DOX alone treated group (Figure 88).

A

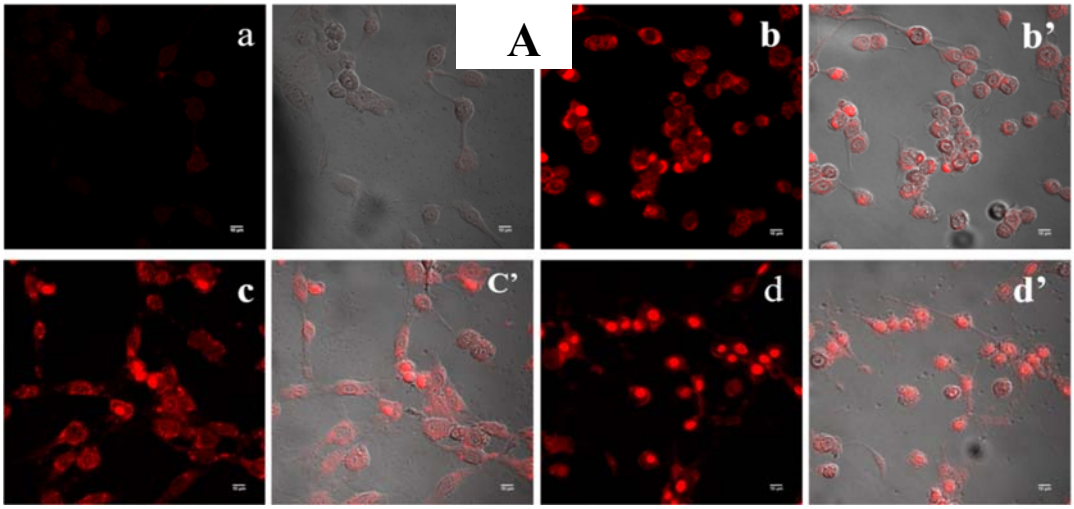

B

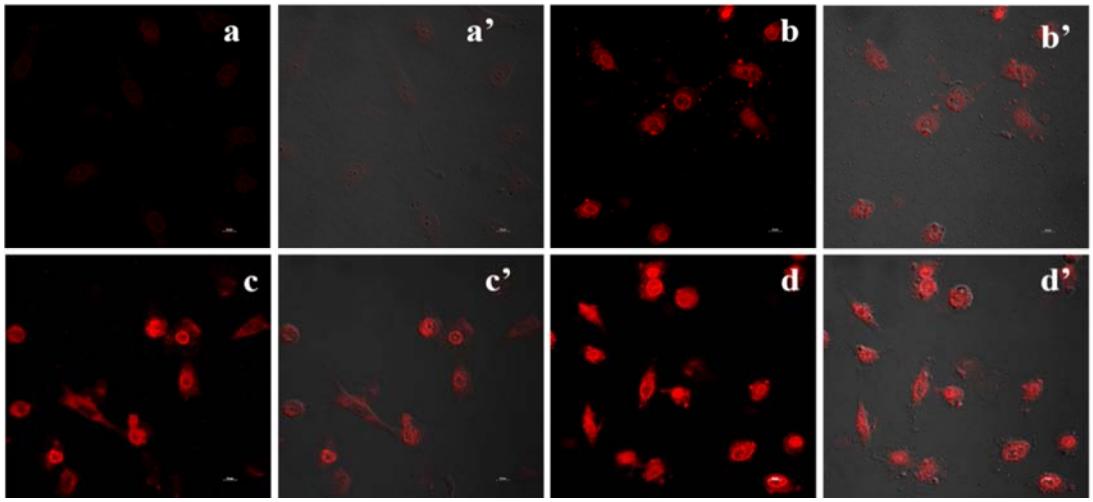

C

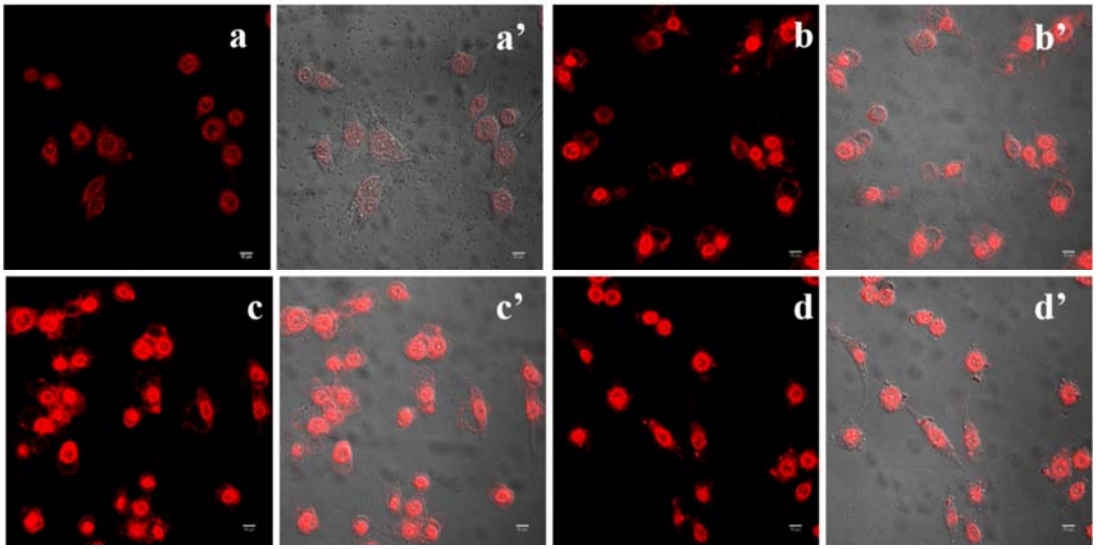

Figure 88: Efflux pump inhibition study A) C6 cells B) A549 cells C) HeLa cells where in all the cells, notation (a) DOX alone treated cell (a') bright field merged image of a (b) cells pretreated with PPDBA I nanoplex at 4:1 ratio followed with DOX (b') bright field merged image of b (c) cells pretreated with PPDBA II nanoplex at 4:1 ratio followed with DOX (c') bright field merged image of c, and (d) PPDBA III nanoplexes 4:1 exposed cells followed with DOX treatment (d') bright filed merged image of d. The magnification is 60x.

4.4.5.10 Efflux pump inhibition studies using flow cytometry

The efflux pump inhibition studies were performed in both P-gp expressed cell lines i.e C6 and A549 and P-gp negative cell lines such as HeLa using PPDBA nanoplexes and the anticancer drug, DOX. The percentage of cells retaining the anticancer drug DOX following nanoplexes/ DOX treatment in the cancer cells were determined using flow cytometry. The control group was cells treated with DOX alone (3μM). The nanoplexes were PPDBA I, II and III with the polymer to DNA ratios 3:1 and 4:1. As shown in Figure 89, the percentage of cells retaining DOX was remarkably higher in the polyplexes pretreated group compared to the DOX alone treated control group. In both C6 and A549, > 75% of cells retained DOX by the nanoplexes pretreated group compared to the control group, which was around 30%. The results were in accordance with the confocal microscopy analysis. Among the nanoplexes, the cells retaining DOX was found to be high in both PPDBA II and III compared to PPDBA I nanoplexes pretreated group. However, the

P-gp negative cell line i.e HeLa, the percentage of cells retaining DOX was found to be more or less the same in both control and PPDBA nanoplexes pretreated group (Figure 89).

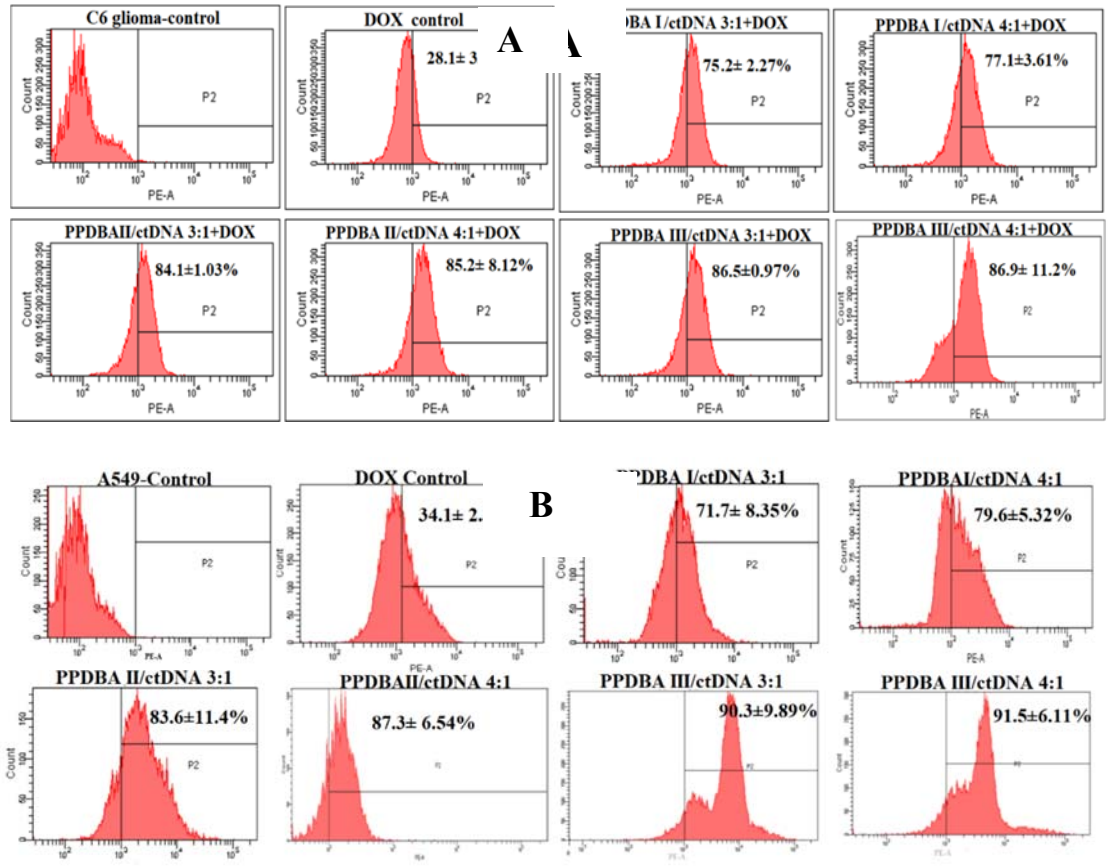

A

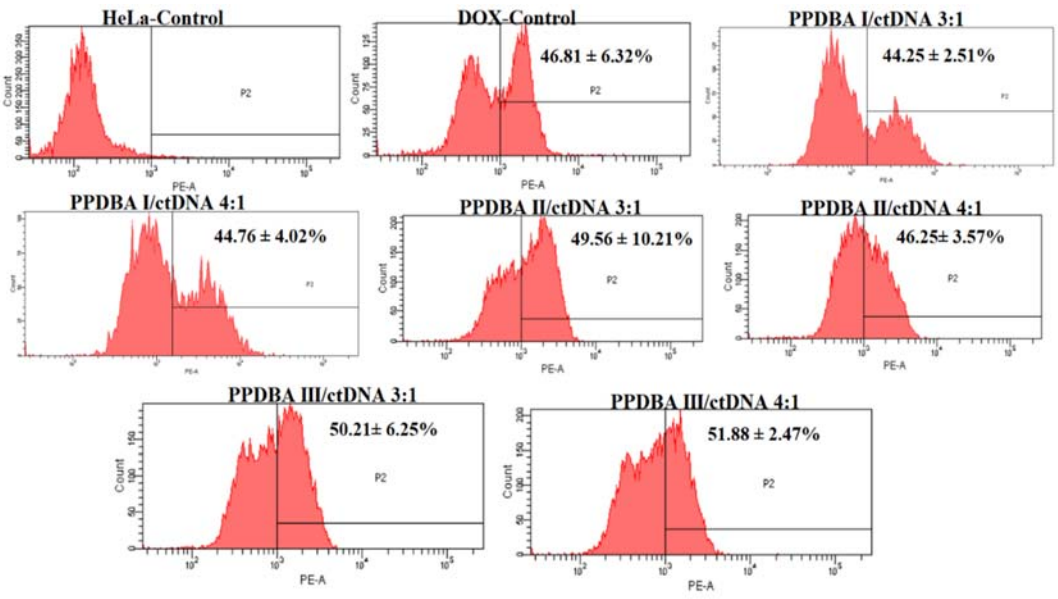

Figure 89: Efflux pump inhibition studies using flow cytometry where A) C6 cells B) A549 and C) HeLa cells. The percentage of cells retaining DOX following PPDBA I/II/III nanoplexes pretreatment and DOX exposure. The DOX alone treated cells is the control group.

4.4.5.11 DOX retention kinetics

The intracellular DOX retention was quantitatively measured at different time intervals (1-8hr) by analyzing the concentration of DOX in the cell lysate at each time point, normalized to the total cellular protein. The intracellular retention of DOX was significantly lower in the control group where the cells were treated with free DOX (3µM) alone. As seen in Figure 90, the concentration of DOX in the PPDBA I, II, III nanoplex treated cells were high as compared to the controls. However, both PPDBA II and III showed the highest retention compared to PPDBA I. In C6 cells, PPDBA I nanoplexes pretreated group showed the maximum retention of DOX at the 4^{th} hr i.e 0.228µg of DOX /mg of protein, whereas PPDBA II and III showed 0.244 and 0.235 µg of DOX /mg of protein respectively. The concentration of DOX was found to be decreasing over time after it reaches the maximum value at the 4^{th} hour. However, the concentration remained high till the 8^{th} hour which was 0.18 µg DOX /mg of protein in the case of PPDBA II and 0.135 and 0.174 µg /mg of protein for PPDBA I and III respectively. In the case of A549, the cells treated with PPDBA I, II and III nanoplexes showed the peak value of DOX concentration

at the 4th hour which was 0.235, 0.258 and 0.241 µg of DOX /mg of protein respectively. The highest value was noted for PPDBA II nanoplexes pretreated cells. After attaining the peak level, the concentration of DOX in the nanoplexes pretreated group lowers with time. However, it maintained a significant difference with the control group even at the 8th hour. Throughout the study, the DOX concentration in the control group was <0.1 µg/mg protein which was much lower than that observed with the nanoplex treated groups. On the contrary, HeLa cells didn't show any significant difference in the concentration of DOX in both the controls and the PPDBA I, II and III polyplexes pretreated group.

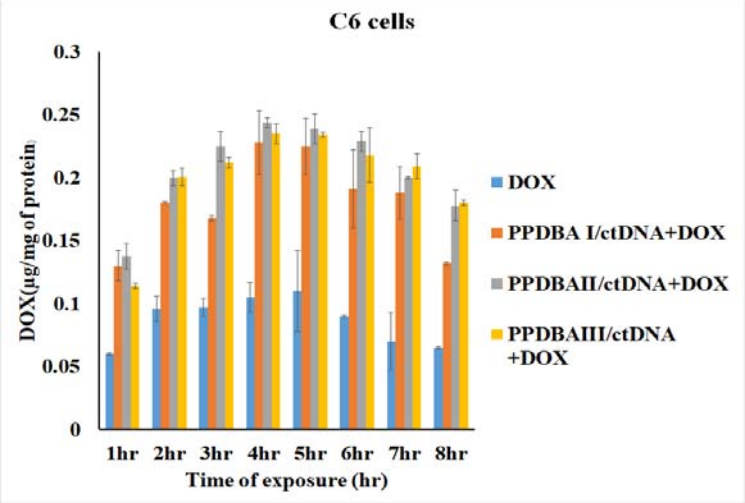

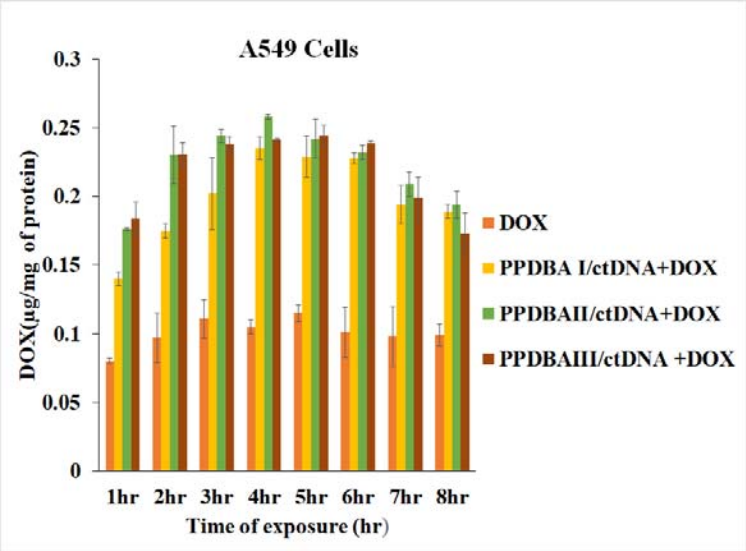

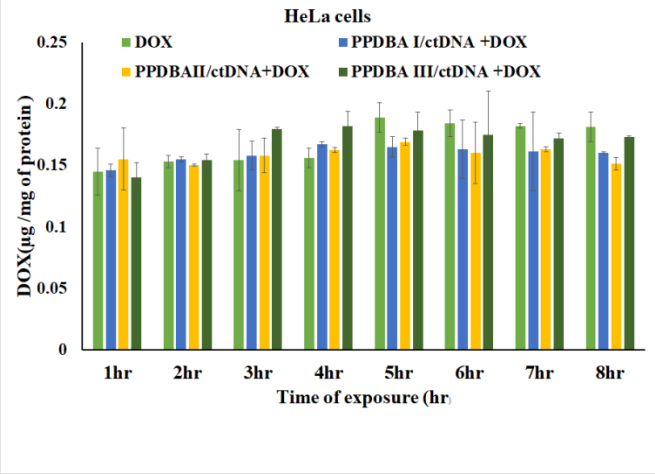

Figure 90: The DOX retention in cell lines C6 cells, A549 and HeLa using drug (DOX) alone and PPDBAI/ ctDNA 4:1, PPDBA II/ctDNA 4:1and PPDBA III/ctDNA 4:1 nanoplex pretreated, followed by DOX. The concentration of the drug is normalized to the total protein content of the cells. P is <0.001 between the control and polyplexes treated group upto 7th hour in C6 and A549. No significance observed in HeLa.

4.4.5.12 Role of glutathione

This study was intended to investigate how the influence of reducing environment affects the accumulation of DOX in presence of PPDBA polyplexes. To verify this role, initially the presence of glutathione in C6 cells was investigated by using the dye monochlorobimane. The glutathione level in the PPDBA nanoplexes and DOX treated cells were compared with the normal untreated

cells and the buthionine sulfoximine (BSO) treated cells. As seen in Figure 91, a remarkable increase in the fluorescence intensity was observed in the polyplexes and DOX treated cells compared with the normal and BSO treated cells. Here, as expected, the level of glutathione was very low in the BSO pretreated cells as compared to the normal and polyplexes treated cells which was indicated by less fluorescence intensity in C6 cells. It was clear from the image that the intensity of blue fluorescence was high in presence of PPDBA and DOX.

To further confirm that the disulfide containing PPDBA polymers were effective in promoting drug retention in cancer cell lines in reductive environment, the cells were initially pre incubated with glutathione monoester for 2hrs, followed by nanoplex treatment for another 2hrs before the addition of DOX. It was noted that a remarkable enhancement in the the cell fluorescence intensity of DOX was observed in the GSH monoester and PPDBA nanoplex pre treated cells compared with the cells that did not receive GSH monoester pre incubation (Figure 92). Similarly, the addition of buthionine sulfoximine pre exposure to the cells followed by PPDBA nanoplexes and DOX treatment showed a reduction in the fluorescence intensity of DOX. The same observation has been quantified by analyzing the concentration of DOX in the C6 cells following BSO preexposure and nanoplex/DOX treatment and/or PPDBA nanoplexes /DOX treatment with or without glutathione monoester preexposure (Figure 93).

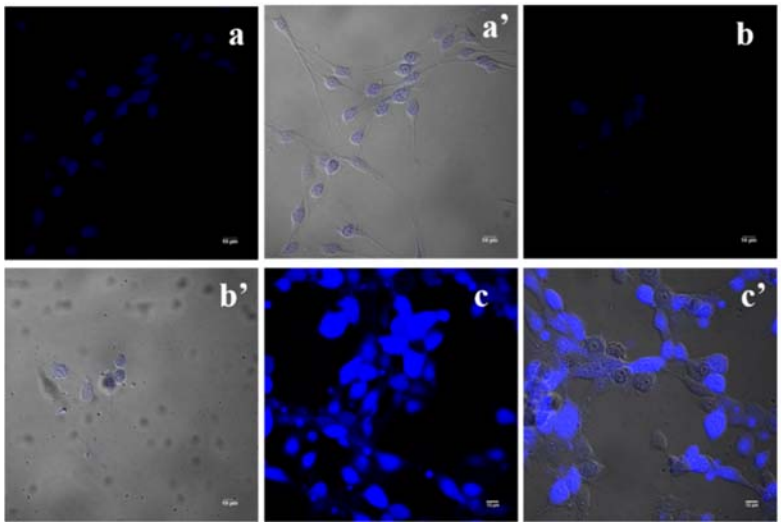

Figure 91: Role of GSH (a) glutathione level in untreated C6 cells (a') bright field merged image of a (b) cells pretreated buthionine sulfoximine followed with nanoplex treatment (b') bright field merged image of b (c) cells pretreated with PPDBA II nanoplex at 4:1 ratio followed with DOX (c') bright field merged image of c, Magnification 60x.

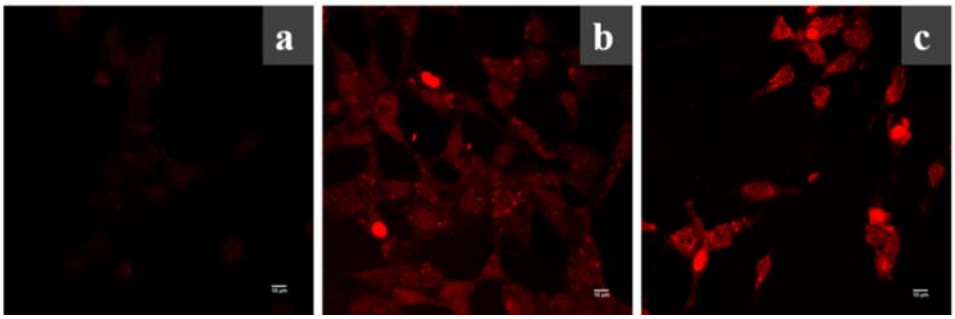

Figure 92: Role of GSH in DOX retention in C6 cells a) Cells pretreated with buthionine sulfoximine and PPDBA II 4:1 nanoplex followed by DOX treatment b) PPDBA nanoplex pretreated, followed by DOX treatement c) Glutathione monoester pretreated followed by PPDBA II 4:1 nanoplexes and DOX. Magnification 60x.

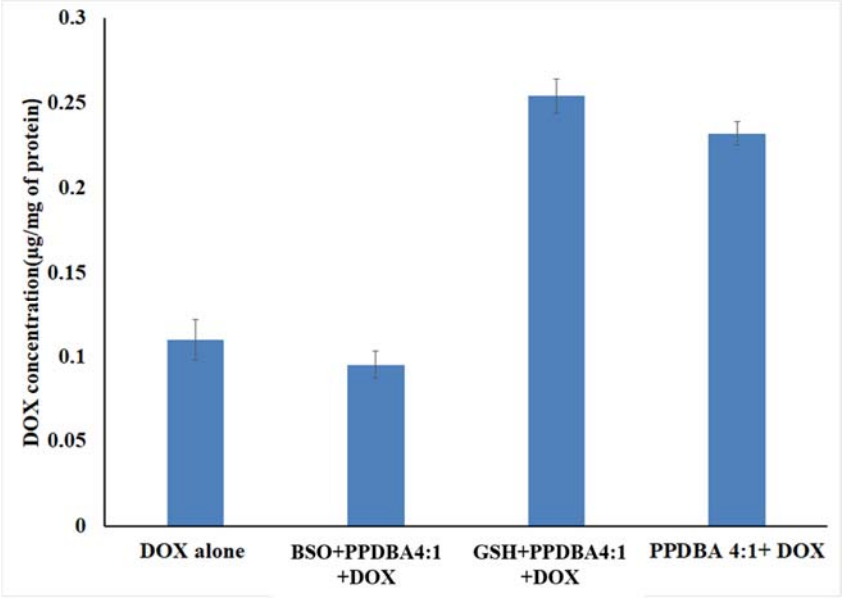

Figure 93: Accumulation of DOX in DOX alone treated cells and cells pretreated with BSO followed by nanoplexes and DOX treated cells and glutathione monoester pretreated followed by nanoplexes and DOX treated cells and finally, the nanoplexes and DOX treated cells. No significant difference seen between the DOX alone and PPDBA 4:1/BSO/DOX treated group. There is significant difference ($P<0.001$) between DOX accumulation in GSH/PPDBA 4:1/DOX and DOX alone.

4.4.5.13 DOX mediated cytotoxicity

The efflux pump inhibition studies demonstrated that the disulfide containing PPDBA nanoplexes can enhance DOX retention in drug resistant cells. Therefore, it is also expected that PPDBA pretreatment can enhance drug-mediated cytotoxicity in the cancer cells. Here, the cells i.e A549 and HeLa were first incubated with nanoplexes for 2hrs, followed by DOX at varying concentrations for different time periods viz., 24, 48 and 72hrs. The MTT assay was carried out thus to determine the dose response in different cancer cells based on DOX alone and nanoplexes/DOX treatment. The dose-response in A549 and HeLa cells are given in Figure 94. In the case of A549, the percentage inhibition in response to drug concentration was found to be higher in the nanoplexes pretreated group compared to DOX alone treated control group over time.

The inhibition rate increased with increasing drug concentration. It is evident from the Figure that the P-gp expressed cell, A549 is more sensitive to DOX in the polyplexes pretreated group i.e 83% inhibition in 10µM DOX against 64% inhibition in the DOX alone treated group(10µM) in 24hrs incubation which was further enhanced to 88% in 48hrs. On the other hand, HeLa cells showed high sensitivity to both nanoplexes/DOX and DOX alone treatment. In HeLa, the percentage inhibition was found to be 88% in the nanoplexes pretreated group whereas it was 86% in DOX alone control at the DOX concentration of 10 µM in 24 hrs which further enhanced in 48 and 72hrs.

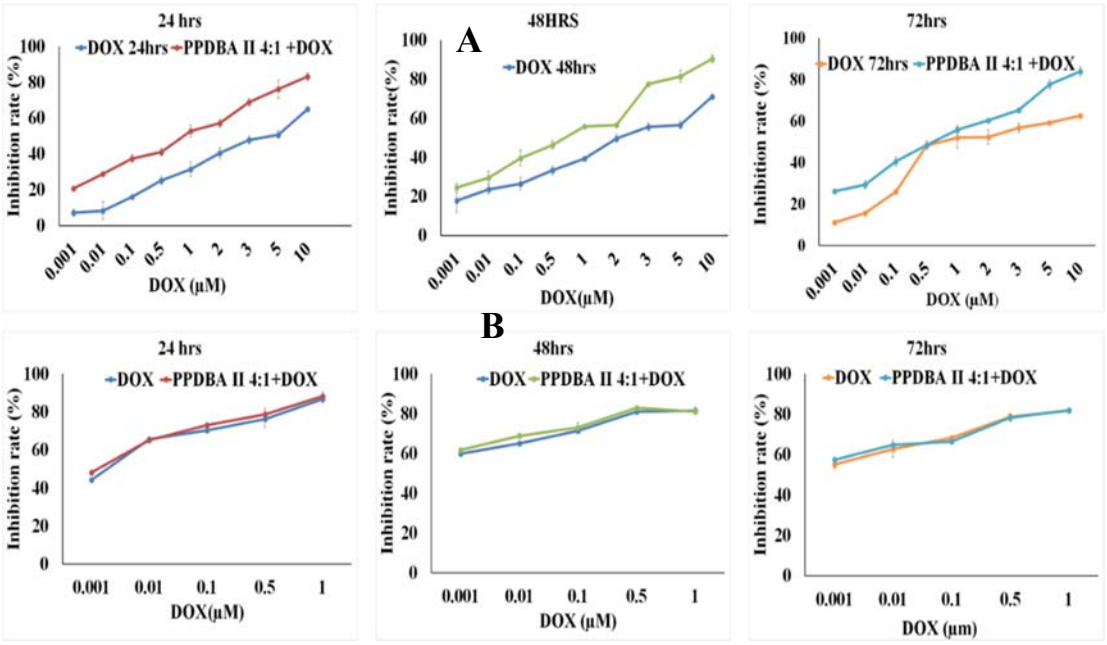

Figure 94: Dose response curves A) A549 and B) HeLa cells where the percentage inhibition was analysed at different time points such as 24hr, 48hr and 72hrs against different concentrations of DOX. DOX concentration are given in µM.

The IC50 values was calculated using DOX and PPDBA nanoplex/DOX in C6, A549 and HeLa cells and are given in Table 13. As shown in the Table, the IC50 values using DOX alone are 4.49 and 3.13µM for A549 and C6 respectively whereas HeLa cells showed an IC50 value of 0.004µM.

However, a remarkable decrease in the IC50 value of DOX was observed in the PPDBA nanoplex pre treated cells of C6 (0.183) and A549 (0.882) when compared to IC50 of DOX alone treated counterpart. HeLa cells on other hand, showed more or less the same result in the control as well as PPDBA nanoplex pretreated cells and are shown to be more sensitive to the drug, DOX. The IC50 values are 5 times lower than the DOX alone treated counterpart in A549.

Cell lines	DOX alone	PPDBAII/ctDNA 4:1 + DOX
HeLa	0.004	0.0025
A549	4.49	0.882
C6	3.13	0.183

Table 13: IC50 values of DOX alone and PPDBAII 4:1 nanoplex along with DOX treated cells at 24hrs. The values are given in μM of Doxorubicin.

Similarly, further evidence on the thiolated nanoplexes overcoming drug resistance was obtained by comparing the ratio of IC50 values of A549 and HeLa cells exposed with both DOX alone and or nanoplexes/ DOX. As shown in Figure 95, the ratio or the resistance factor for DOX alone was 1122 fold higher in A549 compared to HeLa cells (i.e IC50 of A549 is 1122 fold higher than IC50 of HeLa). In contrast, the resistance factor for nanoplexes pretreated cells in A549 is 352 fold as compared to the nanoplexes pretreated cells of HeLa.

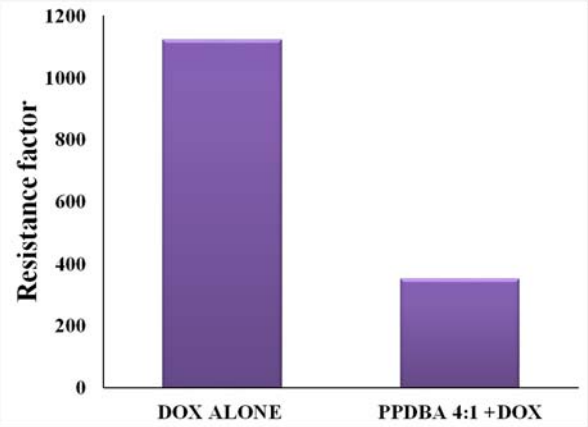

Figure 95: Resistance factor for 24h time point. The resistance factor is the ratio of IC50 of A549 to the IC50 of HeLa.

4.4.5.14 P-gp immunostaining

The P-gp or efflux pump plays an important role in causing multidrug resistance in cancer. The presence of P-gp in cancer cell C6, A549 and HeLa were identified by immunostaining using P-gp specific antibody. The green fluorescence corresponds to the expression of Pgp in the cancer cells. As shown in Figure 96, the intensity of green fluorescence was found to be high in the untreated control cells and DOX treated cells of both A549 and C6 cells. On the contrary, the expression P-gp was found to be lowered or minimised in the PPDBA 4:1 polyplex pretreated cells of both A549 and C6 as was indicated by the low intensity of green fluorescence in the cells. However, in the case of HeLa cells, the green fluorescence was absent in the untreated control cells as well as nanoplex/DOX treated cells.

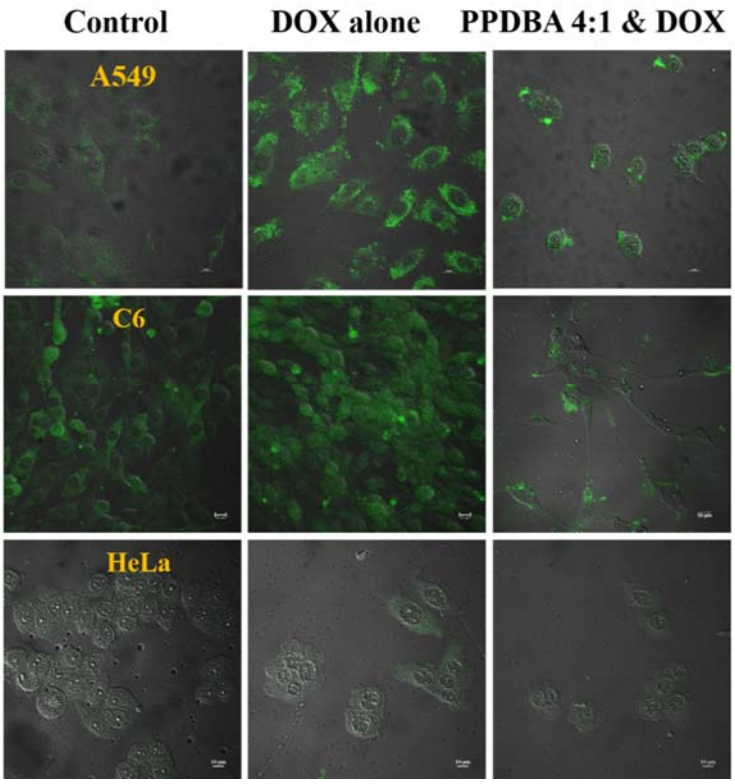

Figure 96: P-gp immunostaning in different cancer cell lines such as C6, A549 and HeLa cells. The green fluorescence corresponds to P-gp expression. The P-gp expression in normal and DOX treated cells are compared with PPDBA II 4:1 nanoplexes pretreated and DOX treated cells. The magnification is 60x.

4.4.5.15 Release study

The drug release from the PPDBA drug nanocomplex was determined at pH 7.4 and 6.8. Initally the drug DOX was intercalated with DNA before forming nanoplexes with PPDBA polymer. The PPDBA/ctDNA/DOX nanocomplex was incubated in PBS at different pH 7.4 and 6.8 to examine drug release at different physiological conditions such as blood circulation and tumor microenvironment respectively. The drug loading efficacy was found to be 85%,. DNA.The size and zeta potential values of the PPDBA/ctDNA /DOX complex was found to be 149nm and +7.01mV respectively. The cumulative drug release profile of both PPDBA/DOX at different pH is given in Figure 97. As shown in Figure, the drug release profile was found to be

pH dependent and was released more at pH 6.8 compared to pH 7.4. It was observed that around 60% of bound drug was released in 24hrs at pH 6.8 against around 52% at pH 7.4. There was no burst release seen in both pH values.

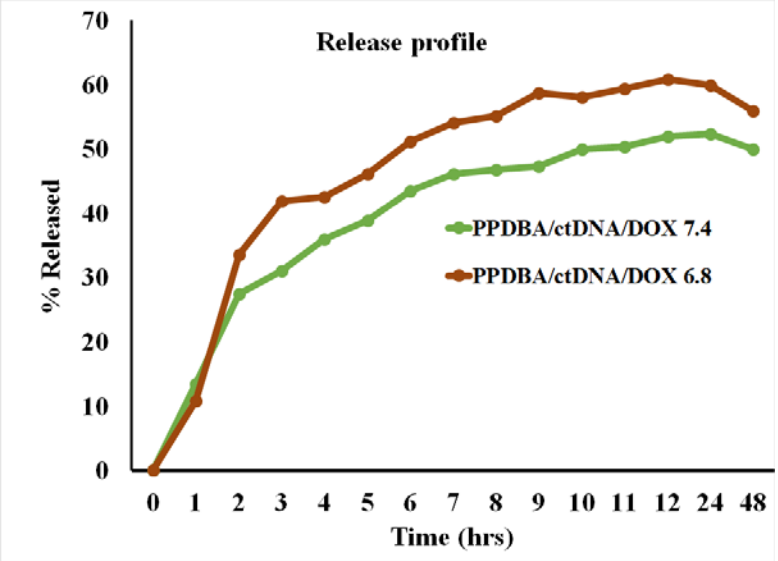

Figure 97: Release profile of doxorubicin from the drug loaded PPDBA II nanoplex at pH 6.8 and 7.4.

4.4.5.16 Synergisitic effect of therapeutic gene and drug

The synergistic effect of the drug and gene was evaluated in C6 cells. The PPDBA/p53 of ratio 4:1 was used for the study. The synergistic effect was determined using p53 gene and anticancer drug DOX in the cancer cell line where different molar concentrations of DOX (0.5, 1 and 1.5 µM) were used. The percentage cell death in the C6 cells following p53 transfection and DOX treatment was monitored via flow cytometry using PI staining. As shown in the Figure 98, PPDBA mediated transfection of p53 in C6 cells along with 0.5µM DOX treatment caused 87% cell death whereas 1µM DOX and 1.5 µM DOX caused 98 % and 99% cell death respectively.

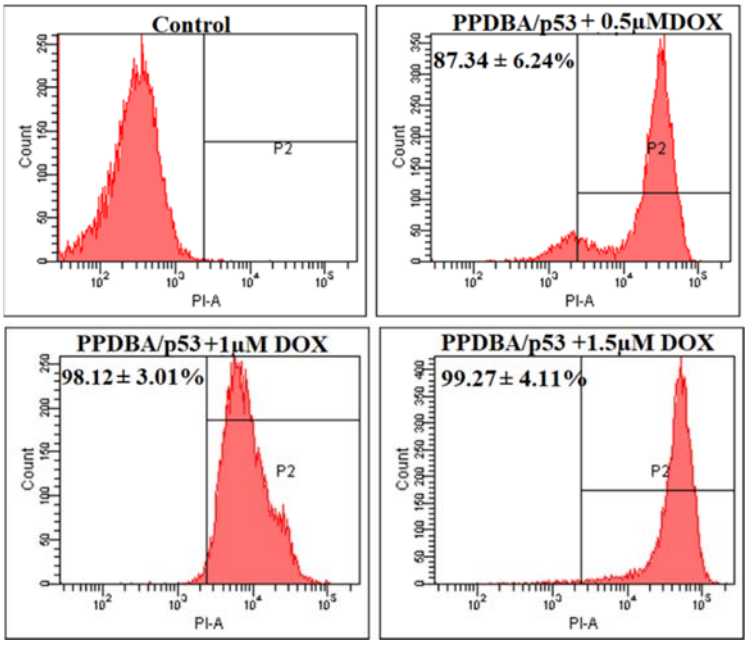

Figure 98: Synergistic effect of the drug and gene was evaluated in C6 cells. Cells were treated with PPDBA/p53 nanoplexes and varying concentration of DOX. Flow cytometry analysis was done to analyse the cell death.

4.5.1 *In vivo* organ distribution of PPDBA nanoplexes

The study on *in vivo* organ distribution of PPDBA nanoplexes was carried out to investigate its possible site of accumulation in the body. The distribution of PPDBA nanoplexes has been studied by both qualitative and quantitative methods. The qualitative methods initially involve the conjugation of polymer with NIR fluorophore DYLight 750. Following the injection of the conjugated polymer based nanoplexes, the corresponding fluorescence signals in the body was visualized using an *in vivo* imaging technique. The quantitative approach was by tagging the PPDBA polymer with rhodamine and the presence of the tagged polymer in different organs were determined at different time points following injection of nanoplexes in the tail vein of mice. As seen in the Figure 99, the fluorescence signals were completely absent in the vital organs like brain, heart, lungs and spleen but the signals were prominently seen in organs like liver and kidney in the 3hr post injection of polyplexes. In the 6^{th} hour, the fluorescence was found to be more intense

in the liver and kidney indicating that most of the polyplexes accumulated there. The quantitative analysis also showed enhanced concentration of tagged polymer in the liver and kidney in 3rd and 6th hour post injection (Figure 100). As seen in Figure 100, the presence of polymer was totally absent in brain, heart, lungs and spleen and was not showing any tendency to accumulate in these organs over time as noted in the *in vivo* imaging. It is interesting to note that PPDBA polyplexes exhibited more remarkable liver targeting property. By 24 hr, the intensity of fluorescence appeared to be reduced in the liver whereas the signal was found to be high in the kidney in both quantitative and qualitative approaches (Figure 99 and 100).

A

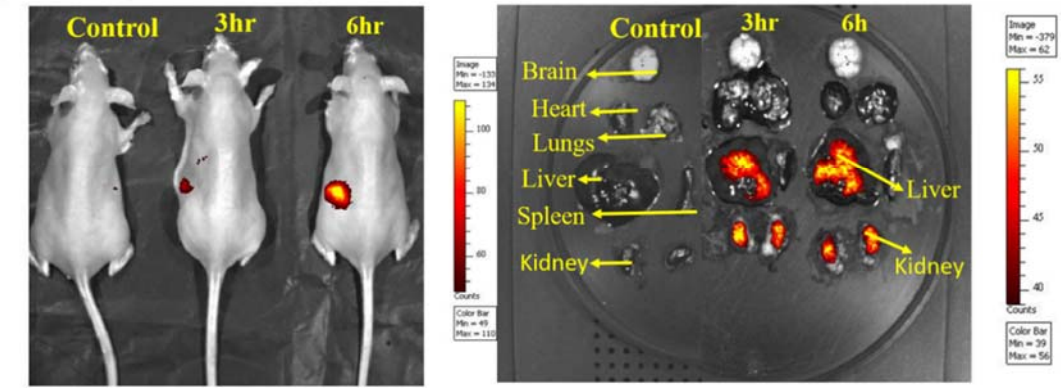

B

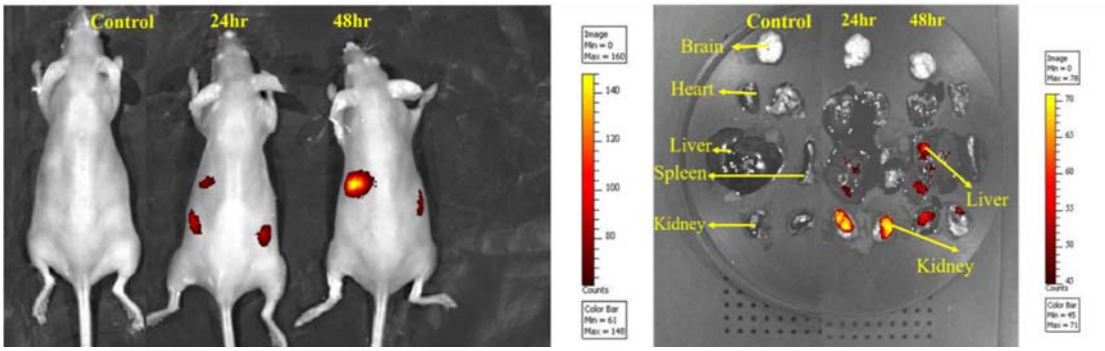

Figure 99 : Organ distribution of PPDBA polyplexes A) *in vivo* imaging of BALB/c mice post injection of PPDBA nanoplexes at 3 and 6 hrs and different organs following dissection. Similarly, B) the distribution of PPDBA nanoplexes following 24 and 48hrs post injection and different organs following dissection. The normal control is the untreated mcie injected with saline only.

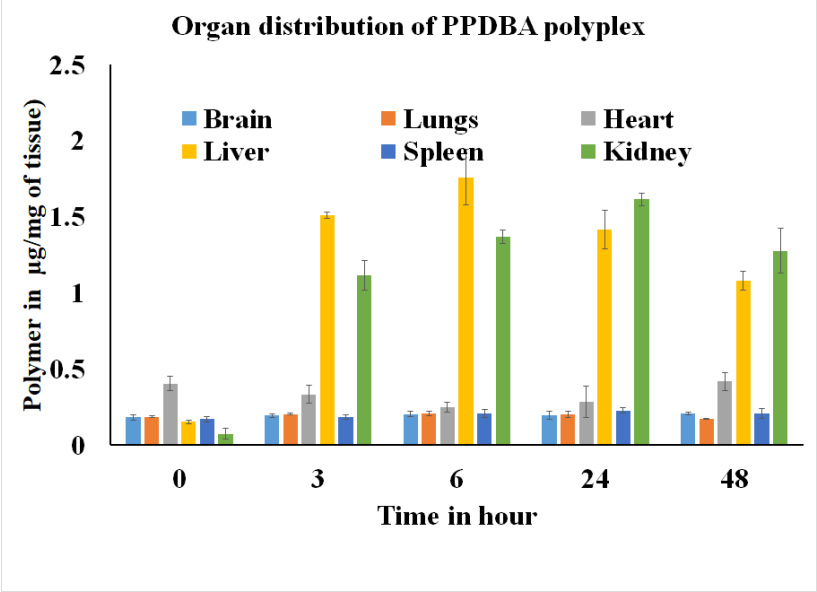

Figure 100: The quantitative measurement of the distribution of PPDBA polyplexes in different organs where n=3.

4.5.2 Antitumor efficacy of PPDBA/p53-DOX nanocomplex in BALB/c mice model

The nanocomplex (PPDBA/p53/DOX) was prepared by initially intercalating the drug DOX with p53 plasmid and later by complexation with PPDBA polymer. The nanocomplexes were intratumorally injected into the mice model at every alternate days for 35 days. Similarly, both DOX alone and PPDBA/p53 nanoplexes were also given to mice as separate injections and evaluated the change in tumor volume. As in Figure 101, compared to the untreated control

animals, the percentage reduction in tumor volume was observed to be more remarkable in the tumor mice treated with PDBA/p53 and PPDBA/p53/DOX nanocomplexes. Infact, higher reduction of almost 20% from the initial tumor size was observed in the PPDBA/p53/DOX treated animals compared to PPDBA/p53 nanoplexes treated animals where it showed almost 11% reduction from the initial tumor size. As in Figure 101, though the drug alone treated animals initially showed a reduction in the tumor volume, the tumor size continues to increase on the 5th day onwards. However, the percentage tumor growth was found to be lower than the untreated control. Both the untreated control and DOX alone treated animals died before the completion of the experiment, indicating its poor survival.

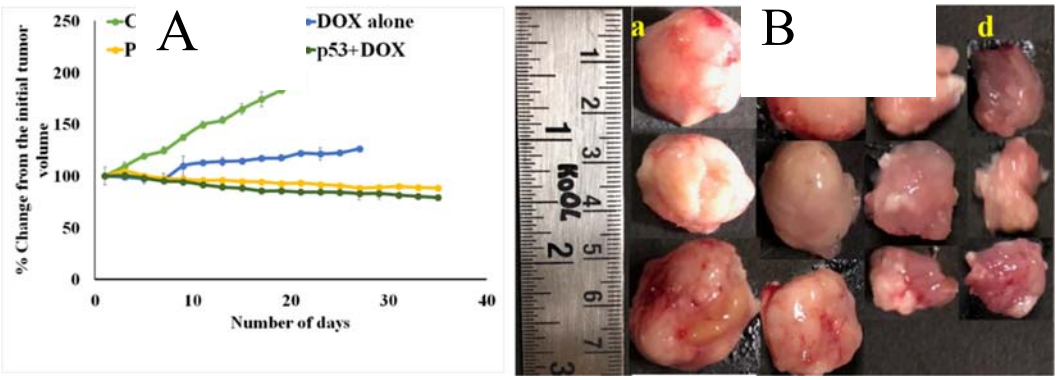

Figure 101: Antitumor activity of PPDBA/p53/DOX in the BALB/c mice model. Each group consist of 3 mice, n=3 A) percentage reduction of tumor from the initial tumor volume B) tumor size a) control group b) DOX alone treated c) PPDBA/p53 treated d) PPDBA/p53/DOX nanocomplex treated mice.

CHAPTER 5
DISCUSSION

Gene therapy holds great promise for the treatment of cancer. Non-viral gene delivery vectors are gaining recognition over viral vectors due to its safety and non-immunogenicity. Cationic polymers have proved successful as transfection reagents for gene delivery applications. Polyplexes which are formed due to the condensation of polycations and DNA via electrostatic interaction is the most widely used gene delivery vectors. Various factors including molecular weight, surface charge, hydrophilicity and structure of polymers affect the gene transfection efficacy of cationic polymers. Therefore, optimization of these characteristics of cationic polymers is necessary to attain a successful non-viral gene transfer. Non-viral vectors need to overcome both intracellular as well as extracellular barriers in order to deliver the nucleic acid cargo to the specified intracellular locations. Different strategies have been explored to impart required functionalities on nanocarriers for the successful transfer of gene to target cells.

5.1 Pullulan-PEI

Pullulan is a non-ionic polysaccharide which is non-toxic, non-immunogenic, non-mutagenic and non-carcinogenic in nature and is widely used for various biomedical applications. Polyethyleneimine (PEI) is one of most successful gene delivery vehicles, however, its toxicity remains a major obstacle for its use in *in vivo* conditions. Here, the conjugation of pullulan to PEI was carried out to minimize the cytotoxicity and improve the transfection efficiency.

5.2. Synthesis and characterization of pullulan-PEI-cysteine (PPSS) and pullulan-PEI- mercaptosuccinic acid (PPMSS)

Branched-chain polyethylenimine (25kDa) is one of the most promising gene delivery vectors containing a high density of amines. Pullulan is a water-soluble polysaccharide with

flexible hydrophilic chain and is nontoxic, non- immunogenic and biocompatible in nature. The conjugation of pullulan with PEI reduces the high charge density of the latter which in turn minimizes the systemic side effect of PEI. Apart from this, the incorporation of cysteine, a natural amino acid on to the pullulan-PEI backbone (PPSS) reduces the surface charge and enhances the compatibility of these polymers. However, there is always a need for improved colloidal stability, targetability and easy release of DNA. In view of developing nanoplexes with improved colloidal stability and efficient release of DNA, pullulan-PEI was further modified with mercaptosuccinic acid. This modification imparts additional carboxyl groups in addition to thiol groups. It is reported that MSA can act as a ligand to target cancer cells (Lin et al., 2016). And the additional free carboxylate group offer electrostatic repulsion required to maintain the stability of nanoparticles in circulation and provides easy intracellular dissociation of polyplexes. The disulfide bonds formed as a result of oxidation of thiol group in both PPSS and PPMSS ensures the stability of nanoplexes in the oxidative extracellular milieu and at the same time, release the therapeutic gene in the reductive intracellular environment. The ^{1}HNMR confirms the conjugation of pullulan, PEI and cysteine and mercaptosuccinic acid in both PPSS and PPMSS respectively. As seen in the results of PPSS (Figure 6) and PPMSS (Figure 29), both polymers and its corresponding control groups i.e. PEI-CYS (S-S) and PEI-MSA, showed the characteristic PEI repeating units i.e. (-CH2-CH2-NH)n representing at signal δ2.5 -2.6ppm. The signals at δ 5.2 -5.3 & δ 4.5 to 5.4 ppm represent the anomeric protons of pullulan observed in PPSS and PPMSS respectively. Most importantly, the two ethylene groups neighboring a disulfide linkage was indicated at δ2.7-2.8 ppm in both PPSS and PPMSS. The –SH protons of alkyl thiols in the MSA was clearly observed at δ 1.2 and δ 1.8 ppm in PEI-MSA whereas it is meagerly visible in PPMSS and PPSS, due to the presence of pullulan in the compound.

FTIR spectra were used to further confirm the conjugation of pullulan, PEI, cysteine and/or mecaptosuccinic acid. The FTIR spectra of PPSS and PPMSS are depicted in Figure 7 and 30 respectively. Herein, a broad absorption band visible in PPSS near 3200cm^{-1} is attributed to the –NH and –OH stretching vibrations of pullulan and PEI. The peaks at 2931cm^{-1} is indicative of the –CH stretching vibrations of PEI. Similarly, peaks at 1628cm^{-1} visible in PPSS corresponds to the C=O stretching of amide I band. A broad absorption peak observed in both pullulan PEI and PPMSS at around 3200 cm^{-1} is due to –OH /-NH stretching vibrations of pullulan and PEI. However, the peaks at 1629cm^{-1} in PEI-MSA and 1655cm^{-1} of PPMSS, are indicative of the C=O stretching of amide I band. Together, these informations indicate the successful formation of PPSS and PPMSS.

The amino content of PPSSI and PPMSS and the corresponding control groups are given in Table 2 (PPSS) and Table 6 (PPMSS). As in Table 2, both the control groups such as PEI-CYS(S-S) I and II showed high amino content compared with the corresponding polymer, PPSSI and II. There is a remarkable reduction in the amino content of PPSSI and II was observed when compared to PPI and PPII, indicating that the conjugation with cysteine further reduced the free amino content in pullulan-PEI (Table 2). Simiarly, the amino content was found to be high in the control group i.e PEI-MSA compared to the corresponding pullulan based derivatives in PPMSS (Table 6). The decrease in amino content in PPMSS polymers is indicative of the successful conjugation of PEI with pullulan and later to the thiol bearing group. The amino content is indicative of the net positive charge in the polymer which in turn determines the gene transfer efficacy. More the amino content greater is the net positive charge on the polymer surface and higher is its interaction with the negatively charged plasma membrane. It should be noted that both very high and low amino content is not suitable for gene delivery applications as it negatively affects the polymer interaction

with the membrane. Hence, an optimum level of the amino group is needed in the polymer chain to maintain a stable polyplex in circulation and also to have an efficient cellular uptake mechanism.

The thiol/disulfide content of both polymers PPSS and PPMSS and its controls were also analyzed and are given in Table 3 & 5. PPSSI showed the highest thiol/disulfide content compared to PPSSII because the amount of cysteine initially added to the pullulan-PEI backbone was highest in PPSSI compared to II. In the case of PPMSS polymers, PPMSSIII showed the highest thiol content compared to PPMSS I and II. The formation of disulfide linkage is also critical as it determines the overall stability of the polymer and susceptibility of the polyplexes in the intracellular redox environment. Furthermore, the free thiol group resulting from the selective intracellular reduction of disulfide linkage is important for efflux pump inhibition in cancer cells.

The cellular trafficking of nanoplexes typically involves endocytosis which involves the direct transmission to the lysosome via endosome following its passage through the cell membrane. The pH of an early endosome is 7.2 which drop to around 5 just before it fuses with the lysosome. The drop in pH in the lysosome and the presence of hydrolytic enzymes causes rapid degradation of the polyplexes and disintegration of DNA (Xiang et al., 2012). Hence, it is considered a challenging step in the intracellular transport of DNA, so the carrier should have an endosomolytic property to protect the therapeutics and aid in its escape from the endosome before it gets degraded in the lysosome. The branched PEI (25K) possess protonable amino groups exhibiting low pKa and hence exhibit good buffering ability at pH range 5 to 7 (Abouelmagd et al., 2012). As shown in the result PPSS (Figure 8) and PPMSS (Figure 31) and its corresponding control groups showed more or less the same buffering capabilities. However, the values of the control groups were higher than that of the corresponding pullulan based polymers and slightly lower than that of PEI alone. Both PPSS/PPMSS and its control groups maintained a good buffering ability which implies that

the endosomolytic properties of PEI are not adversely affected by the multiple modifications. Again, it should be noted that because disulfides are readily reduced in the presence of protons (Yuhe et al., 2011), increasing the number of thiols on the polymeric backbone improves the polymers buffering ability. The above statement was found to be true in case of PPSSI and its control groups as it contained higher disulfide content as compared to PPSS II counterparts. The buffering ability of PPMSS was slightly higher compared to PPSS. This is due to the fact that surface modification with each MSA provides one replaceable hydrogen that will undergo protonation at low pH. This result suggests that these polymers have the buffering ability in the pH range of 7-5 and are capable of escaping the endosomal barrier and release their cargo into the cytosol.

The fundamental design criteria of a gene delivery vector involves its ability to condense DNA into small nano-sized structure to facilitates cellular internalization and protect it from both extracellular and intracellular nuclease degradation. Here, the particle size of both PPSS (Figure 9) and PPMSS (Figure 32) was smaller than 200nm, which is advantageous as it is not only readily endocytosed into the cells for transfection; they can also escape from splenic filtration. As the polymer concentration increases, the electrostatic interaction between the polymer and DNA also increases, resulting in the tight condensation of the molecules leading to a decrease in particle size. In the case of PPSS I, the optimum size was recorded at ratios 2:1 and 4:1. Similarly, in PPSS II and PPMSS, the optimum size was formed at 3:1 and 4:1 polyplexes ratios. In both cases, the particle size was in the range of 100-165nm. The control groups i.e PEI-CYS(S-S) I/II and PEI-MSA also showed the particle size of <200nm.

The zeta potential value is an indicator of the net charge of the polymer/DNA nanoparticles. As shown in Figure 9 and 32, the zeta potential of both PPSS and PPMSS were positive. However,

compared to the corresponding control groups namely PEICYS(S-S) and PEI-MSA, the values of zeta potential were lesser and the net reduction in the positive charge is due to the charge masking effect of both pullulan and disulfide linkages in PPSS and PPMSS. As seen in Figure 9 & 32, the zeta potential of PPSS was higher than that of PPMSS. This could be due to the additional shielding effect of the extra alkyl group present in the PPMSS polyplexes compared to PPSS where the charges remained < 20mV. However, the value approached almost 24mV in PPSS. On the other hand, the zeta potential of the control groups were >25mV which is due to the total lack of charge masking effect from pullulan (Figure 9 & 32). The net positive charge is advantageous because the repulsive forces between them provide stability in the colloidal system by preventing aggregation of nanoparticles along with improving cellular internalization, however charges above 25mV causes cellular toxicity. Here, the DLS measurements confirmed the improved stability and good dispersion.

Agarose gel electrophoresis was carried out to investigate the ability of the polymers to condense DNA. For each polymer, polyplexes were formed at various polymer to DNA ratios ranging from 1:1 to 5:1. In the case of PPSS I & II polymers (Figure 10), except the initial ratio of 1:1, all polyplexes inhibited the mobility of DNA, which is in total agreement with the zeta potential values obtained. Except for the first polymer: DNA ratio, all were positively charged and hence inhibited the DNA mobility in the electrophoresis gel towards the anode. More the positive charge, greater will be its electrostatic interaction with the negatively charged DNA and lesser will be its migration towards the anode. However, at initial ratios, the amount of polymer is less which resulted in an inadequate interaction with the DNA. In contrast, the control groups were all retained in the well even at the initial polymer to DNA ratio of 1:1. In case of PPMSS (Figure 33), the DNA was completely retained in the well in all polymer to DNA ratios (1:1 to 5:1) just like the

corresponding control group, which is again in total agreement with the zeta potential values obtained. The DNA retardation at 1:1 ratio shows that the surface charge of the PPMSS polymer is sufficient to cause the DNA condensation and the charge masking effect of pullulan had little influence on the formation of nanocomplexes.

Again, the stability of nanoplexes in presence of plasma proteins was demonstrated in agarose gel electrophoresis. The results are given in Figure 10 and 33 for PPSS and PPMSS polymers respectively. The plasma proteins are anionic in nature and hence when incubated with polyplexes, it was expected that the proteins will have a competition with DNA for binding with polymer and hence will replace DNA from the polymer. However, it was observed that none of the DNA from the selected polyplexes ratios of PPSS and PPMSS have released from the polymer on exposing with the plasma proteins. Hence, no trace of DNA was observed in the agarose gel. On the other hand, the DNA was observed to be confined in the well region, indicating the strong interaction between the polymer and DNA, showing the stability of polyplexes in circulation.

The reversible cross-linking of the polymer with disulfide bonds provides a way to maintain the stability of the polyplexes in the extracellular environment while inducing the efficient release of DNA from the polyplexes after their movement into the reductive intracellular cytoplasmic compartment (Klein and Wagner, 2014). In order to evaluate the effect of reductive environment on nanoplexes, they were treated with DTT (mimicking the intracellular glutathione level). As shown in Figure 11 and 34, the size of the polyplexes of both polymers i.e. PPSS I/II and PPMSS gradually increased via incubation with DTT over time. Moreover, the particle size of PPSSI/PPMSS 4:1 nanoplexes was significantly higher (>400nm) than the untreated counterparts. It is concluded that reductive cleavage of disulfide bonds in the catiomer influenced the ionic interactions between the charged surfaces resulting in the formation of larger aggregates. This

observation indicates the responsiveness of these polyplexes to a thiol-rich environment and its role in the intracellular delivery of biologics. It is known that the electrostatic interaction forms the major driving force for the formation of polyplexes; however, disulfide linkages also exert some additional weak forces like hydrogen bonding and dipole interaction to contribute to the stability of the polyplexes (Lin and Engbersen, 2009). It should be noted that the reduction in disulfide bonds removes the effect of these additional forces and causes further loosening of the DNA interaction with the polymer. The influence of DTT on stability of polyplexes was further demonstrated in agarose gel electrophoresis (Figure 12 and 35). Following enlargement in particle size on exposure with DTT, it was expected a simultaneous release of DNA from the nanocomplexes. However, as shown in the results (Figure 12), the PPSS nanoplexes remain stable and the bound DNA was not released from the complexes upon exposure with DTT. A similar observation was seen in the case of PPMSS polyplexes on incubation with DTT (Figure 35). However, in both cases, when the nanoplexes were exposed with DTT and heparin together, where heparin mimic the intracellular anionic condition, the DNA was found to be released from the nanocomplexes (Figure 12 & 35). This implies that the unpacking and release of DNA from the polyplexes demand further assistance from the cytosolic anionic fractions.

The biodistribution of nanoparticles following its systemic delivery is largely dependent on the nature of proteins that adheres on to the nanoparticles surfaces over time. The proteins that bind most strongly to the polymeric nanoparticles (NP) includes albumin, immunoglobulin, fibrinogen, apolipoproteins, and proteins from the complement cascade system (Ilinskaya and Dobrovolskaia, 2016). The binding of complement proteins and immunoglobulins promotes particle opsonization leading to recognition by the mononuclear phagocyte system (MPS) and rapid clearance of NP from the bloodstream. The MPS capture involves macrophage phagocytosis

in the liver and splenic filtration, this, in turn, reduces the plasma half-life of nanoparticles. Hence, several strategies have been developed to enhance the blood residence time of cationic nanoparticles. The plasma protein interaction with PPSS and PPMSS polymers was demonstrated in PAGE studies. As seen in the results, both PPSS (Figure 13) and PPMSS (Figure 36) reduced the adsorption of proteins on to their surfaces on incubating with plasma, which is evidenced by the appearance of protein bands in PAGE as similar to plasma. This lack of adsorption of proteins is mainly due to hydrophilicity and steric repulsion effect of pullulan. On the other hand, both PEI and PEI derivatives showed significant absence of plasma protein bands in PAGE as compared to plasma alone and pullulan derivatives. This is due to the increased adsorption of plasma proteins on to both PEI/PEI derivatives, resulting in the absence of protein bands in the gel. However, as compared to PEI alone, the PEI derivatives showed a reduction in protein adsorption and presence of protein bands in the gel. This is due to the fact that the presence of disulfide linkages in PEI derivatives limits the adsorption of proteins. Hence it is concluded that both the presence of pullulan and disulfide linkages together contributes to the prevention of protein adsorption on to PPSS and PPMSS. Again, the surface charge of the polymer is another important factor which determines the protein interaction. From the results, Figure 9 & 32, it has been observed that the surface charge is highest in PEI which was then followed by PEI derivatives and then pullulan based derivatives. Here, the adsorption of proteins also followed the same trend. This result implies that an increase in charge density is associated with an increase in plasma protein adsorption. The charge shielding effect of both pullulan and thiol-containing groups largely reduced the adsorption of plasma proteins on to PPSS and PPMSS.

Though cationic polymers like PEI exhibits relatively high gene transfection, their therapeutic application is largely hampered due to high cytotoxicity. Free PEI usually destabilizes

the cellular membrane, causes necrosis related cytotoxicity and further elicits signals for cellular apoptosis. Thus, cytotoxicity can be minimized by using biodegradable polyplexes. The incorporation of disulfide linkages to the polymer chain not only enhance intracellular degradability of the polymer but may also lead to low cytotoxicity (Yan and Li, 2016). Herein, both PPSS and PPMSS, the nanoplexes interaction with different cell lines such as C6, A549, HeLa and fibroblast cell, L929 were evaluated and is shown in Figure 14 & 37. The results shows that both PPSS and PPMSS exhibit >85% viability in all the cell lines tested. In the case of polyplexes, polymer is ionically complexed with DNA and the exposed cationic groups are lower compared to free polymer. Hence, here it can be concluded that these nanoplexes are non-toxic and could be suitable for gene delivery applications. The cytotoxic study conducted in L929 further supported the above statement with the fact that the nanoplexes of PPSS and PPMSS are non-toxic to the normal cells.

The cellular uptake of nanoplexes formulated with PPSSI/II (Figure 15), PPMSS (Figure 38) and its corresponding control groups (Figure 16 & 38) were examined using confocal microscopy and flow cytometry in C6 cells. The results demonstrated the successful localization of ctDNA into the cytosol and nucleus. This infers that both PPSS and PPMSS polymers are efficient gene delivery vectors capable to transfer the gene to the host cell nucleus. The diffused appearance of green fluorescence in the cytosol reflects the presence of nanoplexes in that region. The appearance of intense green fluorescence in the nucleus can be related to the polyplex dissociation in the cytosol and subsequent translocation of DNA to the nucleus. However, the confirmation of this statement can be obtained from the polymer trafficking studies detailed in the next section. Again, the difference in the intensity of green fluorescence observed in the nuclear region between PPSSI and PPSSII nanoplexes can be attributed to the effect of disulfide linkages, where the former

possess higher disulfide bonds and hence it is possible to have an easy disintegration of polyplexes in the cytosol and subsequent appearance of DNA in the nucleus. Similarly, both PPSS and PPMSS nanoplexes maintained the normal spindle-shaped morphology of C6 cells, indicating that these polymers are non-toxic in nature. Additionally, it was reported earlier that MSA can be utilized as a ligand to target cancer cells. Hence, the addition of MSA in the pullulan-PEI backbone strengthen its suitability (PPMSS) as a vector for gene delivery. On the contrary, both control groups of PPSS (Figure 16) and PPMSS (Figure 38) exhibited neither cellular nor nuclear uptake and displayed notable necrosis of cell with fragmented Hoechst stained nucleus. This is due to the fact that the charge shielding effect of pullulan was totally lacking and hence resulting in the enhanced cytotoxic effect of PEI. The flow cytometry analysis also supports the observation in confocal microscopy and showed >75% cellular uptake for PPMSS (Figure 39) against >85% in PPSS (Figure 17). This result infers that both are good vectors in terms of intracellular transport of DNA.

The positively charged polyplexes usually bind to the heparan sulfate proteoglycan in the cell membrane by electrostatic interaction which is then taken into the cell via endocytosis (Yameen et al., 2014). The three important endocytosis pathways include clathrin-mediated, caveolae-mediated endocytosis, and macropinocytosis. Chlorpromazine inhibits the clathrin-mediated endocytosis by inducing a loss of clathrin and adaptor protein complex from the surface of the cell. Similarly, filipin inhibits the caveolae-mediated endocytosis through depletion of cholesterol from the cell membrane by forming inclusion complexes with cholesterol. Amiloride inhibits macropinocytosis via an unknown mechanism. The individual exposure of these inhibitors was thought to prevent or reduce the entry of nanoplexes. However as seen in the results (Figure 18 & 40), it was observed that whichever pathway is inhibited, presence of nanoplexes was found

inside the cells. Hence, it is concluded these nanoplexes take multiple entry pathways to get inside the cell.

The polymer trafficking studies were performed in C6 cells using selected nanoplex ratios of PPSS (4:1) and PPMSS (4:1) to analyze the intracellular location of nanoplexes over time and hence to acquire a qualitative description of the transport process. Here, the polymer and DNA were labeled with rhodamine and YOYO-I respectively and the nucleus was stained with Hoechst. As seen in the result (Figure 19), in the case of PPSSI nanoplexes yellow fluorescent spots (representing both tagged DNA & polymer together) were found in the cytoplasm during the 1st hour and near the nuclear membrane, indicating that the DNA is still associated with the polymer. However, the YOYO-I-DNA was found confined in the nuclear region in the 2nd hour whereas the rhodamine tagged polymer was seen only in the cytoplasm. This observation infers the successful unpacking of PPSS I nanoplexes and the appearance of DNA in the nuclei and presence of rhodamine tagged polymer in the cytosol.

In the case of PPMSS nanoplexes, as seen in Figure 41, the rhodamine tagged polymer gets dissociated from the DNA in the 1st hour following nanoplex internalization. This indicates relatively easy unpacking of polyplexes and subsequent translocation of DNA to the nuclei. More intense red fluorescence observed inside the cytoplasm in the 2nd hour represent complete dissociation of polyplexes. However, in both cases, over time, the intensity of red fluorescence becomes minimal and mostly confined to the cell membrane region, indicating that PPSS/PPMSS polyplexes, following unpacking and release of DNA is subsequently exocytosed. Here, both the polymers contain inter and intra disulfide linkages, which in presence of intracellular reductive environment undergoes reduction at the disulfide bond resulting in the polyplex unpacking and release of DNA. The unpacking of the polyplexes which contain PEI was made easy by the

presence of pullulan in the compound as it reduces the charge density in PEI. In addition, the easy unpacking of PPMSS polyplexes observed in Figure 41, was due to the loosened association of polymer and DNA, contributed by the combined activity of reducing environment, the presence of pullulan and a free carboxyl group in MSA. In this line, it should be noted that the failure of many cationic gene delivery systems is due to the tightened polymer-DNA interaction, poor vector unpacking and hence minimal transfection efficiency (Guo et al., 2012). Since both the polymers are successful in cellular uptake, vector unpacking and further translocation of DNA to the nuclei, this can be a promising vector for intracellular delivery of therapeutic gene.

The transfection efficiency of the polymer, PPSS, and PPMSS was evaluated using the p53 plasmid in C6 cells. Here, both qualitative and quantitative evaluation of the transfection potency of the polymer was determined using confocal microscopy and flow cytometry respectively. The transgene expression of p53 is indicated by the presence of dead cells. Hence, the transfection efficiency was indirectly measured by the presence of dead cells in the transfected cells. As seen in the results, the cell death was found to be high in cells transfected with both PPSS I (Figure 20) and PPMSS nanoplexes (Figure 42), which was analyzed by means of the live and dead assay. Similarly, the quantification of dead cells was carried out by flow cytometry using PI staining and which further substantiated the observation obtained in the microscopic analysis. In flow cytometry, >75% cell death was shown by PPMSS (Figure 43) nanoplexes and> 85% was recorded for PPSS I nanoplexes treated cells (Figure 21). Interestingly, although PPSS II nanoplexes showed good cellular uptake in C6 cells (>85%), it turned out to be poor in terms of transfection efficiency with only 15% cell death was shown in flow cytometry and a low number of dead cells (red) observed in LDA (Figure 22). The possible explanation could be that PPSS II contained comparatively low reduction sensitive disulfide linkages and together with a strong

interaction of pDNA to the polymer might have lowered the unpacking of polyplexes and hence showed poor transgene expression of p53. However, the extensive inter and intra disulfide linkages in PPSSI together with charge masking effect of pullulan enhanced the reductive cleavage and easy unpacking of polyplexes. This observation established the significance of disulfide linkages in the cellular unpacking of nanoplexes. In this line, it should be noted that similar to PPSSII, PPMSS also contained less thiol content, but the transfection efficiency was high (Figure 42 & 43). This disparity in the observation is due to the fact that PPMSS possess extra carboxyl group in each MSA molecule, which further aid in the effective release of nucleic acid.

Annexin V-FITC/propidium iodide staining was carried out to analyze the percentage of cell death caused by apoptosis. As seen in Figure 22 & 44, the percentage of apoptosis was measured based on the sum of early and late apoptotic cells (Q2+Q4) in annexin V staining. From the results it is evident that the cell death was due to the apoptosis mediated by PPSS (Figure 22) and PPMSS polyplexes (Figure 44) based transfection, which is >75% & >85% respectively. The successful intracellular transfection of p53 by these polymers (PPSS & PPMSS) are related to the nanocomplex formation, endosomal escape via good buffering ability caused by the presence of amine groups in the polymer, vector unpacking mediated by the combined influence of pullulan and disulfide linkages and finally translocation of p53 plasmid to the nucleus to initiate the process of apoptosis.

Again, to further confirm the expression of the p53 in the transfected cells, p53 immunostaining method was adopted. As seen in the results (Figure 23 & 45), the intensity of green fluorescence indicates the expression of the p53 in the cells. It is interesting to note that expression of p53 is higher in those cells treated with both PPSSI (Figure 23) and PPMSS (Figure 45) nanoplexes, whereas it was low in PPSSII nanoplexes treated cells. These results indicate that

the cell death is mediated by the transfection of p53 alone. Hence it is proved that both the polymers PPSS and PPMSS are superior gene delivery vectors.

The drug efflux transporters are generally overexpressed in most of the cancer cells which mediate active effluxing of anticancer drugs from the cell. Among which P-glycoprotein (P-gp) is most important as it shows broad substrate specificity and is a major obstacle in anticancer therapy. Herein, the efflux pump inhibition studies are meant to evaluate the potential of the thiolated polymers in inhibiting the drug efflux pump in cancer cells.

In this study, appropriate cell lines were chosen by using a known P-gp inhibitor, verapamil. Verapamil is a calcium channel blocker and mainly function to block the P-gp mediated effluxing. As shown in the result (Figure 24), the incubation of cells with verapamil followed by DOX treatment has enhanced the drug retention in the cells which reached up to 3µg/mg of protein in A549 and 2.5µg/mg of protein in C6 cells. On the other hand, in the control cells which are DOX alone treated have a retention value of 0.09 µg of DOX /mg of protein and 0.06 µg/mg of protein in A549 and C6 respectively. These results demonstrated that both A549 and C6 are P-gp overexpressed cells and hence the presence of verapamil has blocked the P-gp activity in the membrane resulting in the enhanced retention of DOX on DOX treatment. The control cells which were not exposed with verapamil treatment have actively effluxed the anticancer drug DOX from within the cells resulting in the low DOX retention in the cells. On the contrary, HeLa cells showed the same value (~0.18 µg/mg of protein) of DOX retention i.e. in both controls as well as verapamil pretreated cells. These findings indicated that the presence of P-gp is critical for the differential accumulation of DOX in different cell lines and that P-gp activity was totally lacking in the HeLa cells. Herein, both C6 and A549 which was responding to the verapamil pretreatment were selected

as P-gp positive cells and HeLa cells which was unresponsive to verapamil was chosen as P-gp negative cell for farther studies.

A series of experiments on the thiolated polymers have been carried out to evaluate its potency in inhibiting efflux pump in cancer cells. In this line, a qualitative determination of the efflux pump inhibition property of both PPSS and PPMSS was evaluated in different cell lines using confocal microscopy. Herein, the anticancer drug, DOX act as an indicator of P-gp activity in the cell. The DOX retention mediated by PPSS I polyplexes of ratios 2:1 and 4:1 were carried out in cell lines such as C6 (Figure 25), A549 (Figure 26), and HeLa (Figure 28) cells. Similarly, the retention of DOX mediated by PPMSS polyplexes of ratios 3:1 and 4:1 in cell lines such as C6 (Figure 46), A549 (Figure 47), and HeLa (Figure 48) respectively. The red fluorescence corresponding to the presence of DOX was high in both PPSS and PPMSS polyplexes pretreated cells as compared to the DOX alone treated control cells of C6 and A549. The enhanced presence of DOX on exposure to the polyplexes in C6 and A549 indicates the inhibition of P-gp activity by the polymer. The reduced P-gp activity resulted in the enhanced accumulation of anticancer drug DOX in these cells which otherwise leads to the active effluxing of drugs as was seen with the controls. In HeLa cells (Figure 27 and 48), the red fluorescence corresponding to DOX was more or less same in both the polyplexes pretreated one and DOX alone treated cells. This is due to the fact that the cell line itself is P-gp negative and hence the drug DOX can easily diffuse into the cell and accumulate there.

The flow cytometry analysis also showed a similar result where the percentage of cells containing DOX was found to be high in the polyplexes pretreated cells of C6 and A549. In PPSS I 2:1 and 4:1 pretreated group, the percentage of cells retaining DOX was 70% and 78% in C6 cells where as 69% and 75% in A549 cells respectively (Table 4).

In PPMSS polyplexes 3:1 and 4:1 pretreated cells, the percentage of cells containing DOX was found to be 67% and 81% in C6 and 70% and 78% in A549 respectively (Table 7). However, in the control group of C6 and A549, only 30% and 34% of cells were retaining DOX respectively, indicating the active effluxing of DOX from within the cells by the membrane P-gp. However, the high percentage of cells retaining DOX in the polyplexes pretreated group indicated the inhibition of membrane P-gp activity by the PPSS/PPMSS polymer. Both confocal and flow cytometry analysis showed that the polymer have a direct influence on the membrane P-gp activity and its interaction have caused the conformational change in the P-gp resulting in the blockage of its function.

Further, the retention of DOX at different time intervals was quantitatively determined by analyzing the concentration of DOX in cell lysate, normalized to the total protein content of the cells. As shown in Figure 28, the retention of DOX mediated by the PPSS I polyplexes was found to be significantly high ($P<0.001$) compared to the corresponding control group i.e. drug alone treated cells of C6 and A549. The concentration of DOX initially used was 3μM. In C6 cells, the nanoplexes pretreated cells showed a gradual increase in DOX retention and exhibited the highest retention of DOX at the 2nd hour i.e. 0.18 μg/mg of protein. From the 3rd hour onwards, the concentration of DOX was found to be decreasing with time. The control cells showed a drug retention of <0.1 μg/mg of protein at all time points. However, it is interesting to note that even in the 7th hour, the retention of DOX in the polyplexes pretreated group was significantly higher than that in the control group i. e $P <0.001$. Similarly, in the case of cells treated with nanoplexes of PPMSS (Figure 49), the concentration of DOX in C6 cells attained a peak value of 0.14 μg/mg of protein in the 2nd hour and then decreased with respect to time. Similar observation was seen in the A549 cells also, where PPSS (Figure 28) and PPMSS (Figure 49) pretreated group showed

a peak concentration of 0.182 µg/mg protein at 4th hour and 0.16µg /mg protein at 3rd hr respectively. Here also, a significant difference in the concentration of DOX in both controls as well as polyplexes pretreated group was observed. This results clearly indicate the influence of thiolated polymers on the membrane P-gp activity. Even though the concentration of DOX declined with time, the level of DOX remained high even in 8th hour in case of A549 compared to C6 cells. Though the nanoplex influence on P-gp was same in different cell lines, the degree of sustainability varies which depend on the nature of cells. The gradual increase in DOX concentration followed by a decrease over time infers that either the effect of thiolated polymer, PPSS and PPMSS on P-gp activity is time dependant and is reversible or the polymer may get exocytosed over a period of time. The intracellular trafficking studies have shown that the polymer is slowly getting localised near the cell membarne and is eliminated from the cells. Besides, there are reports in literature which state that the activity of thiomers in the cellular efflux pump is completely reversible (Werle, 2008). However, it is interesting to note that the PPSS and PPMSS interaction with the P-gp was not completely diminished even at 7th hour as was evidenced by the high DOX retention in the cells compared to the control. This is in agreement with the intracellular polymer tracking studies, which showed polymer interaction with the membrane till the 7th hour. However, the control cells maintained a low concentration of DOX in C6 and A549 due to the active effluxing of DOX by the cells. On the other hand, HeLa cells didn't show any significant difference in the concentration of DOX in the control as well as nanoplexes pretreated group (Figure 28 & 49). This is due to the absence of P-gp activity in the membrane which in turn led to the enhanced accumulation of DOX in the cells. Hence it is concluded that both PPSS/PPMSS polymer have an inhibitory effect on P-gp which result in the reversal of drug resistance in cancer cells C6 and A549 with the simultaneous accumulation of DOX over time.

5.3 Synthesis and characterization of pullulan-PEI-3,3 dithiodipropionic acid (PPDPA) and pullulan-PEI-4,4 dithiodibutyric acid (PPDBA)

The parent compound, pullulan-PEI has been acylated and thiolated simultaneously using 3,3 dithiodipropionate (DPA) and 4,4 dithiodibutyrate (DBA) to form the pullulan-PEI-3,3 dithiodipropionic acid (PPDPA) and pullulan-PEI-4,4 dithiodibutyric acid (PPDBA) respectively. Both DPA and DBA contained an in built disulfide linkages in it and its incorporation to the pullulan-PEI backbone impart redox sensitivity to the polymer and also the acyl content help in the easy dissociation of the nanoplexes in the cytosol. Though PEI is considered as the superior gene transfection agent, the *in vivo* application is limited due to the difficulty in the timely unpacking of the PEI/plasmid DNA complexes and high cellular toxicity. It was reported that the hydrophobic-hydrophilic modification has been applied to enhance cell binding, confer protection from enzymatic degradation and facilitate the intracellular pDNA dissociation to mediate favorable gene transfection.

Synthesis of PPDPA and PPDBA was established by means of analytical techniques such as ^{1}HNMR, FTIR, Ellman's assay and $CuSO_4$ assay. As shown in the results, among the PPDPA (Table 9) and PPDBA (Table 12) polymers, PPDPA I and PPDBA I showed the highest amino content compared to the corresponding polymers of PPDPA/PPDBAII and PPDPA/PPDBA III. This due to the fact that as the amount of DPA/DBA increases, more number of primary amines of PEI in pullulan-PEI get involved in the amide linkage formation resulting in the reduction of free amino group in the pullulan-PEI. The control groups i.e PDPA and PDBA showed high amino content as compared to the corresponding pullulan based derivatives. The amino content of the polymer is crucial as it contributes to the surface charge of vectors, cellular uptake, endosomal escape, and vector unpacking.

As seen in the results (Table 8 and 11), the thiol/disulfide content of the polymers was in the reverse order as that of amino content. It increases with the amount of DPA/DBA added to the parent compound, pullulan-PEI. Likewise, PPDPA III/PPDBAIII contained the higher thiol/disulfide compared to PPDPAI/II and PPDBA I/II. The formation of disulfide linkages is crucial as it contributes to the stability of the polymer in circulation and related to the polyplexes susceptibility in the intracellular redox environment for the easy release of the therapeutic gene. The free thiol group which is formed in the polymers are crucial as it plays an important role in the efflux pump inhibition in cancer cells.

The successful formation of PPDPA and PPDBA and its corresponding control groups were verified by ^{1}HNMR. As given in results of PPDPA (Figure 50) and PPDBA (Figure 71), the signals at δ 2.5- 2.6ppm corresponds to the characteristic peaks of PEI, i.e –(CH2-CH2-NH) which was clearly observed in both pullulan derivatives such as PPDPA and PPDBA, its corresponding control groups and the parent compound, pullulan-PEI. Similarly, the broad signals at the region from δ 3.4 -3.9 ppm was associated with –CH and –CH_2 backbone of pullulan and was observed in representative polymers of PPDPA/PPDBA and the parent compound, pullulan-PEI. This indicates the successful conjugation of PEI and dithiodipropinic acid or dithiodibutyric acid. The presence of disulfide linkages in the polymer was also confirmed by the presence of signals at δ 2.7-2.8ppm which denote the two ethylene groups neighboring a disulfide linkage. This signal was present in both PPDPA/PPDBA and its control group, PDPA/PDBA. Similarly, the peaks corresponding to the anomeric protons observed in the maltotriose units in pullulan and the presence of –OH groups in the polymer were identified.

The FTIR spectra also provide information about the conjugation and formation of PPDPA (Figure 51) and PPDBA (Figure 72). The prominent broad band near 3283 cm^{-1} in PPDPA and

3212 cm^{-1} in PPDBA represent the overlapping –OH and –NH stretching vibrations of pullulan and PEI. The sharp peak at 3268cm^{-1} and 3272 cm^{-1} correspond to PDPA and PDBA respectively indicate the –NH stretching vibrations of PEI. Similarly, the peaks near 1629 cm^{-1} and 1635 cm^{-1} in PPDPA polymers are representing the amide I bond due to C=O stretching. In PPDBA, the peaks at 1627cm^{-1} and 1624cm^{-1} in the control group respectively was assigned to the amide I bond due to C=O stretching and peaks at 1459cm^{-1} in both was due to the –NH bending of amide II bonding. Other additional peaks of PPDPA and PPDBA and its corresponding controls are detailed in the result section.

The non-viral gene delivery system should possess a certain mechanism to facilitate its escape from the endosome in order to avoid trafficking to the lysosome or recycle back to the cell membrane. Here, the buffering ability of the polymer was analyzed in the broad pH range of 10 to 4, mimicking the pH variations in endosome maturation. As shown in the result (Figure 52 and 73), PEI showed the highest buffering ability whereas the modified polymers such as PPDPA and PPDBA showed comparatively lower buffering capabilities. Though in comparison with native PEI, both PPDPA and PPDBA polymers showed lesser buffering capacity, it is adequate enough to allow an endosomal escape. Apart from primary amino groups, the secondary and tertiary amines of PEI which are not participating in the acylation or conjugation with pullulan, also contribute towards buffering capacity in both PPDPAs and PPDBAs. The presence of hydrophilic/hydrophobic moieties in.PPDPA/PPDBA also contributed to the enhanced buffering capacity. This is because the hydrophilic nature of pullulan makes the PEI extend more freely in the medium against the restriction offered by the hydrophobic moieties such as DPA and DBA in the polymers. However, there were slight variations in the buffering capabilities of different polymer groups in PPDPA and PPDBA. Among the polymers, PPDPA I showed the highest

buffering ability, followed by PPDPA III and then PPDPA II. The slight difference in the buffering capabilities between PPDPA II and III might be because of the conformational differences between the two polymers and the differences in the amount of disulfide content (Figure 52). Similarly, in the case of PPDBA (Figure 73), the PPDBA I possess high buffering capacity compared to PPDBA II and III. On the other hand, the control groups such as PDPA I/II/III and PDBA I/II/III were showing higher endosomolytic property than that of the corresponding pullulan based polymers. This is largely due to more amino density in the control groups compared with the pullulan based derivatives.

Both particle size and zeta potential determine the biodistribution and pharmacokinetic properties of the nanoparticles in circulation. Alteration in size and charge can have a profound effect on the behavior of nanoparticles in the biological environment. As seen in the result, Figure 53 and 74, it is interesting to note that the PPDPA I polyplex though attained a particle size of <200nm in all the polymer to DNA ratios ranging from 1:1 to 5:1, failed to attain a positive surface charge. On the other hand, PPDPA II/III polymers and PPDBA I/II/III polymer based polyplexes all attained positive surface charges except in the initial polyplex ratios (1:1). All the polyplexes have maintained a particle size of <200nm, which is ideal for gene delivery applications. The primary driving force for nano complex formation is electrostatic interactions, however, some weak forces derived from the physicochemical and structural properties of cationic polymers such as hydrogen bonding, dipole interaction and hydrophobic interaction may also contribute to DNA condensation and nanocomplex formation (Lin and Engbersen, 2009). As illustrated in results (Figure 53 and 74), PPDPA/ctDNA and PPDBA/ctDNA formed stable nanocomplexes with a polydispersity index of 0.1-0.3. The smaller PDI indicated that polyelectrolyte complexes which are formed are much-defined particles with uniform distribution. The initial negative charge at 1:1

polyplex ratio observed in PPDPA and PPDBA indicated that the amount of polymer was insufficient to completely condense DNA. However, as the polymer concentration increases, the condensation of DNA also improves significantly resulting in the formation of nanosized complexes with stable positive charge. However, in the case of PPDPA I, the positive zeta potential was obtained at above 5:1 ratio (Figure 53). It should be noted that the presence of large moieties on the particle surface change the plane of shear to a farther distance from the surface which may lead to reduction in the measured zeta potential values even if the particle surface charge is high (Quaglia et al., 2009). On the contrary, all the polyplexes of control groups such as PDPA I/II/III and PDBA I/II/III possess remarkably high zeta potential (>25mV) values compared to pullulan based counterparts. The high positive charge exhibited by the control groups are not advantageous as it can cause deleterious effects on blood cells such as RBC, WBC, platelets etc or can interact with proteins leading to other side effects. The size and zeta values of PPDPA and PPDBA are adequate for cellular internalization processes and also minimize cellular toxicity.

The strength of polyplex formation and or the polymer condensation ability was evidenced by agarose gel electrophoresis. As seen in the results (Figure 54 and 75), complete retardation of DNA was observed in the control groups such as PDPA I/II/III and PDBA I/II/III at all polyplexes ratios demonstrating the strong interaction between the polymer and DNA. However, the results were not identical with PPDPA I, II and III (Figure 54), the DNA was not retained in the well in case of PPDPA I polyplexes of ratios ranging from 1:1-5:1 and the initial two polyplexes ratios of PPDPA II and III. Similarly, in PPDBA I/II/III (Figure 75), complete retardation of DNA was observed only at the polymer to DNA ratio greater than 1:1. All the results are in accordance with the zeta potential values obtained in the previous study (Figure 53 and 74). This infers that more polymer concentration is necessary to form an adequate compaction with the DNA. The gel

retardation studies on the pullulan derivatives thus confirmed that both PPDPAs and PPDBAs form stable nanocomplexes. In this line, it is also important to mention about the role disulfide bond in DNA condensation. As reported earlier disulfide bond is longer than the ethylene C-C bond i.e. 0.203 vs 0.154 nm and which implies that disulfide containing polymeric chains have a higher degree of flexibility than carbon analogs without disulfide linkages. Hence the relatively free chain foldings and movements of disulfide-containing cationic polymers can also expect to contribute to the enhanced polymer/DNA interaction and condensation (Yan and Engbersen, 2009).

The stability of the polyplexes was also assessed by incubating with plasma. The plasma proteins are negatively charged, hence it was expected that the interaction might cause the removal of DNA from the polymer. However, as in Figure 54 and 75, the DNA was found to be confined in the well region. This observation implies the strong interaction of the polymer with the DNA indicating its stability in the extracellular medium.

Reversible disulfide cross-linking is an attractive strategy to bestow polymeric nanomedicines with high *in vivo* stability and rapid intracellular release of therapeutic cargo. The significant difference in glutathione concentration between the intracellular and extracellular compartments gives a rationale for the intracellular delivery of therapeutics using disulfide cross-linked compounds with tailored property to promptly dissociate under physiological conditions in the cytosol. Both PPDPA and PPDBA polyplexes have been investigated for its reduction sensitive property by exposing to the reductive agent, DTT. The results showed that both the selected polyplex ratios of the polymer PPDPA I/II/III (Figure 55) and PPDBA I/II/III (Figure 76) were responsive to reduction conditions and it formed large aggregates in presence of DTT over time. The size reached around 280nm in PPDBA polyplexes with a net increase of around 100nm from

the DTT-untreated counterpart. A similar result was observed in PPDPA polyplexes as well. However, the size variation of PPDPA and PPDBA polyplexes was not as bigger as that was observed in PPSS and PPMSS, where it formed particle size up to 450nm in 4h. Both PPSS and PPMSS are formed via selective oxidation of thiol group in the polymer chain and hence there is wider opportunity to form both intra as well as intermolecular disulfide linkages. On the other hand, in both PPDPA and PPDBA, the disulfide linkages remain within the polymer, hence there are no chances of disulfide formation between the chains. This, in turn, has reflected in the particle size variation of these polymers on exposing with the reducing agent. It is known that the higher degree of flexibility of the disulfide linkages imparts free chain movement and folding of disulfide-containing cationic polymers which in turn contribute to the polymer/DNA interactions. Hence, the reduction of disulfide linkages changed the binding capabilities of the polymer to DNA.

Again, It was observed in the previous finding of PPSS and PPMSS (Figure 10 & 33), that the property of reduction sensitivity alone was not able to release DNA from the polymer and hence the influence of anionic components in the cell are also crucial in the complete unpacking of the polyplexes. Similarly, the unpacking of PPDPA polyplexes was carried out with DTT/ heparin combined treatment (Figure 56). On the other hand, PPDBA polymers showed a partial release of DNA on exposing with DTT (Figure 77), Here, the interaction of the polymer with DNA might be much weaker than the corresponding PPDPA and which is contributed by the enhanced presence of acyl content in the PPDBA polymer which leads to loosened interaction of the polymer with DNA. This indicates that the disulfide containing pullulan based polymers i.e PPDPA and PPDBA are reduction sensitive and are capable of unpacking the carrier vector to release the therapeutic gene of interest to the cytoplasm of the target cell.

For nanoscale materials, the surface area to volume ratio is far greater than larger particles, which in turn implies that more proteins will bind on nanoparticle than a particle of larger size (Mazzafero et al., 2010). Protein binding is established as one of the important factors influencing the *in vivo* biodistributions of nanoparticles. Certain components of the plasma protein may enhance the uptake of coated materials by the cells of the reticuloendothelial system (RES). The longer a nanoparticle remains in circulation, greater the chances of it to enter the target cell (Yameen et al., 2014). Herein, the protein binding of PPDPAs/PPDBAs polymers was examined by performing native PAGE by incubating samples with serum proteins (Figure 57 & 78). It has been observed that all the pullulan based polymers showed more or less similar protein profile as in serum in PAGE. This result implies that the surface functionalities in both PPDPAs and PPDBAs prevented the eventual binding of serum proteins on to the surfaces. Most of the failures in the *in vivo* experiments of nanoparticles are basically due to the particle size enhancement and aggregation on exposure to the blood proteins and subsequent removal via the RES. It is clear that the presence of pullulan in the polymers provided protein/opsonization resistance properties by minimizing the interaction between the particle surface and serum proteins. The protein distribution profile in the corresponding control groups i.e. PDPAs and PDBAs also showed an improvement in preventing protein adsorption compared to PEI (Figure 57 and 78). Herein, the presence of propionate and butyrate chain that is conjugated to PEI might have exerted a steric hindrance and thereby minimized the protein adsorption. On the other hand, in PPDPA and PPDBA, pullulan provides a hydrophilic surface that sterically prevents access of proteins. This feature of pullulan based derivatives can enhance the blood half-life and circulation time, suggesting that it can further enhance the homing of therapeutics and are compatible to use for systemic circulation.

The cytotoxicity of the PPDPA I, II, III and PPDBA I, II, III nanoplexes was investigated using MTT assay. The MTT assay was performed in C6, HeLa, A549 and L929 cells. The cells were incubated with polyplexes for a period of 24h. Cationic polymers such as PEI are toxic to cells due to their strong interactions with plasma membrane or interaction with negatively charged cell components. However, the results showed that both PPDPAs (Figure 58) and PPDBAs (Figure 79) exhibit a significantly lower cytotoxicity in comparison with the corresponding control groups i.e PDPAs and PDBAs. The pullulan based derivatives showed >85% cell viability in all the cell lines tested, and which implies that the nanoplexes are non-toxic and safe to use in systemic circulation.

The cellular uptake of the selected polyplexes ratios of PPDPA I/II/III and PPDBA I/II/III and its corresponding control groups were analyzed in C6 cells. Herein, the DNA was tagged with YOYO-I. As shown in Figure 59, the selected nanoplexes ratios of PPDPA I (10:1 and 25:1) and similarly, PPDPA II (3:1 and 4:1) and PPDPA III (3:1 and 4:1) were all showing good cellular uptake and which are indicated by the appearance of green fluorescence in the cytoplasm as well as in the nucleus. Similarly, the selected polyplexes ratios of PPDBA I/II and III (3:1 and 4:1) also showed enhanced cellular internalization (Figure 80). In both cases, the intensity of green fluorescence was found to be more intense in the nuclei and more or less diffused in the cytoplasm. This indicates that the presence of YOYO tagged DNA is more specifically confined to the nuclear region than the cytoplasmic region. The cellular uptake process is also quantified by flow cytometry analysis. As given in the results (Figure 60 and 81), the percentage of cells showing polyplex uptake was high in PPDPA/PPDBA I and II nanoplex treated cells compared with PPDPA/PPDBA III, which could be related to the surface charge and nanoplex formation. On the other hand, the cellular uptake of nanoplexes using PDPA/PDBA I, II and III with YOYO tagged

DNA showed neither cellular nor nuclear uptake and the cells was visibly damaged due to the high cellular toxicity by the polymer.

It is known that the cationic carrier DNA complexes enter cells by means of endocytosis. The endocytosis pathway includes clathrin-mediated endocytosis, caveolae-mediated and macropinocytosis. The respective endocytosis inhibitor includes chlorpromazine, filipin, and amiloride. As seen in results (Figure 61 and 82), the individual pretreatment of the cells using these inhibitors, followed by nanoplex exposure have not affected the entry of nanoplexes into the cells. It was expected that the inhibitor might cause reduction or complete prevention of the entry of nanoplexes, but no significant influence was observed in the nanoplex entry which implies that each time the closure of one pathway made the nanoplexes to avail an alternate way to get inside and hence the entry of pullulan based nanoplexes are considered multi-channeled.

To further elucidate gene delivery efficacy of the polymer, the intracellular movement of the PPDPA/PPDBA polyplexes was determined by tagging both polymer and DNA with rhodamine and YOYO-1 dye respectively and monitored via confocal microscopy. The selected polyplexes ratio of both the polymers was chosen for the study i.e PPDPA/PPDBA 4:1. The polyplex transportation, unpacking, and distribution occurred in more or less similar manner in both the polymers. As seen in Figure 62 and 83, following 1h post transfection, there was a faint red fluorescence corresponding to the polyplexes found distributed throughout the cell membrane and green fluorescence corresponding to YOYO-1-DNA was seen in the nuclei overlapped with Hoechst. By 2h post-transfection, the intensity and number of fluorescent particles increased and most of the YOYO-I-DNA represented by green fluorescence was distributed in the nuclei than in the cytoplasmic compartment. This indicated the faster and efficient nanoplex unpacking and release of DNA into the cytoplasm and further transportation to the nuclei. But the appearance of

many yellow fluorescence dots located inside the cells at the 2nd hour inferred that the polyplexes unpacking was not complete. Interestingly, in the fourth hour, the intensity of green fluorescence was more prominent and was seen coincided with the Hoechst stained nuclei. This indicated polyplex unpacking and enhanced migration of YOYO-I-DNA to the nuclei. By 7hr post-transfection, the red fluorescence was noted in large patches on the cell surface in both polyplexes (PPDPA/PPDBA) indicate that the following unpacking, the polymer moves towards the cell membrane and possibly out of the cell. It was observed that following cellular transport, the nanoplexes undergo reduction responsive vector unpacking in the cytoplasm which leads to DNA release and further transportation to the nuclei. The polymer is subsequently removed from the cell.

The transfection studies of the selected polyplexes ratios of PPDPA I/II/III and PPDBA I/II/III was determined following complexation with the p53 plasmid in C6 cells. The p53 mediated cell death was qualitatively analyzed via live and dead assay using confocal microscopy, whereas the cell death was quantified by means of PI staining and annexin V staining using flow cytometry. As shown in the results, Figure 63 and 84, the dead cells appeared to be high in cells transfected with PPDPA I and PPDBA I nanoplexes compared to PPDPA II/PPDBA II and PPDPA III and PPDBA III. Similarly, the cell death quantified by means of PI staining also followed the same pattern where the order of cell death is PPDPA I>PPDPA II> PPDPA III and PPDBA I>PPDBA II>PPDBA III (Figure 64 and 85). The annexin staining data shown in Figure 65 and 86, indicates that there is a disparity in the percentage of cellular death as quantified by PI staining alone and Annexin V staining. This difference is prominent especially in case of PPDPA I/PPDBA I nanoplex treated cells, eg. 92% was noted in PPDPA I 25:1 by PI staining which was 65% in annexin staining. This is due to the fact that the polymers with a low degree of acylation and

disulfide content such as PPDPA I might contain excess polymer after condensation with the plasmid, which could possibly contribute to some extent of toxicity which in turn lead to cell death by necrosis. Hence, the high cell death recorded by PI staining might be contributed by both necrosis as well as apoptosis together. On the other hand, PPDPA II /PPDBA II which showed a difference of nearly <10% in both these techniques, indicating that mainly the cell death is based on p53 mediated apoptosis. In both cases, the transfection efficiency is higher in PPDPA II and PPDBAII compared to PPDPAII and PPDBAIII. Here, the combination of factors such as improved cellular uptake, optimal buffering capacity and finally dissociation of the polyplexes in the cytoplasm due to less compact complexes contributes to the transfection efficiency. However, the transfection efficiency of PPDPAII /PPDBAII is comparatively lower than in PPSS and PPMSS because of the lack of extensive disulfide linkages (both intra and inter disulfide bonds) in PPDPA and PPDBA. Hence in the former, extensive reduction in the disulfide linkages, together with optimal buffering and polyplex dissociation contributes to the enhanced transfection efficiency.

The expression of the p53 gene in the transfected cells was directly measured by means of p53 immunofluorescence using confocal microscopy. As in the results, Figure 66 and 87, both PPDPA and PPDBA polyplexes showed enhanced expression of p53 in the cytosol compared with the untreated control cells, where the intensity of green fluorescence was minimal. This indicates that transfection of p53 plasmid-mediated by PPDPA/PPDBA polymers lead to transgene expression of p53 in the cancer cell line. As compared to PPDBA I/II, the presence of p53 was found to be minimal in PPDBA III, which is in total agreement with annexin V results detailed above.

Further, efflux pump inhibition ability of the thiolated polymers i.e PPDPA I, II III and PPDBAI, II, III were evaluated using the selected nanoplexes ratios of the polymer. However, the control groups PDPA/PDBA I, II, and III were not selected for this study as they were toxic in nature. The anticancer drug doxorubicin (DOX) is a substrate of P-gp, hence the efflux and or accumulation of DOX in the cancer cell was taken as the index for P-gp activity. As seen in Figure 67-68 and 88, both C6 and A549, did not show any detectable level of DOX in the drug alone treated control group, indicating the overexpression of P-gp and the corresponding effluxing of DOX. On the contrary, the pretreatment with the PPDPA I, II, III (Figure 67-68) and /or PPDBA I, II III nanoplexes (Figure 88) enhanced the overall accumulation of DOX in A549 and C6 cells indicated by intense red fluorescence in confocal microscopy. The PPDPA/PPDBA I, II, and III nanoplexes pretreated cells also exhibited >80% of cells retaining DOX by flow cytometry analysis (Table 10 & Figure 89). This indicated that both PPDPA/PPDBA polymers have influenced the P-gp to inhibit its activity which in turn has reflected in the enhanced accumulation of DOX in the C6 and A549 cells. Among the PPDPA/PPDBA I, II, III polymers, the percentage of cells retaining DOX in the nanoplex pretreated group was in the order of PPDPA/PPDBA III>PPDPA/PPDBAII>PPDPA/PPDBA I in both C6 and A549 cells. A similar observation was seen in confocal images with the intensity of red fluorescence was of the same order as shown above. The enhanced DOX retention in C6 and A549 on the preexposure of the PPDPA/PPDBA nanoplexes is mainly due to the fact that the thiolated polymers can directly form disulfide linkages with the membrane P-gp protein and inhibit its efflux pump activity. It should also be noted that more the disulfide/thiol content of the polymer, greater will be its interaction with the membrane P-gp activity to inhibit. This has been evidenced by the enhanced accumulation of DOX observed in both PPDPAII/III and PPDBAII/III compared to PPDPA/PPDBA I. Additionally, it

should be noted that P-gp is an integral protein which is embedded in the phospholipid bilayer of the plasma membrane and hence any difference in the membrane composition can cause an adverse impact on the activity of P-gp. Since the P-gp protein is specifically concentrated in the lipid raft, the lipophilicity of the polymers especially PPDPA II/III and PPDBA II/III and its subsequent interaction with the plasma membrane can also cause a change in the membrane chemical composition and microenvironment and which in turn can also impair the activity of P-gp (Oriowski et al., 2006). Additionally, being a thiomer, the PPDPA/PPDBA polymers have an inherent ability to interact with the P-gp directly and hence inhibiting the efflux pump activity. Overall, all these resulted in the inhibition of membrane P-gp activity and which further enhanced the accumulation of the anticancer drug, DOX in C6 and A549. In the meantime, no differences between free DOX and the nanoplex treated group was detected in the HeLa cells(Figure 69 & 88), indicated that P-gp activity was totally lacking in the HeLa cells. The same finding was observed in the flow cytometry analysis where the percentage of cells retaining DOX was found to be the same in the nanoplexes pretreated and DOX alone treated cells (Table 10 and Figure 89).

The intracellular DOX accumulation at different time points was analyzed by measuring the DOX in the cell lysate and normalizing it to the total protein content of the cells. Due to the active effluxing of DOX by C6 and A549, the intracellular concentration was less when treated with free DOX (Figure 70 & 90) As shown in the results, the concentration of DOX increases with time in the nanoplexes (PPDPA I,II,III and PPDBA I,II,III) pretreated group. Of which the more pronounced effect was observed in the PPDPAII/III and PPDBAII/III nanoplexes treated group compared with PPDPAI/PPDBA I.

In the case of cells treated with nanoplexes of PPDPA III and PPDPAII, the cellular DOX level in A549 reached up to 0.239 µg/mg protein and 0.230µg/mg of protein respectively.

Similarly, the cells treated with PPDBAI,II and III nanoplexes showed the peak value 0.235, 0.258 and 0.241 µg of DOX /mg of protein respectively in A549 cells at the 4th hour. On the other hand, the cells treated with nanoplexes of PPDPA I/II/III showed the maximum level at the 2nd hour and which was 0.222, 0.210, 0.242 µg/mg of DOX. In C6 cells, PPDBA I nanoplexes pretreated group showed the maximum retention of DOX at the 4th hr i.e 0.228µg DOX /mg protein, whereas PPDBA II and III showed 0.244 and 0.235 µg DOX /mg protein respectively (Figure 90). Following the peak level, the concentration of DOX in both PPDPA/PPDBA nanoplex treated cells was found to decrease with time. However, there was a significant difference in the DOX retention between the control as well as polyplexes pretreated group ($P<0.001$) even at the 7th hour in both C6 and A549. However, the HeLa cells in both DOX alone and polyplexes pretreated conditions showed more or less the same concentration of DOX in the cells. Owing to the efflux of DOX by the P-gp in C6/A549, it was not surprising that the intracellular accumulation of DOX in C6/A549 was significantly lower than that in HeLa cells when incubated with DOX alone. However, the DOX retention in the nanoplexes pretreated group in C6/A549 was comparable to HeLa, indicating that the senstivity of C6 and A549 was increased in presence of the nanoplexes. However, it should be noted that the cellular level of DOX in C6/A549 was decreasing with time indicated that the influence of polymers on P-gp activity is reversible and transient. Among the thiolated polymers i.e PPSS, PPMSS, PPDPA and PPDBA, the nanoplexes of PPDBA II 4:1 was showing the highest level of DOX retention in both C6 and A549 cells and hence it was selected for further studies on efflux pump inhibition.

To further investigate how the reducing environment affects the intracellular accumulation of DOX in presence of PPDBA nanoplexes, the glutathione level was initially determined in presence and absence of nanoplexes in C6 cells. Additionally, the level of glutathione was

determined in presence of buthionine sulfoximine (BSO) and nanoplexes. The drug, buthionine sulfoximine is an inhibitor of glutathione transferase (GST) enzyme, and hence inhibit the synthesis of glutathione in the cell. As shown in Figure 91, a remarkable increase in the glutathione level was observed in the PPDBA nanoplexes treated cells compared to the normal cells. This is mainly due to the fact that glutathione selectively reduces the disulfide linkages in the PPDBA polymers resulting in the enhanced activity of glutathione in the cells on exposure with the nanoplexes. On the otherhand, the cells treated initially with BSO followed by nanoplexes exposure showed a low level of glutathione in C6 cells as was shown by less fluorescence intensity in confocal microscopy (Figure 91). Further, the intracellular retention of DOX was determined in the reducing environment in the presence of PPDBA polyplexes in C6 cells. Previous studies on DOX accumulation have shown that PPDBA 4:1 nanoplexes pretreatment caused significant accumulation of DOX in C6 cells. To further investigate the interaction between a reducing environment and accumulation of DOX, intracellular glutathione level was further increased by preincubating the C6 cells with glutathione monoester and determined its influence on DOX retention. Glutathione monoester once inside the cell undergo rapid cleavage of ester linkages to release free glutathione inside the cells. As shown in Figure 92 and 93, a remarkable enhancement in the cell fluorescence intensity of DOX was observed in the GSH monoester and PPDBA nanoplex pre-treated cells compared with the cells that did not receive GSH monoester preincubation. In addition, the buthionine sulfoximine (BSO) pre-exposure to the cells followed by PPDBA nanoplexes and DOX treatment showed a reduction in the fluorescence intensity of DOX. This is due to the fact that BSO inhibits the synthesis of glutathione which in turn resulted in the low accumulation of DOX in these cells. It is reported that the enhanced level of glutathione in cancer cells usually contributes to chemoresistance due to its elevated antioxidant activity

(Forman et al., 2009). However, the observation here (Figure 92 &93) showed that GSH has a role in the cellular retention of DOX and that the presence of GSH have caused the selective reduction of disulfide linkages in the PPDBA polymers to release free thiol groups in the polymer. This in turn has resulted in the inhibition of P-gp by establishing disulfide linkages with the membrane P-gp protein. The observation also implies that more the disulfide content in the polymer greater will be the selective reduction by GSH and hence better will be the cellular accumulation of DOX. In addition, the low accumulation of DOX in the BSO pretreated cells also emphasized the significance of glutathione in the cellular retention of DOX.

The efflux pump inhibition studies have shown an enhanced accumulation of anticancer drug DOX in the resistant cell lines when it was preexposed with the PPDBA II 4:1 nanoplexes. Hence it is important to determine the cytotoxic effect of the anticancer drugs in the nanoplexes pretreated cells to find out how the influence of nanoparticle exposure improves the sensitivity of cancer cells towards anticancer drugs. The cytotoxicity of DOX alone and PPDBA nanoplexes in combination with DOX were investigated in HeLa and A549 cells by MTT assay. As seen in results (Figure 94), the percentage inhibition caused by DOX alone and nanoplexes/DOX-treatment in the cancer cells was determined after incubation for 24, 48 and 72 hrs. It was observed that the percentage inhibition was found to be high in the nanoplexes pretreated cells compared to the DOX alone treated cells in A549. This observation suggest that PPDBA nanoplexes can circumvent the P-gp mediated effluxing of the drug by reversibly inhibiting its activity. The drug DOX accumulated in the cell can easily diffuse into the nucleus and intercalate DNA to exert its cytotoxic effect. Compared to 24hrs, the percentage inhibition was high in 48 and 72hrs which imply that the inhibition rate is concentration and incubation time-dependent in A549 cells. At the highest drug concentration of 10μM of DOX, the inhibition was 83% in nanoparticle exposed cells

against 64% in the control cells in 24hrs in A549. This has further increased to 92% in the nanoparticle exposed cells in 48hrs. Meanwhile, the drug-sensitive HeLa cells were equally sensitive to both DOX alone and PPDBA preexposed/DOX-treated cells, the inhibition percentage was observed as >85% in the 24hrs in HeLa. As in A549, the cell death was dose-dependent in HeLa cells. As in result (Figure 24), the percentage inhibition of PPDBA nanoplexes pretreated cells in A549 was similar to the drug sensitive HeLa cells. This provides evidence that the ability of PPDBA polymers to prevent drug efflux from drug-resistant cells leads to enhanced drug mediated inhibition.

The anticancer effect was further quantified by half maximal inhibitory concentration or IC50 (illustrated in Table 13). The IC50 was found to be 0.004,4.14 & 3.13μM for DOX alone treated cells of HeLa, A549 and C6 cells respectively. A significant decrease in the IC50 of DOX in the PPDBA nanoplex pre-treated cells was observed in drug-resistant cell lines such as C6 and A549 (i.e IC50 is 0.183 & 0.882) when compared with the free drug treatment, owing to the enhanced retention of DOX. The cytotoxicity of DOX was significantly improved in the resistant cell lines such as C6 and A549 treated with PPDBA nanoplexes/DOX. Further evidence of PPDBA nanoplexes on circumventing the drug efflux mediated resistance(MDR) is provided by comparing the ratio of IC50 of A549 and HeLa cells treated with DOX alone and PPDBA/DOX and the Resistance Factor (RF) was thereby calculated. As shown in Figure 95, the RF values of DOX alone was 1122, whereas it is 352 in the PPDBA nanoplexes/DOX treatment. It indicated that the PPDBA nanoplexes enhanced the sensitivity against the resistant cells and the MDR effect was partly overcome.

The overexpression of P-gp is the most important factor contributing to the phenomenon of multidrug resistance (MDR) in cancer.The expression of P-gp in C6, A549, and HeLa cells were

evaluated by means of immunostaining using P-gp specific antibody. As shown in Figure 96, the green fluorescence corresponding to the presence of P-gp was observed in both normal as well as DOX-treated control cells of A549 and C6 cells. It was observed that the expression of P-gp was high in the DOX-treated control cells of C6 and A549 compared to the normal cells, owing to the overexpression of P-gp by DOX. This observation is in fact in agreement with the previous reports which showed that doxorubicin influences the P-gp expression levels in cancer cells (Ye et al., 2008). P-gp overexpression is indicative of active effluxing of anticancer drug which results in an increased resistance of cancer cells to chemotherapeutic drugs. On the contrary, the expression of P-gp was lowered or minimized in the PPDBA II 4:1 nanoplexes pretreated cells of A549 and C6. This is in agreement with the previous finding on DOX retention in these cell lines i.e. C6 and A549, where a high concentration of DOX was observed in the PPDBA polyplex pretreated cells. On the other hand, the control cells showed a minimal level DOX retention in these cells due to the overexpression of P-gp in the membrane. However, no observable influence on membrane P-gp was seen in the HeLa cells where the presence of DOX has only sparingly enhanced the P-gp. Hence it is evident that the HeLa cells are sensitive and it showed enhanced retention of DOX in all efflux pump studies. From this observation, it is concluded that the PPDBA polymer minimizes the cellular P-gp activity by two possible mechanisms and thus contributing to the enhanced sensitivity of anticancer drugs.

(a) Firstly, this may be due to the fact that in the presence of redox environment, PPDBA polymer undergoes a reduction in the disulfide linkage and form a thiol group bearing polymer which may interact with the free thiol group of the cysteine residue of the membrane P-gp, changes its conformation and interferes the efflux processes.

(b) Secondly, the possible interaction of butyl chain in PPDBA with the cell membrane leading to change in membrane microenvironment and subsequent conformational change in the P-gp membrane protein.

The drug release study of PPDBA/ctDNA-DOX nanocomplex was performed at different pH 7.4 and 6.8 which corresponds to the systemic circulation and tumor microenvironment respectively. Initially, the drug DOX was intercalated with the DNA before forming the nanoplex with the PPDBA polymer. The drug loading efficacy was 85%, indicating a strong affinity between the drug DOX and DNA. The size and zeta potential of the drug loaded nanoplex, PPDBA II/ctDNA 4:1 was found to be 149nm and + 7.01 mV respectively, indicating that the presence of DOX in the PPDBA nanoplex has not remarkably changed the DNA affinity towards the polymer. The cumulative drug release profile of the PPDBA/ctDNA/DOX nanocomplexes is given in Figure 97. It was observed that the drug release was pH dependent and was found to be higher at low pH. The DOX release from the PPDBA II nanoplexes was around 60% at pH 6.8, whereas it was only around 52% at 7.4. The higher drug release observed as the pH lowered from 7.4 to 6.8, was probably caused by the enhanced protonation of the drug, DOX and the resultant destabilization and increased electrostatic repulsion between the polymer and the drug. It should be also noted that no burst release occurred at both pH indicating that drug DOX is loaded within in the carrier and the interaction is strong enough to hold strongly. At respective pH with respect to time and ionization the drug is slowly released from the carrier. The enhanced release of drug DOX at pH 6.8 is advantageous as it is corresponding to the pH in the tumor microenvironment and it was observed a sustained release of drug 48hrs. This will ensure a continuous release of the drug to the

tumor site over a period of time. A slight change in the pH does have an influence on the release profile of the polymer.

The synergistic effect of the drug DOX and gene, the p53 plasmid was evaluated in C6 cells. It was observed that the IC50 of DOX in C6 cell was 3μM and the percentage of cell death caused by the transfection of p53 gene mediated by PPDBA polymer was 59%. As shown in Figure 98, the cells treated with PPDBA/p53 nanoplex along with DOX enhanced the cell death in comparison with individual treatment. The C6 cells treated with fixed amount PPDBA/p53 nanoplexes and different DOX concentration resulted in 87% cell death at 0.5μM, 87% with 1μM 99% with 1.5 μM respectively. This is because transfecting cancer cells with wild-type p53 result in the reactivation of apoptotic pathways as well as improvement of the cytotoxic effect of DNA damaging anticancer agents such as DOX. Therefore, the addition of gene and DOX can synergistically increase the sensitivity of cancer cells to result in a greater therapeutic outcome. The importance of this finding is that the dose of chemotherapeutic drugs which causes undesirable side effects can be brought down without compromising the needed high cell death. Hence it is effective for tumor treatment.

It should be noted that the nanoparticles have the ability to penetrate different physiological barriers and accumulate in organs to cause potential toxicity. Hence it is essential to determine the *in vivo* behavior of PPDBA nanoparticles before using it for therapeutic applications. Though the PPDBA nanoplexes was proved nontoxic in the *in vitro* conditions, it is essential to evaluate the behavior of the nanoparticles in the *in vivo* situations. *In vivo* biodistribution of the nanoplexes was evaluated in BALB/c mice. As seen in Figure 99, the fluorescence signals corresponding to PPDBA nanoplexes were completely absent in the vital organs such as brain, heart, lungs and spleen in 3rd hr, 6hr, 24hr and 48hrs. The quantitative data given in Figure 100, also showed that

the nanoplexes in circulation was not accumulating in any vital organs and was not interfering the physiological functions of these organs. The mice also appeared healthy even after 48hrs of injecting with the polymers, indicating that there was no deleterious interaction between the nanoplexes and blood components. The cationic polymers are expected to have an interaction with the blood components and blood proteins to have hematological and immunological problems. Also, the spleen was totally absent from any signals corresponding to the polymer, which infers that there was no sequestration of nanoplexes occurred. Absence in the lungs indicates that there was no aggregation of nanoparticles in blood which otherwise lead to retention and embolism in the lung capillaries. This observation showed that though the polymer is cationic in nature, the presence of pullulan in the PPDBA polymer reduced protein adsorption and complement activation via hydrophilicity and steric repulsion effects. This in turn has extended the blood half-life of the PPDBA nanoparticles. As in Figure 99 and 100, the PPDBA nanoplexes were appeared both in liver and kidney in the 3rd hour and 6th hour. Pullulan is reported to have liver targeting property and as shown in the results, polyplexes appeared more in the liver. However, in the 24hrs, the level minimized in the liver whereas the excretion via the kidney has simultaneously increased, indicating the nanoplexes removal from the body. The accumulation of the nanoplexes in the liver also indicates its normal pathway of excretion from the body. At 48th hour, though the level of nanoplexes were lowered in the liver and kidney, its presence was still seen. This shows that the nanoparticles have an extended blood half-life and the nanoparticle carriers remain in the blood stream long enough to reach or recognize the therapeutic site of action. The nanoplexes are simultaneously eliminated from the body via the kidney.

The combined gene/ drug delivery hold great promise for the treatment of cancer as it suppress or reverse tumor growth and disease progression. However, this strategy requires the development of

safe and stable delivery system that can be delivered systemically to the tumor cells. Here, the PPDBA polymeric nanoparticles were demonstrated as non-toxic and superior gene/drug delivery vector. Anti-tumor effect of the dual delivery of gene and anticancer drug was evaluated in tumor bearing mice. The effect of combination delivery system on tumor size reduction was studied in the mice tumor model, where the injection was given directly to the tumor region in every alternate day for 35 days. The results are given in Figure 101. Treatment of tumors by direct injection is a clinically relevant technique (Pisters et al., 2004). As shown in the results, although DOX injection decreases the tumor volume in the first 5days, the size of the tumor was found increasing thereafter. This is due to the fact that the tumor cells become resistant to the anticancer drug DOX resulting in the continuous growth of tumor even after repeated injection of DOX to the tumor site. However, it is interesting to note that treatment with PPDBA/p53 nanoplexes were more effective in sustaining tumor growth inhibition compared to untreated and DOX treated controls. Furthermore, the percentage reduction of tumor was more pronounced in the combined delivery of drug/gene using PPDBA polymer. The injection with PPDBA/p53/DOX nanocomplex has reduced the tumor volume by almost 20% from the initial tumor size (Figure 101). The injection was given at different tumor location such as at top side and the base of the tumor to result in more uniform availability of nanoplexes throughout the tissue. It should be noted that the uniform distribution of nanoparticles in the tumor site is critical for better efficacy. Although multiple genes are involved in the carcinogenesis, the majority of cancers demonstrate mutation in p53 gene or other defects in the p53 pathway. In this study, it was observed that the gene therapy approach using PPDBA polymer successfully replaced the wild type p53 function as was evidenced by the inhibition in the progression of tumor growth in mice. It should be noted that the mutation in p53 not only contribute to the tumor progression, but also increases the expression of MDR1, which in turn resulted in

chemoresistance. The restoration of p53 in the tumor cells have enhanced the sensitivity of these cells to chemotherapeutics resulting in the enhanced reduction in the tumor growth progression.

: Chapter 6 Summary and Conclusion

Chemotherapy is one of the potential treatment approaches along with surgery and radiation therapy to treat cancers. However, the side effects such as systemic toxicity contributed by non-specific drug accumulation, bone marrow suppression, and low bioavailability have often limited its application. In addition, addressing the problem of multidrug resistance is quite limited. Due to multidrug resistance (MDR) most cancer cells develop resistance to a variety of structurally unrelated chemotherapeutic agents resulting in minimal cell death and expansion of drug-resistant tumors. Tumor cells are characterized by genetic heterogeneity and hence the treatment using a single therapeutic agent often results in a poor clinical outcome. Over the past two decades, gene therapy has gained great attention as an alternative strategy for the treatment of cancer. Recently, combination therapies using anticancer drugs and the therapeutic gene have been identified as a promising strategy to enhance therapeutic efficacy and decrease drug resistance. This has been carried out by either concurrently targeting multiple components in a single pathway or across multiple interrelated pathways. In this line, this study mainly focused on the synthesis of disulfide cross-linked pullulan based cationic polymers to simultaneously carry out gene delivery and efflux pump inhibition to overcome multidrug resistance and enhance the sensitivity of cancer cells for chemotherapeutics.

The disulfide cross-linked cationic pullulan has been synthesized by incorporating the thiol-containing group to the polymer pullulan-PEI, where PEI is a polyamine polymer which imparts

cationicity to pullulan which in turn impart gene transfer efficacy. Here, pullulan is the base material, which is a water-soluble, non-toxic, non-immunogenic and non-carcinogenic polysaccharide which has been widely used for pharmaceutical and chemical manipulation due to its attractive biological and physicochemical features. Pullulan has shown prolonged circulation time due to its electric neutrality and also exhibit liver targeting capability due to its high affinity for asialoglycoprotein receptor (ASGPR) in the liver. It was reported previously that the conjugation of pullulan to PEI have effectively minimized the cytotoxicity associated with the charge density of PEI and also displayed good transfection efficacy. Here, the incorporation of thiol/disulfide group to the pullulan-PEI backbone is intended to bestow dual functions i.e. gene delivery and efflux pump inhibition.

Two categories of polymers were synthesized based on the incorporation of the thiol group to the pullulan-PEI backbone.

Category I: Here, the thiol-bearing group was conjugated to pullulan-PEI and the subsequent oxidation step to form disulfide cross-linked polymer. The polymers formed in category I is pullulan-PEI-cysteine (PPSS I and PPSSII) and pullulan-PEI-mercaptosuccinic acid (PPMSS).

Category II; The second category involves direct incorporation of in-built disulfide containing moieties on to the pullulan-PEI. The category II polymers are pullulan-PEI-3,3 dithiodipropionic acid (PPDPAI, PPDPAII, PPDPAIII) and pullulan-PEI-4,4 dithiodibutyric acid (PPDBA I, PPDBAII, PPDBAIII).

The control groups were composed of PEI and thiol/disulfide group alone ie. PEI-cysteine (PEICYS(S-S I/II)), PEI-mercaptosuccinic acid (PEI-MSA), PEI-3,3 dithiodipropionic acid (PDPAI, II, III) and PEI-4,4 dithiodibutyric acid (PDBAI, II, III).

The physicochemical characterization of the polymers PPSS and PPMSS (category I polymers) were carried out by using ^{1}HNMR and FTIR and confirmed the conjugation of pullulan, PEI and cysteine or mercaptosuccinic acid respectively. The amino content of the polymers (PPSS and PPMSS) which is related to the net positive charge and gene delivery efficacy was determined by $CuSO_4$ assay. The thiol/disulfide content of the polymers was also verified by using Ellman's and/or NTSB assay. Both physicochemical and biological properties of the nanoparticles are highly dependent on the polymer to DNA ratio and hence a range of ratios (1:1-5:1) was screened to identify the optimal ratio at which DNA is condensed into small positively charged particles. The selected nanoplexes of PPSSI (2:1 & 4:1) and PPSSII (3:1 & 4:1) were showing a particle size of <200nm and a positive zeta potential value, <20mV which in fact is adequate for gene delivery applications. The gel retardation assay proved the strong interaction of the polymers to DNA and confirmed the stability of the nanoplexes in circulation. Both PPSS and PPMSS displayed high buffering ability comparable to PEI, which infers the endosomolytic property of the polymer. The plasma protein interactions of the pullulan based polymers i.e PPSS and PPMSS showed the presence of all plasma protein bands on PAGE analysis. This indicated minimal protein adsorption on to the polymer surface which inturn infers its better compatibility as well as probable higher blood circulation time and bioavailability of the nanoplexes. The cytotoxicity assay of the PPSS and PPMSS nanoplexes in different cancer cells (C6/A549/HeLa) and normal fibroblast cells (L929) showed >85% cell viability which establishes that the polymer is non cytotoxic and safe to use. On the contrary, the control group showed a viability of <50% in these cell lines due to the cytotoxic effect of PEI. The cellular uptake studies showed the presence of tagged nucleic acid in the cytoplasm as well as nuclei. The endocytosis inhibitor studies indicated that the nanoplexes take multiple pathways to get internalized into the cell. The polymer trafficking kinetics of PPSS

and PPMSS indicated the successful unpacking of nanoplexes, delivery of DNA and subsequent exocytosis of the polymer. The transfection efficiency of the polymer was confirmed by both qualitative and quantitative methods.. The p53 protein expression in transfected cells was established by immunocytochemistry analysis. Annexin V staining proved that the cell death is mainly mediated by the apoptosis followed by the transfection using nanoplexes.

The efflux pump inhibition study was performed in C6, A549, and HeLa where the selection of cell lines was initially carried out using the known P-gp inhibitor, verapamil. The anticancer drug DOX was used as an index for P-gp activity. The efflux pump inhibition study showed that the nanoplexes of PPSS and PPMSS were effective in retaining DOX in the cancer cells which otherwise was rapidly removed from the cells via enhanced P-gp activity. The DOX retention was confirmed both qualitatively (confocal analysis) and quantitatively (flow cytometry) in both P-gp positive cell lines i.e C6 and A549 and P-gp negative cells i.e HeLa.

In Category II polymers: The conjugation of 3,3 dithiodipropionic acid and 4,4 dithiodibutyric acid to pullulan-PEI was confirmed via ^{1}HNMR and FTIR. The amino and thiol content of the polymers PPDPA and PPDBA were quantified by using $CuSO_4$ and Ellman's assay respectively. The size and zeta potential values of nanoplexes at different polymer to DNA ratios of both PPDPA/PPDBA polymers were <200nm and within +15mV respectively. The polymers showed good buffering ability pH range of 7-5 and displayed good DNA complexation ability as seen from gel retardation studies. The stability studies indicated that the nanoplexes of PPDPA/PPDBA are responsive to the intracellular reductive environment and the subsequent release of DNA is dependent on the combined influence of intracellular reducing agent and anionic conditions inside the cell. The PAGE analysis showed that the pullulan derivatives minimized protein adsorption on to their surfaces. The MTT assay of the selected nanoplexes ratios of PPDPA

I, II, III, and PPDBA I, II, III showed >85% of cell viability in all the cell lines tested against <50% viability exhibited by the control group nanoplex treated cells. The nanoplexes of PPDPAI, II, III, and PPDBA I, II, III showed enhanced cellular uptake at all the ratios and endocytosis inhibitor study indicated that the nanoplexes are taking a multiple entry pathway for cellular internalization. The polymer trafficking studies indicated the nanoplexes unpacks and the DNA gets localized into the nucleus. The polymer remains in cytoplasm and subsequently exocytosed. The nanoplexes of PPDPA I, II, III, and PPDBA I, II, III showed high transfection efficiency as indicated by cell death mediated by the p53 plasmid. The transfection efficacy was highest in the PPDPAI and PPDBA I compared to PPDBA II/III and PPDPA II/III. This could be related to the cellular uptake, endosomal escape, and unpacking of polyplexes. The efflux pump inhibition efficacy of the selected nanoplexes ratios of the polymer PPDPA I, II, III, and PPDBA I, II, III was evaluated in P-gp positive cell lines C6, A549, and P-gp negative HeLa cells. There was a significant enhancement in the retention of DOX in the polyplexes pretreated group of resistant cell lines compared to the DOX alone treated counterpart.

Among all the four polymers, though PPSS I nanoplexes showed the highest transfection efficacy, the efflux pump inhibition property was found to be highest with the PPDBA II at 4:1 ratio and hence this has been chosen for further studies. Furthermore, the percentage inhibition caused by the drug DOX was found be high in the PPDBA nanoplexes pretreated group of C6 and A549 compared to the drug alone treated control group. There was a corresponding decrease in the IC50 value of the C6 and A549 cell lines following treatment with nanoplexes. The release studies of the PPDBA/ctDNA/DOX nano complex showed a higher release at pH 6.8 than at physiological pH, which is advantageous as the tumor pH is also the same. The glutathione level in cancer usually contributes to chemoresistance due to the enhanced detoxification of anticancer drugs. But here

the enhanced glutathione level in the drug-resistant cancer cells contributes to the increased retention of DOX in the presence of PPDBA nanoplexes. Moreover, the influence of thiolated nanoplexes on the expression of P-gp was confirmed by P-gp immunofluorescence. Above all, the synergistic effect of both gene, p53 and the drug DOX enhanced the sensitivity of cancer cells towards chemotherapeutics which results in a greater therapeutic outcome.

The *in vivo* biodistributions of the PPDBA nanoplexes in BALB/c mice showed that the nanoplexes were eliminated from the body via kidney over time and was not found accumulating in the vital organs like brain, lungs, heart, and spleen. This indicated that the nanoplexes are well suitable for therapeutic applications. The antitumor activity of the nanoplexes in the tumor-induced mice showed that the co-delivery of drug and gene contributed to the remarkable reduction in the tumor volume which is related to the increased chemosensitivity mediated by the p53 activity.

As a conclusion, the multifunctional thiolated pullulan based polymer act as a simultaneous gene delivery vector and efflux pump inhibitor which could synergistically enhance the chemotherapeutic effect of anticancer drug DOX and overcome drug resistance. The combination of p53/DOX delivery along with P-gp inhibition by the PPDBA polymer reduced the dose of an anticancer drug used for cell death. This low dosage would be advantageous in reducing the side effects associated with chemotherapeutics. It is thus an effective treatment strategy for combating cancer. As a future work, the mechanism of P-gp inhibition by the thiolated polymer needs to be elucidated further.

References

Abbasi M, Lavasanifar A, Uludag H (2013) Recent attempts at RNAi-mediated P-glycoprotein downregulation for reversal of multidrug resistance in cancer. *Med Res Rev* 33(1): 33-53.

Abdallah, HM, Al-Abd, AM, El-Dine RS, El-Halawany AM (2015) P-glycoprotein inhibitors of natural origin as potential tumor chemo-sensitizers: A review. *J Adv Res* 6: 45–62.

Abouelmagd SA, Hyun H, Yeo Y (2014) Extracellularly activaTable nanocarriers for drug delivery to tumors. *Expert Opin Drug Deliv* 11: 1601–1618.

Adjei IM, Sharma B, Labhasetwar V (2014) Nanoparticles: cellular uptake and cytotoxicity. *Adv Exp Med Biol* 811:73-91.

Akinc A, Thomas M, Klibanov AM, Langer R (2005) Exploring polyethylenimine-mediated DNA transfection and the proton sponge hypothesis. *J Gene Med* 7: 657–663.

Alakhova DY, Kabanov AV (2014) Pluronics and MDR Reversal: An Update. *Mol Pharm* 11: 2566–2578.

Alfarouk KO, Stock CM, Taylor S, Walsh M, Muddathir AK (2015) Resistance to cancer chemotherapy: failure in drug response from ADME to P-gp. *Cancer Cell Int* 15: 71-82.

Allmeroth M, Moderegger D , Gündel D , Buchholz HG, Mohr N, Koynov K, Rösch F, Thews O, Zentel R (2013) PEGylation of HPMA-based block copolymers enhances tumor accumulation in vivo: a quantitative study using radiolabeling and positron emission tomography. *J Control Release* 172:77-85.

Al-Shawi MK, Omote H (2005) The Remarkable Transport Mechanism of P-glycoprotein; a Multidrug Transporter. *J Bioenerg Biomembr* 37: 489–496.

Backos DS , Franklin CC, Reigan P (2012) The role of glutathione in brain tumor drug resistance. *Biochem Pharmacol* 83: 1005-1012.

Baguley BC (2010) Multiple drug resistance mechanisms in cancer. *Mol. Biotechnol* 46 (3): 308–316.

Ballestar E, Esteller M (2008) Epigenetic gene regulation in cancer. *Adv Genet* 61:247-267.

Bao X, Wang W, Wang C, Wang Y, .Zhou J (2014) chitosan- graft-PEI-candesartan conjugate for targeted co-delivery of drug and gene in anti angiogenesis cancer therapy. *Biomaterials* 35: 8450-5466.

Batrakova EV, Li S, Brynskikh AM, Sharma AK, Li Y, et al. (2010) Effects of Pluronic and Doxorubicin on Drug Uptake, Cellular Metabolism, Apoptosis and Tumor Inhibition in Animal Models of MDR Cancers. *J Control Release* 143(3): 290–301.

Binkhathlan Z, Lavasanifar A. P-glycoprotein inhibition as a therapeutic approach for overcoming multidrug resistance in cancer: current status and future perspectives. *Curr Cancer Drug Targets* 13:326-346.

Bonengel S, Bernkop-Schnürch A (2014) Thiomers--from bench to market.*J Control Release* 195:120-129.

Bonner DK, Zhao X, Buss H, Langer R, Hammond PT (2013) Crosslinked linear polyethylenimine enhances delivery of DNA to the cytoplasm. *J Control Release* 167(1):101-107.

Bouard D, Alazard-Dany N, Cosset FL (2009). Viral vectors: from virology to transgene expression. *Br J Pharmacol* 157(2): 153–165.

Breier A, Gibalova L, Seres M, Barancik M, Sulova Z (2013) New insight into p-glycoprotein as a drug target. Anticancer Agents. *Med Chem*13:159-170.

Bremner KH, Seymour LW, Logan A, Read ML (2004) Factors influencing the ability of nuclear localization sequence peptides to enhance nonviral gene delivery. *Bioconjug Chem* 15:152–161.

Breunig M, Lungwitz W, Liebl R, Goepferich A (2012) Breaking up the correlation between efficacy and toxicity for nonviral gene delivery. *Proc. Natl. Acad. Sci. U.S.A* 104: 14454–14459.

Brumbach JH , Lin C, Yockman J, Kim WJ, Blevins KA, et al (2010) Mixtures of poly(triethylenetetramine/cystaminebisacrylamide)andpoly(triethylenetetramine/cystamine bisacrylamide)-g-poly(ethylene glycol) for improved gene delivery. *Bioconjug chem* 21(10): 1753-1761.

Carlisle RC, Etrych T, Briggs SS, Preece JA, Ulbrich K, Seymour LW (2004) Polymer-coated polyethylenimine/DNA complexes designed for triggered activation by intracellular reduction. *J Gene Med* 6(3):337-344.

Chico I, Kang MH, and Bergan R (2001) Phase I study of infusional paclitaxel in combination with the P- glycoprotein antagonist PSC833. *J Clin Oncol* 19:832-842.

Choi S , Lee KD (2008) Enhanced gene delivery using disulfide-crosslinked low molecular weight polyethylenimine with listeriolysin o-polyethylenimine disulfide conjugate. *J Control Release* 131(1):70-76.

Collins M, Thrasher A (2015) Gene therapy: progress and predictions. *Proc Biol Sci* 282: 1821-1832.

Cuvier C, Roblot-Treupel L, Millot JM, Lizard G, Chevillard S, et al.(1992) Doxorubicin-loaded nanospheres bypass tumor cell multidrug resistance. *Biochem. Pharmacol* 44 (3): 509–517.

Deng HX, Wang Y, Ding QR, Li DL, Wei YQ (2017) Gene therapy research in Asia. *Gene Ther* 24:572-577.

Dunnhaupt S, Barthelmes J, Rahmat D, Leithner K, Thurner CC, Friedl H, Bernkop-Schnurch A (2012) S-Protected Thiolated Chitosan for Oral Delivery of Hydrophilic

Macromolecules: Evaluation of Permeation Enhancing and Efflux Pump Inhibitory Properties. *Mol. pharmaceutics* 9:1331−1341.
Elbayoumi TA, Torchilin VP (2007) Enhanced Cytotoxicity of Monoclonal Anticancer Antibody 2C5-Modified Doxorubicin-Loaded PEGylated Liposomes against Various Tumor Cell Lines. *Eur J Pharm Sci 32(3): 159–168.*

Fan H, Hu QD, Xu FD, Liang WQ, Tang GP, Yang WP (2012) *In vivo* treatment of tumors using host-guest conjugated nanoparticles functionalized with doxorubicin and the therapeutic gene pTRAIL. *Biomaterials* 33: 1428-1436.
Filomeni G, Rotilio G, Ciriolo MR (2002) Cell signalling and the glutathione redox system.*Biochem. Pharmacol* 64: 1057–1064.
Föger F, Malaivijitnond S, Wannaprasert T, Huck C, Bernkop-Schnürch A, Werle M (2008) Effect of a thiolated polymer on oral paclitaxel absorption and tumor growth in rats. *J drug target* 16:149-155.
Foger F, Hoyer H, Kafedjiiski K, Thaurer A, Bernkop-Schnurch A (2006) *In vivo* comparison of various polymeric and low molecular mass inhibitors of intestinal P-glycoprotein. *Biomaterials* 27: 5855-5860.

Forman HJ, Zhang H, Rinna A (2009) Glutathione: Overview of its protective roles, measurement, and biosynthesis. *Mol Aspects Med* 30: 1–12.

Ganjavi H, Gee M, Narendran A, Parkinson N, Krishnamoorthy N, Freedman MH, Malkin D (2006) Adenovirus-mediated p53 gene therapy in osteosarcoma cell lines: sensitization to cisplatin and doxorubicin. *Cancer Gene Ther* 13: 415–419.
Ganoth A, Merimi KC, Peer D (2015) Overcoming multidrug resistance with nanomedicines. *Expert Opin Drug Deliv* 12:223-238.
Gillet JP, Gottesman MM (2010) Mechanisms of multidrug resistance in cancer. *Methods Mol Biol* 596:47-76.

Glasgow MD, Chougule MB (2015) Recent Developments in Active Tumor Targeted multifunctional Nanoparticles for Combination Chemotherapy in Cancer Treatment and Imaging. *J Biomed Nanotechnol* 11:1859-1898.

Gosselin MA, Guo W, Lee RJ (2002) Efficient gene transfer using reversibly cross-linked low molecular weight polyethylenimine. *Bioconjug Chem* 12(6):989-994.

Gottesman MM, Fojo T, Bates SE (2002) Multidrug resistance in cancer: Role of ATP dependent transporters. *Nat Rev Cancer* 2(1):48-58.

Grade M, Difilippantonio MJ, Camps J (2015) Patterns of Chromosomal Aberrations in Solid Tumors. *Recent Results Cancer Res* 200: 115-142.

Guans X (2015) Cancer metastases: challenges and opportunities. *Acta Pharm Sin B* 5: 402-418.

Guo G, Cui Y (2015) New perspective on targeting the tumor suppressor p53 pathway in the tumor microenvironment to enhance the efficacy of immunotherapy. *J Immunother Cancer* 3: 9-15.
Guo X, Huang L (2012) Recent Advances in Nonviral Vectors for Gene Delivery. *Acc. Chem. Res* 45: 971−979.

Gyarmati B, Némethy A, Szilágyi A (2013) Reversible disulphide formation in polymer networks: A versatile functional group from synthesis to applications. *Eur polym J* 49: 1268-1286.
Haberland A, Böttger M (2005) Nuclear proteins as gene-transfer vectors. *Biotechnol Appl Biochem* 42:97-106.

Han L, Huang RQ, Li JF, Liu S, Huang S, Jiang C (2011) Plasmid pORF-hTRAIL and doxorubicin co-delivery targeting to tumor using peptide- conjugated polyamido amine dendrimer. *Biomaterials* 32 (4):1242–1252.

Han X, Fang Q, Yao F, Wang X, Wang J (2009) The heterogeneous nature of polyethylenimine-DNA complex formation affects transient gene expression. *Cytotechnology* 60(1-3): 63–75.

Hanahan D, Weinberg RA (2011) Hallmarks of cancer: the next generation. *Cell* 144:646-674.
Hardee CL, Arévalo-Soliz LM, Hornstein BD, Zechiedrich L (2017) Review Advances in Non-Viral DNA Vectors for Gene Therapy. *Genes* 8: 1-22.
Hickman MA, Malone RW, Lehmann-Bruinsma K, Sih TR, Knoell D, Szoka FC, Walzem R, Carlson DM, Powell JS (1994) Gene expression following direct injection of DNA into liver. *Hum Gene Ther* 5: 1477-1483.
Hientz K, Mohr A, Guha DB, Efferth T (2017) The role of p53 in cancer drug resistance and targeted chemotherapy. *Oncotarget* 8: 8921–8946.

Hientz K, Mohr A, Bhakta-Guha D, Efferth T (2017). The role of p53 in cancer drug resistance and targeted chemotherapy. *Oncotarget* 8(5): 8921–8946.

Hoon JJ, Christensen LV, Yockman JW, Zhong Z, Engbersen GF, et al. (2007) Reducible poly(amido ethylenimine) directed to enhance RNA interference. *Biomaterials* 28(10) : 1912-1917.

Hwang DW, Son S, Jang J, Youn H, Lee S, et al. (2011) A brain-targeted rabies virus glycoprotein-disulfide linked PEI nanocarrier for delivery of neurogenic microRNA. *Biomaterials* 32(21):4968-4975.

Ilinskaya AN, Dobrovolskaia MA (2016) Interaction between Nanoparticles and Plasma Proteins: Effects on Nanoparticle Biodistribution and Toxicity. In: Vauthier C., Ponchel G. (eds) *Polymer Nanoparticles for Nanomedicines*. Springer, Cham, pp-524-545.

Immordino ML, Dosio F, Cattel L (2006) Stealth liposomes: review of the basic science, rationale and clinical applications, existing and potential. *Int. J. Nanomedicine* 1(3): 297-315.

Iqbal J , Shahnaz G, Perera G, Hintzen F, Sarti F, Bernkop-Schnürch A (2012) Thiolated chitosan: development and *in vivo* evaluation of an oral delivery system for leuprolide. *Eur J Pharm Biopharm* 80(1):95-102.
Jaramillo AC, Al Saig F, Cloos J, Jansen G, Peters GJ (2018) How to overcome ATP-binding cassette drug efflux transporter-mediated drug resistance?. *Cancer Drug Resist* 1:6-29.
Jensen KS, Hansen RE, Winther JR (2009) Kinetic and Thermodynamic Aspects of Cellular Thiol-Disulfide Redox Regulation. *Antioxid. Redox Signaling* 11: 1047–1058.

Jha S, Sharma PK, Malviya R (2016) Hyperthermia: Role and Risk Factor for Cancer Treatment. *Achiev. Life Sci* 10: 161-167.
Jhaveri AM Torchilin VP (2014) Multifunctional polymeric micelles for delivery of drugs andsiRNA. *Front.Pharmacol* 5:77-89.
Kakizawa Y, Kataoka K(2015) ,Block copolymer micelles for delivery of gene and related compounds. *Adv.Drug Deliv.Rev* 54:203-222.
Khalil I, Kogure K, Akita H, Harashima H (2006) Uptake pathways and subsequent intracellular trafficking in nonviral gene delivery. *Pharmacol Rev* 58:32–45.
Kim T, Kim SW (2011) Bioreducible polymers for gene delivery. *React Funct Polym* 17: 344–349.
Klein PM, Müller K, Gutmann C, Kos P, Krhac Levacic A, et al. (2015) Twin disulfides as opportunity for improving stability and transfection efficiency of oligoaminoethane polyplexes. *J Control Release* 205:109-119.
Klein PM, Wagner E (2014) Bioreducible polycations as shuttles for therapeutic nucleic acid and protein transfection. *Antioxid Redox Signal* 21(5):804-817.
Ko NR, Cheong J, Noronha A, Wilds CJ, Oh JK (2015) Reductively-sheddable cationic nanocarriers for dual chemotherapy and genetherapy with enhanced release. *Colloids Surf.B: Biointerfaces* 126 : 178–187.
Kotterman MA, Chalberg TW, Schaffer DV (2015) Viral Vectors for Gene Therapy: Translational and Clinical Outlook. *Annu. Rev. Biomed. Eng* 17: 63-89.
Krakhmal NV, Zavyalova MV, Denisov EV, Vtorushin SV, Perelmuter VM (2015) Cancer Invasion: Patterns and Mechanisms. *Acta Naturae 7*: 17–28.
Krishna R, Mayer LD (2000) Multidrug resistance (MDR) in cancer. Mechanisms, reversal using modulators of MDR and the role of MDR modulators in influencing the pharmacokinetics of anticancer drugs. *Eur J Pharm Sci* 11:265-283.
Laffleur F, Bernkop-Schnürch A (2012). Thiomers: promising platform for macromolecular drug delivery. *Future Med Chem* 4: 2205-2216.

Lee TK, Han JS, Fan ST (2011) Gene delivery using a receptor-mediated gene transfer system targeted to hepatocellular carcinoma cells. *Int. J. Cancer* 93:393–400.

Lee Y, Mo H, Koo H, Park JY, Cho MY, et al. (2007) Visualization of the degradation of a disulfide polymer, linear poly(ethylenimine sulfide), for gene delivery. *Bioconjug Chem* 18(1):13-8.

Li Y,Xu B,Bai T,Liu W (2015)Co-delivery of doxorubicin and tumor-suppressing p53 gene using a POSS-based star-shaped polymer for cancer therapy. *Biomaterials* 55: 12–23.

Lin C, Engbersen JFJ (2009) The role of the disulfide group in disulfide-based polymeric gene carriers. *Expert Opin. Drug Deliv 6(4):421-439.*

Lin C, Lou B (2012) Bioreducible Cationic Polymers for Gene Transfection. [Intech]:China.Available:http://www.intechopen.com/books/biomedicine/bioreducible-cationic-polymers-for-gene-therapy

Lin C, Zhong Z, Lok MC, Jiang X, Hennink WE, et al. (2007) Novel bioreducible poly(amido amine)s for highly efficient gene delivery. *Bioconjugate Chem* 18: 138–145.

Lin G, Wang X, Yin F, Yong KT (2015) Passive tumor targeting and imaging by using mercaptosuccinic acid-coated near-infrared quantum dots. *Int J Nanomedicine* 10:335-345.

Liu S, Guo Y, Huang R, Li J, Huang S, Kuang Y, et al. (2012) Gene and doxorubicin co-delivery system for targeting therapy of glioma. *Biomaterials* 33:4907–4916.

Longley DB, Johnston PG (2005) Molecular mechanisms of drug resistance. *J. Pathol* 205 (2): 275–292.

Luebeck EG, Moolgavkar SH (2002) Multistage Carcinogenesis and the Incidence of Colorectal Cancer. *Proc. Natl. Acad. Sci* 99: 15095-15100.

Ma D, Lin QM, Zhang LM, Liang YY, Xue W (2014) Astar-shaped porphyrin-arginine functionalized poly (L-lysine) copolymer for photo- enhanced drug and gene co-delivery. *Biomaterials* 35 (14): 4357–4367.

Ma J, Du LF, Chen M, Wang HH, Xing LX, et al. (2013) Drug-loaded nano-microcapsules delivery system mediated by ultrasound-targeted microbubble destruction: A promising therapy. *Method. Biomed Rep* 1(4): 506–510.

McKenzie DL, Kwok KY, Rice KG (2000) A potent new class of reductively activated peptide gene delivery agents. *J Biol Chem* 275(14): 9970-9977.

Meadows KL, Hurwitz HI (2012) Anti-VEGF Therapies in the Clinic. *Cold Spring Harb. Perspect Med* 2: 65-77.

Mendoza-Rodríguez CA, Cerbón MA (2001) Tumor suppressor gene p53: mechanisms of action in cell proliferation and death. *Rev Invest Clin* 53:266-273.

Miyata K, Kakizawa Y, Nishiyama N, Harada A, Yamasaki Y, et al (2004) Block Catiomer Polyplexes with Regulated Densities of Charge and Disulfide Cross-Linking Directed To Enhance Gene Expression. *J. Am. Chem. Soc* 126 (8): 2355–2361

Morris LG, Chan TA (2015) Therapeutic targeting of tumor suppressor genes. *Cancer* 121: 1357-1368.

Mukhtar E, Adhami VM, Mukhtar H (2014) Targeting Microtubules by Natural Agents for Cancer Therapy. *Mol Cancer Ther* 13: 275–284.

Noone AM, Howlader N, Krapcho M, Miller D, Brest A, Yu M, Ruhl J, Tatalovich Z, Mariotto A, Lewis DR, Chen HS, Feuer EJ, Cronin KA (2018) SEER Cancer Statistics Review, 1975-2015, Available : https://seer.cancer.gov/csr/1975_2015/ (accessed april 2018).

Orlowski S, Martin S, Escargueil A (2006) P-glycoprotein and 'lipid rafts': some ambiguous mutual relationships (floating on them, building them or meeting them by chance?) *Cell. Mol. Life Sci 63*: 1038-1059.

Ou M, Wang XL, Xu R, Chang CW, Bull DA, Kim SW (2008) Novel Biodegradable Poly(disulfide amine)s for Gene Delivery with High Efficiency and Low Cytotoxicity. *Bioconjug Chem 19(3): 626–633.*
Oupický D, Parker AL, Seymour LW (2004) Laterally Stabilized Complexes of DNA with Linear Reducible Polycations: Strategy for Triggered Intracellular Activation of DNA Delivery Vectors. *J. Am. Chem. Soc* 124 (1): 8–9.

Pack DW, Hoffman AS, Pun S, Stayton PS (2005) Design and development of polymers for gene delivery. *Nat. Rev. Drug Discovery* 4: 581–593.
Palleria C, Paolo AD, Giofrè A, Caglioti C, Leuzzi G, Siniscalchi A, et al. (2013) Pharmacokinetic drug-drug interaction and their implication in clinical management. *J Res Med Sci* 18(7): 601–610.

Palmberger TF, Laffleur F, Greindl M, Bernkop-Schnürch A (2015) *In vivo* evaluation of anionic thiolated polymers as oral delivery systems for efflux pump inhibition. *Int J Pharm* 491(1-2):318-22.

Pan B, Yao KS, Monia BP, Dean NM, McKay RA, Hamilton TC, O'Dwyer PJ (2002) Reversal of cisplatin resistance in human ovarian cancer cell lines by a c-jun antisense oligodeoxynucleotide (ISIS 10582): evidence for the role of transcription factor overexpression in determining resistant phenotype. *Biochem Pharmacol* 63: 1699-1707.

Peng Q, Hu C, Cheng J, Zhong Z, Zhuo R (2009) Influence of disulfide density and molecular weight on disulfide cross-linked polyethylenimine as gene vectors. *Bioconjug Chem* 20(2): 340-346.

Pérez-Herrero E, Fernández-Medarde A (2015) Advanced targeted therapies in cancer: Drug nanocarriers, the future of chemotherapy. *Eur J Pharm Biopharm* 93:52-79.

Ping Y , Wu D, Kumar JN, Cheng W, Lay CL, et al. (2013) Redox-responsive hyperbranched poly (amido amine)s with tertiary amino cores for gene delivery. *Biomacromolecules* 14(6): 2083-94.

Pisters LL,Pettaway CA, Troncoso P, McDonnel TJ, Stephens LC, Wood CG (2004) Evidence that transfer of functional p53 protein results in increased apoptosis in prostate cancer. *Clin Cancer Res* 10: 1217-1226.

Qian Y , Chen X (2010) Tumor suppression by p53: making cells senescent. *Histol Histopathol* 25:515-526.

Quaglia F, Ostacolo I, Mazzaglia A, Villari V, Zaccaria D, Sciortino MT (2009) The intracellular effects of non-ionic amphiphilic cyclodextrin nanoparticles in the delivery of anticancer drugs. *Biomaterials* 30: 374-382.

Quail DF, Joyce JA (2013) Microenvironmental regulation of tumor progression and metastasis. *Nat Med* 19(11): 1423–1437.

Rahmat D, Sakloetsakun D, Shahnaz G, Sarti F, Laffleur F, Schnürch AB (2012) HEC-cysteamine conjugates: influence of degree of thiolation on efflux pump inhibitory and permeation enhancing properties. *Int J Pharm* 422(1-2):40-46.

Rejman J, Bragonzi A, Conese M (2005) Role of clathrin- and caveolae-mediated endocytosis in gene transfer mediated by lipo- and polyplexes. *Mol Ther* 12: 468–474.

Risnayanti C, Jang YS, Lee J, Jun Ahn H (2018) PLGA nanoparticles co-delivering MDR1 and BCL2 siRNA for overcoming resistance of paclitaxel and cisplatin in recurrent or advanced ovarian cancer. *Sci Rep* 8: 7498-7506.

Saad M, Garbuzenko OB, Minko T (2008) Co-delivery of siRNA and an anticancer drug for treatment of multidrug-resistant cancer. *Nanomedicine (Lond)* 3(6): 761–776.

Saito G, Swanson JA, Lee KD (2003). Drug delivery strategy utilizing conjugation viareversible disulfide linkages: role and site of cellular reducing activities. *Adv Drug Deliv Rev* 55(2):199–215.

Schafer FQ, Buettner GR (2001) Redox environment of the cell as viewed through the redox state of the glutathione disulfide/glutathione couple. *Free Radical Biol. Med* 30: 1191–1212.

Schmitz T, Bravo-Osuna I, Vauthier C, Ponchel G, Loretz B, Bernkop-Schnürch A (2007) Development and *in vitro* evaluation of a thiomer-based nanoparticulate gene delivery system. *Biomaterials* 28(3): 524-531.

Schmitz T, Bravo-Osuna I, Vauthier C, Ponchel G, Loretz B, Bernkop-Schnürch A (2007) Development and *in vitro* evaluation of a thiomer-based nanoparticulate gene delivery system. *Biomaterials* 28(3):524-531.

Schneider R, Barakat A, Pippen J, Osborne C (2011) Aromatase inhibitors in the treatment of breast cancer in post-menopausal female patients: an update. *Breast Cancer (Dove Med Press)* 3:113-125.

Seo SJ, Lee SY, Choi SJ, Kim HW (2015) Tumor targeting co-delivery of drug and gene from temperature triggered micelles. *Macromol.Biosci* 15:1198–1204.

Siegel RL, Miller KD, Jemal A (2016) Cancer statistics. *CA Cancer J Clin* **66**:7-13.

Singh B, Maharjan S, Park TE , Jiang T, Kang SK, Choi YJ, Cho CS. Tuning the buffering capacity of polyethylenimine with glycerol molecules for efficient gene delivery: staying in or out of the endosomes. *Macromol Biosci* 15:622-35.

Sleiman RG, Esmerian M.O, Kobeissy H, Dbaibo G (2013) p53 and Ceramide as Collaborators in the Stress Response. *Int J Mol Sci 14*: 4982–5012.

Son S, Singha K, Kim WJ (2010) Bioreducible BPEI-SS-PEG-cNGR polymer as a tumor targeted nonviral gene carrier. *Biomaterials* 31(24):6344-6354.

Son S, Namgung R, Kim J, Singha K, Kim WJ (2012) Bioreducible polymers for gene silencing and delivery. *Acc Chem Res* 45:1100-1112.

Staud F, Ceckova M, Micuda S, Pavek P (2010) Expression and function of p-glycoprotein in normal tissues: effect on pharmacokinetics. *Methods Mol Biol* 596:199-222.

Sullivan R, Alatise OI, Anderson BO, Audisio R, Autier P, Aggarwal A (2015) Global cancer surgery: delivering safe, affordable, and timely cancer surgery. *Lancet Oncol* 16: 1193-1224.

Sun TM, Du DZ, Yao YD, Mao CD, Dou S, et al. (2011) Simultaneous delivery of siRNA and paclitaxel via 'two in onw' micelleplex promotes synergistic tumor suppression. *ACS Nano* 5: 1483-1494.

Sunoqrot S, Bugno J, Lantvit D, Burdette JE, Hong S (2014). Prolonged Blood Circulation and Enhanced Tumor Accumulation of Folate-Targeted Dendrimer-Polymer Hybrid Nanoparticles. *J Control Release*191: 115–122.

Tagde A, Singh H, Kang MH, Reynolds CP (2014) The glutathione synthesis inhibitor buthionine sulfoximine synergistically enhanced melphalan activity against preclinical models of multiple myeloma. *Blood Cancer J* 4: 229-241.

Tang YC, Yin C (2014) Enhnaced antitumor efficacy of folate modified amphiphilic nanoparticles through co-delivery of chemotherapeutic drugs and genes. *Biomaterials* 35: 6369-6378.

Torre LA, Goding Sauer AM, Chen MS, Singer MK, Jemal A, Siegel RL (2016) Cancer Statistics for Asian Americans, Native Hawaiians, and Pacific Islanders, 2015: Convergence of incidence between males and females. *CA Cancer J Clin* 66: 182–202.

Tran S, DeGiovanni PJ, Piel B, Rai P (2017) Cancer nanomedicine: a review of recent success in drug delivery. *Clin Transl Med* 6: 44-55.

Tsouris V,Joo MK, Kim SH, Kwon IL, Won YY (2014) Nanocarriers that enable co-delivery of chemotherapy and RNAi agents for treatment of drug-resistant cancer. *Biotechnol. Adv* 32: 1037-1050.

Vasiliu T, Cojocaru C, Rotaru A, Pricope G, Pinteala M, Clima L (2017) Optimization of Polyplex Formation between DNA Oligonucleotide and Poly(L-Lysine): Experimental Study and Modeling Approach. *Int. J. Mol. Sci 18*: 1291-1310.

Wang D, Xu, X, Zhang X, Sun B, Wang L (2018) Codelivery of doxorubicin and MDR1-siRNA by mesoporous silica nanoparticles-polymerpolyethylenimine to improve oral squamous carcinoma treatment. *Int J Nanomedicine* 13: 187–198.

Wang Y, Ke CY, Weijie Beh C, Liu SQ, Goh SH, Yang YY (2007)The self-assembly of biodegradable cationic polymer micelles as vectors for gene transfection. *Biomaterials* 28(35):5358-5368.

Wendel E, Stanchina D, Fridman JS, Malina A, Ray A, et al.Survival signalling by Akt and eIF4E in oncogenisis and cancer therapy. *Nature* 428: 332-337.

Werle M (2008) Natural and Synthetic Polymers as Inhibitors of Drug Efflux Pumps. *Pharm Res* 25(3): 500–511.

Winther JR, Thorpe C (2014) Quantification of Thiols and Disulfides. *Biochim Biophys Acta* 1840: 838-846.

Wu G, Fang YZ, Yang S, Lupton JR, Turner ND (2004). Glutathione metabolism and its implications for health. *J Nutr* 134(3):489–492.

Xiang SN, Tong HJ, Shi Q, Fernandes JC, Jin T, Dai KR, Zhang XL (2012) Uptake mechanisms of non-viral gene delivery. *J.Controlled Release* 158: 371−378.

Xiaowei D, Russell JM (2010) Nanomedicinal strategies to treat multidrug-resistant tumors: current progress. *Nanomedicine (Lond)* 5(4):597-615.

Xu Q, Xia Y, Wang CH, Pack DW (2012) Monodisperse double-walled microspheres loaded with chitosan-p53 nanoparticles and doxorubicin for combined gene therapy and chemotherapy. *J Control Release* 163(2):130-135.

Yameen B, Choi WI, Vilos C, Swami A, Shi J, Farokhzad OC (2014) Insight into Nanoparticle Cellular Uptake and Intracellular Targeting. *J. Controlled Release* 190: 485−499.

Yan L, Xingde L (2016) Biodegradable Stimuli-Responsive Polymeric Micelles for Treatment of Malignancy.*Curr Pharm Biotechnol* 17(3): 227–236.

Yang C, Wu T, Qi Y, Zhang Z (2018) Recent Advances in the Application of Vitamin E TPGS for Drug Delivery. *Theranostics* 8: 464–485.

Yang H , Ding R, Tong Z, Huang J, Shen L , et al. (2016) siRNA Targeting of MDR1 Reverses Multidrug Resistance in a Nude Mouse Model of Doxorubicin-resistant Human Hepatocellular Carcinoma. *Anticancer Res* 36(6):2675-2682.

Yang X, lyer AK, Singh A, Choy E, Hornicek FJ, Amiji MM, Duan Z(2015) *MDR1* siRNA loaded hyaluronic acid-based CD44 targeted nanoparticle systems circumvent paclitaxel resistance in ovarian cancer. *Sci Rep* 5: 8509 -8520.

Yin H, Kanasty RL, Eltoukhy AA, Vegas AJ , Dorkin JR, Anderson DG (2014) Non-viral vectors for gene-based therapy. *Nat Rev Genet* 15: 541–555.

Yin, Q, Shen, J,.Chen L, Zhang Z, Gu W, Li Y (2010) Overcoming multidrug resistance by co-delivery of Mdr-1andsurvivin-targeting RNA with reduction-responsible cationicpoly(beta-aminoesters). *Biomaterials* 33 :6495–6506.

You YZ, Manickam DS, Zhou QH, Oupicky D (2007) Reducible poly(2-dimethylaminoethyl methacrylate): Synthesis, cytotoxicity, and gene delivery activity. *J Control Release* 122(3): 217–225.

Young JL, Benoit JN, Dean DA (2003) Transfer and Expression of Plasmids in the Intact Vasculature. *Gene Ther* 10: 1465-1470.

Yuan Y, Cai T, Xia X, Zhang R , Chiba P, Cai Y (2016) Nanoparticle delivery of anticancer drugs overcomes multidrug resistance in breast cancer. *Drug Deliv* 23:3350-3357.

Yuhe W, Meng Z, Fenghua M, Jing Z, Rui P, Zhiyuan Z (2011) Branched Polyethylenimine Derivatives with Reductively Cleavable Periphery for Safe and Efficient *In Vitro* Gene Transfer. *Biomacromolecules* 12: 1032–1049.

Zahreddine H, Borden K (2013) Mechanisms and insights into drug resistance in cancer. *Front Pharmacol* 4: 28-34.

Zhan C, Wei X, Qia J,Feng L, Zhu J, Lu W (2012) Co-delivery of TRAIL gene enhances the anti-glioblastoma effect of paclitaxel invitro and invivo. *J.Control.Release*160: 630–636.

Zhang M, Liu E, Cui Y, Huang Y (2017) Nanotechnology-based combination therapy for overcoming multidrug-resistant cancer. *Cancer Biol Med* 14:212–227.

Zhang P,.Hu L,Yin Q,Zhang Z, Feng L, Li L (2015) Transferrin-conjugated polyphosphoester hybrid micelle loading paclitaxel for brain targeting delivery : Synthesis, preparation and *in vivo* evaluation. *J control.Release* 159:429-434.

Zhong Z, Feijen J, Lok MC, Hennink WE, Christensen LV, et al. (2005) Low molecular weight linear polyethylenimine-b-poly(ethylene glycol)-b-polyethylenimine triblock copolymers: synthesis, characterization, and *in vitro* gene transfer properties. *Biomacromolecules* 6:3440-3448.

Zhu L, ,Perche F, Wang T, Torchilin P (2013) Matrix metalloproteinase 2- sensitive multifunctional polymeric micelles for tumor specific co-delivery of siRNA and hydrophobic drugs. *Biomaterials* 35: 4213-4222.

Zugates GT, Daniel GA, Steven RL, Ingrid EBL, Langer EB (2006) Synthesis of Poly(β-amino ester)s with Thiol-Reactive Side Chains for DNA Delivery. *J. Am. Chem. Soc* 128 : 12726–12734.

List of publications

1. Priya S.S, Rekha M.R (2017) Redox sensitive cationic pullulan for efficient gene transfection and drug retention in C6 glioma cells. *International Journal of Pharmaceutics*, 530: 401-414.
2. Priya.S.S, Rekha M.R (2016) Disulphide cross linked pullulan based cationic polymer for improved gene delivery and efflux pump inhibition. *Colloids and Surfaces B: Bio-interfaces*, 146: 879-887.
3. Priya S.S, Rekha M.R (2018) Thiol redox-sensitive cationic polymers for dual delivery of drug and gene. *Therapeutic delivery*, 9: 751-773. (*Review*)
4. Priya S. S and Rekha M. R (2016) Pullulan based multifunctional thiolated polymers for efficient gene delivery and efflux pump inhibition with enhanced doxorubicin retention in c6 glioma cell Front. *Bioeng. Biotechnol*.
5. Sherly.M. Caroline, S.S. Priya, M.R Rekha (2017) Cationic polyelectrolyte vectors in gene delivery. Particulate technology for delivery of therapeutics,) 395-417, *Springer Nature (Book Chapter)*.
6. Priya S.S, Rekha M.R. Nullifying tumor efflux pump by 3,3 dithiodipropionate modified pullulan: Formulation of low dose anticancer chemotherapeutics (under revision)
7. Priya S.S, Rekha.M.R. Disulfide corss linked polyethyleneimine mediated transfection and efflux pump inhibition in C6 glioma cells (under revision)